



**Australian Government**

**Geoscience Australia**

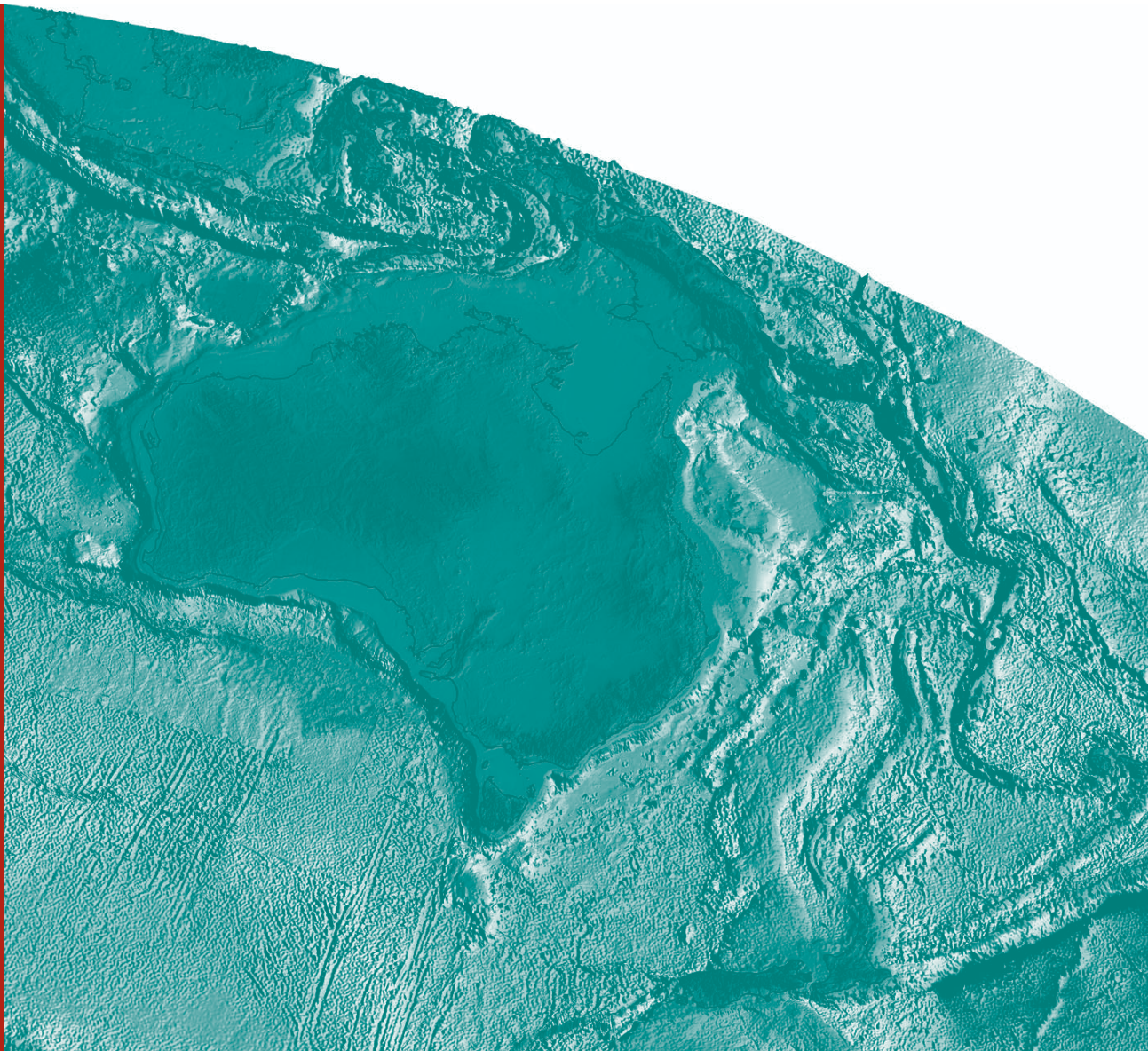
# Compilation of SHRIMP U-Pb geochronological data

Yilgarn Craton, Western Australia, 2004-2006

*Sircombe, K.N., Cassidy, K.F., Champion, D.C. & Tripp, G.*

**Record**

**2007/01**



# Compilation of SHRIMP U-Pb geochronological data, Yilgarn Craton, Western Australia, 2004-2006

GEOSCIENCE AUSTRALIA  
RECORD 2007/01

by

K.N. Sircombe<sup>1</sup>  
K.F. Cassidy<sup>1,2</sup>  
D.C. Champion<sup>1</sup>  
G. Tripp<sup>3</sup>



**Australian Government**

**Geoscience Australia**

- 
1. Geoscience Australia, GPO Box 378, Canberra, ACT 2601
  2. Rubicon Resources Limited, PO Box 1380, West Perth, WA 6872
  3. Barrick Australia-Pacific, PO Box 1662, Kalgoorlie, WA 6433

**Department of Industry, Tourism & Resources**

Minister for Industry, Tourism & Resources: The Hon. Ian Macfarlane, MP

Parliamentary Secretary: The Hon. Bob Baldwin, MP

Secretary: Mark Paterson

**Geoscience Australia**

Chief Executive Officer: Dr Neil Williams

© Commonwealth of Australia, 2007

This work is copyright. Apart from any fair dealings for the purpose of study, research, criticism, or review, as permitted under the *Copyright Act 1968*, no part may be reproduced by any process without written permission. Copyright is the responsibility of the Chief Executive Officer, Geoscience Australia. Requests and enquiries should be directed to the **Chief Executive Officer, Geoscience Australia, GPO Box 378 Canberra ACT 2601**.

Geoscience Australia has tried to make the information in this product as accurate as possible. However, it does not guarantee that the information is totally accurate or complete. Therefore, you should not solely rely on this information when making a commercial decision.

**ISSN 1448-2177**

**ISBN 978 1 921236 09 9 (Hardcopy)**

**ISBN 978 1 921236 10 5 (Web)**

**GeoCat # 64996**

<p><b>Bibliographic reference:</b> Sircombe, K.N., Cassidy, K.F., Champion, D.C. and Tripp, G., 2007. Compilation of SHRIMP U-Pb geochronological data, Yilgarn Craton, Western Australia, 2004-2006. Geoscience Australia Record 2007/01.</p>
--

# Contents

List of Figures .....	iv
List of Tables .....	x
Introduction.....	1
Analytical procedures .....	4
<b>Part 1: Southwest Yilgarn</b> .....	10
2003967051: biotite granodiorite, Nippering Quarry.....	10
2003967056: biotite syenogranite, Blackburn Mine .....	16
2003967058: foliated biotite monzogranite, Puntaping Rock.....	22
2003967065: biotite-two pyroxene quartzofeldspathic gneiss (granulite), Nairibin Rock.....	28
2003967068: biotite quartzofeldspathic gneiss, Lake Dumbleyung .....	35
2003969212: biotite tonalite, Narrogin Quarry .....	41
2004967003: banded biotite quartzofeldspathic augen gneiss, Tweed River .....	46
2004967004: Gibraltar quartz monzonite .....	52
2004967007: biotite monzogranite dyke, Dinninup.....	59
2004967009: biotite granite, Wilyungulup Spring.....	65
2004967550: biotite syenogranite dyke, Nanicup Bridge.....	73
2004968001A: meta-psammite, Wheatley .....	78
2004969008: biotite granodiorite, Newlgalup .....	87
<b>Part 2: Eastern Yilgarn</b> .....	93
2002967002: biotite quartzofeldspathic gneiss, Moon Rock .....	93
2002967003: biotite quartzofeldspathic gneiss, Kirgella Rockhole.....	98
2002967004: biotite monzogranite, Lords Bore .....	104
2004967308: volcanic meta-sandstone, Kanowna Belle.....	110
2004967310: volcanic meta-sandstone, Kanowna Belle.....	117
2004967316: volcanic meta-sandstone, Kanowna Belle.....	122
2004967325: meta-dacite, Kanowna Belle .....	129
2004967366: meta-sandstone, Long Wong prospect .....	136
2004967367: volcanic meta-sandstone, Three-in-Hand prospect .....	144
2004967369: porphyritic micro-diorite sill, Three-in-Hand prospect.....	153
2004967372: meta-conglomerate, Bee-Eater prospect .....	160
2004967377: Owen monzogranite .....	164
2004967500: meta-sandstone, Toppin Hill .....	169
2004967506: meta-rhyolite, Toppin Hill .....	175
Acknowledgements .....	181
References.....	182



# List of Figures

**Figure 1.** Location of Yilgarn Craton study areas detailed in Figure 2 and Figure 3. .... 1

**Figure 2.** Approximate locations of samples from the Eastern Goldfields study area presented in this Record. The geology, towns and coastline are derived from Geoscience Australia’s national geoscience database. .... 2

**Figure 3.** Approximate locations of samples from the southwest Yilgarn study area presented in this Record. The geology, towns and coastline are derived from Geoscience Australia’s national geoscience database. .... 3

**Figure 4.** An illustration of the difference between (A) a conventional Wetherill concordia plot with highly correlated error ellipses and (B) a Tera-Wasserburg concordia plot with no error correlation. .... 7

**Figure 5.** Tera-Wasserburg concordia plot illustrating potential graphical interpretation of the dispersion of plotted results. Zero-age Pb-loss is revealed by dispersion parallel to the x-axis. Ancient discordia chords (e.g. ancient Pb-loss or resetting) will be seen as dispersion toward the lower-right. Any mixing with common-Pb can be seen as dispersion toward the upper-left. .... 7

**Figure 6.** Concordia plot illustrating the concept of zero-age discordance lines. Analysis (a) is concordant; analysis (b) is ~2.5% discordant, i.e.  $^{207}\text{Pb}/^{206}\text{Pb}$  age is 2750 Ma, and assuming zero-age Pb-loss the  $^{206}\text{Pb}/^{238}\text{U}$  age is 2680 Ma, the difference of 70 Myr is ~2.5% of the  $^{207}\text{Pb}/^{206}\text{Pb}$  age; analysis (c) is 4.5% discordant; analysis (d) is >5% discordant. Analyses are typically discarded from further interpretation at -5% and +5% discordance. .... 8

**Figure 7.** Illustration of concordia contour diagrams (from Sircombe 2006). A) Tera-Wasserburg diagram with analyses represented by conventional error ellipses and illustrating the visual clutter caused by large volumes of geochronological data in complex samples. B) The equivalent concordia contour diagram to (A) where the bivariate normal distributions represented by the error ellipses have been summed to produced an overall distribution which has been contoured to illustrate distinct modes and relationships. .... 9

**Figure 8.** Representative images (transmitted light on left, cathodoluminescence on right) for sample 2003967051: biotite granodiorite, Nippering Quarry. SHRIMP analysis spots are labelled. .... 12

**Figure 9.** Tera-Wasserburg concordia plot for zircons from sample 2003967051: biotite granodiorite, Nippering Quarry. White-filled symbols are used to define the age of the sample; discordant and/or high common-Pb analyses are light grey. .... 13

**Figure 10.** Tera-Wasserburg concordia plot for zircons from sample 2003967051: biotite granodiorite, Nippering Quarry. White-filled symbols are used to define the age of the sample; dark grey ellipse indicates concordia age; cross-hatch fill indicates possible inheritance; vertical hatch fill indicates possible Pb-loss; discordant and/or high common-Pb analyses are light grey. .... 14

**Figure 11.** Representative images (transmitted light on left, cathodoluminescence on right) for sample 2003967056: biotite syenogranite, Blackburn Mine. SHRIMP analysis spots are labelled. .... 18

**Figure 12.** Tera-Wasserburg concordia plot for zircons from sample 2003967056: biotite syenogranite, Blackburn Mine. White-filled symbols are used to define the age of the sample; discordant and/or high common-Pb analyses are light grey. .... 19

**Figure 13.** Tera-Wasserburg concordia contour plot of sample 2003967056: biotite syenogranite, Blackburn Mine illustrating the smearing of isotopic values. .... 20

**Figure 14.** Representative images (transmitted light on left, cathodoluminescence on right) for sample 2003967058: foliated biotite monzogranite, Puntaping Rock. SHRIMP analysis spots are labelled. .... 24

**Figure 15.** Tera-Wasserburg concordia plot for zircons from sample 2003967058: foliated biotite monzogranite, Puntaping Rock. White-filled symbols are used to define the age of the sample; discordant and/or high common-Pb analyses are light grey; vertical hatching and cross hatching indicate apparently concordant analyses considered affected by Pb-loss. .... 25

**Figure 16.** Tera-Wasserburg concordia plot for zircons from sample 2003967058: foliated biotite monzogranite, Puntaping Rock concentrating on the concordant group yielding a concordia age of  $2673 \pm 9$  Ma indicated by the dark ellipse. ....26

**Figure 17.** Representative images (transmitted light on left, cathodoluminescence on right) for sample 2003967065: biotite-two pyroxene quartzofeldspathic gneiss (granulite), Nairibin Rock. SHRIMP analysis spots are labelled. ....30

**Figure 18.** Tera-Wasserburg concordia plot for zircons from sample 2003967065: biotite-two pyroxene quartzofeldspathic gneiss (granulite), Nairibin Rock. Cross-hatch symbol indicates protolith analyses; vertical hatching indicate analyses interpreted as metamorphic; diagonal hatching indicates a possible mixed analysis; discordant and/or high common-Pb analyses are light grey. ....31

**Figure 19.** Tera-Wasserburg concordia plot for zircons from sample 2003967065: biotite-two pyroxene quartzofeldspathic gneiss (granulite), Nairibin Rock focussing on the concordant analyses. Cross-hatch symbol indicates protolith analyses; vertical hatching indicate analyses interpreted as metamorphic; diagonal hatching indicates a possible mixed analysis; discordant and/or high common-Pb analyses are light grey. ....32

**Figure 20.** Plot of zircon age in relation to  $^{232}\text{Th}/^{238}\text{U}$  ratio for concordant zircons from 2003967065: biotite-two pyroxene quartzofeldspathic gneiss (granulite), Nairibin Rock illustrating two distinct clusters. Triangular markers indicate the older cluster and square markers indicate the younger cluster. A possibly blended analysis (#6.1) is indicated with the diamond marker. The red markers indicate the median and median absolute deviation in both dimensions for each cluster. ....33

**Figure 21.** Representative images (transmitted light on left, cathodoluminescence on right) for sample 2003967068: biotite quartzofeldspathic gneiss, Lake Dumbleyung. SHRIMP analysis spots are labelled. ....37

**Figure 22.** Tera-Wasserburg concordia plot for zircons from sample 2003967068: biotite quartzofeldspathic gneiss, Lake Dumbleyung. White-filled symbols are used to define the age of the sample; discordant and/or high common-Pb analyses are light grey; vertical hatching indicates inheritance; cross-hatching indicates analyses regarded as younger outliers possibly due to Pb-loss. ....38

**Figure 23.** Tera-Wasserburg concordia plot for zircons from sample 2003967068: biotite quartzofeldspathic gneiss, Lake Dumbleyung focussing on the concordant analyses yielding a concordia age of  $2650 \pm 7$  Ma. ....39

**Figure 24.** Representative images (transmitted light on left, cathodoluminescence on right) for sample 2003969212: biotite tonalite, Narrogin Quarry. SHRIMP analysis spots are labelled. ....43

**Figure 25.** Tera-Wasserburg concordia plot for zircons from sample 2003969212: biotite tonalite, Narrogin Quarry. White-filled symbols are < 10% discordant; light grey symbols indicate analyses > 10% discordant and/or high common-Pb. ....44

**Figure 26.** Representative images (transmitted light on left, cathodoluminescence on right) for sample 2004967003: banded biotite quartzofeldspathic augen gneiss, Tweed River. SHRIMP analysis spots are labelled. Note difference between hyacinth and yellow coloured grains as discussed in the text. ....48

**Figure 27.** Tera-Wasserburg concordia plot for zircons from sample 2004967003: banded biotite quartzofeldspathic augen gneiss, Tweed River. Colouring of error ellipses illustrates the relationship between reverse discordance and uranium content. ....49

**Figure 28.** Tera-Wasserburg concordia plot for zircons from sample 2004967003: banded biotite quartzofeldspathic augen gneiss, Tweed River focussing on the lower-U, concordant hyacinth-coloured zircons which yield a concordia age of  $2658 \pm 7$  Ma. ....50

**Figure 29.** Representative images (transmitted light on left, cathodoluminescence on right) for sample 2004967004: Gibraltar quartz monzonite. SHRIMP analysis spots are labelled. ....54

**Figure 30.** Tera-Wasserburg concordia plot for zircons from sample 2004967004: Gibraltar quartz monzonite. 2004967004: Plus-symbol hatching indicates older cluster and vertical hatching indicates younger cluster as discussed in text; diagonal hatching indicates group of analyses with >1000 ppm U; discordant and/or high common-Pb analyses are light grey; Inset: inherited analyses. ....55

**Figure 31.** Concordia contour diagram of sample 2004967004: Gibraltar quartz monzonite illustrating concordant clusters: a dominant cluster 2630 – 2620 Ma and a broader cluster 2650 – 2690 Ma. ....56

**Figure 32.** Plot of zircon age in relation to U content for zircons from sample 2004967004: Gibraltar quartz monzonite 2004967004: illustrating two potential clusters. As discussed in text: triangular markers indicate older cluster, square markers indicate younger cluster and diamond markers indicate concordant analyses with > 1000 ppm. The red markers and error bars indicate the median and median absolute deviation for each cluster. ....57

**Figure 33.** Plot of zircon age in relation to  $^{232}\text{Th}/^{238}\text{U}$  ratio for zircons from sample 2004967004: illustrating two potential clusters. As discussed in text: Triangular markers indicate older cluster, square markers indicate younger cluster and diamond markers indicate concordant analyses with > 1000 ppm. The red markers and error bars indicate the median and median absolute deviation for each cluster. ....57

**Figure 34.** Representative images (transmitted light on left, cathodoluminescence on right) for sample 2004967007: biotite monzogranite dyke, Dinninup. SHRIMP analysis spots are labelled. ....61

**Figure 35.** Tera-Wasserburg concordia plot for zircons from sample 2004967007: biotite monzogranite dyke, Dinninup. White-filled error ellipses indicate analyses used for calculating concordia age of  $2610 \pm 7$  Ma (indicated by dark grey error ellipse). Vertical hatch indicates analysis interpreted as inheritance; diagonal hatch indicates analysis considered as a blend; light-grey fill indicates analyses with high common-Pb. ....62

**Figure 36.** Plot of zircon age in relation to  $^{232}\text{Th}/^{238}\text{U}$  ratio for zircons from sample 2004967007: biotite monzogranite dyke, Dinninup illustrating a weak correlation toward higher ratio values for younger zircon analyses as discussed in text. ....63

**Figure 37.** Representative images (transmitted light on left, cathodoluminescence on right) for sample 2004967009: biotite granite, Wilyungulup Spring. SHRIMP analysis spots are labelled. ....67

**Figure 38.** Tera-Wasserburg concordia plot for zircons from sample 2004967009: biotite granite, Wilyungulup Spring. The two concordant clusters discussed in text are indicated by vertical and cross hatching; discordant and/or high common-Pb analyses are light grey. ....68

**Figure 39.** Concordia contour plot for zircons from sample 2004967009: biotite granite, Wilyungulup Spring (effectively the equivalent of **Figure 38**) illustrating the two clusters at ~2690 Ma and ~2640 Ma discussed in the text. ....69

**Figure 40.** Plot of zircon age in relation to U content for zircons from sample 2004967009: biotite granite, Wilyungulup Spring illustrating two potential clusters. Triangular markers indicate the older cluster and square markers indicate the younger cluster. The red markers and error bars indicate the median and median absolute deviation for each cluster. ....70

**Figure 41.** Plot of zircon age in relation to  $^{232}\text{Th}/^{238}\text{U}$  ratio for zircons from sample 2004967009: biotite granite, Wilyungulup Spring illustrating two potential clusters. Triangular markers indicate the older cluster and square markers indicate the younger cluster. The red markers and error bars indicate the median and median absolute deviation for each cluster. ....70

**Figure 42.** Probability density distribution and histogram plot of concordant  $^{207}\text{Pb}/^{206}\text{Pb}$  ages from sample 2004967009: biotite granite, Wilyungulup Spring with mixture modelled age components shown. ....71

**Figure 43.** Representative images (transmitted light on left, cathodoluminescence on right) for sample 2004967550: biotite syenogranite dyke, Nanicip Bridge. SHRIMP analysis spots are labelled. ....75

**Figure 44.** Tera-Wasserburg concordia plot for zircons from sample 2004967550: biotite syenogranite dyke, Nanicip Bridge. Two outliers are indicated by vertical hatching; discordant and/or high common-Pb analyses are light grey. ....76

**Figure 45.** Representative images (transmitted light on left, cathodoluminescence on right) for sample 2004968001A: meta-psammite, Wheatley. SHRIMP analysis spots are labelled. ....80

**Figure 46.** Tera-Wasserburg concordia plot for zircons from sample 2004968001A: meta-psammite, Wheatley. Cross-hatch pattern indicate distinctly older analyses; vertical hatch indicates analyses with U > 1000 ppm; white filled ellipses indicate bulk of concordant analyses; discordant and/or high common-Pb analyses are light grey. ....81

**Figure 47.** Concordia contour plot for zircons from sample 2004968001A: meta-psammite, Wheatley (effectively the equivalent of **Figure 46**) illustrating the broad range of analyses from 2700 to 2600 Ma with a dominant mode ~2640 Ma. .... 82

**Figure 48.** Plot of zircon age in relation to U content for concordant zircons from 2004968001A: meta-psammite, Wheatley illustrating a trend toward younger ages with higher U contents. Square markers indicate analyses U > 1000 ppm. Diamond markers indicate older analyses. .... 83

**Figure 49.** Plot of zircon age in relation to  $^{232}\text{Th}/^{238}\text{U}$  ratio for concordant zircons from 2004968001A: meta-psammite, Wheatley. Square markers indicate analyses U > 1000 ppm. .... 83

**Figure 50.** Probability density distribution and histogram plot of  $^{207}\text{Pb}/^{206}\text{Pb}$  ages from sample 2004968001A: meta-psammite, Wheatley with mixture modelled age components shown. Light grey distribution depicts all ages including discordant analyses – subsequent distributions have been scaled to this; medium grey distribution depicts concordant analyses with U < 1000 ppm which is the basis for mixture modelled age components; dark grey distribution depicts concordant analyses with U > 1000 ppm. .... 84

**Figure 51.** Representative images (transmitted light on left, cathodoluminescence on right) for sample 2004969008: biotite granodiorite, Newlgalup. SHRIMP analysis spots are labelled. 89

**Figure 52.** Tera-Wasserburg concordia plot for zircons from sample 2004969008: biotite granodiorite, Newlgalup. The two concordant clusters discussed in the text and interpreted from Figure 53 are indicated by white fill and cross hatching; an analytically suspicious result is indicated in light grey. The dark-grey ellipses indicate concordia ages calculated at  $2651 \pm 11$  Ma and  $2610 \pm 8$  Ma. .... 90

**Figure 53.** Concordia contour plot for zircons from sample 2004969008: biotite granodiorite, Newlgalup illustrating the two prominent clusters at ~2650 Ma and ~2610 Ma. .... 91

**Figure 54.** Representative images (transmitted light on left, cathodoluminescence on right) for sample 2002967002: biotite quartzofeldspathic gneiss, Moon Rock. SHRIMP analysis spots are labelled. .... 95

**Figure 55.** Tera-Wasserburg concordia plot for zircons from sample 2002967002: biotite quartzofeldspathic gneiss, Moon Rock. White-filled symbols are used to define the age of the sample; discordant and/or high common-Pb analyses are light grey; outliers have vertical hatching; the cross-pattern indicates one concordant analysis of bright CL zoning as described in the text. .... 96

**Figure 56.** Representative images (transmitted light on left, cathodoluminescence on right) for sample 2002967003: biotite quartzofeldspathic gneiss, Kirgella Rockhole. SHRIMP analysis spots are labelled. .... 100

**Figure 57.** Tera-Wasserburg concordia plot for zircons from sample 2002967003: biotite quartzofeldspathic gneiss, Kirgella Rockhole. Insert diagram is a detailed view of the ~2730 Ma group. White-filled symbols are used to define the age of the sample; cross-hatch indicates analyses considered as inheritance; discordant and/or high common-Pb analyses are light grey; outliers have vertical hatching as described in the text. .... 101

**Figure 58.** Concordia contour plot for zircons in the ~2730 Ma group from sample 2002967003: biotite quartzofeldspathic gneiss, Kirgella Rockhole. .... 102

**Figure 59.** Representative images (transmitted light on left, cathodoluminescence on right) for sample 2002967004: biotite monzogranite, Lords Bore. SHRIMP analysis spots are labelled. .... 106

**Figure 60.** Tera-Wasserburg concordia plot for zircons from sample 2002967004: biotite monzogranite, Lords Bore. White-filled symbols are used to define the age of the sample; discordant and/or high common-Pb analyses are light grey; inherited analyses have vertical striping. .... 107

**Figure 61.** Tera-Wasserburg concordia contour plot of sample 2002967004: biotite monzogranite, Lords Bore illustrating the distinction between the two clusters at 2700 Ma and 2638 Ma. Only data within 5% discordance are included in the distribution. .... 108

**Figure 62.** Representative images (transmitted light on left, cathodoluminescence on right) for sample 2004967308: volcanic meta-sandstone, Kanowna Belle. SHRIMP analysis spots are labelled. .... 112

**Figure 63.** Tera-Wasserburg concordia plot for zircons from sample 2004967308: volcanic meta-sandstone, Kanowna Belle. White-filled symbols are used to define the age of the sample as discussed in text; discordant and/or high common-Pb analyses are light grey; cross hatch indicates analyses interpreted as inheritance..... 113

**Figure 64.** Tera-Wasserburg concordia contour plot for two sets of analyses from sample 2004967308: volcanic meta-sandstone, Kanowna Belle..... 114

**Figure 65.** Probability density distribution and histogram plot of  $^{207}\text{Pb}/^{206}\text{Pb}$  ages from sample 2004967308: volcanic meta-sandstone, Kanowna Belle..... 115

**Figure 66.** Complete image (transmitted light on left, cathodoluminescence on right) for sample 2004967310: volcanic meta-sandstone, Kanowna Belle. SHRIMP analysis spots are labelled. .... 119

**Figure 67.** Tera-Wasserburg concordia plot for zircons from sample 2004967310: volcanic meta-sandstone, Kanowna Belle. White-filled symbols are used to define the age of the sample as discussed in text. .... 120

**Figure 68.** Representative images (transmitted light on left, cathodoluminescence on right) for sample 2004967316: volcanic meta-sandstone, Kanowna Belle. SHRIMP analysis spots are labelled. .... 124

**Figure 69.** Tera-Wasserburg concordia plot for zircons from sample 2004967316: volcanic meta-sandstone, Kanowna Belle. Only analyses with <1% common-Pb have been plotted as white-filled symbols. .... 125

**Figure 70.** Tera-Wasserburg contour concordia plot for concordant zircons from sample 2004967316: volcanic meta-sandstone, Kanowna Belle. Only analyses with <1% common-Pb have been used to calculate the distribution. .... 126

**Figure 71.** Probability density distribution and histogram plot of  $^{207}\text{Pb}/^{206}\text{Pb}$  ages from sample 2004967316: volcanic meta-sandstone, Kanowna Belle with mixture modelled age components shown. Only analyses with <1% common-Pb have been used to calculate the distribution and age components. Because of the low quantity of data the modelled age components should be considered as tentative. .... 127

**Figure 72.** Representative images (transmitted light on left, cathodoluminescence on right) for sample 2004967325: meta-dacite, Kanowna Belle. SHRIMP analysis spots are labelled. ... 131

**Figure 73.** Tera-Wasserburg concordia plot for zircons from sample 2004967325: meta-dacite, Kanowna Belle. The two concordant clusters discussed in text are indicated by white fill and vertical hatching; discordant and/or high common-Pb analyses are light grey. .... 132

**Figure 74.** Concordia contour plot for zircons from sample 2004967325: meta-dacite, Kanowna Belle illustrating the dominant cluster at ~2700 Ma and a minor cluster at ~2665 Ma. .... 133

**Figure 75.** Plot of zircon age in relation to  $^{232}\text{Th}/^{238}\text{U}$  ratio for zircons from sample 2004967325: meta-dacite, Kanowna Belle illustrating possible weak correlation ( $\rho^2$ : 0.28). .... 134

**Figure 76.** Probability density distribution and histogram plot of concordant  $^{207}\text{Pb}/^{206}\text{Pb}$  ages from sample 2004967325: meta-dacite, Kanowna Belle with mixture modelled age components shown. .... 134

**Figure 77.** Representative images (transmitted light on left, cathodoluminescence on right) for sample 2004967366: meta-sandstone, Long Wong prospect. SHRIMP analysis spots are labelled. .... 138

**Figure 78.** Tera-Wasserburg concordia plot for zircons from sample 2004967366: meta-sandstone, Long Wong prospect. Analyses in the main concordant cluster are indicated by white fill; analyses possibly affected by Pb-loss have vertical hatching; inherited analyses have a cross-hatch fill and discordant and/or high common-Pb analyses are light grey. .... 139

**Figure 79.** Concordia contour plot for zircons from sample 2004967366: meta-sandstone, Long Wong prospect illustrating the dominant cluster at ~2720 Ma and probable dispersion toward lower left. .... 140

**Figure 80.** Probability density distribution and histogram plot of concordant  $^{207}\text{Pb}/^{206}\text{Pb}$  ages from sample 2004967366: meta-sandstone, Long Wong prospect with mixture modelled age components shown. .... 141

**Figure 81.** Representative images (transmitted light on left, cathodoluminescence on right) for sample 2004967367: volcanic meta-sandstone, Three-in-Hand prospect. SHRIMP analysis spots are labelled. .... 146



**Figure 82.** Tera-Wasserburg concordia plot for zircons from sample 2004967367: volcanic meta-sandstone, Three-in-Hand prospect. Analyses in the main concordant cluster are indicated by white fill; rims have vertical hatching; discordant and/or high common-Pb analyses are light grey. .... 147

**Figure 83.** Tera-Wasserburg concordia plot for core and rim analyses from sample 2004967367: volcanic meta-sandstone, Three-in-Hand prospect. Analyses from zircon cores are indicated by thick line on the error ellipses; dashed error ellipses indicate corresponding analyses from rims. .... 148

**Figure 84.** Concordia contour plot for zircons from sample 2004967367: volcanic meta-sandstone, Three-in-Hand prospect illustrating the dominant cluster at ~2700 Ma and probable dispersion toward lower left. .... 149

**Figure 85.** Probability density distribution and histogram plot of concordant  $^{207}\text{Pb}/^{206}\text{Pb}$  ages from sample 2004967367: volcanic meta-sandstone, Three-in-Hand prospect with mixture modelled age components shown. .... 150

**Figure 86.** Representative images (transmitted light on left, cathodoluminescence on right) for sample 2004967369: porphyritic micro-diorite sill, Three-in-Hand prospect. SHRIMP analysis spots are labelled. .... 155

**Figure 87.** Tera-Wasserburg concordia plot for zircons from sample 2004967369: porphyritic micro-diorite sill, Three-in-Hand prospect. The main concordant clusters discussed in the text are represented by white-filled symbols and the young outliers from this group are indicated by vertical hatching; discordant and/or high common-Pb analyses are light grey. .... 156

**Figure 88.** Concordia contour plot for zircons from sample 2004967369: porphyritic micro-diorite sill, Three-in-Hand prospect, illustrating the dominant cluster at ~2680 Ma with minor dispersion toward lower right. .... 157

**Figure 89.** Complete image (transmitted light on left, cathodoluminescence on right) of sample 2004967372: meta-conglomerate, Bee-Eater prospect. SHRIMP analysis spots are labelled. .... 162

**Figure 90.** Tera-Wasserburg concordia plot for zircons from sample 2004967372: meta-conglomerate, Bee-Eater prospect. The main concordant cluster discussed in text is represented by white-filled symbols with the concordant age ellipse represented by the dark grey fill; discordant and/or high common-Pb analyses are light grey. .... 163

**Figure 91.** Representative images (transmitted light on left, cathodoluminescence on right) for sample 2004967377: Owen monzogranite. SHRIMP analysis spots are labelled. .... 166

**Figure 92.** Tera-Wasserburg concordia plot for zircons from sample 2004967377: Owen monzogranite. The main concordant cluster used to calculate a concordia age of  $2655 \pm 15$  Ma is represented by white-filled symbols; discordant and/or high common-Pb analyses are light grey. .... 167

**Figure 93.** Representative images (transmitted light on left, cathodoluminescence on right) for sample 2004967500: meta-sandstone, Toppin Hill. SHRIMP analysis spots are labelled. The white streaking is due to the over-bright luminescence of accidentally included apatite grains. .... 171

**Figure 94.** Tera-Wasserburg concordia plot for zircons from sample 2004967500: meta-sandstone, Toppin Hill. White-filled symbols are used to define the age of the sample; discordant and/or high common-Pb analyses are light grey; vertical hatch indicates analyses with possible Pb-loss; cross hatch indicates analyses on cores identified by CL imaging. Data with instrument induced exaggerated uncertainties have not been plotted. .... 172

**Figure 95.** Tera-Wasserburg concordia plot for two sets of analyses from sample 2004967500: meta-sandstone, Toppin Hill with potential core-rim relationship. Core analyses are indicated by thick border on error ellipses; corresponding rim analyses have dashed borders. Although the ages suggest that core analyses are older than rim analyses, there is no significant statistical difference between the two. .... 173

**Figure 96.** Representative images (transmitted light on left, cathodoluminescence on right) for sample 2004967506: meta-rhyolite, Toppin Hill. SHRIMP analysis spots are labelled. .... 177

**Figure 97.** Tera-Wasserburg concordia plot for zircons from sample 2004967506: meta-rhyolite, Toppin Hill. White-filled symbols are used to define the age of the sample; discordant and/or high common-Pb analyses are light grey; cross-hatch fill indicates possible inheritance; vertical hatch fill indicates possible Pb-loss. .... 178

**Figure 98.** Tera-Wasserburg concordia plot for concordant zircons from sample 2004967506: meta-rhyolite, Toppin Hill.  $^{207}\text{Pb}/^{206}\text{Pb}$  ages ( $\pm 2\sigma$ ) uncertainties used for calculating weighted mean shown in inset. .... 179

## List of Tables

<b>Table 1.</b> Standard run table for SHRIMP analyses in this project.....	5
<b>Table 2.</b> SHRIMP analytical results for zircon from sample 2003967051: biotite granodiorite, Nippering Quarry. ....	15
<b>Table 3.</b> SHRIMP analytical results for zircon from sample 2003967056: biotite syenogranite, Blackburn Mine.....	21
<b>Table 4.</b> SHRIMP analytical results for zircon from sample 2003967058: foliated biotite monzogranite, Puntaping Rock. ....	27
<b>Table 5.</b> SHRIMP analytical results for zircon from sample 2003967065: biotite-two pyroxene quartzofeldspathic gneiss (granulite), Nairibin Rock.....	34
<b>Table 6.</b> SHRIMP analytical results for zircon from sample 2003967068: biotite quartzofeldspathic gneiss, Lake Dumbleyung.....	40
<b>Table 7.</b> SHRIMP analytical results for zircon from sample 2003969212: biotite tonalite, Narrogin Quarry. ....	45
<b>Table 8.</b> SHRIMP analytical results for zircon from sample 2004967003: banded biotite quartzofeldspathic augen gneiss, Tweed River. ....	51
<b>Table 9.</b> SHRIMP analytical results for zircon from sample 2004967004: Gibraltar quartz monzonite.....	58
<b>Table 10.</b> SHRIMP analytical results for zircon from sample 2004967007: biotite monzogranite dyke, Dinninup.....	64
<b>Table 11.</b> SHRIMP analytical results for zircon from sample 2004967009: biotite granite, Wilyungulup Spring. ....	72
<b>Table 12.</b> SHRIMP analytical results for zircon from sample 2004967550: biotite syenogranite dyke, Nanicip Bridge.....	77
<b>Table 13.</b> SHRIMP analytical results for zircon from sample 2004968001A: meta-psammite, Wheatley. ....	85
<b>Table 14.</b> SHRIMP analytical results for zircon from sample 2004969008: biotite granodiorite, Newlgalup. ....	92
<b>Table 15.</b> SHRIMP analytical results for zircon from sample 2002967002: biotite quartzofeldspathic gneiss, Moon Rock. ....	97
<b>Table 16.</b> SHRIMP analytical results for zircon from sample 2002967003: biotite quartzofeldspathic gneiss, Kirgella Rockhole.....	103
<b>Table 17.</b> SHRIMP analytical results for zircon from sample 2002967004: biotite monzogranite, Lords Bore.....	109
<b>Table 18.</b> SHRIMP analytical results for zircon from sample 2004967308: volcanic meta-sandstone, Kanowna Belle. ....	116
<b>Table 19.</b> SHRIMP analytical results for zircon from sample 2004967310: volcanic meta-sandstone, Kanowna Belle. ....	121
<b>Table 20.</b> SHRIMP analytical results for zircon from sample 2004967316: volcanic meta-sandstone, Kanowna Belle. ....	128
<b>Table 21.</b> SHRIMP analytical results for zircon from sample 2004967325: meta-dacite, Kanowna Belle. ....	135
<b>Table 22.</b> SHRIMP analytical results for zircon from sample 2004967366: meta-sandstone, Long Wong prospect. ....	142
<b>Table 23.</b> SHRIMP analytical results for zircon from sample 2004967367: volcanic meta-sandstone, Three-in-Hand prospect.....	151

<b>Table 24.</b> SHRIMP analytical results for zircon from sample 2004967369: porphyritic micro-diorite sill, Three-in-Hand prospect. ....	158
<b>Table 25.</b> SHRIMP analytical results for zircon from sample 2004967372: meta-conglomerate, Bee-Eater prospect. ....	163
<b>Table 26.</b> SHRIMP analytical results for zircon from sample 2004967377: Owen monzogranite. ....	168
<b>Table 27.</b> SHRIMP analytical results for zircon from sample 2004967500: meta-sandstone, Toppin Hill. ....	174
<b>Table 28.</b> SHRIMP analytical results for zircon from sample 2004967506: meta-rhyolite, Toppin Hill. ....	180

# Introduction

This Record contains zircon U-Pb geochronological data obtained between February 2004 and October 2006 on rocks from the Yilgarn Craton, Western Australia. Sampling locations are shown in Figures 1 to 3.

The data were collected as part of Geoscience Australia's Western Australia south-west gneiss terrane Pilot Project and the Predictive Mineral Discovery Co-operative Research Centre's Y2 and Y4 Projects. The results are helping meet the objective of providing an improved geological and metallogenic framework in the Yilgarn Craton and help provide geochronological constraints on geodynamic and tectonic models for the region.

The Record describes the analysed samples and data obtained from them, and provides brief discussion of their geochronological interpretation. The broader geological implications of the data will be published elsewhere. The complete data files are stored in the Geoscience Australia geochronology database, OZCHRON ([www.ga.gov.au](http://www.ga.gov.au)).



**Figure 1.** Location of Yilgarn Craton study areas detailed in [Figure 2](#) and [Figure 3](#).

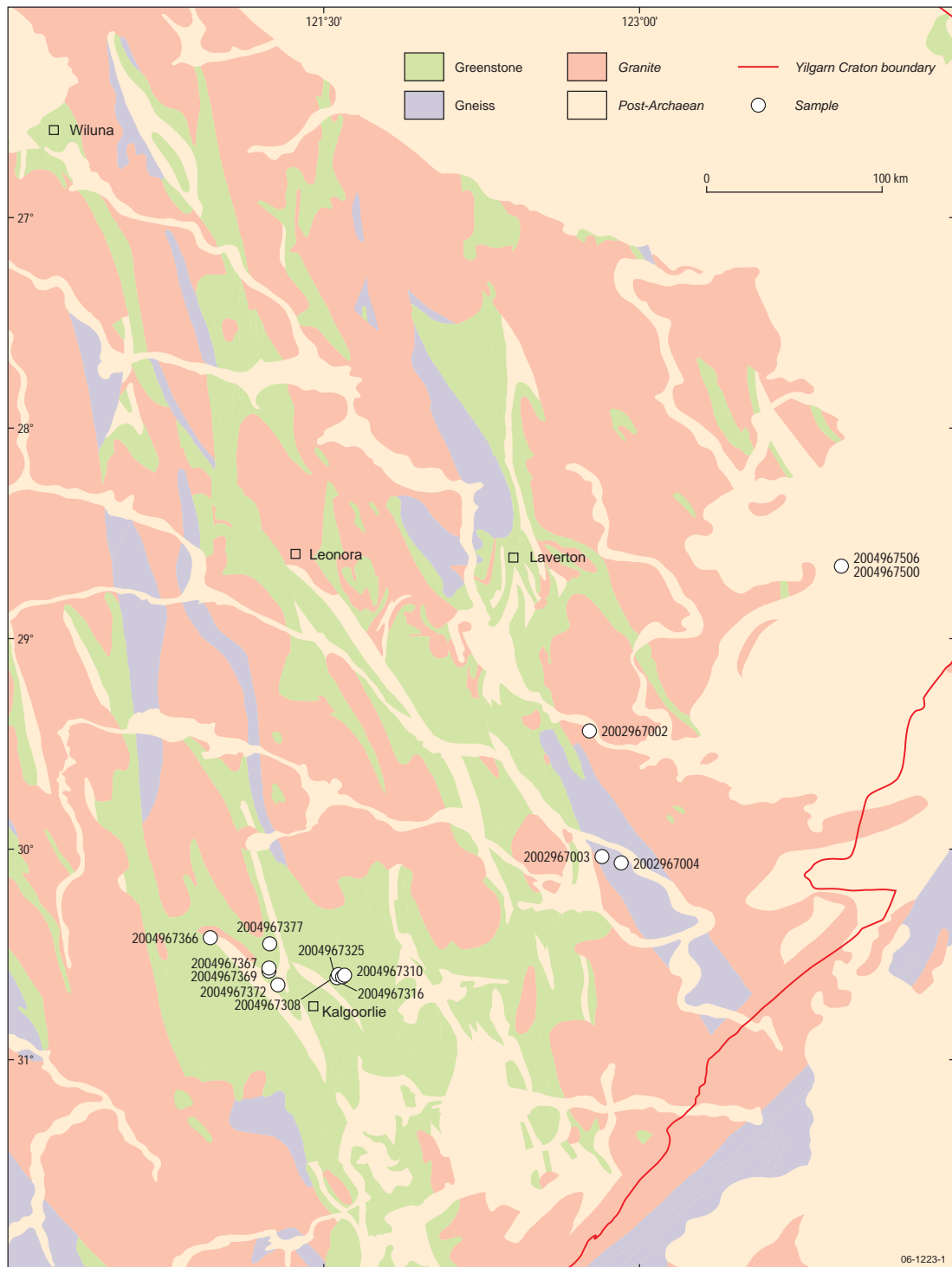


**Figure 2.** Approximate locations of samples from the Eastern Goldfields study area presented in this Record. The geology, towns and coastline are derived from Geoscience Australia's national geoscience database.



**Figure 3.** Approximate locations of samples from the southwest Yilgarn study area presented in this Record. The geology, towns and coastline are derived from Geoscience Australia's national geoscience database.

# Analytical procedures

## SAMPLE PROCESSING

Sampling involved the splitting of boulders to access fresh rock, although blasting of solid outcrop was required for some samples. Other samples were obtained from drillcore in collaboration with company geologists. The locations of field samples ( $\pm 50$  m) were determined using a hand-held GPS; drillcore collar locations were obtained from company data. Sample locations in this Record are referred to the Geocentric Datum of Australia 1994 (GDA94) through Map Grid Australia (MGA) coordinates, Zones 50 and 51.

At the field site, the rock was broken into fist-size fragments, having regard to cleanliness at all times, to avoid contamination of the sample. Typically, the sample weighed between 10 kg and 20 kg, sometimes more if a low zircon yield was suspected, but less if only drillcore was available. In the mineral separation lab at Geoscience Australia each rock was cleaned and broken down to 2–5 cm pieces using a pre-cleaned hydraulic splitter. The pieces were ultrasonically washed in water, dried under heat lamps and crushed using a jaw crusher or Rocklabs Boyd crusher. Milling used a Rocklabs Continuous Ring Mill.

For samples where magmatic age is the primary geochronological focus, zircon selection was biased towards the least magnetic, clearest grains, without discrimination between grain morphologies. The initial mineral-density separation was undertaken using a Wilfley table, reducing the sample to about 5% of its original weight. The highly magnetic grains were then removed using a hand magnet. A second density separation stage, using Tetrabromoethane (2.96 g/ml), was followed by magnetic separation using a Frantz isodynamic separator. The nonmagnetic fraction then went to a third density separation in Methylene Iodide (3.3 g/ml) and additional Frantz magnetic barrier separation. Where possible, approximately 100–150 zircon grains per sample were handpicked for mounting. For the metasedimentary samples, where zircon provenance is the main factor, zircons were hand-picked without discrimination from the heavy mineral concentrate.

The zircon grains were encapsulated in epoxy, together with similar quantities of zircon standards QGNG (Daly et al. 1998) or TEMORA (Black et al. 2003), and a small quantity of standard SL13 for composition calibration. The mounts were polished to expose grains in section, and all grains were photographed in transmitted and reflected light, and imaged by cathodoluminescence (CL) on a Hitachi S2250 NSEM located at the Australian National University.

All SHRIMP mounts were ultrasonically cleaned in petroleum spirit and a 10% Extran solution, triple rinsed in quartz-distilled water, and dried overnight at 30°C in an oven prior to coating with high-purity gold.

## DATA ACQUISITION FOR ZIRCON

SHRIMP analyses were undertaken on the SHRIMP-II instruments located at the John de Laeter Centre of Mass Spectrometry (JdL Centre), Curtin University of Technology, Perth, Western Australia and the SHRIMP-RG instrument in the Research School of Earth Sciences at the Australian National University, Canberra, using procedures developed from Compston et al. (1984). In general, attempts were



made to analyse examples of all identified grain types. To minimise potential surface contaminants, the ion probe  $O_2^-$  beam was rastered across the surface of the sample for 3 minutes prior to analysis. Data were acquired over seven scans through the mass sequence as listed in Table 1. The primary beam typically produced a 20–30  $\mu\text{m}$  elliptical spot with a beam strength of between 2 and 3 nA, although occasionally up to ~5 nA. The mass resolution at 1% peak height was typically 4,500 to 5,500 with secondary ion sensitivity on SL13 >15 cps/ppm Pb/nA.

This acquisition phase of the project coincided with two major events at the John de Laeter Centre of Mass Spectrometry. The first was the arrival of new SHRIMP-II instrument at the end of 2003 ('SHRIMP-B'). Some analyses are the product of sessions on this instrument early in 2004 while understanding of the instrument's nuances was still developing and, unfortunately, reflect their experimental nature in lower precision in some data. Eventually, SHRIMP-B proved to be a very reliable and stable analytical instrument, frequently reaching high levels of mass resolution, sensitivity and precision.

The second event was a major overall and upgrade of the older instrument, SHRIMP-A, which had been originally installed in 1994. Prior to this procedure in August and September 2004, instrument performance was frequently compromised by component failure and this is also reflected in the quality of some data.

Because of the early experimental nature of early SHRIMP-B sessions and scheduling to reduce exposure to poor performance on SHRIMP-A, most analytical sessions were over 24 hour periods. This is contrast to the previous geochronological compilations (Fletcher et al. 2001; Dunphy et al. 2003) which were typically over 48-hour periods.

**Table 1.** Standard run table for SHRIMP analyses in this project.

NOMINAL ATOMIC MASS	SPECIES	COUNT TIME (s)
196	$^{164}\text{Zr}^{16}\text{O}_2$	2
204	$^{204}\text{Pb}$	10
204.05	Background	10
206	$^{206}\text{Pb}$	10
207	$^{207}\text{Pb}$	40
208	$^{208}\text{Pb}$	10
238	$^{238}\text{U}$	5
248	$^{232}\text{Th}^{16}\text{O}$	5
254	$^{238}\text{U}^{16}\text{O}$	2

#### DATA REDUCTION FOR ZIRCON

QGNG and TEMORA were used for calibration of U/Pb and SL13 for U content (238 ppm U; Claoue-Long et al. 1995). The reference  $^{206}\text{Pb}/^{238}\text{U}$  age for QGNG, determined by replicate analyses using thermal ionisation mass spectrometry (TIMS) is  $1842.0 \pm 3.1$  Ma (Black et al. 2003). Note that this is a revised value that differs very slightly from previous reports (Fletcher et al. 2001; Dunphy et al. 2003), but will only have a trivial impact on comparing ages between reports.

Data reduction used SQUID 1.1 (Ludwig 2002). Where appropriate, the canonical value of 2.0 has been used as the slope of the  $\ln[\text{Pb}/\text{U}]:\ln[\text{UO}/\text{U}]$  calibration line (Claoue-Long et al. 1995). In some cases a different value for the slope has been sufficiently well-established to justify its use.

Common-lead in the calibration standards is assumed to be surface contaminant and thus corrections were based on the isotopic composition of atmospheric lead in Perth, Western Australia which differs very slightly from the previously assumed Broken Hill galena composition<sup>1</sup>. For the standard QGNG, corrections were based on measured <sup>204</sup>Pb and for TEMORA corrections were based on measured <sup>207</sup>Pb. Samples were corrected using <sup>204</sup>Pb measurements and an isotopic composition calculated using the Stacey and Kramers lead isotopic evolution model (Stacey and Kramers 1975) based on the <sup>207</sup>Pb/<sup>206</sup>Pb age of the sample. This method is the default in the SQUID data reduction package. This differs from previous reports which used the isotopic composition of Broken Hill galena in sample corrections. However, data are only used for age determinations if the common-Pb component is sufficiently small that corrections of the <sup>207</sup>Pb/<sup>206</sup>Pb ratio and age are insensitive to the choice of common-Pb composition (particularly in the Archaean age range). Analyses requiring large corrections are typically discordant and presumed to have experienced some open-system disturbance making their interpretation unreliable.

## DATA PRESENTATION

All tabulated data are common-Pb corrected. Assuming zero-age Pb-loss, discordance is calculated as:

$$Disc. = \left( 1 - \frac{{}^{206}Pb / {}^{238}U \text{ age}}{{}^{207}Pb / {}^{206}Pb \text{ age}} \right) \times 100 \quad (1)$$

This equation is fundamentally different from the default method used in SQUID 1.1 and is thus calculated independently. The concordance value (simply  $100 - \text{discordance}$ ) was used in previous reports (Fletcher et al. 2001; Dunphy et al. 2003).

Data from individual analyses are shown in Tera-Wasserburg concordia plots (Tera and Wasserburg 1972) at  $\pm 1\sigma$  precision. The errors in Tera-Wasserburg concordia plots have minimal correlation so better illustrate sample complexity than Wetherill-style concordia plots (Wetherill 1956) where the errors are often highly correlated and thus produce elongated ellipses and visually crowded plots (Figure 4).

---

<sup>1</sup> In the previous reports of Fletcher et al. (2001) and Dunphy et al. (2003), common-Pb contamination was assumed to be largely derived from the deposition of airborne alkyllead pollution manufactured from Broken Hill lead ore. The isotopic composition was approximated by a Stacey and Kramers single-stage Pb-evolution model at 1600 Ma (<sup>206</sup>Pb/<sup>204</sup>Pb: 15.959, <sup>207</sup>Pb/<sup>206</sup>Pb: 0.962, <sup>208</sup>Pb/<sup>206</sup>Pb: 2.230). The Pb-isotopic composition of aerosols in Perth, Western Australia, is actually slightly more radiogenic, reflecting the contribution of alkyllead in Western Australian fuel sourced from Singaporean petrol refineries (<sup>206</sup>Pb/<sup>204</sup>Pb:  $16.64 \pm 0.04$ , <sup>207</sup>Pb/<sup>206</sup>Pb:  $0.926 \pm 0.001$ , <sup>208</sup>Pb/<sup>206</sup>Pb:  $2.181 \pm 0.002$ ; Bollhöfer and Rosman, 2000).



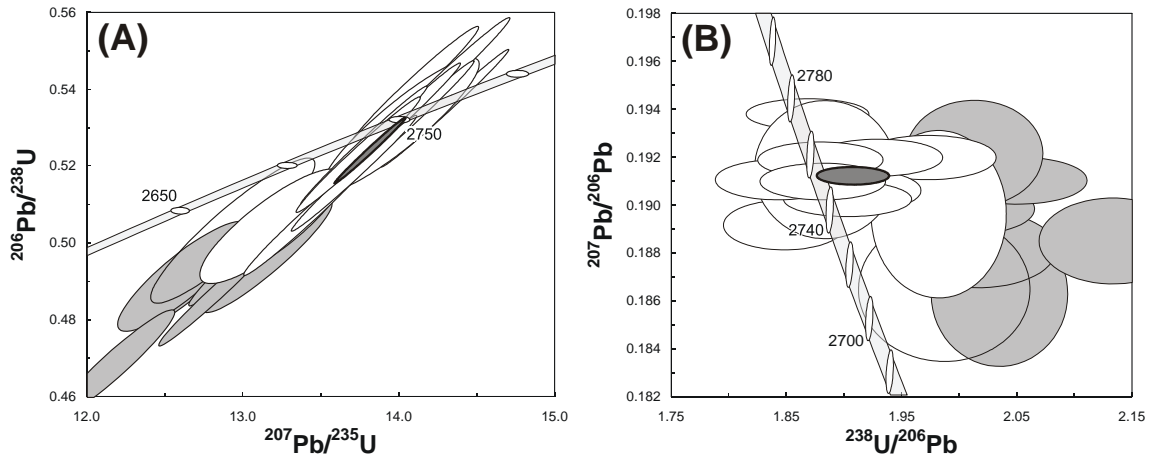


**Figure 4.** An illustration of the difference between (A) a conventional Wetherill concordia plot with highly correlated error ellipses and (B) a Tera-Wasserburg concordia plot with no error correlation.

The graphical interpretations possible in a Wetherill concordia plots are also available in a Tera-Wasserburg plot with slight modifications as illustrated in Figure 5.

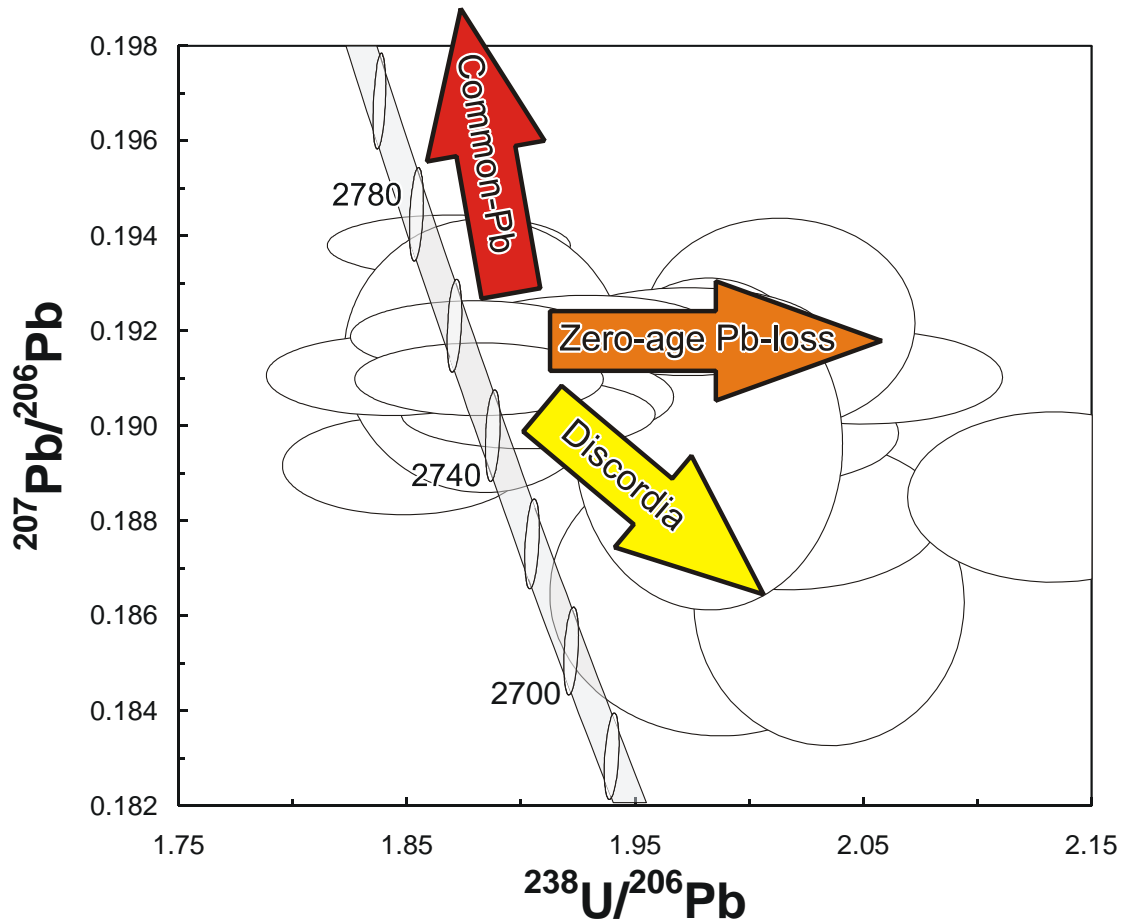


**Figure 5.** Tera-Wasserburg concordia plot illustrating potential graphical interpretation of the dispersion of plotted results. Zero-age Pb-loss is revealed by dispersion parallel to the x-axis. Ancient discordia chords (e.g. ancient Pb-loss or resetting) will be seen as dispersion toward the lower-right. Any mixing with common-Pb can be seen as dispersion toward the upper-left.

The concordia plots are also shown with a ‘band’ representing concordia rather than a single line. This reflects the uncertainties in the measurements of the uranium isotope decay constants as recommended by (Ludwig 2000). A further innovation is plotting zero-age discordance lines on the concordia plot at -5%, 1%, 2%, 3%, 4% and 5% intervals (Figure 6). It should be noted that these lines only represent discordance calculated assuming zero-age Pb-loss (see previous formula) and thus have no relevance to discussion of discordance due to ancient Pb-loss events.

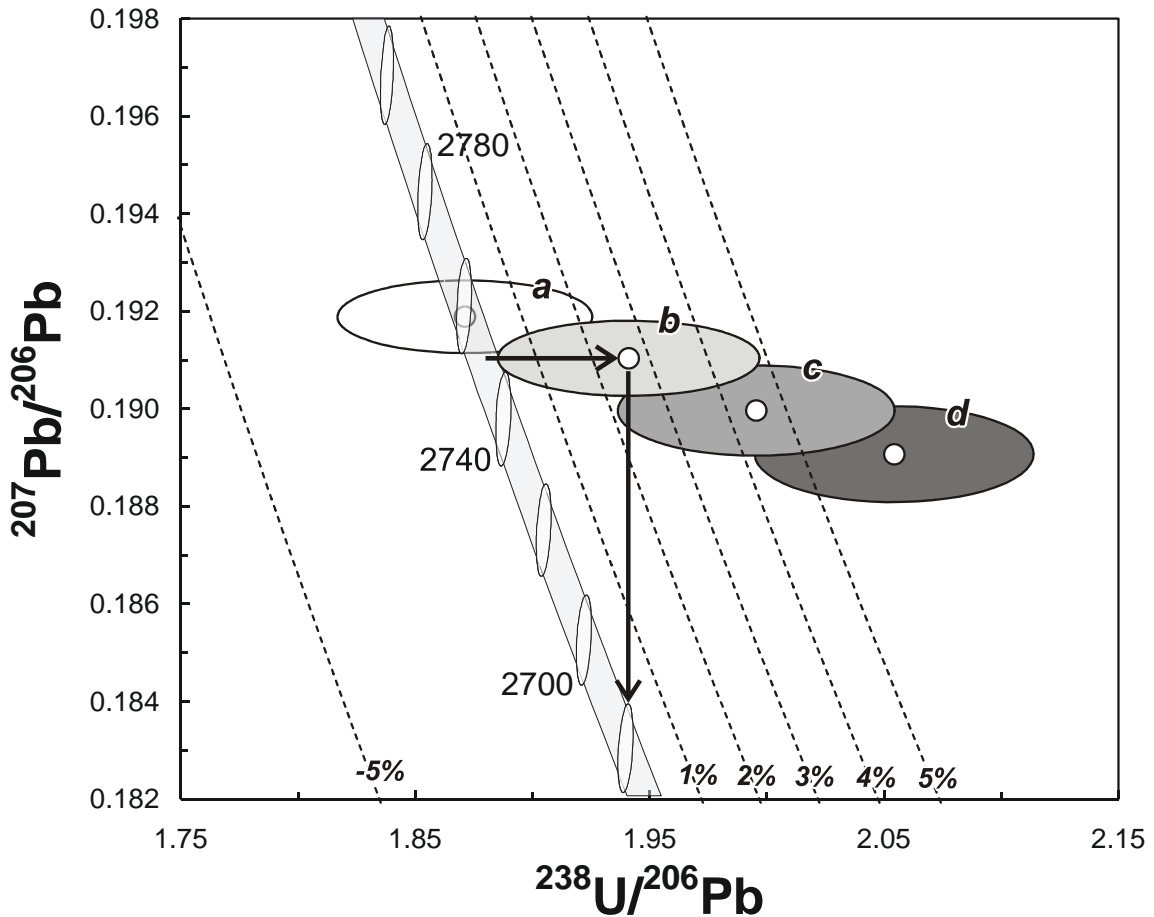


**Figure 6.** Concordia plot illustrating the concept of zero-age discordance lines. Analysis (a) is concordant; analysis (b) is ~2.5% discordant, i.e.  $^{207}\text{Pb}/^{206}\text{Pb}$  age is 2750 Ma, and assuming zero-age Pb-loss the  $^{206}\text{Pb}/^{238}\text{U}$  age is 2680 Ma, the difference of 70 Myr is ~2.5% of the  $^{207}\text{Pb}/^{206}\text{Pb}$  age; analysis (c) is 4.5% discordant; analysis (d) is >5% discordant. Analyses are typically discarded from further interpretation at -5% and +5% discordance.

After filtering during data-processing explained below, there are two methods for calculating a single age from the data. The simplest is the weighted mean  $^{207}\text{Pb}/^{206}\text{Pb}$  ages determined from grouped data, although this method assumes concordance. The second method is the ‘Concordia Age’ (Ludwig 1998) which uses two dimensions of data (e.g.  $^{207}\text{Pb}/^{206}\text{Pb}$  and  $^{206}\text{Pb}/^{238}\text{U}$ ) to calculate a weighted mean age and provide a quantitative test of the assumption of concordance. Both weighted mean values are given in the text with 95% confidence levels.

For samples containing a range of ages where resolving individual age components cannot be done objectively (typically, although not exclusively, detrital samples), a

mixture modelling approach is used based on the algorithm of Sambridge and Compston (1994). This method estimates the most likely ages and proportions in a set of age data although it should be carefully noted that results are models of the age distribution rather than ‘absolute’ determined ages and need to be treated with caution in further interpretation.

The final ages are rounded off to integers and the corresponding uncertainties are rounded up to cover the range that is required by additional decimal places (e.g.  $2660.2 \pm 5.2$  Ma rounds to  $2660 \pm 6$  Ma).

### CONCORDIA CONTOUR DIAGRAMS

The salient features of a U-Pb concordia diagram (e.g. Wetherill style:  $^{206}\text{Pb}/^{238}\text{U}$  vs.  $^{207}\text{Pb}/^{235}\text{U}$  or Tera-Wasserburg style  $^{238}\text{U}/^{206}\text{Pb}$  vs.  $^{207}\text{Pb}/^{206}\text{Pb}$ ) such as local modes and relative discordance are frequently obscured in diagrams based on large sets of data. Simplifying and plotting the data as univariate ages can aid interpretation, but the discordance filtering of such data is arbitrary. A new approach has been used where the individual analyses are treated as bivariate normal distributions and their values are summed across an x-y grid to produce a 3-dimensional probability distribution (Sircombe 2006). This distribution can then be contoured and colour-mapped to illustrate features relevant to a concordia line (Figure 7). This approach, as is frequently demonstrated in this Record, can greatly aid the visualisation and interpretation of complex sets of geochronological data.

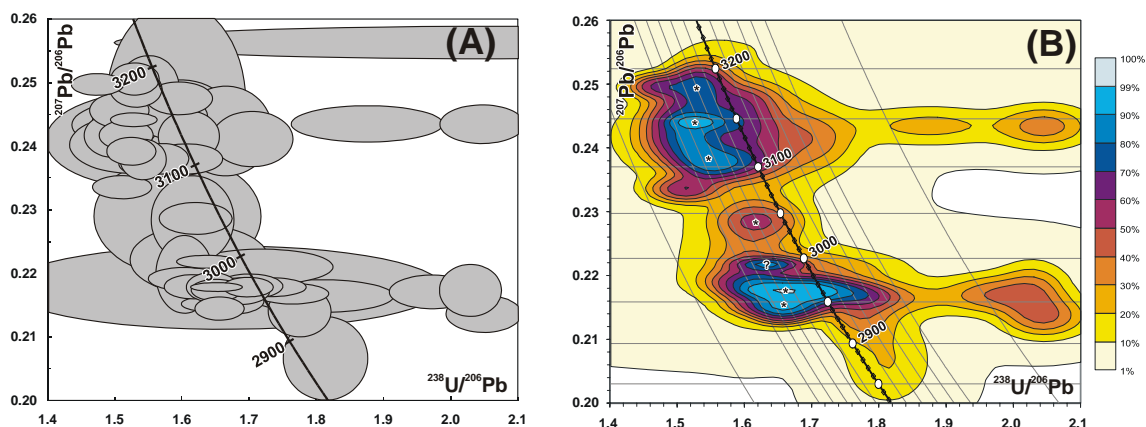


**Figure 7.** Illustration of concordia contour diagrams (from Sircombe 2006). A) Tera-Wasserburg diagram with analyses represented by conventional error ellipses and illustrating the visual clutter caused by large volumes of geochronological data in complex samples. B) The equivalent concordia contour diagram to (A) where the bivariate normal distributions represented by the error ellipses have been summed to produced an overall distribution which has been contoured to illustrate distinct modes and relationships.

## Part 1: Southwest Yilgarn

### 2003967051: biotite granodiorite, Nippering Quarry

#### SAMPLE INFORMATION

**1:250,000 sheet:** Dumbleyung (SI5007)

**1:100,000 sheet:** Dumbleyung (2431)

**MGA:** 557699 mE 6316491 mN

**Location:** Sample taken from the northwest wall of the Nippering quarry, 11 kms west of Dumbleyung.

**Description:** This rock is a variably foliated, grey, seriate to variably feldspar-porphyritic, medium-grained biotite granodiorite. It forms part of a complex series of biotite granite phases that intrude nebulitic quartzofeldspathic migmatite, garnet-cordierite-biotite- and clinopyroxene-biotite-bearing quartzofeldspathic gneiss and minor amphibolite. The granodiorite phase is cut by several, light grey, biotite monzogranite phases and all phases are intruded by pegmatite veins and sub-vertical Proterozoic dolerite dykes.

The sample is characterised by a granular texture. Principal minerals are quartz (35%), K-feldspar (30%), plagioclase (25%) and biotite (8-10%), with K-feldspar $\approx$ plagioclase. Accessory phases include trace titanite, apatite, monazite, zircon, fluorite, pyrrhotite and anhedral opaque minerals. The rock contains minor myrmekitic quartz-plagioclase and quartz-biotite intergrowth. The rock is very weakly recrystallised with quartz displaying minor undulose extinction, deformation lamellae and rare subgrains. Alteration is limited to weak to moderate saussuritization of plagioclase by white mica, clinoziosite/epidote, and moderate replacement of biotite by chlorite, epidote, opaque minerals and white mica.

#### DESCRIPTION OF ZIRCONS

**Shape:** Subhedral grains with moderate rounding of crystal faces (Figure 8).

**Size:** 50 to 100 microns.

**Colour/clarity:** Colourless and clear.

**Quality:** Fair to good. Frequent fractures and inclusions.

**CL zoning:** Prominent concentric zoning with occasional complex embayments (Figure 8).



#### CONCURRENT STANDARD DATA

**Pb/U reprod.(2s):** 1.1%

**Err. of mean (2s):** 2.7%

**Standard:** TEMORA

**Analyses:** 12

**Notes:** The TEMORA standard was used on this sample as part of development trials early in this phase of the project. QGNG was also analysed concurrently to monitor  $^{207}\text{Pb}/^{206}\text{Pb}$  ratios. The Pb/U calibration slope is non-default at 1.66. The scatter most probably reflects poor instrument stability on SHRIMP-A and the resulting errors should be propagated through the unknowns. Although this large error will contribute to  $^{206}\text{Pb}/^{238}\text{U}$  age errors it will have no impact on  $^{207}\text{Pb}/^{206}\text{Pb}$  ages which are used here.

#### SAMPLE DATA

Twenty-nine analyses were made on twenty-nine grains (Table 2). Fifteen of the analyses are >5% discordant although these analyses produce a good discordia chord and concordia intercepts at  $2668 \pm 13$  Ma and  $843 \pm 27$  Ma (MSWD: 5.6) (Figure 9). The lower intercept value clearly indicates a non-zero age Pb-loss event.

Discarding two outliers from the concordant analyses, one possibly inherited with a notably high Th content and one possibly indicative of Pb-loss (#10.1 and #16.1 respectively) yields a concordia age of  $2661.9 \pm 9.9$  Ma (95% conf.; MSWD: 3.9; prob. conc. 0.05). The high MSWD and low probability of concordance would suggest that this age may be affected by a minor ancient Pb-loss event and should be treated with caution.



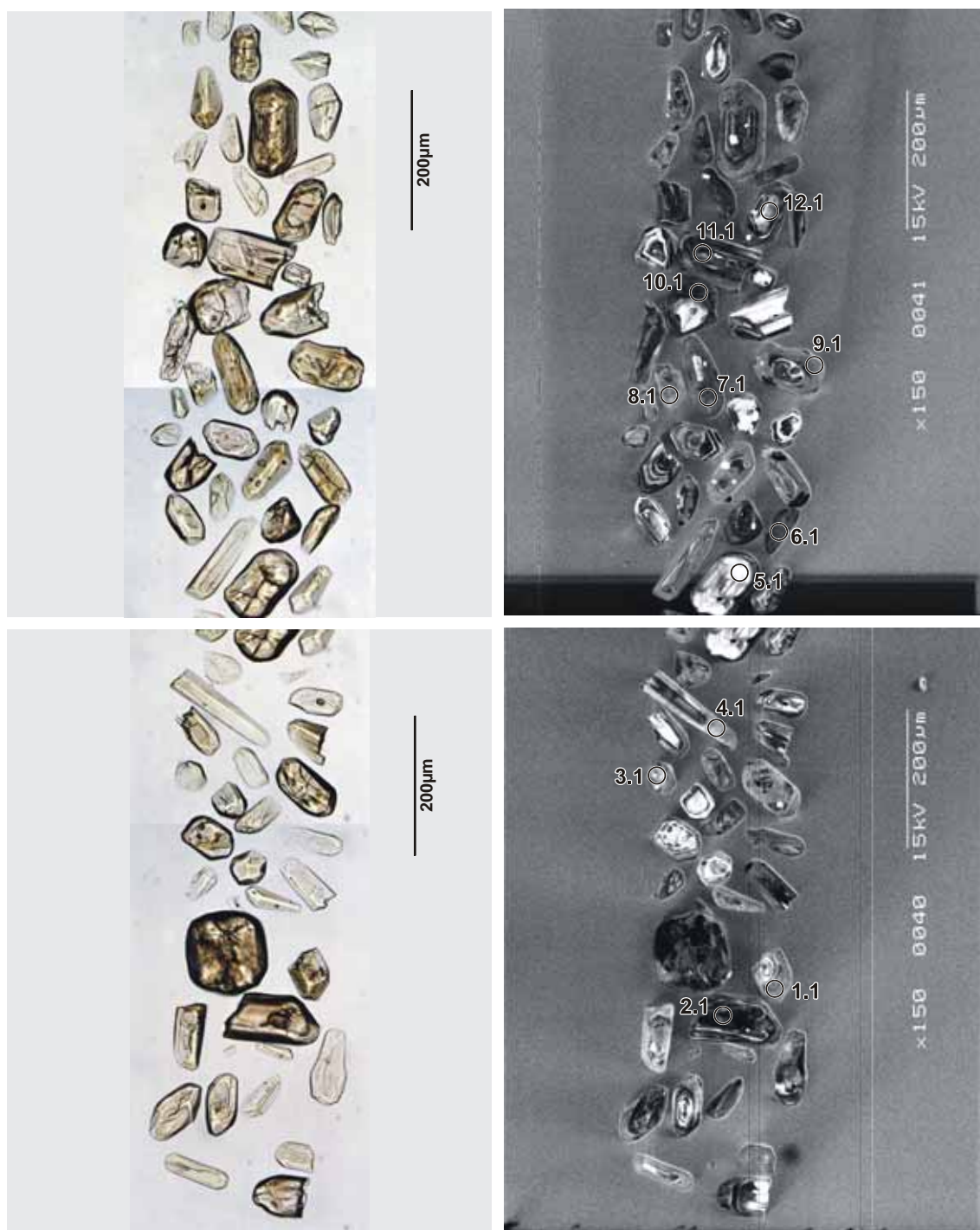


**Figure 8.** Representative images (transmitted light on left, cathodoluminescence on right) for sample 2003967051: biotite granodiorite, Nippering Quarry. SHRIMP analysis spots are labelled.

#### GEOCHRONOLOGICAL INTERPRETATION

The magmatic age of the granodiorite is tentatively interpreted as  $2662 \pm 10$  Ma and the zircons have been strongly influenced by a Neoproterozoic Pb-loss event.



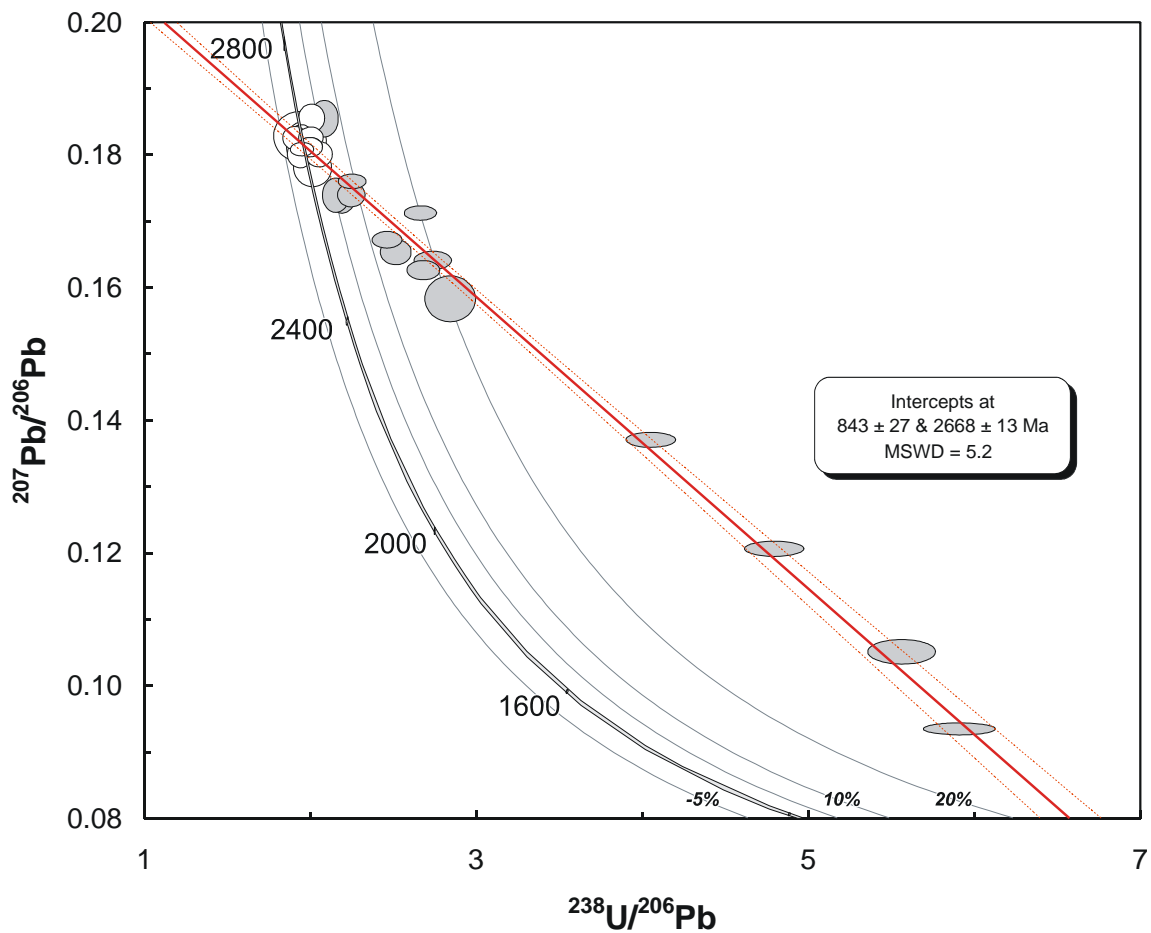


**Figure 9.** Tera-Wasserburg concordia plot for zircons from sample 2003967051: biotite granodiorite, Nippering Quarry. White-filled symbols are used to define the age of the sample; discordant and/or high common-Pb analyses are light grey.

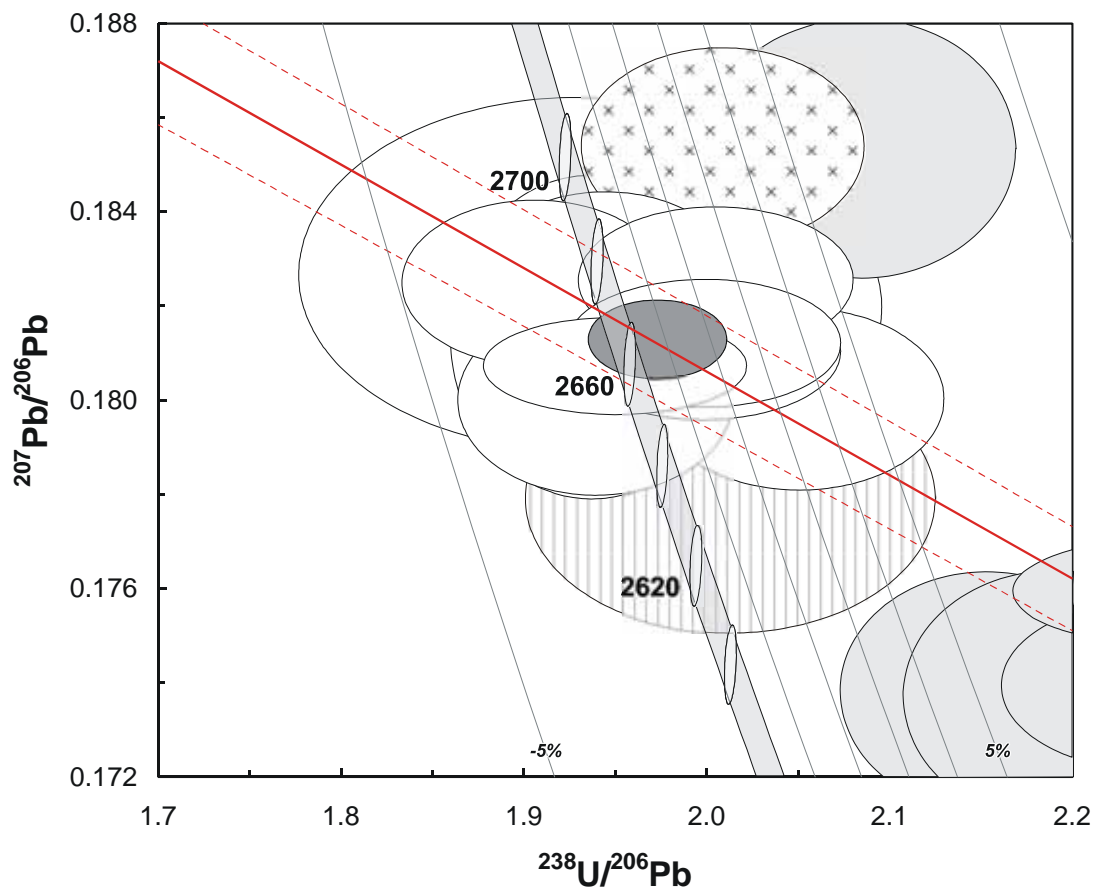


**Figure 10.** Tera-Wasserburg concordia plot for zircons from sample 2003967051: biotite granodiorite, Nippering Quarry. White-filled symbols are used to define the age of the sample; dark grey ellipse indicates concordia age; cross-hatch fill indicates possible inheritance; vertical hatch fill indicates possible Pb-loss; discordant and/or high common-Pb analyses are light grey.

Table 2. SHRIMP analytical results for zircon from sample 2003967051: biotite granodiorite, Nippering Quarry.

Grain. Spot	U (ppm)	Th (ppm)	% comm 206	<sup>207</sup> Pb / <sup>206</sup> Pb	±	<sup>206</sup> Pb / <sup>238</sup> U	±	<sup>207</sup> Pb / <sup>235</sup> U	±	% Disc.	<sup>207</sup> Pb / <sup>206</sup> Pb Age (Ma)	±
<i>Main</i>												
24.1	211	203	0.043	0.1800	0.0008	0.5157	0.0082	12.8006	0.2118	-1.1	2653.0	7.7
3.1	313	262	0.020	0.1800	0.0008	0.4875	0.0077	12.1022	0.1973	3.5	2653.2	7.3
18.1	198	197	-0.044	0.1807	0.0008	0.5007	0.0082	12.4777	0.2117	1.6	2659.7	7.7
4.1	1437	94	0.004	0.1807	0.0004	0.5129	0.0077	12.7817	0.1951	-0.3	2659.7	3.9
26.1	412	283	-0.016	0.1810	0.0006	0.5005	0.0077	12.4944	0.1965	1.7	2662.5	5.4
17.1	575	65	0.011	0.1812	0.0006	0.5003	0.0076	12.5018	0.1949	1.8	2664.1	5.1
12.1	199	202	-0.046	0.1814	0.0014	0.5163	0.0084	12.9098	0.2338	-0.7	2665.3	12.9
5.1	96	75	-0.009	0.1820	0.0012	0.4971	0.0085	12.4711	0.2280	2.6	2670.9	10.8
2.1	563	423	0.007	0.1825	0.0007	0.5246	0.0082	13.2024	0.2128	-1.6	2675.8	6.6
25.1	837	540	-0.042	0.1826	0.0008	0.5141	0.0078	12.9414	0.2039	0.1	2676.4	7.0
11.1	448	418	0.001	0.1826	0.0006	0.4988	0.0077	12.5559	0.1978	2.5	2676.5	5.8
28.1	551	438	-0.009	0.1827	0.0015	0.5184	0.0168	13.0582	0.4370	-0.5	2677.6	13.9
<i>Pb-loss?</i>												
10.1	422	269	-0.012	0.1779	0.0012	0.4968	0.0113	12.1861	0.2889	1.3	2633.5	11.0
<i>Inheritance? High Th</i>												
16.1	371	832	-0.075	0.1854	0.0009	0.4978	0.0079	12.7275	0.2097	3.6	2702.0	7.6
<i>Discordant</i>												
7.1	1507	72	0.021	0.0931	0.0004	0.1690	0.0025	2.1694	0.0337	32.4	1489.5	7.5
13.1	1557	67	-0.029	0.1048	0.0008	0.1795	0.0027	2.5930	0.0432	37.8	1710.3	13.3
6.1	1272	96	0.010	0.1203	0.0005	0.2084	0.0031	3.4576	0.0539	37.8	1961.4	6.9
9.1	1337	83	-0.038	0.1368	0.0005	0.2464	0.0037	4.6500	0.0718	35.1	2187.7	5.9
8.1	1193	188	0.019	0.1582	0.0014	0.3518	0.0077	7.6708	0.1809	20.2	2436.1	15.4
1.1	542	110	0.067	0.1625	0.0006	0.3727	0.0057	8.3498	0.1311	17.7	2481.6	6.4
21.1	631	528	-0.046	0.1640	0.0006	0.3652	0.0062	8.2569	0.1440	19.6	2497.1	5.8
19.1	1059	198	0.000	0.1652	0.0008	0.3975	0.0060	9.0565	0.1437	14.0	2510.1	8.0
20.1	776	867	-0.039	0.1671	0.0005	0.4059	0.0062	9.3499	0.1449	13.2	2528.7	5.0
27.1	1274	116	0.012	0.1711	0.0005	0.3755	0.0057	8.8594	0.1356	20.0	2568.8	4.5
15.1	455	472	-0.019	0.1737	0.0011	0.4567	0.0070	10.9401	0.1815	6.5	2593.9	10.4
22.1	709	700	0.000	0.1738	0.0010	0.4644	0.0071	11.1300	0.1817	5.2	2594.7	9.9
29.1	796	825	0.050	0.1739	0.0007	0.4455	0.0068	10.6834	0.1683	8.5	2595.8	7.1
14.1	1090	281	0.021	0.1759	0.0005	0.4442	0.0067	10.7743	0.1658	9.4	2614.8	4.3
23.1	97	80	-0.220	0.1854	0.0011	0.4798	0.0080	12.2640	0.2183	6.5	2701.7	10.1

Data are at 1σ precision. All Pb data are common-Pb corrected based on <sup>204</sup>Pb measurements. Mount: Z3581; Instrument: JdL Centre SHRIMP-A; Acquisition: 27 April 2004.



## 2003967056: biotite syenogranite, Blackburn Mine

### SAMPLE INFORMATION

**1:250,000 sheet:** Dumbleyung (SI5007)

**1:100,000 sheet:** Katanning (2430)

**MGA:** 584189 mE 6288395 mN

**Location:** This sample was taken from outcrop about 10 m below ground level in the northwest corner of Blackburn open-pit at Jinkas Hill, about 10km north of Badgebup Siding.

**Description:** This rock is a light grey-green-pink, foliated to banded, seriate to sparsely K-feldspar-porphyrific, fine-coarse grained biotite syenogranite. It is the least-altered main phase of a series of gently east-dipping, strongly foliated and variably altered syenogranite sheet-like bodies that intrude a succession of highly-deformed (isoclinally folded, strongly lineated) biotite amphibolite and meta-sedimentary rocks. Coarse-grained pegmatitic and biotite-poor and biotite-rich syenogranitic layers give the rock a banded appearance. The intrusions are variably altered and contain quartz-plagioclase-pyroxene-sulfide (molybdenite, chalcopyrite) veins away from the sample site. At the sample site, the rock is cut by minor, thin quartz-plagioclase-pyroxene layers.

The sample is characterised by a granular to granoblastic texture. Principal minerals are quartz (30%), K-feldspar (35-40%), plagioclase (20%), pyroxene (5-8%) and biotite (5-8%), with K-feldspar > plagioclase. K-feldspar, dominantly microcline, forms phenocrysts to 2 cm in length. Hypersthene and clinopyroxene (diopside) are both present and are subhedral to anhedral. Accessory phases include trace apatite, zircon and anhedral opaque minerals. The rock has minor myrmekitic quartz-biotite and quartz-plagioclase intergrowth. The rock is weakly recrystallised with quartz displaying weak to moderate subgrain development and deformation lamellae and, in places, biotite is strongly aligned. Quartz-plagioclase-pyroxene forms bands and veins up to several cm thick. Alteration is limited to weak to moderate saussuritization of plagioclase by white mica/muscovite and epidote, variable replacement of pyroxene by chlorite, actinolite and sericite, and moderate replacement of biotite by chlorite, epidote, opaque oxides and muscovite.

### DESCRIPTION OF ZIRCONS

**Shape:** Generally stubby, well rounded grains with only occasional euhedral crystal faces ([Figure 11](#)).

**Size:** ~50 - ~100 microns



**Colour/clarity:** Colourless to pale brown  
**Quality:** Frequent cracks and inclusions  
**CL zoning:** Strong concentric zoning with frequent complex embayments and occasional bright rims too narrow to analyse (Figure 11).

#### CONCURRENT STANDARD DATA

**Pb/U reprod.(2s):** 2.5%  
**Err. of mean (2s):** 0.8%  
**Standard:** TEMORA  
**Analyses:** 14 (one discarded with high common-Pb)  
**Notes:** Reproducibility of Pb/U ratios is reasonable.

#### SAMPLE DATA

Thirty-three analyses were made on thirty-three grains (Table 3). Five analyses are > 5% discordant, and the remaining analyses are generally concordant with ages well scattered between ~2550 Ma and ~2680 Ma with no statistically plausible single population (Figure 12 and Figure 13). The U and Th content of the analysed grains are remarkably high with median values of 1186 and 954 ppm respectively. However, there is no apparent correlation with age and Th/U content. Analyses targeted at zircons with bright CL patterns associated with rims also have a wide range of ages. One younger age (#1.1) – also the analysis with the highest U content of 3009 ppm – is suggestive of Pb-loss but there is no apparent discordia chord.



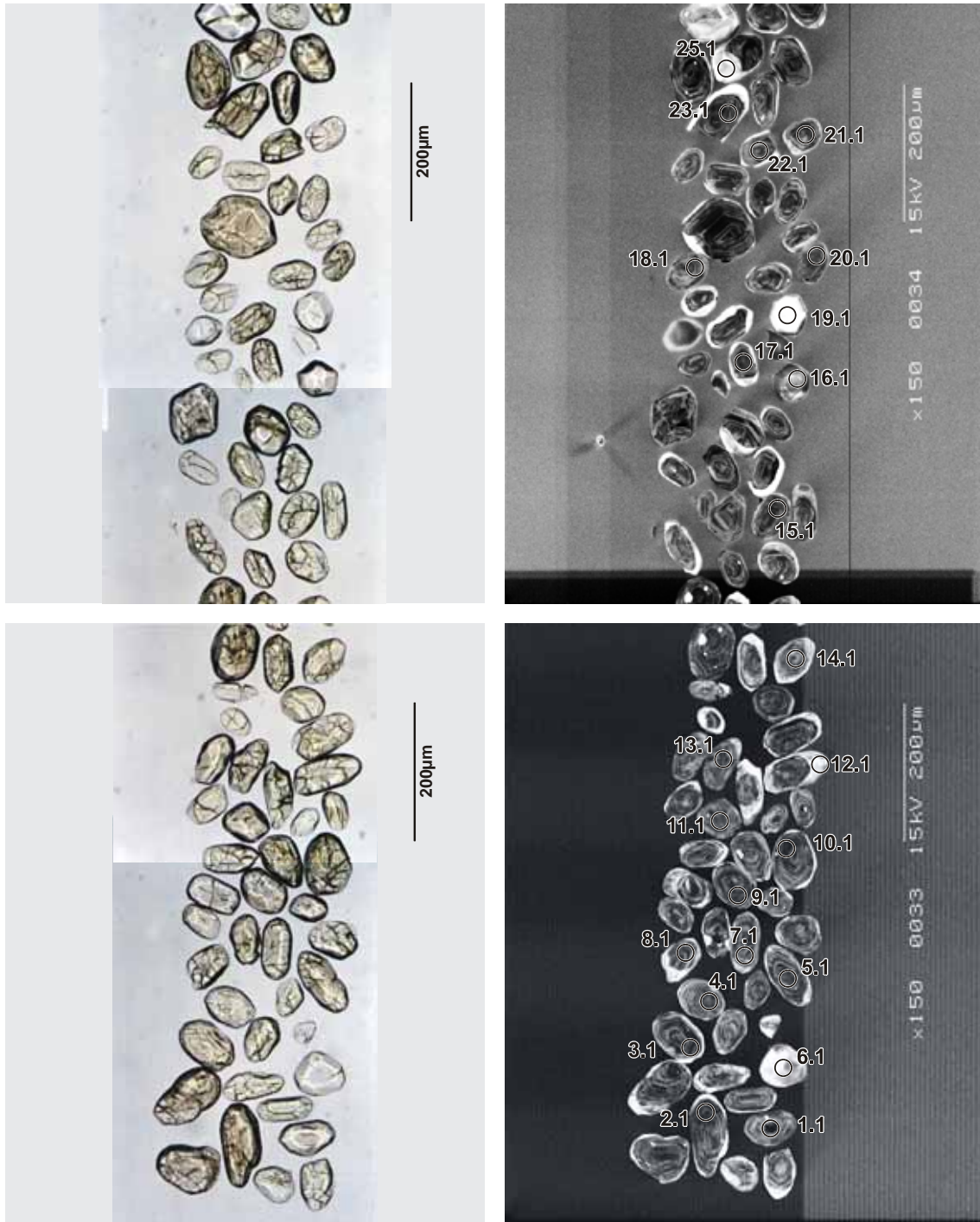


**Figure 11.** Representative images (transmitted light on left, cathodoluminescence on right) for sample 2003967056: biotite syenogranite, Blackburn Mine. SHRIMP analysis spots are labelled.

### GEOCHRONOLOGICAL INTERPRETATION

There are two possible interpretations of these data.

The first interpretation is that the ages represent a mixed provenance in the original protolith to the monzogranite. The generally rounded zircon shape could be interpreted as indicative of a detrital origin, although that scenario requires a later magmatic phase without significant zircon growth.

The second interpretation is that the ages represent the formation of igneous high-U zircon ~2670 Ma, but the rock was subject to continuing high temperature for tens of millions of years that resulted in Pb diffusion seen as an indistinct discordia chord or smearing along concordia. The complexity of the zircon growth patterns seen in CL imaging could indicate a series of high-temperature events whose effect on the U-Pb isotopic values was further exaggerated by high U content.

The second scenario is more likely, but the data preclude an accurate assessment of the original age of zircon formation.

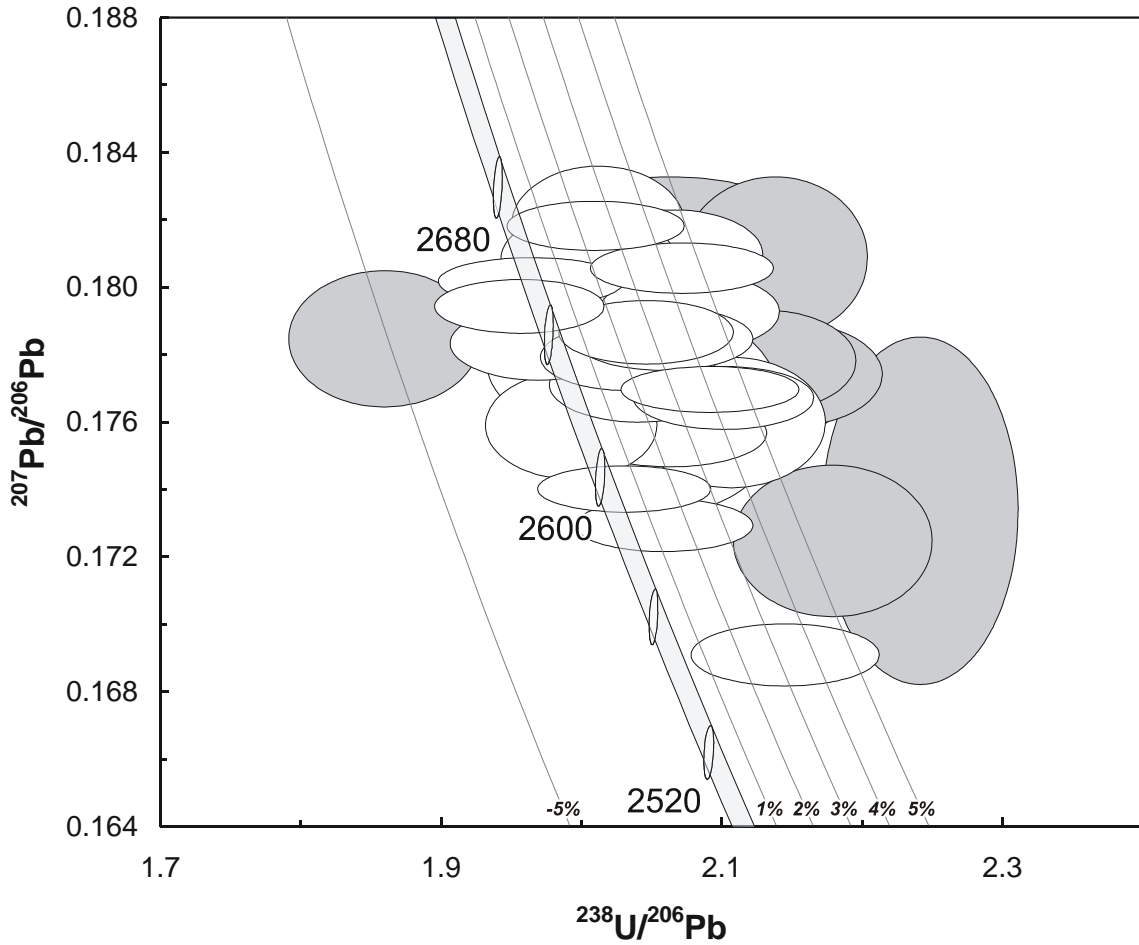


**Figure 12.** Tera-Wasserburg concordia plot for zircons from sample 2003967056: biotite syenogranite, Blackburn Mine. White-filled symbols are used to define the age of the sample; discordant and/or high common-Pb analyses are light grey.

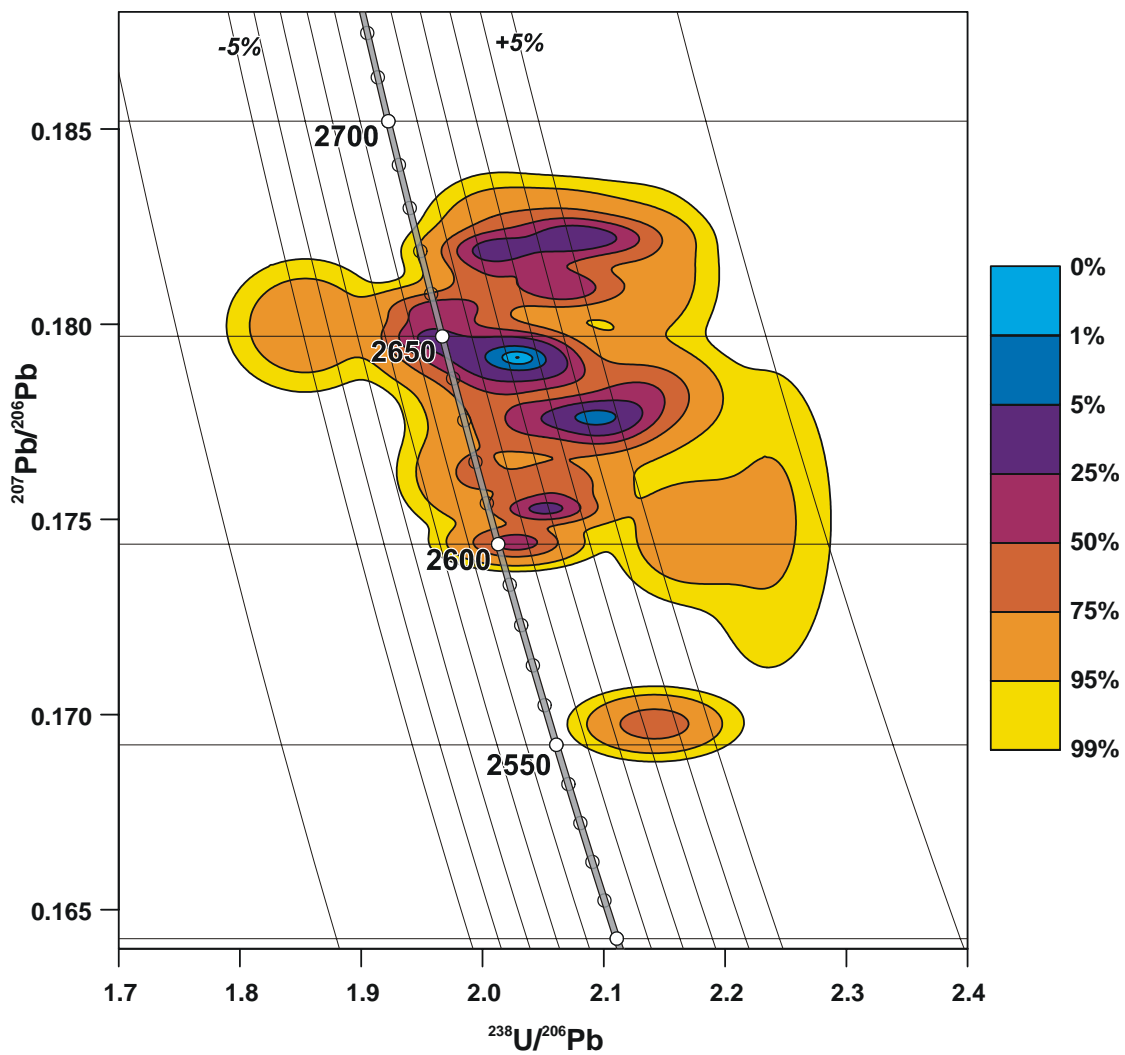


**Figure 13.** Tera-Wasserburg concordia contour plot of sample 2003967056: biotite syenogranite, Blackburn Mine illustrating the smearing of isotopic values.

**Table 3.** SHRIMP analytical results for zircon from sample 2003967056: biotite syenogranite, Blackburn Mine.

Grain. Spot	U (ppm)	Th (ppm)	% comm 206	$^{207}\text{Pb}$ $/^{206}\text{Pb}$	$\pm$	$^{206}\text{Pb}$ $/^{238}\text{U}$	$\pm$	$^{207}\text{Pb}$ $/^{235}\text{U}$	$\pm$	% Disc.	$^{207}\text{Pb}$ $/^{206}\text{Pb}$ Age (Ma)	$\pm$
<i>Protolith ages?</i>												
1.1	3009	2211	0.073	0.1691	0.0004	0.4666	0.0060	10.8785	0.1420	3	2548.8	3.8
31.1	2081	1893	0.257	0.1730	0.0003	0.4862	0.0061	11.5936	0.1466	1	2586.4	3.1
24.1	1471	1324	0.042	0.1740	0.0003	0.4930	0.0062	11.8308	0.1495	1	2596.8	2.7
13.1	1186	784	0.020	0.1757	0.0004	0.4853	0.0067	11.7548	0.1640	2	2612.5	3.9
23.1	1493	1264	0.030	0.1759	0.0006	0.5024	0.0063	12.1854	0.1592	0	2614.8	6.1
17.1	968	629	0.201	0.1760	0.0008	0.4751	0.0062	11.5292	0.1580	4	2615.5	7.4
19.1*	107	77	0.123	0.1763	0.0012	0.4846	0.0075	11.7806	0.1990	3	2618.6	11.4
29.1	1527	1415	0.065	0.1767	0.0004	0.4763	0.0060	11.6057	0.1475	4	2622.4	3.6
15.1	1238	965	0.601	0.1768	0.0006	0.4722	0.0062	11.5140	0.1559	5	2623.4	5.5
20.1	1638	1519	0.077	0.1770	0.0003	0.4786	0.0060	11.6783	0.1469	4	2624.8	2.6
9.1	1227	918	0.039	0.1771	0.0005	0.4908	0.0062	11.9862	0.1546	2	2626.1	4.3
26.1*	236	298	0.053	0.1778	0.0008	0.5006	0.0069	12.2743	0.1793	1	2632.8	7.7
18.1	1477	1274	0.138	0.1780	0.0004	0.4922	0.0063	12.0762	0.1561	2	2633.9	3.8
21.1	989	417	0.098	0.1783	0.0004	0.5083	0.0066	12.5002	0.1657	0	2637.6	4.1
5.1	833	592	0.039	0.1785	0.0004	0.4862	0.0062	11.9659	0.1538	3	2638.9	3.5
12.1*	233	107	0.165	0.1785	0.0008	0.5385	0.0081	13.2539	0.2087	-5	2638.9	7.7
6.1*	359	342	0.029	0.1786	0.0006	0.4971	0.0065	12.2403	0.1654	1	2639.7	5.3
33.1	1648	1380	0.070	0.1787	0.0004	0.4892	0.0061	12.0531	0.1528	3	2640.7	3.6
16.1*	358	436	0.044	0.1790	0.0006	0.4983	0.0065	12.2950	0.1662	1	2643.3	5.4
32.1	1078	738	0.332	0.1793	0.0005	0.4819	0.0061	11.9122	0.1540	4	2646.2	4.4
30.1	1023	1089	0.029	0.1795	0.0003	0.5120	0.0065	12.6674	0.1624	-1	2647.8	3.0
14.1	1399	1179	0.024	0.1802	0.0003	0.5096	0.0070	12.6604	0.1752	0	2654.4	2.7
28.1	1482	1239	0.035	0.1806	0.0003	0.4832	0.0062	12.0301	0.1568	5	2658.2	2.8
10.1	1148	842	0.023	0.1809	0.0006	0.4994	0.0063	12.4535	0.1614	2	2660.7	5.1
7.1	1369	614	0.052	0.1810	0.0005	0.4846	0.0061	12.0924	0.1559	5	2661.9	4.9
2.1	1075	794	0.031	0.1818	0.0007	0.4976	0.0063	12.4760	0.1658	3	2669.6	6.6
3.1	1469	1026	0.008	0.1818	0.0003	0.4980	0.0064	12.4853	0.1628	2	2669.7	2.7
8.1	956	647	0.062	0.1820	0.0005	0.4848	0.0082	12.1667	0.2095	5	2671.3	4.8
<i>Discordant</i>												
25.1*	297	379	0.242	0.1725	0.0009	0.4592	0.0061	10.9221	0.1567	6	2582.0	8.9
11.1	1379	1122	0.178	0.1734	0.0021	0.4465	0.0057	10.6741	0.1877	9	2590.7	20.2
22.1	1182	1158	0.082	0.1774	0.0006	0.4658	0.0059	11.3963	0.1488	7	2629.0	5.9
4.1	1193	954	0.031	0.1778	0.0006	0.4700	0.0059	11.5242	0.1509	6	2632.7	5.7
27.1	1163	1142	0.042	0.1809	0.0010	0.4681	0.0059	11.6764	0.1599	8	2661.2	8.9

Data are at  $1\sigma$  precision. All Pb data are common-Pb corrected based on  $^{204}\text{Pb}$  measurements. Mount: Z3581; Instrument: JdL Centre SHRIMP-A; Acquisition: 14 March 2004. Grain-spot labels marked with an asterisk indicate analyses made on zircon with bright CL patterns possibly consistent with rim structures as discussed in text.



## 2003967058: foliated biotite monzogranite, Puntaping Rock

### SAMPLE INFORMATION

**1:250,000 sheet:** Dumbleyung (SI5007)

**1:100,000 sheet:** Wagin (2331)

**MGA:** 537085 mE 6312638 mN

**Location:** This sample taken from blasted rock on Puntaping Rock, about 5 km east of Wagin.

**Description:** This rock is a white-grey, foliated to weakly banded, seriate to sparsely feldspar-porphyratic, fine-medium grained biotite monzogranite. The monzogranite contains a strong foliation that dips gently (~15°) east. Biotite schlieren, nebulous biotite banding, thin coarse-grained quartz-feldspar-rich 'segregations' and variations in grain size give the rock a weakly banded appearance. The rock is cut by minor pegmatite veins (10-30 cm thick), narrow shear zones, and late dextral faults. Minor thin dolerite dykes cut all phases and fabrics.

The sample is characterised by a granular to granoblastic texture. Principal minerals are quartz (40%), plagioclase (30%), K-feldspar (25%) and biotite (5-10%), with plagioclase > K-feldspar. Accessory phases include trace apatite, secondary titanite, zircon, anhedral opaque minerals and altered allanite. The rock has minor micrographic quartz-K-feldspar and myrmekitic quartz-plagioclase intergrowth. Quartz displays moderate subgrain development with sutured grain boundaries and some undulose extinction. Biotite is weakly to moderately aligned. Alteration is limited to very weak saussuritization of plagioclase by white mica, epidote, and very minor replacement of biotite by chlorite, epidote, and opaque minerals.

### DESCRIPTION OF ZIRCONS

**Shape:** Generally sub-euhedral stubby prismatic grains ([Figure 14](#)).

**Size:** 60 to 120 microns

**Colour/clarity:** Clear to pale yellow. Generally clear.

**Quality:** Fair. Inclusions and cracks common with some complex zoning optically visible.

**CL zoning:** Broadly concentric zoning with occasional complex embayments. Potentially high-U and metamict bands in some zoned grains apparent ([Figure 14](#)).



#### CONCURRENT STANDARD DATA

**Pb/U reprod.(2s):** 1.7%

**Err. of mean (2s):** 4.8%

**Standard:** TEMORA

**Analyses:** 12

**Notes:** The reproducibility of the standard is good.

#### SAMPLE DATA

Twenty-eight analyses were made on twenty-eight grains (Table 4). Thirteen analyses are > 5% discordant and there is the suggestion of an ancient Pb-loss discordia from ~2700 Ma (Figure 15). There appears to be no relationship between the CL compositional pattern of the analysed grains and the concordance and age of the analyses. There are two notably younger and apparently concordant grains (#2.1 and #7.1). Analysis #2.1 also has one of the highest U content values at 1084 ppm which raises suspicion about the reliability of the age result. Analysis #7.1 is somewhat mysterious in the context of this sample and without further analysis at this stage is tentatively also assumed to have also been affected by Pb-loss. Of the remaining concordant analyses, a further three analyses (#16.1, #20.1 and #26.1) are outliers from the main group and possibly also affected by ancient Pb-loss.

The remaining ten analyses form a coherent cluster (Figure 16) and yield a concordia age of  $2673 \pm 9$  Ma ( $2\sigma$ , MSWD of concordance = 0.16, Probability of concordance = 0.69).





**Figure 14.** Representative images (transmitted light on left, cathodoluminescence on right) for sample 2003967058: foliated biotite monzogranite, Puntaping Rock. SHRIMP analysis spots are labelled.

#### GEOCHRONOLOGICAL INTERPRETATION

The common concentric zoning of the zircons suggests that the grains have a common igneous origin and the age of  $2673 \pm 9$  Ma is interpreted as the age of the igneous protolith to the gneiss. The metamorphism that formed the gneiss may have caused the ancient Pb-loss seen in the sample. Analysis #7.1 may possibly represent a later



zircon forming event, although there is no certain evidence in these data to confirm or deny this.

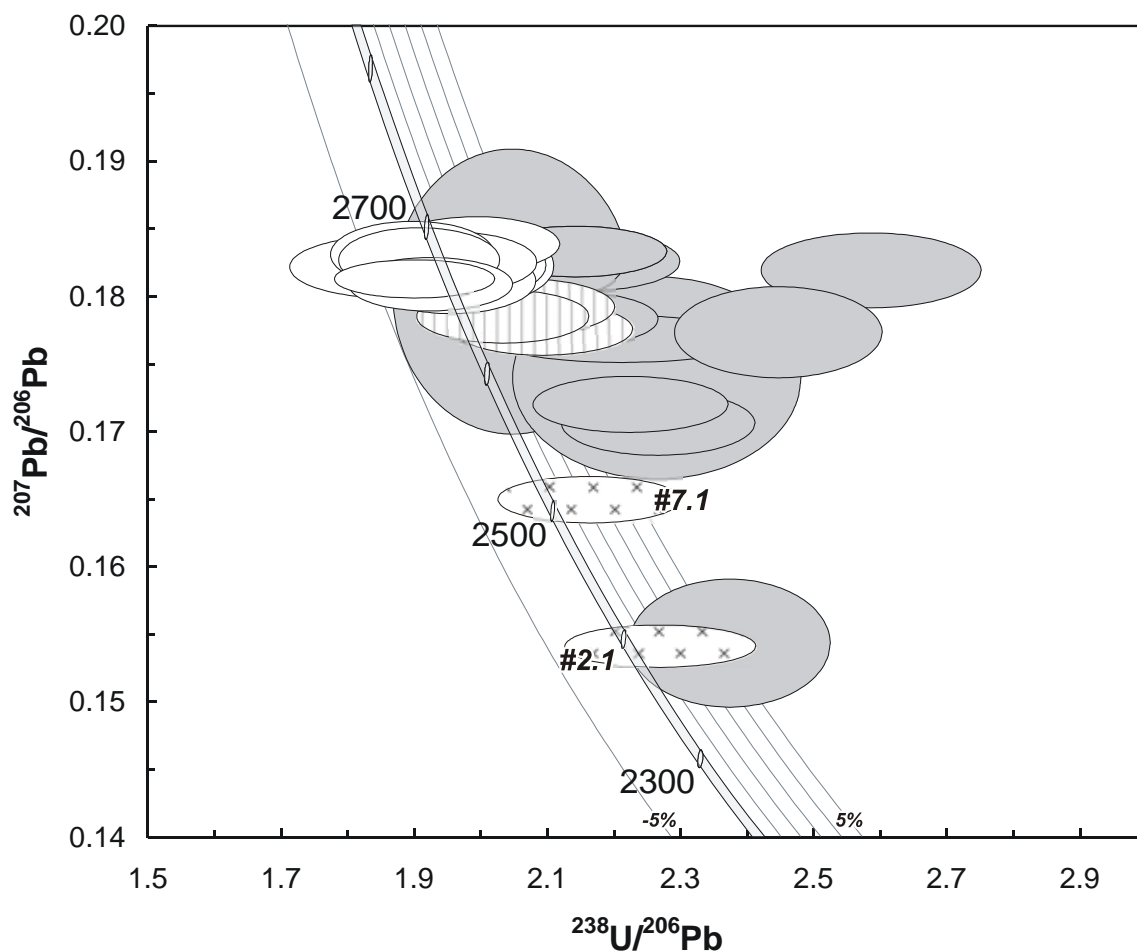


**Figure 15.** Tera-Wasserburg concordia plot for zircons from sample 2003967058: foliated biotite monzogranite, Puntaping Rock. White-filled symbols are used to define the age of the sample; discordant and/or high common-Pb analyses are light grey; vertical hatching and cross hatching indicate apparently concordant analyses considered affected by Pb-loss.

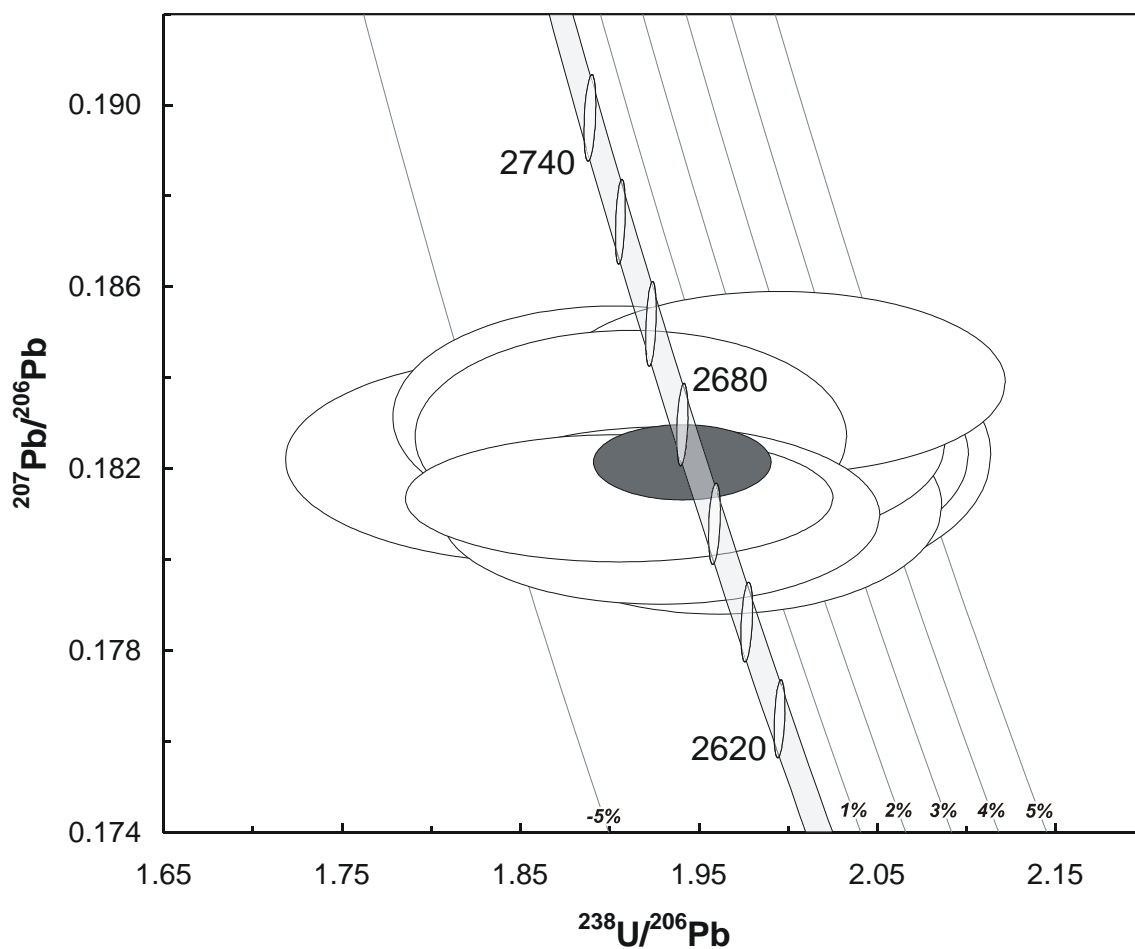


**Figure 16.** Tera-Wasserburg concordia plot for zircons from sample 2003967058: foliated biotite monzogranite, Puntaping Rock concentrating on the concordant group yielding a concordia age of  $2673 \pm 9$  Ma indicated by the dark ellipse.

**Table 4.** SHRIMP analytical results for zircon from sample 2003967058: foliated biotite monzogranite, Puntaping Rock.

Grain Spot	U (ppm)	Th (ppm)	% comm 206	$^{207}\text{Pb}/^{206}\text{Pb}$	$\pm$	$^{206}\text{Pb}/^{238}\text{U}$	$\pm$	$^{207}\text{Pb}/^{235}\text{U}$	$\pm$	% Disc.	$^{207}\text{Pb}/^{206}\text{Pb}$ Age (Ma)	$\pm$
<i>Protolith age?</i>												
19.1	429	130	0.104	0.1810	0.0008	0.5187	0.0135	12.9428	0.3423	-1.2	2661.7	7.3
14.1	503	148	0.117	0.1812	0.0010	0.5101	0.0133	12.7431	0.3391	0.3	2663.7	9.0
1.1	822	579	0.024	0.1813	0.0006	0.5251	0.0135	13.1297	0.3410	-2.1	2665.2	5.3
25.1	509	273	-0.016	0.1822	0.0009	0.5351	0.0177	13.4435	0.4505	-3.4	2673.1	8.6
12.1	429	229	0.290	0.1823	0.0012	0.5036	0.0132	12.6589	0.3409	1.7	2674.0	10.7
4.2	296	134	0.113	0.1823	0.0010	0.5070	0.0134	12.7441	0.3447	1.1	2674.0	9.4
11.1	445	213	0.161	0.1826	0.0009	0.5097	0.0133	12.8312	0.3412	0.8	2676.3	8.3
15.1	705	344	0.223	0.1827	0.0010	0.5233	0.0135	13.1825	0.3480	-1.3	2677.6	8.7
24.1	250	86	-0.025	0.1831	0.0010	0.5262	0.0139	13.2865	0.3591	-1.6	2681.5	9.0
21.1	556	340	0.198	0.1839	0.0008	0.5014	0.0130	12.7137	0.3350	2.6	2688.4	7.4
<i>Pb-loss?</i>												
26.1	364	119	-0.025	0.1777	0.0008	0.4769	0.0125	11.6809	0.3097	4.5	2631.1	7.4
16.1	558	207	0.220	0.1786	0.0008	0.4911	0.0127	12.0922	0.3185	2.4	2639.8	7.4
20.1	478	185	0.186	0.1793	0.0008	0.4827	0.0126	11.9321	0.3155	4.0	2646.2	7.7
2.1	1084	689	0.616	0.1543	0.0006	0.4401	0.0113	9.3660	0.2441	1.8	2394.5	7.0
7.1	788	530	0.164	0.1651	0.0007	0.4618	0.0120	10.5109	0.2761	2.4	2508.5	7.2
<i>Discordant/High common-Pb</i>												
4.1	1548	66	1.069	0.1545	0.0019	0.4209	0.0108	8.9676	0.2568	5.5	2396.7	21.3
22.1	738	289	0.547	0.1707	0.0010	0.4407	0.0115	10.3754	0.2769	8.2	2564.9	9.5
18.1	492	249	0.063	0.1721	0.0008	0.4491	0.0120	10.6570	0.2898	7.3	2578.4	8.2
27.1	838	285	0.537	0.1740	0.0030	0.4411	0.0171	10.5843	0.4506	9.3	2596.8	29.1
17.1	965	437	0.114	0.1769	0.0007	0.4513	0.0165	11.0079	0.4046	8.5	2624.1	6.6
9.1	697	272	0.450	0.1774	0.0014	0.4083	0.0106	9.9883	0.2697	16.0	2628.9	12.8
3.1	1039	506	0.340	0.1784	0.0008	0.4688	0.0121	11.5312	0.3028	6.0	2637.9	7.7
8.1	575	204	1.310	0.1804	0.0043	0.4877	0.0175	12.1305	0.5221	3.6	2656.4	39.4
23.1	430	258	0.899	0.1820	0.0011	0.3864	0.0101	9.6949	0.2599	21.1	2670.9	10.3
10.1	588	288	0.413	0.1824	0.0011	0.4799	0.0125	12.0697	0.3226	5.5	2674.8	10.0
13.1	479	138	0.439	0.1826	0.0009	0.4621	0.0120	11.6358	0.3080	8.5	2676.8	8.0
5.1	685	304	0.240	0.1834	0.0008	0.4662	0.0121	11.7872	0.3094	8.1	2683.5	6.8
6.1	685	304	0.240	0.1834	0.0008	0.4662	0.0121	11.7872	0.3094	8.1	2683.5	6.8

Data are at  $1\sigma$  precision. All Pb data are common-Pb corrected based on  $^{204}\text{Pb}$  measurements. Mount: Z3581; Instrument: JdL Centre SHRIMP-A; Acquisition: 9 April 2004.



## 2003967065: biotite-two pyroxene quartzofeldspathic gneiss (granulite), Nairibin Rock

### SAMPLE INFORMATION

**1:250,000 sheet:** Dumbleyung (SI5007)

**1:100,000 sheet:** Dumbleyung (2431)

**MGA:** 585590 mE 6310720 mN

**Location:** This sample was hammered from blasted rock on the south side of the road.

**Description:** This rock is a dark grey, banded, variably quartz-feldspar-porphyrific, fine-medium grained, biotite-two pyroxene quartzofeldspathic gneiss. The gneiss contains biotite-rich seams, felsic layers and segregations, some of which may represent leucosome. The seams, layers and segregations are strongly deformed and boudinaged. Variations in grain size and biotite and/or pyroxene content result in the rock having a banded appearance. Foliated and locally folded medium-coarse-grained seriate to feldspar-porphyrific biotite granite dykes intrude the gneiss. The rock also contains minor, thin quartz-rich veins.

The sample is characterised by a granoblastic texture. Principal minerals are quartz (35%), plagioclase (~40%), ortho- and clinopyroxene (~15%), biotite (8-10%), K-feldspar (~5%), with orthopyroxene~clinopyroxene and plagioclase»K-feldspar. Accessory phases include apatite, zircon and anhedral opaque minerals. The rock contains minor quartz-biotite intergrowth. Biotite and pyroxene exhibit strong alignment forming a strong fabric. Quartz shows weak to moderate subgrain development and very minor undulose extinction. Alteration is limited with very weak saussuritization of plagioclase by white mica and epidote, very minor replacement of biotite by chlorite and opaque oxides, and very minor replacement of pyroxene by chlorite, actinolite and sericite.

### DESCRIPTION OF ZIRCONS

**Shape:** Sub-euhedral to rounded ([Figure 17](#)).

**Size:** 50 – 100 microns.

**Colour/clarity:** Mostly clear.

**Quality:** Few cracks and inclusions.

**CL zoning:** Complex banding and embayments frequently with oscillatory zoned cores and homogeneous rims ([Figure 17](#)).



#### CONCURRENT STANDARD DATA

**Pb/U reprod.(2s):** 0.75%

**Err. of mean (2s):** 2.19%

**Standard:** QGNG

**Analyses:** 12 (one discarded as young outlier).

**Notes:** Reproducibility of standard is good.

#### SAMPLE DATA

Thirty-one analyses were made on twenty-nine grains. Nineteen analyses are > 5% discordant although these analyses produce a good discordia chord and concordia intercepts at  $2671 \pm 17$  Ma and  $993 \pm 66$  Ma (Figure 18). The lower intercept value clearly indicates a non-zero age Pb-loss event.

One further analysis (#15.1) can be discarded with possible Pb-loss and a closer examination of the concordant analyses (Figure 19) indicates a strong correlation with  $^{232}\text{Th}/^{238}\text{U}$  ratio (Figure 20). The difference between these two clusters also largely corresponds to a difference in CL pattern with the older cluster with higher  $^{232}\text{Th}/^{238}\text{U}$  ratio associated with oscillatory zoned cores and the younger cluster with lower  $^{232}\text{Th}/^{238}\text{U}$  ratio associated with homogeneously zoned rims and mantles. Analysis #27 clearly demonstrates a significant difference in age ( $2679.1 \pm 16.0$  Ma and  $2649.2 \pm 7.0$  Ma),  $^{232}\text{Th}/^{238}\text{U}$  ratio and CL pattern between core and rim (Figure 17, Figure 20).

The older cluster has a median  $^{232}\text{Th}/^{238}\text{U}$  ratio value of 0.63 and yields a weighted mean  $^{207}\text{Pb}/^{206}\text{Pb}$  age of  $2677.8 \pm 6.0$  (MSWD: 0.64). The younger cluster has a median  $^{232}\text{Th}/^{238}\text{U}$  ratio value of 0.26 and yields a weighted mean  $^{207}\text{Pb}/^{206}\text{Pb}$  age of  $2645.9 \pm 3.3$  (MSWD: 0.64).



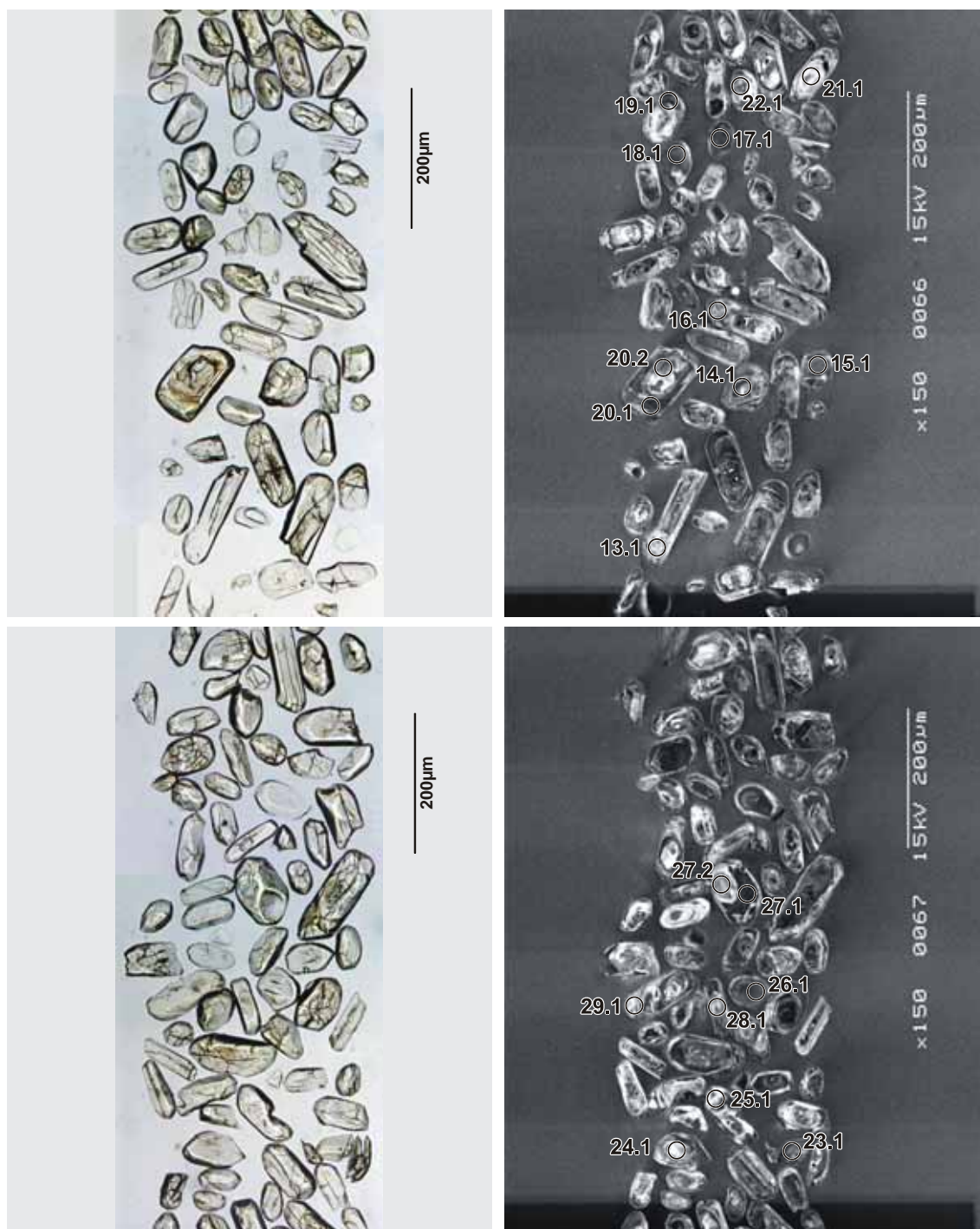


**Figure 17.** Representative images (transmitted light on left, cathodoluminescence on right) for sample 2003967065: biotite-two pyroxene quartzofeldspathic gneiss (granulite), Nairibin Rock. SHRIMP analysis spots are labelled.

#### GEOCHRONOLOGICAL INTERPRETATION

The age of  $2678 \pm 6$  Ma is interpreted as the igneous age of the protolith to the gneiss. The age  $2646 \pm 4$  Ma is interpreted as the age of metamorphism.

The significance of the  $993 \pm 66$  Ma lower intercept age is unclear within the context of these data, but it may be associated with tectonism in the Albany-Fraser orogen.



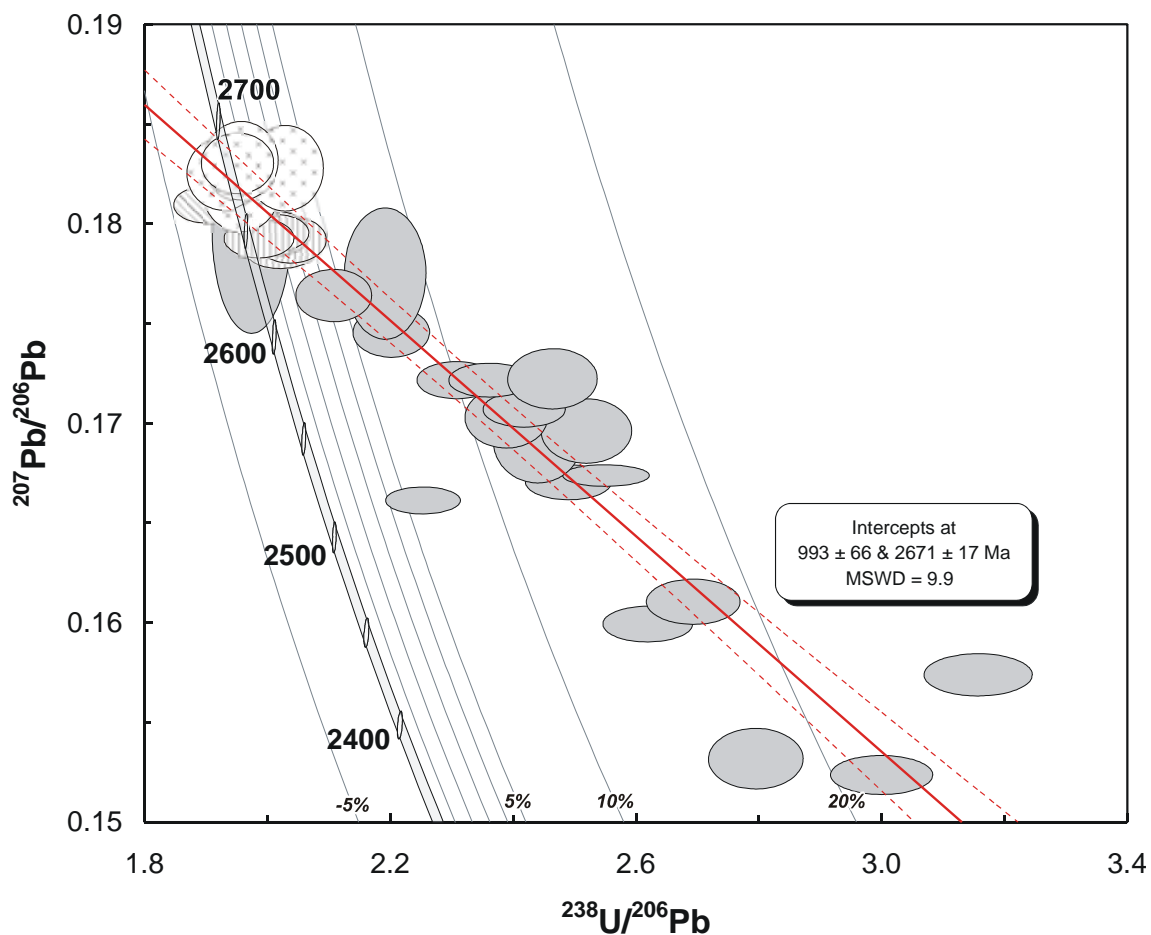


**Figure 18.** Tera-Wasserburg concordia plot for zircons from sample 2003967065: biotite-two pyroxene quartzofeldspathic gneiss (granulite), Nairibin Rock. Cross-hatch symbol indicates protolith analyses; vertical hatching indicate analyses interpreted as metamorphic; diagonal hatching indicates a possible mixed analysis; discordant and/or high common-Pb analyses are light grey.

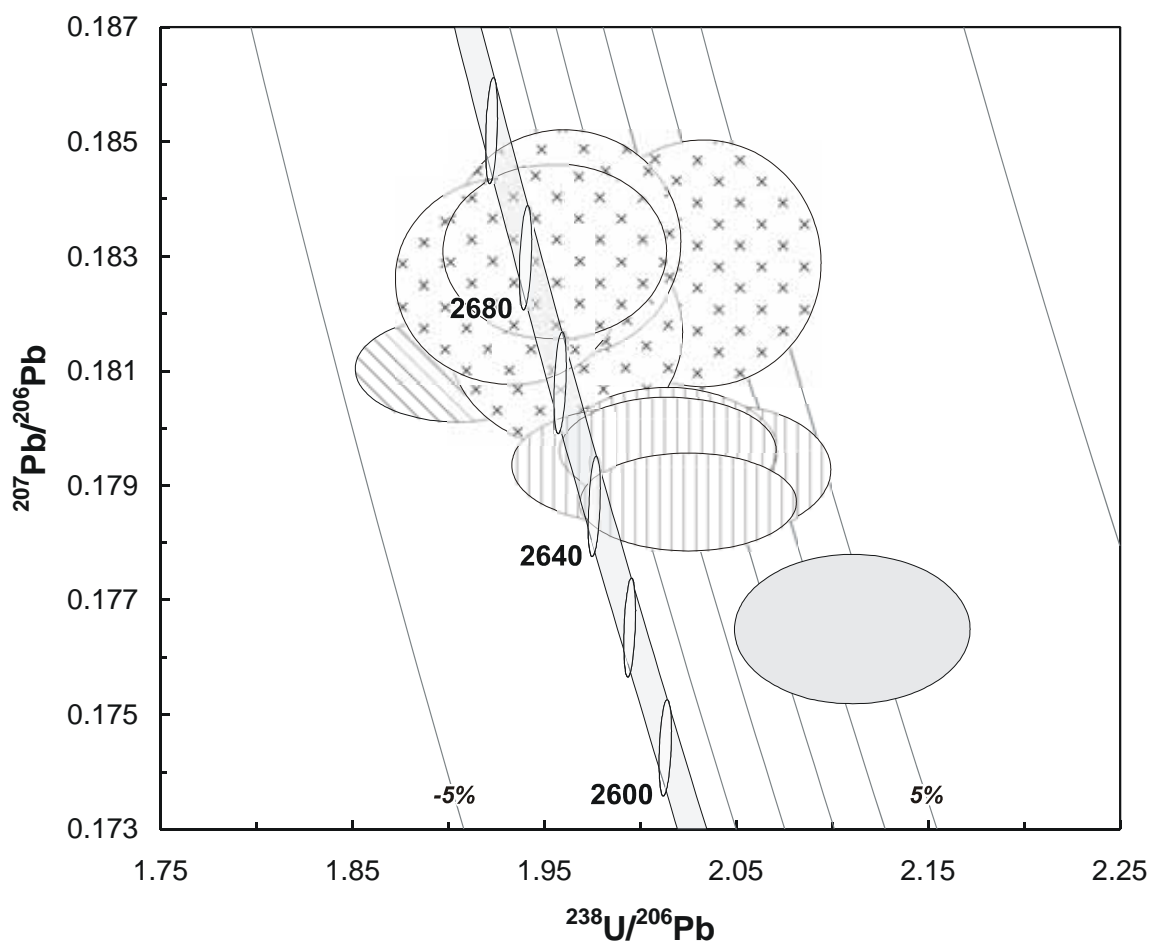


**Figure 19.** Tera-Wasserburg concordia plot for zircons from sample 2003967065: biotite-two pyroxene quartzofeldspathic gneiss (granulite), Nairibin Rock focussing on the concordant analyses. Cross-hatch symbol indicates protolith analyses; vertical hatching indicate analyses interpreted as metamorphic; diagonal hatching indicates a possible mixed analysis; discordant and/or high common-Pb analyses are light grey.

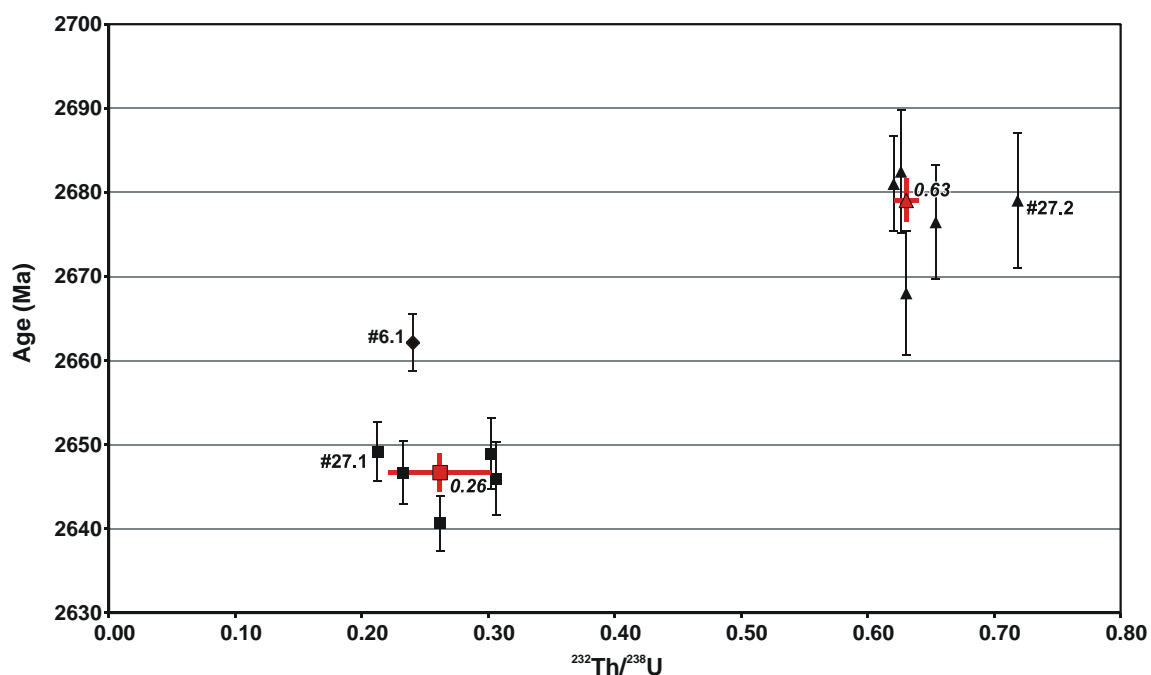


**Figure 20.** Plot of zircon age in relation to  $^{232}\text{Th}/^{238}\text{U}$  ratio for concordant zircons from 2003967065: biotite-two pyroxene quartzofeldspathic gneiss (granulite), Nairibin Rock illustrating two distinct clusters. Triangular markers indicate the older cluster and square markers indicate the younger cluster. A possibly blended analysis (#6.1) is indicated with the diamond marker. The red markers indicate the median and median absolute deviation in both dimensions for each cluster.

**Table 5.** SHRIMP analytical results for zircon from sample 2003967065: biotite-two pyroxene quartzofeldspathic gneiss (granulite), Nairibin Rock.

Grain.Spot	U (ppm)	Th (ppm)	% comm 206	<sup>207</sup> Pb / <sup>206</sup> Pb	±	<sup>206</sup> Pb / <sup>238</sup> U	±	<sup>207</sup> Pb / <sup>235</sup> U	±	% Disc.	<sup>207</sup> Pb / <sup>206</sup> Pb Age (Ma)	±
<i>Metamorphism</i>												
25.1	865	219	0.023	0.1787	0.0003	0.4941	0.0056	12.1741	0.1408	2.0	2640.7	3.2
18.1	473	140	0.021	0.1793	0.0005	0.4901	0.0057	12.1140	0.1450	2.8	2646.0	4.3
9.1	904	203	0.035	0.1793	0.0004	0.5030	0.0058	12.4370	0.1470	0.8	2646.7	3.7
26.1	498	146	-0.005	0.1796	0.0005	0.4969	0.0058	12.3029	0.1468	1.8	2648.9	4.2
27.1	676	139	-0.007	0.1796	0.0004	0.4967	0.0057	12.3005	0.1434	1.9	2649.2	3.5
<i>Protolith</i>												
21.1	185	113	0.065	0.1817	0.0008	0.5104	0.0066	12.7844	0.1743	0.4	2668.0	7.4
22.1	197	125	0.106	0.1826	0.0007	0.5181	0.0065	13.0417	0.1730	-0.5	2676.5	6.8
27.2	249	173	0.044	0.1829	0.0009	0.4923	0.0061	12.4139	0.1662	3.7	2679.1	8.0
2.1	190	114	0.026	0.1831	0.0006	0.5118	0.0063	12.9195	0.1640	0.6	2681.0	5.7
24.1	204	123	-0.011	0.1832	0.0008	0.5104	0.0065	12.8964	0.1729	0.9	2682.5	7.3
<i>Blended analysis?</i>												
6.1	572	133	0.079	0.1810	0.0004	0.5257	0.0060	13.1200	0.1515	-2.3	2662.1	3.4
<i>Minor Pb-loss</i>												
15.1	369	252	0.015	0.1765	0.0005	0.4740	0.0056	11.5331	0.1419	4.5	2619.8	5.1
<i>Discordant/high common-Pb</i>												
1.1	1432	258	0.202	0.1304	0.0005	0.2601	0.0029	4.6780	0.0556	29.2	2103.9	7.1
20.1	1065	192	0.117	0.1523	0.0004	0.3334	0.0038	7.0025	0.0815	21.8	2372.2	4.5
10.1	1789	209	0.035	0.1531	0.0006	0.3578	0.0040	7.5545	0.0899	17.2	2381.1	6.9
19.1	1028	290	0.215	0.1574	0.0004	0.3168	0.0036	6.8743	0.0806	26.9	2427.6	4.6
4.1	612	71	0.057	0.1599	0.0004	0.3817	0.0043	8.4163	0.0975	15.1	2454.8	3.9
23.1	665	182	0.113	0.1610	0.0005	0.3712	0.0043	8.2429	0.0977	17.5	2466.5	4.8
17.1	3766	256	0.006	0.1661	0.0003	0.4435	0.0049	10.1584	0.1137	6.1	2519.1	2.8
7.1	1242	190	0.052	0.1671	0.0004	0.4014	0.0046	9.2467	0.1072	14.0	2528.4	3.6
5.1	1387	133	0.032	0.1674	0.0002	0.3918	0.0044	9.0421	0.1031	15.8	2531.7	2.2
8.1	329	103	0.140	0.1692	0.0009	0.4096	0.0050	9.5556	0.1267	13.2	2549.8	8.8
14.1	369	111	0.081	0.1696	0.0007	0.3968	0.0047	9.2824	0.1159	15.6	2554.1	6.5
16.1	957	245	0.319	0.1703	0.0006	0.4184	0.0048	9.8252	0.1175	12.0	2560.6	6.1
13.1	923	224	0.099	0.1707	0.0004	0.4133	0.0047	9.7291	0.1125	13.0	2564.7	3.6
29.1	827	233	0.070	0.1722	0.0004	0.4329	0.0050	10.2788	0.1198	10.1	2579.1	3.7
12.1	949	235	0.044	0.1722	0.0004	0.4234	0.0049	10.0519	0.1171	11.8	2579.1	3.4
28.1	279	113	0.044	0.1722	0.0006	0.4057	0.0049	9.6355	0.1222	14.9	2579.6	6.0
3.1	422	162	0.163	0.1746	0.0005	0.4537	0.0052	10.9228	0.1302	7.3	2602.3	4.9
11.1	316	192	0.074	0.1776	0.0014	0.4559	0.0056	11.1615	0.1618	7.9	2630.1	12.7
20.2	186	99	1.329	0.1797	0.0021	0.5062	0.0066	12.5428	0.2210	0.4	2650.3	19.6

Data are at 1 $\sigma$  precision. All Pb data are common-Pb corrected based on <sup>204</sup>Pb measurements. Mount: Z3582; Instrument: JdL Centre SHRIMP-A; Acquisition: 4 May 2004.



## 2003967068: biotite quartzofeldspathic gneiss, Lake Dumbleyung

### SAMPLE INFORMATION

**1:250,000 sheet:** Dumbleyung (SI5007)

**1:100,000 sheet:** Dumbleyung (2431)

**MGA:** 558228 mE 6313195 mN

**Location:** This sample was hammered from a boulder near outcrop at the Lake Dumbleyung yacht club.

**Description:** This rock is a grey-pink, weakly altered, variably deformed and banded, seriate to sparsely feldspar-porphyritic, fine-medium grained, biotite quartzofeldspathic gneiss. The gneiss has a strong, moderately east-dipping, fabric defined principally by biotite. Biotite schlieren, nebulitic in places, and variations in grain size and modal abundance of plagioclase, K-feldspar and biotite result in the felsic gneiss displaying weak compositional layering. Biotite forms prominent lineation in places. The gneiss forms part of sequence of felsic, garnet-biotite-bearing and lesser mafic gneiss that is intruded by pink-grey, variably-deformed, strongly K-feldspar-porphyritic, medium-grained biotite monzogranite veins, dykes and larger bodies. The monzogranite also contains a moderate-strong foliation, which is generally parallel to the gneissosity, indicating possibly syn-kinematic emplacement of these intrusions. Thin shear zones oblique to the main foliation truncate the gneiss and granite. All phases are cut by relatively common, thin pegmatite and quartz veins.

The sample has a granular to granoblastic texture. Principal minerals are quartz (30%), plagioclase (32-35%), K-feldspar (28-30%) and biotite (5-8%), with plagioclase > K-feldspar. Accessory phases include trace apatite, zircon, monazite and anhedral opaque minerals. Potassium feldspar is dominantly anhedral grains of microcline that are interstitial to plagioclase. Very minor myrmekitic quartz-plagioclase intergrowth is associated with margins of K-feldspar grains. The rock displays minor recrystallization, with quartz displaying very minor undulose extinction and subgrain development, particularly at grain margins. There is a weak mineral alignment defined by biotite. Plagioclase shows patchy replacement by white mica, epidote, chlorite and carbonate. Biotite is weakly to moderately replaced by chlorite, white mica, epidote and opaque minerals.

### DESCRIPTION OF ZIRCONS

**Shape:** Sub-euhedral to rounded ([Figure 21](#)).

**Size:** 100 to 150 microns.

**Colour/clarity:** Mostly clear.



**Quality:** Generally good, with common inclusions and cracks.  
**CL zoning:** Broadly concordant zoning with some complex embayments, truncations and occasional sector-zoning (Figure 21).

#### CONCURRENT STANDARD DATA

**Pb/U reprod.(2s):** 1.04%

**Err. of mean (2s):** 3.07%

**Standard:** QGNG

**Analyses:** 12 (one discarded with anomalously high age)

**Notes:**

#### SAMPLE DATA

Thirty-five analyses were made on thirty-three grains (Table 6; Figure 22). Five analyses are > 5% discordant or have high common-Pb. A couple of grains (#16 and #18) exhibited potential core-rim structures (Figure 21), but no significant age relationship was discovered. Two analyses (#27 and #34) have significant older ages, although analysis #34.1 could be the result of a two-component mixture in the same spot. The only notable difference in physical appearance of these two grains is that grain #27 has the lowest U content of the whole analytical session at 126 ppm.

The bulk of the analyses form a tight concordant cluster of which only three analyses (#3.1, #9.1 and #28.1) are discarded as outliers, possibly a function of minor Pb-loss. The remaining 25 analyses yield a good quality concordia age of  $2650 \pm 7$  Ma (95% confidence; MSWD of concordance = 1.5; Probability of concordance = 0.22; Figure 23).





**Figure 21.** Representative images (transmitted light on left, cathodoluminescence on right) for sample 2003967068: biotite quartzofeldspathic gneiss, Lake Dumbleyung. SHRIMP analysis spots are labelled.

#### GEOCHRONOLOGICAL INTERPRETATION

The age of  $2650 \pm 7$  Ma is interpreted as an igneous age of the protolith to the gneiss.



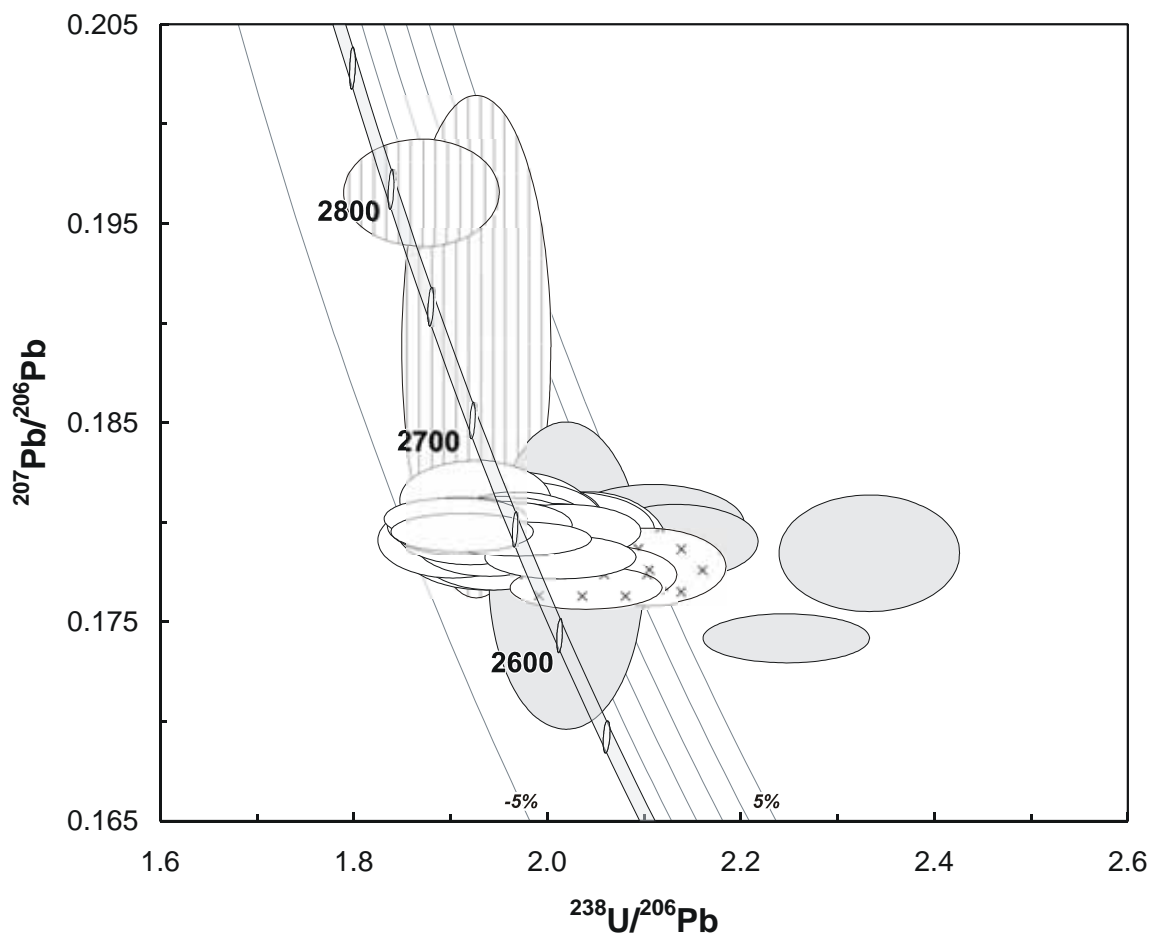


**Figure 22.** Tera-Wasserburg concordia plot for zircons from sample 2003967068: biotite quartzofeldspathic gneiss, Lake Dumbleyung. White-filled symbols are used to define the age of the sample; discordant and/or high common-Pb analyses are light grey; vertical hatching indicates inheritance; cross-hatching indicates analyses regarded as younger outliers possibly due to Pb-loss.

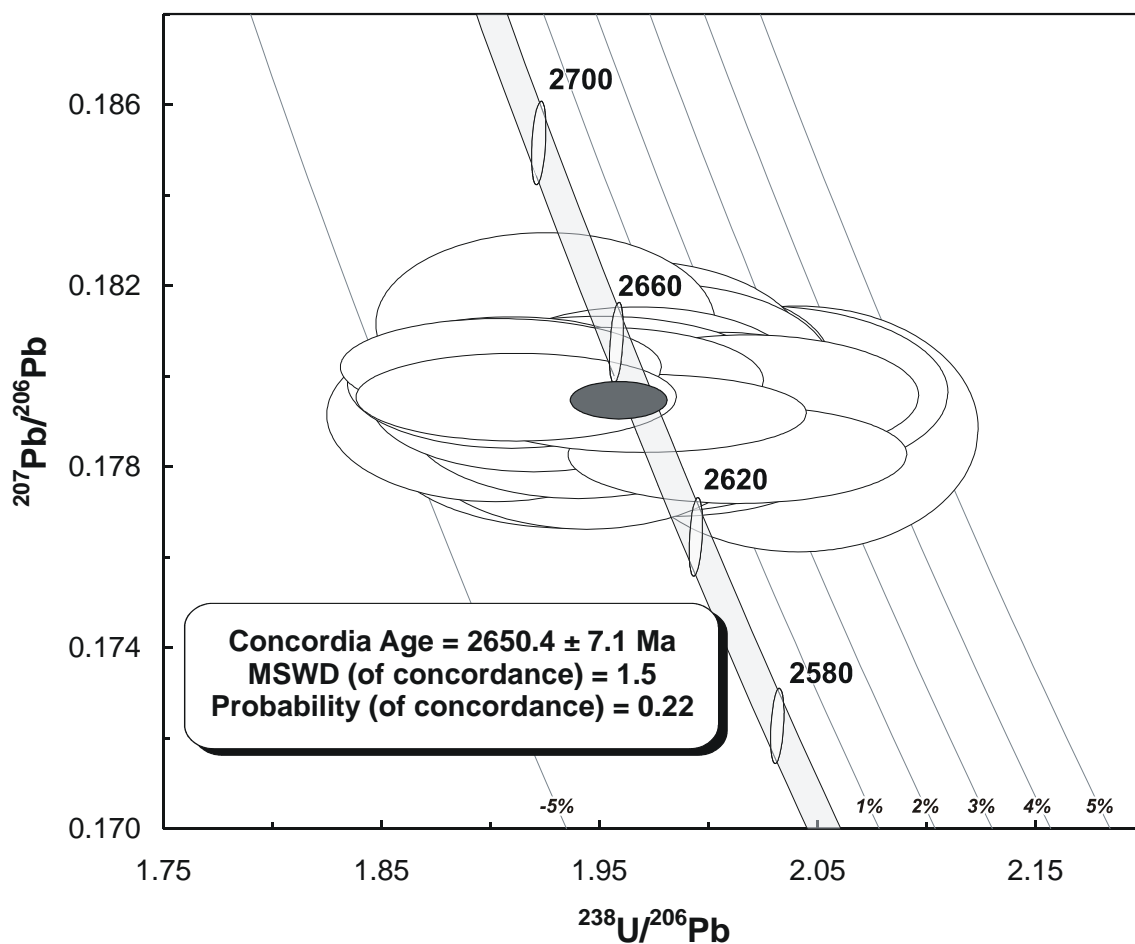


**Figure 23.** Tera-Wasserburg concordia plot for zircons from sample 2003967068: biotite quartzofeldspathic gneiss, Lake Dumbleyung focussing on the concordant analyses yielding a concordia age of  $2650 \pm 7$  Ma.

**Table 6.** SHRIMP analytical results for zircon from sample 2003967068: biotite quartzofeldspathic gneiss, Lake Dumbleyung.

Grain.Spot	U (ppm)	Th (ppm)	% comm 206	$^{207}\text{Pb}/^{206}\text{Pb}$	$\pm$	$^{206}\text{Pb}/^{238}\text{U}$	$\pm$	$^{207}\text{Pb}/^{235}\text{U}$	$\pm$	% Disc.	$^{207}\text{Pb}/^{206}\text{Pb}$ Age (Ma)	$\pm$
<i>Concordant protolith age</i>												
29.1	857	594	0.102	0.1783	0.0004	0.4966	0.0078	12.2080	0.1951	1.4	2637.1	4.1
8.1	236	143	0.005	0.1785	0.0007	0.5162	0.0092	12.7046	0.2326	-1.7	2638.9	6.9
31.1	267	148	0.151	0.1786	0.0008	0.5143	0.0084	12.6626	0.2147	-1.3	2639.7	7.4
11.1	470	244	0.268	0.1787	0.0007	0.5064	0.0085	12.4764	0.2142	0.0	2640.6	6.3
2.1	228	134	0.091	0.1789	0.0011	0.4899	0.0081	12.0818	0.2142	2.7	2642.3	10.3
18.1	313	210	0.036	0.1789	0.0008	0.5042	0.0093	12.4388	0.2356	0.4	2642.9	7.5
7.1	297	175	0.041	0.1791	0.0007	0.5153	0.0084	12.7222	0.2137	-1.3	2644.1	6.6
30.1	206	114	0.043	0.1792	0.0008	0.5257	0.0087	12.9865	0.2234	-2.9	2645.2	7.3
10.1	469	229	0.294	0.1792	0.0009	0.5094	0.0081	12.5884	0.2116	-0.3	2645.6	8.6
16.1	1165	871	0.022	0.1792	0.0004	0.5076	0.0079	12.5432	0.1979	0.0	2645.6	3.3
23.1	389	214	0.136	0.1793	0.0007	0.4990	0.0080	12.3340	0.2049	1.4	2646.1	6.6
33.1	481	250	0.382	0.1795	0.0006	0.5208	0.0083	12.8907	0.2109	-2.1	2648.3	6.0
32.1	896	626	0.015	0.1796	0.0004	0.5230	0.0082	12.9494	0.2055	-2.4	2648.9	3.7
25.1	671	649	0.041	0.1796	0.0006	0.4955	0.0078	12.2690	0.1980	2.1	2649.2	5.1
18.2	246	116	0.045	0.1797	0.0008	0.4947	0.0089	12.2558	0.2268	2.2	2649.8	7.3
13.1	247	167	0.124	0.1797	0.0007	0.5082	0.0084	12.5948	0.2140	0.1	2650.5	6.9
25.1	556	326	0.039	0.1797	0.0005	0.5084	0.0084	12.5999	0.2118	0.0	2650.5	4.7
21.1	355	184	-0.016	0.1799	0.0006	0.5236	0.0085	12.9878	0.2142	-2.4	2652.0	5.5
5.1	550	328	-0.010	0.1799	0.0005	0.5129	0.0082	12.7249	0.2054	-0.6	2652.2	4.5
4.1	522	422	0.014	0.1801	0.0005	0.5129	0.0085	12.7342	0.2145	-0.6	2653.4	4.9
22.1	267	134	0.007	0.1802	0.0008	0.5057	0.0083	12.5630	0.2135	0.6	2654.4	7.2
24.1	680	412	0.043	0.1802	0.0004	0.5249	0.0083	13.0449	0.2087	-2.5	2655.0	4.0
15.1	238	117	0.002	0.1804	0.0007	0.5085	0.0094	12.6474	0.2402	0.2	2656.5	6.7
2.1	244	134	0.001	0.1805	0.0009	0.5086	0.0084	12.6544	0.2182	0.2	2657.0	8.0
20.1	240	170	0.134	0.1812	0.0008	0.5193	0.0086	12.9743	0.2227	-1.2	2663.8	7.6
<i>Young outliers/Pb-loss?</i>												
3.1	852	666	0.130	0.1768	0.0004	0.4903	0.0077	11.9511	0.1904	1.9	2622.9	4.2
9.1	473	176	0.215	0.1774	0.0006	0.4882	0.0083	11.9419	0.2063	2.5	2628.8	5.8
28.1	572	401	0.302	0.1778	0.0008	0.4756	0.0075	11.6622	0.1920	4.7	2632.8	7.4
<i>Inheritance</i>												
34.1	410	266	0.090	0.1889	0.0052	0.5191	0.0085	13.5210	0.4307	1.4	2732.5	45.0
27.1	126	105	0.096	0.1967	0.0011	0.5347	0.0094	14.4997	0.2682	1.3	2798.7	9.2
<i>Discordant/High common-Pb</i>												
14.1	1004	284	0.185	0.1742	0.0005	0.4451	0.0070	10.6913	0.1709	8.7	2598.4	4.9
12.1	586	519	1.122	0.1774	0.0032	0.4952	0.0080	12.1087	0.2914	1.3	2628.3	29.6
6.1	307	144	0.785	0.1785	0.0012	0.4286	0.0070	10.5487	0.1860	12.9	2638.9	11.2
1.1	502	553	0.400	0.1791	0.0008	0.4686	0.0075	11.5721	0.1914	6.3	2644.5	7.1
16.2	357	269	0.261	0.1800	0.0008	0.4739	0.0086	11.7597	0.2204	5.7	2652.5	7.6

Data are at  $1\sigma$  precision. All Pb data are common-Pb corrected based on  $^{204}\text{Pb}$  measurements. Mount: Z3582; Instrument: JdL Centre SHRIMP-B; Acquisition: 9 June 2004.



## 2003969212: biotite tonalite, Narrogin Quarry

### SAMPLE INFORMATION

**1:250,000 sheet:** Corrigin (SI5003)

**1:100,000 sheet:** Narrogin (2332)

**MGA:** 510152 mE 6355423 mN

**Location:** The sample is from the northwest wall of the Narrogin quarry, about 5 km west of Narrogin.

**Description:** The sample is a grey-white, moderately altered, weakly hornfelsed, seriate to locally sparsely quartz-feldspar-porphyrific, medium-coarse grained biotite tonalite. It contains relatively common pegmatite veins and patches throughout rock, as well as minor biotite schlieren and biotite-rich bands. The banding and pegmatite veins are mainly subhorizontal to locally subvertical. Medium-grained (quartz-)diorite intrudes and hornfelses the biotite tonalite. Both phases are cut by rare thin hornblende-biotite granite dykes and late minor thin dolerite dykes.

The sample is characterised by a micrographic to granophyric texture. Principal minerals are plagioclase (60%), quartz (10%), K-feldspar (<5%) and altered FeMg-silicates (~5-6%), with the remainder comprising fine-grained quartz-feldspar-rich groundmass. Accessory phases include trace zircon, titanite and anhedral opaque minerals. Plagioclase forms variably altered anhedral to subhedral grains, whereas large anhedral quartz grains have weak subgrain development with sutured grain boundaries and undulose extinction. The groundmass is mainly micrographic quartz-feldspar intergrowth, which rims both plagioclase and quartz phenocrysts, and minor secondary chlorite, sericite, biotite, epidote and opaque minerals. Alteration is moderate to intense with FeMg-bearing silicates strongly replaced by chlorite, sericite, secondary biotite, opaque minerals, epidote, titanite and leucoxene, and moderate saussuritization of plagioclase by white mica, epidote and chlorite.

### DESCRIPTION OF ZIRCONS

**Shape:** Sub-euhedral to rounded ([Figure 24](#)).

**Size:** 100 to 200 microns.

**Colour/clarity:** Pale to dark brown. Frequently cloudy and turbid.

**Quality:** Poor. Very common cracks and inclusions. Radial crack patterns frequent. Optically apparent core/rim structures.

**CL zoning:** Weakly banded with very complex embayment and truncation structures ([Figure 24](#)).



#### CONCURRENT STANDARD DATA

**Pb/U reprod.(2s):** 1.72%

**Err. of mean (2s):** 5.03%

**Standard:** QGNG

**Analyses:** 11 (one discarded with anomalously high age)

**Notes:** Due to poor instrument performance the quality of the standard measurements in this session is also very low. There is insufficient data to subdivide the session for calibration.

#### SAMPLE DATA

Twenty-two analyses were made on twenty-one grains (Table 7). The predominant feature of the results is the high uranium content (median value 1524 ppm) and subsequent discordance (median value 21%). Only six analyses are less than 10% discordant. The results are widely scattered (Figure 25) and no statistically viable discordia chord can be interpreted (a chord calculated with all data yields intercepts at  $3154 \pm 130$  Ma and  $1285 \pm 180$  Ma with a massive MSWD of 22). There is a weak suggestion of concordant grains ~3240 Ma.

Core and rim structures are apparent, but difficult to analyse. Grain #8 exhibits a distinct core/rim relationship, and although there is a distinct difference in  $^{207}\text{Pb}/^{206}\text{Pb}$  ages between the two analyses (core:  $3248 \pm 47$  Ma; rim:  $2565 \pm 7$  Ma), both ages are discordant. This would suggest that there are two phases of zircon growth in this sample, one around 3240 Ma and another around 2600 Ma.



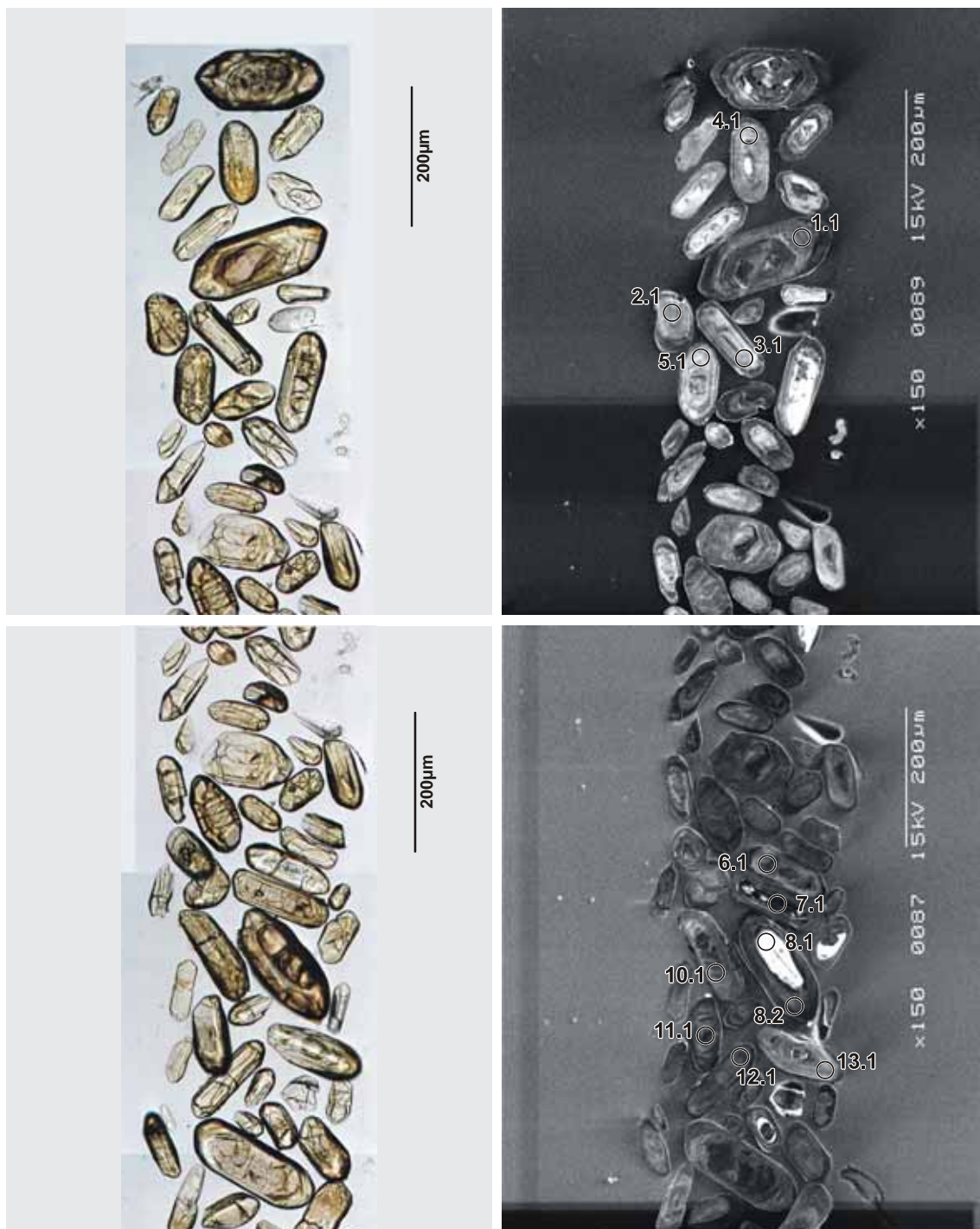


**Figure 24.** Representative images (transmitted light on left, cathodoluminescence on right) for sample 2003969212: biotite tonalite, Narrogin Quarry. SHRIMP analysis spots are labelled.

#### GEOCHRONOLOGICAL INTERPRETATION

The poor quality of these data makes a reliable interpretation practically impossible. There are only a few concordant grains and the only potential cluster is ~3240 Ma. Whether this age represents an inheritance or magmatic age is unclear from these data, although the presence of core/rim structures would suggest the former with a possible magmatic event around 2600 Ma.



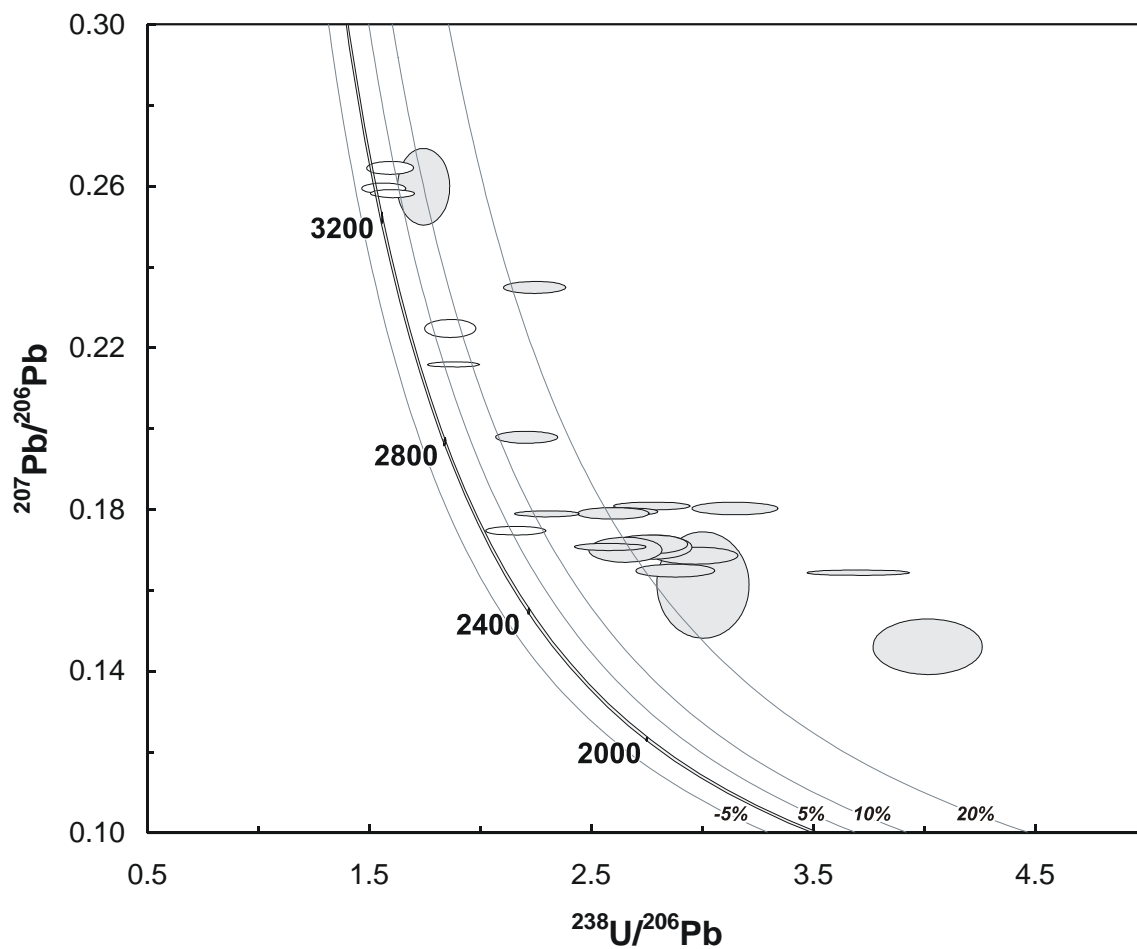


**Figure 25.** Tera-Wasserburg concordia plot for zircons from sample 2003969212: biotite tonalite, Narrogin Quarry. White-filled symbols are < 10% discordant; light grey symbols indicate analyses > 10% discordant and/or high common-Pb.

**Table 7.** SHRIMP analytical results for zircon from sample 2003969212: biotite tonalite, Narrogin Quarry.

Grain.Spot	U (ppm)	Th (ppm)	% comm 206	<sup>207</sup> Pb / <sup>206</sup> Pb	±	<sup>206</sup> Pb / <sup>238</sup> U	±	<sup>207</sup> Pb / <sup>235</sup> U	±	% Disc.	<sup>207</sup> Pb / <sup>206</sup> Pb Age (Ma)	±
<i>Scattered concordant</i>												
20.1	1116	61	0.012	0.1748	0.0004	0.4632	0.0119	11.1643	0.2877	5.8	2604.2	4.2
13.1	2123	160	0.079	0.2160	0.0003	0.5324	0.0134	15.8603	0.4002	6.8	2951.5	1.9
6.1	2196	99	0.045	0.2250	0.0009	0.5367	0.0137	16.6495	0.4299	8.2	3016.9	6.7
11.1	927	186	0.019	0.2585	0.0004	0.6230	0.0158	22.2045	0.5647	3.6	3237.7	2.4
7.1	383	179	-0.004	0.2598	0.0005	0.6393	0.0164	22.8998	0.5908	1.8	3245.3	3.2
14.1	298	121	0.102	0.2650	0.0007	0.6278	0.0168	22.9368	0.6174	4.1	3276.4	3.9
<i>Scattered discordant</i>												
19.1	1939	111	0.130	0.1460	0.0028	0.2493	0.0063	5.0168	0.1589	37.6	2299.1	32.9
2.1	2139	49	0.255	0.1613	0.0054	0.3333	0.0095	7.4101	0.3256	24.9	2468.9	56.6
10.1	3256	182	0.393	0.1643	0.0003	0.2704	0.0068	6.1270	0.1547	38.3	2500.8	2.9
16.1	1320	46	0.339	0.1649	0.0007	0.3475	0.0088	7.8976	0.2023	23.3	2506.1	6.8
22.1	1661	57	0.385	0.1686	0.0008	0.3370	0.0088	7.8319	0.2073	26.4	2543.3	8.4
24.1	1275	21	0.128	0.1701	0.0013	0.3772	0.0096	8.8435	0.2340	19.4	2558.3	12.4
12.1	1621	35	0.152	0.1707	0.0012	0.3600	0.0091	8.4717	0.2228	22.7	2564.5	12.2
8.2	1437	164	0.184	0.1707	0.0004	0.3868	0.0098	9.1068	0.2307	17.8	2564.9	3.5
21.1	1685	28	0.404	0.1714	0.0009	0.3620	0.0091	8.5543	0.2210	22.5	2571.0	9.1
23.1	1648	26	0.090	0.1790	0.0003	0.4351	0.0110	10.7350	0.2717	11.9	2643.2	2.5
5.1	1885	125	0.349	0.1791	0.0006	0.3850	0.0097	9.5064	0.2418	20.6	2644.6	5.6
1.1	931	27	0.155	0.1794	0.0004	0.3794	0.0096	9.3861	0.2384	21.7	2647.7	4.1
17.1	2037	297	0.235	0.1803	0.0006	0.3180	0.0080	7.9075	0.2015	33.0	2655.9	5.9
15.1	1491	35	0.220	0.1809	0.0004	0.3611	0.0091	9.0060	0.2280	25.3	2661.0	3.5
4.1	1524	62	0.055	0.1979	0.0006	0.4528	0.0116	12.3578	0.3202	14.3	2809.2	5.0
18.1	515	89	0.113	0.2352	0.0006	0.4461	0.0114	14.4657	0.3699	23.0	3087.6	4.1
8.1	67	20	0.134	0.2602	0.0039	0.5735	0.0159	20.5721	0.6475	10.0	3247.7	23.5

Data are at 1 $\sigma$  precision. All Pb data are common-Pb corrected based on <sup>204</sup>Pb measurements. Mount: Z3582; Instrument: JdL Centre SHRIMP-A; Acquisition: 10 July 2004.



## 2004967003: banded biotite quartzofeldspathic augen gneiss, Tweed River

### SAMPLE INFORMATION

**1:250,000 sheet:** Collie (SI5006)

**1:100,000 sheet:** Bridgetown (2130)

**MGA:** 445840 mE 6242772 mN

**Location:** This sample taken from blasted rock on south side of road, about 1 km east of Tweed River.

**Description:** This rock is grey, banded, seriate to moderately quartz-feldspar porphyritic, medium-grained, biotite quartzofeldspathic augen gneiss. Feldspar and quartz porphyroclasts to 4 cm in length form augen in the gneiss. The rock is strongly recrystallised and contains a strong foliation. Biotite-rich seams and schlieren, as well as compositional layering, result in the rock having a strongly banded appearance. Bands range from several millimetres to centimetres in thickness. Rare, thin pegmatite veins cut the gneiss.

The gneiss has a granoblastic to porphyroclastic texture. Principal minerals are quartz (30-35%), K-feldspar (30-35%), plagioclase (20-25%) and biotite (8-10%), with K-feldspar > plagioclase. Accessory phases include apatite, zircon, and anhedral opaque minerals. Anhedral quartz and feldspar form a polygonal mosaic and enclose larger K-feldspar and quartz porphyroclasts. Plagioclase forms anhedral to subhedral grains, whereas anhedral quartz grains have minor subgrain development and undulose extinction. Quartz porphyroclasts display weak subgrain development, deformation lamellae and moderate undulose extinction. K-feldspar, dominantly microcline with patchy minor perthite, forms porphyroclasts generally to 2 cm in length and rarely to 4 cm. Rare myrmekitic quartz-plagioclase intergrowth is associated with margins of K-feldspar grains. Aligned green-brown biotite flakes and weakly aligned quartz porphyroclasts define a strong fabric parallel to banding. Alteration is limited to minor, weak replacement of biotite by epidote, chlorite, and white mica and incipient saussuritisation of plagioclase by epidote and white mica.

### DESCRIPTION OF ZIRCONS

**Shape:** Two distinct sub-populations noted. The dominant population tends to be sub-euhedral frequently elongate prismatic grains; the other tends to be equant, euhedral and frequently fractured ([Figure 26](#)).

**Size:** 50 to 300 microns.



- Colour/clarity:** The dominant prismatic population is yellow to brown coloured and is frequently turbid. The euhedral population is distinctly hyacinth-coloured and tends to be clear.
- Quality:** Yellow population has poor quality with frequent cracks and inclusions. Hyacinth population is generally good with rare cracks or inclusions.
- CL zoning:** Zoning is generally very bland with weak indication of oscillatory and sector zoning in hyacinth sub-population (Figure 26).

#### CONCURRENT STANDARD DATA

**Pb/U reprod.(2s):** 4.1%

**Err. of mean (2s):** 1.1%

**Standard:** QGNG

**Analyses:** 16

**Notes:** Reproducibility of Pb/U ratios is relatively higher than the typical expectation of normal analytical dispersion. The duoplasmatron was unstable during this session and could not be corrected.

#### SAMPLE DATA

Thirty-five analyses were made on thirty-five grains with twenty analyses on the hyacinth-coloured population and fifteen on the yellow-coloured population (Table 8). Filtering for discordance is very unusual in this sample as the yellow-coloured population has remarkably high U content (median = 5396 ppm) and is strongly reversely discordant (Figure 27), but is not affected by common-Pb content typically expected in high U grains. These features would suggest that the U/Pb calibration for these grains is being perturbed, either by high U content or related compositional features. It is interesting to note that this rock also had a strong presence of monazite and this could indicate that the associated zircon may have compositional differences such as higher P or REE content.

Focussing on the hyacinth-coloured population (median U = 376 ppm) produces a concordia age of  $2658 \pm 7$  Ma (95% confidence; MSWD of concordance: 0.89; Probability of concordance: 0.35). Presuming that Pb/Pb ratios are unaffected by the potential calibration problem, a weighted  $^{207}\text{Pb}/^{206}\text{Pb}$  age for the yellow-coloured grain yields a value of  $2659 \pm 2$  (95% confidence; MSWD: 2.6; two rejects: #11.1 and #28.1). There is no significant age difference between the two zircon populations.



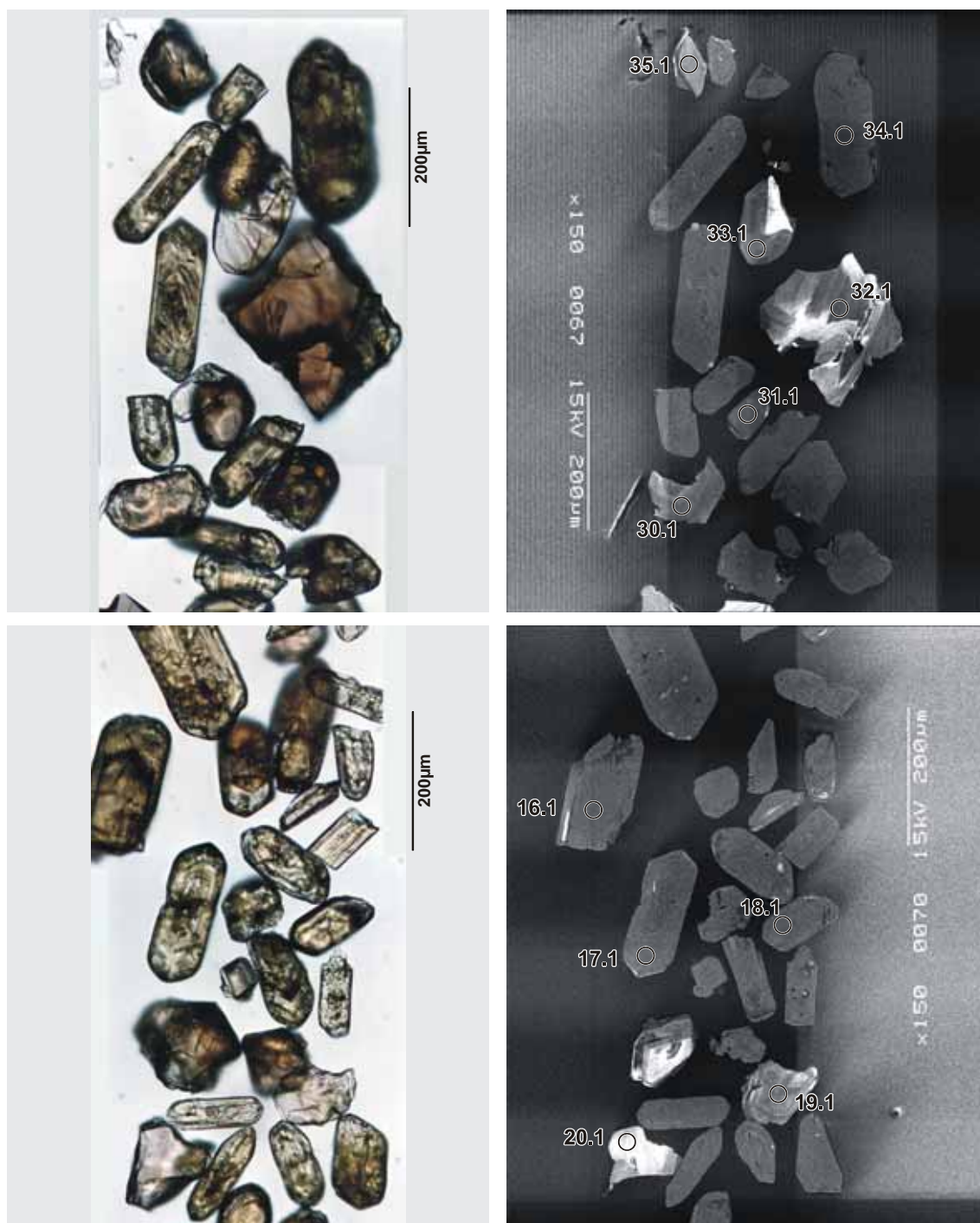


**Figure 26.** Representative images (transmitted light on left, cathodoluminescence on right) for sample 2004967003: banded biotite quartzofeldspathic augen gneiss, Tweed River. SHRIMP analysis spots are labelled. Note difference between hyacinth and yellow coloured grains as discussed in the text.

### GEOCHRONOLOGICAL INTERPRETATION

The complex nature of this sample makes interpretation difficult. There are clearly two zircon phases, but no significant difference in age at  $2658 \pm 7$  Ma (hyacinth population) and  $2659 \pm 2$  Ma (yellow population). It is possible that the two phases represent two closely spaced magmatic phases that were intermingled either prior to, or during, metamorphism.



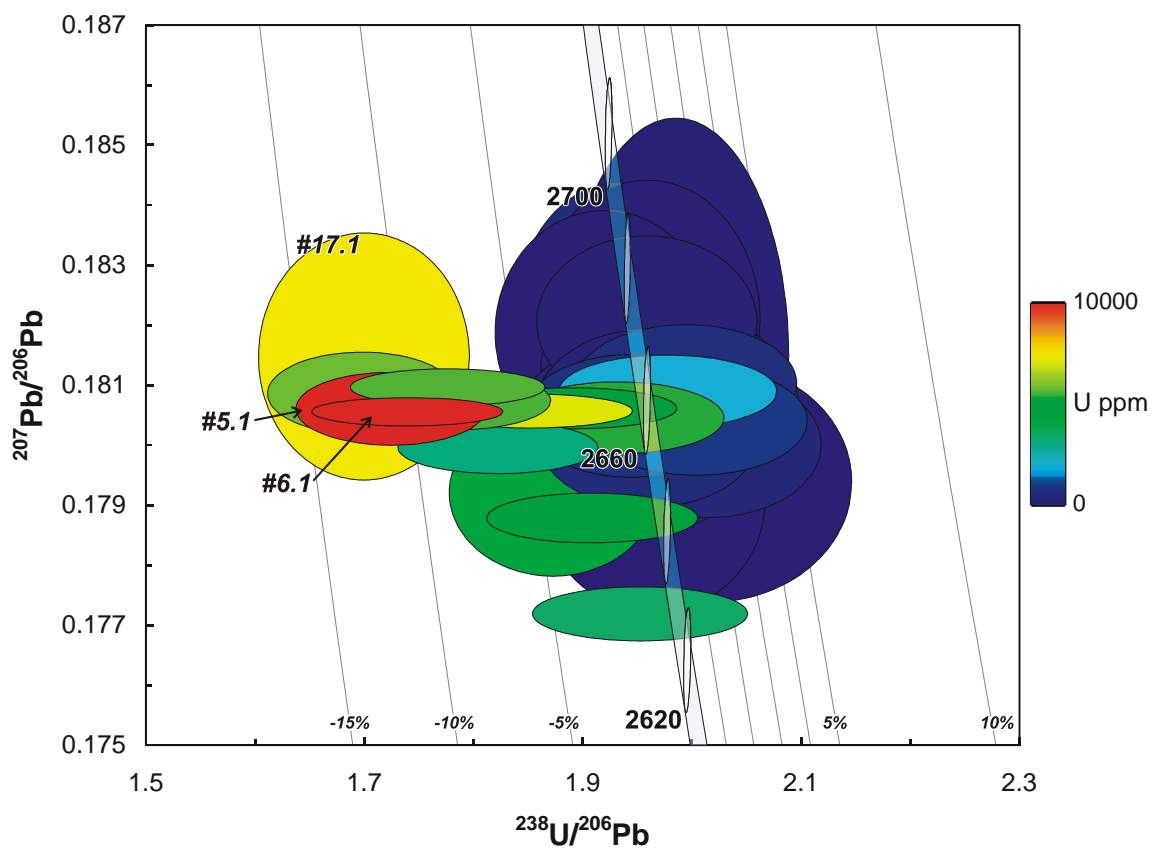


**Figure 27.** Tera-Wasserburg concordia plot for zircons from sample 2004967003: banded biotite quartzofeldspathic augen gneiss, Tweed River. Colouring of error ellipses illustrates the relationship between reverse discordance and uranium content.

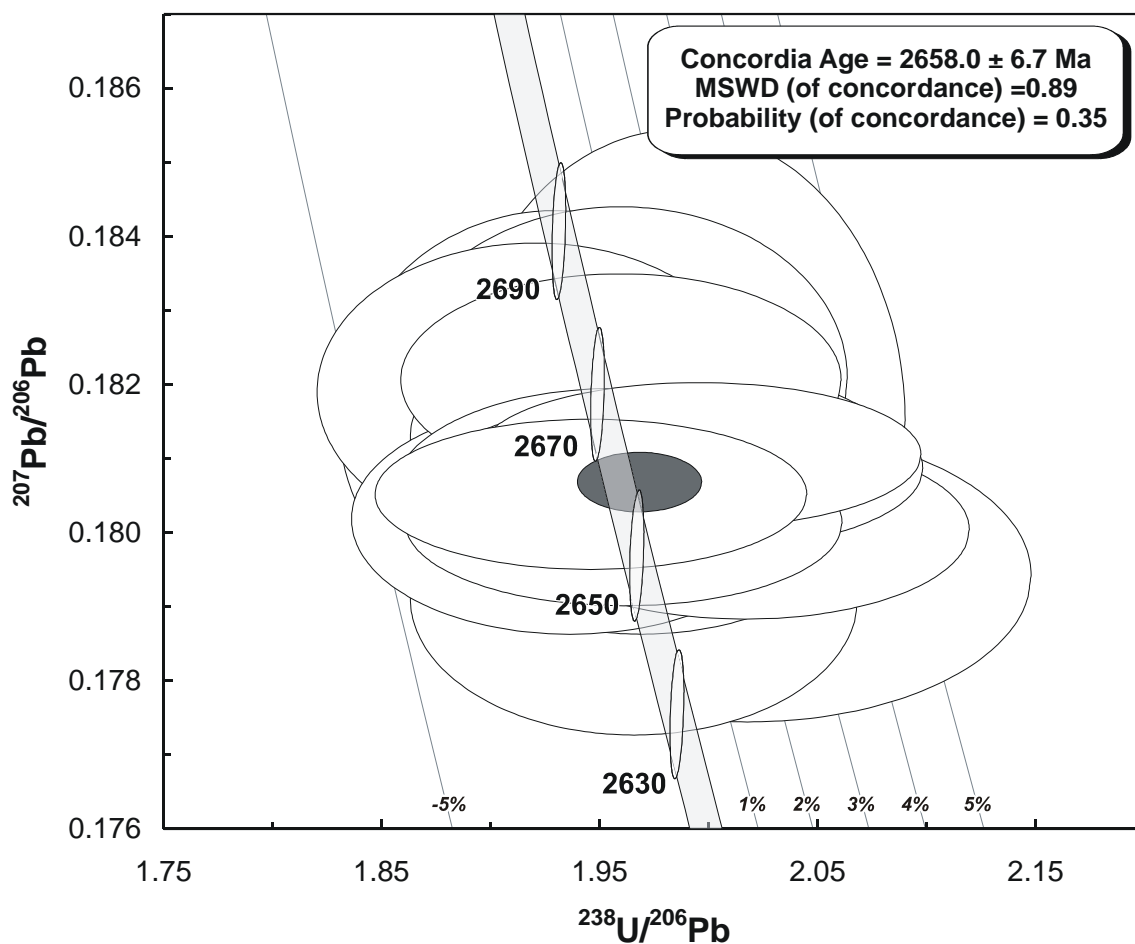


**Figure 28.** Tera-Wasserburg concordia plot for zircons from sample 2004967003: banded biotite quartzofeldspathic augen gneiss, Tweed River focussing on the lower-U, concordant hyacinth-coloured zircons which yield a concordia age of 2658 ± 7 Ma.

**Table 8.** SHRIMP analytical results for zircon from sample 2004967003: banded biotite quartzofeldspathic augen gneiss, Tweed River.

Grain.Spot	U (ppm)	Th (ppm)	% comm 206	<sup>207</sup> Pb / <sup>206</sup> Pb	±	<sup>206</sup> Pb / <sup>238</sup> U	±	<sup>207</sup> Pb / <sup>235</sup> U	±	% Disc.	<sup>207</sup> Pb / <sup>206</sup> Pb Age (Ma)	±
<i>Hyacinth-coloured</i>												
24.1	269	82	0.211	0.1791	0.0008	0.5087	0.0108	12.5635	0.2721	-0.2	2644.7	7.0
1.1	256	106	0.164	0.1794	0.0008	0.4957	0.0130	12.2621	0.3270	2.0	2647.5	7.5
19.1	502	174	0.052	0.1800	0.0005	0.4960	0.0103	12.3131	0.2588	2.1	2653.2	4.5
29.1	584	223	0.023	0.1801	0.0005	0.5100	0.0106	12.6670	0.2657	-0.1	2654.1	4.2
25.1	354	136	0.053	0.1802	0.0006	0.5165	0.0109	12.8314	0.2744	-1.1	2654.6	5.9
21.1	517	196	0.060	0.1803	0.0007	0.5078	0.0106	12.6277	0.2679	0.3	2656.1	6.5
22.1	433	200	0.036	0.1805	0.0005	0.5086	0.0106	12.6574	0.2674	0.2	2657.3	4.7
30.1	718	220	0.072	0.1805	0.0004	0.5139	0.0107	12.7923	0.2670	-0.6	2657.7	3.8
13.1	361	150	0.087	0.1805	0.0006	0.5111	0.0107	12.7232	0.2705	-0.1	2657.9	5.3
20.1	247	114	0.085	0.1807	0.0007	0.5043	0.0107	12.5626	0.2714	1.0	2658.9	6.4
15.1	380	123	0.031	0.1808	0.0006	0.5027	0.0106	12.5338	0.2665	1.3	2660.5	5.3
31.1	575	194	0.064	0.1809	0.0005	0.5010	0.0104	12.4934	0.2618	1.6	2660.9	4.1
8.1	677	316	0.053	0.1811	0.0004	0.5012	0.0104	12.5106	0.2609	1.6	2662.5	3.7
10.1	692	346	0.052	0.1811	0.0007	0.5077	0.0106	12.6757	0.2682	0.6	2662.8	6.5
12.1	372	144	0.133	0.1813	0.0007	0.5091	0.0107	12.7250	0.2713	0.4	2664.7	6.1
35.1	351	142	0.188	0.1815	0.0016	0.5034	0.0107	12.5994	0.2899	1.4	2666.7	14.7
26.1	558	210	0.115	0.1815	0.0012	0.5182	0.0109	12.9703	0.2847	-0.9	2666.9	10.6
33.1	274	109	0.133	0.1819	0.0008	0.5207	0.0111	13.0605	0.2837	-1.2	2670.3	7.5
3.1	356	122	0.038	0.1821	0.0006	0.5103	0.0107	12.8102	0.2723	0.5	2671.8	5.3
32.1	177	87	0.136	0.1821	0.0009	0.5104	0.0110	12.8150	0.2846	0.5	2672.1	8.6
<i>Yellow-coloured</i>												
28.1	3363	163	0.016	0.1772	0.0002	0.5119	0.0105	12.5090	0.2569	-1.4	2627.2	1.7
11.1	4461	289	0.006	0.1788	0.0002	0.5236	0.0108	12.9110	0.2663	-2.7	2642.1	1.6
16.1	3909	648	0.005	0.1792	0.0006	0.5338	0.0110	13.1920	0.2754	-4.2	2645.9	5.2
23.1	3074	227	0.003	0.1800	0.0002	0.5484	0.0113	13.6098	0.2796	-6.2	2652.8	1.6
18.1	829	271	0.065	0.1804	0.0004	0.4989	0.0103	12.4123	0.2581	1.8	2657.0	3.4
2.1	5396	1485	0.008	0.1805	0.0002	0.5174	0.0106	12.8760	0.2645	-1.2	2657.3	2.3
6.1	9783	2512	0.002	0.1806	0.0001	0.5744	0.0118	14.3029	0.2929	-10.1	2658.2	0.9
14.1	7063	1028	0.001	0.1806	0.0001	0.5396	0.0111	13.4367	0.2753	-4.6	2658.4	1.1
5.1	9994	2861	0.001	0.1806	0.0002	0.5796	0.0119	14.4363	0.2961	-10.8	2658.7	2.3
9.1	4730	2003	0.003	0.1806	0.0001	0.5285	0.0108	13.1630	0.2698	-2.9	2658.8	1.3
4.1	5603	1613	0.004	0.1808	0.0002	0.5611	0.0115	13.9859	0.2873	-7.9	2659.9	1.8
34.1	5865	1095	0.007	0.1809	0.0003	0.5887	0.0122	14.6826	0.3059	-12.1	2661.1	2.5
27.1	1901	626	0.013	0.1809	0.0002	0.5054	0.0104	12.6073	0.2601	0.9	2661.3	2.3
7.1	5651	1256	0.003	0.1810	0.0001	0.5626	0.0115	14.0408	0.2877	-8.1	2662.0	1.2
17.1	7362	1844	0.003	0.1815	0.0008	0.5879	0.0136	14.7121	0.3466	-11.8	2666.6	7.6

Data are at 1 $\sigma$  precision. All Pb data are common-Pb corrected based on <sup>204</sup>Pb measurements. Mount: Z4437; Instrument: JdL Centre SHRIMP-B; Acquisition: 22 October 2004.



## 2004967004: Gibraltar quartz monzonite

### SAMPLE INFORMATION

**1:250,000 sheet:** Collie (SI5006)

**1:100,000 sheet:** Bridgetown (2130)

**MGA:** 430760 mE 624494 mN

**Location:** This sample taken from blasted rock on north side of road.

**Description:** This rock is a grey-white to white-pink, lineated, moderately to strongly amphibole-K-feldspar-porphyrific, medium-coarse-grained quartz syenite. It forms part of the Gibraltar quartz monzonite, an elongate intrusion of regional extent, which locally ranges from quartz diorite to syenite. The rock is moderately recrystallised and contains a moderate lineation defined by amphibole. Rounded to elongate amphibole-magnetite xenocrysts to 1-4 cm are locally abundant. The quartz syenite is cut by minor, thin quartz veins.

The sample is characterised by a granular texture. Principal minerals are quartz (~20%), K-feldspar (45-50%), plagioclase (20-25%), secondary amphibole (5-8%) and titanite (1-2%), with K-feldspar > plagioclase. Accessory phases include minor apatite and anhedral opaque minerals, and trace zircon and allanite. Potassium feldspar, mainly microcline and perthite, forms phenocrysts to several centimetres, which contain inclusions of K-feldspar, plagioclase and quartz. Amphibole, principally actinolite and/or hornblende, is secondary in origin and possibly replaces primary pyroxene, and is rimmed by abundant fine-grained epidote and minor secondary biotite. Quartz is variably recrystallised to fine-grained polygonal mosaics around plagioclase and K-feldspar grains, with larger relict quartz grains displaying strong undulose extinction and subgrain development. Plagioclase is moderately altered to albite, clinozoisite/epidote and rare white mica, whereas amphibole is partly replaced by epidote/clinozoisite, secondary biotite, minor chlorite and opaque oxides.

### DESCRIPTION OF ZIRCONS

**Shape:** Euhedral prismatic and fragments (Figure 29).

**Size:** 80 to 200 microns.

**Colour/clarity:** Clear to brown.

**Quality:** Fair to good. Occasional cracks and inclusions.

**CL zoning:** Zoning generally bland. Some prominent concentric zoning and occasional core/rim structures (Figure 29).



#### CONCURRENT STANDARD DATA

**Pb/U reprod.(2s):** 4.6%

**Err. of mean (2s):** 1.6%

**Standard:** QGNG

**Analyses:** 11

**Notes:** Reproducibility of Pb/U ratios is relatively worse than the typical expectation of normal analytical dispersion. The instrument was having technical difficulties with electronic communications and the repeated restarts may explain some scatter.

#### SAMPLE DATA

Thirty-one analyses were made on thirty-one grains with three analyses >5% discordant (Table 9; Figure 30). Two analyses (#6.1 and #14.1) are significantly older and regarded as inherited. Three analyses (#5.1, #15.1 and #18.1) have notably high U content >1000 ppm and have been set aside from subsequent age calculations because of possible calibration issues. The remaining analyses span a range of ages from ~2600 Ma to ~2700 Ma.

Closer inspection would suggest that there are two populations of zircon (Figure 31, Figure 32, Figure 33). The first ranges from ~2650 to ~2700 Ma and tends to have lower U (median: 223 ppm), higher Th/U (median: 0.37) and generally oscillatory zoned CL suggesting an igneous origin. The second cluster occurs at ~2630 Ma and tends to have higher U (median: 377 ppm), lower Th/U (median: 0.19) and generally bland CL suggesting a metamorphic origin.

The youngest cluster can be resolved with mixture modelling of the  $^{207}\text{Pb}/^{206}\text{Pb}$  ages as  $2615 \pm 3$  Ma and  $2625 \pm 3$  Ma. Mixture modelling of the second cluster indicates component ages at  $2653 \pm 4$  Ma,  $2669 \pm 4$  Ma and  $2684 \pm 4$  Ma. The veracity of these model ages is strongly dependent on the number of analyses and should be regarded with caution.



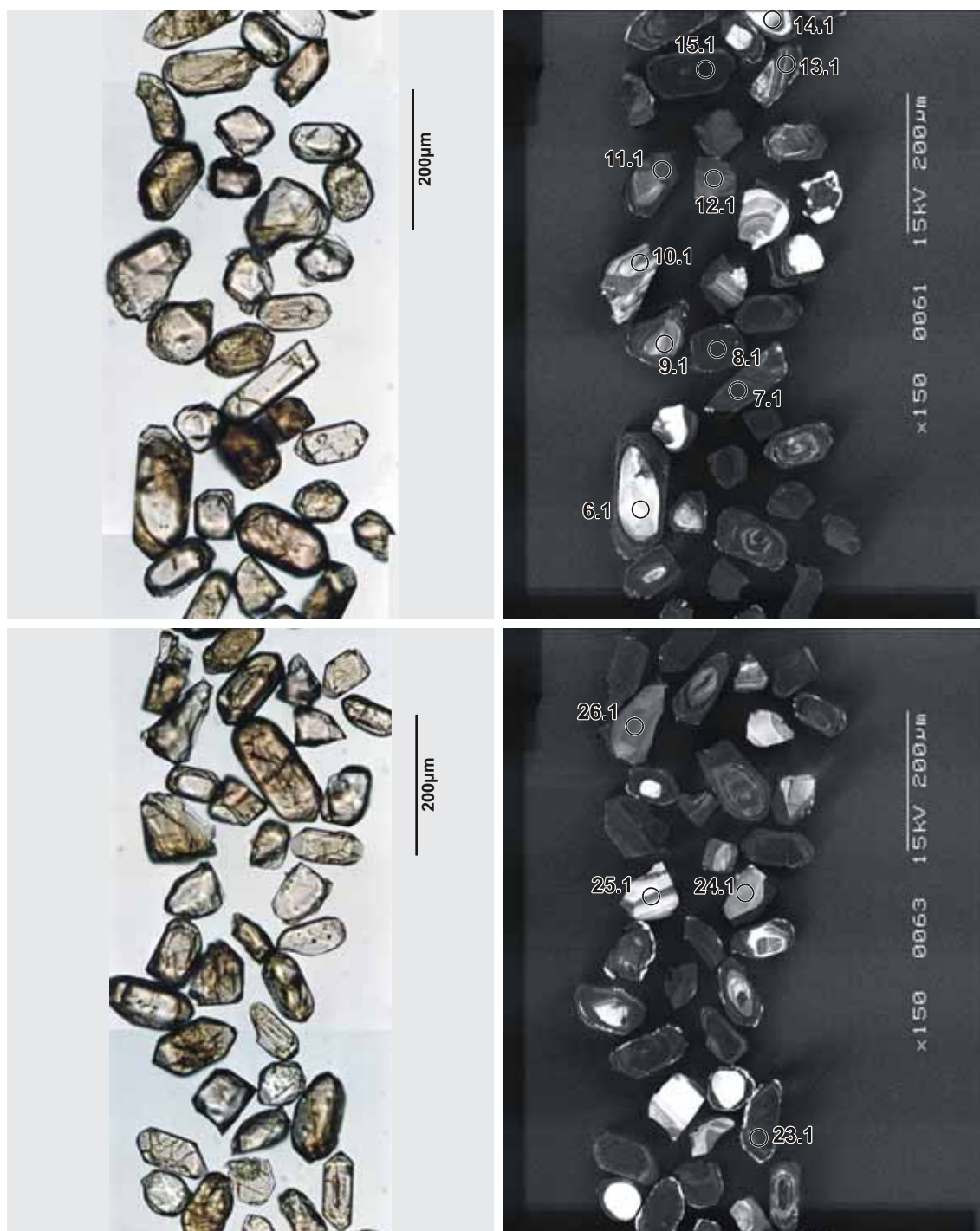


**Figure 29.** Representative images (transmitted light on left, cathodoluminescence on right) for sample 2004967004: Gibraltar quartz monzonite. SHRIMP analysis spots are labelled.

#### **GEOCHRONOLOGICAL INTERPRETATION**

This is a complex population of zircon derived from a complex geological history. The rock has inherited grains from a ~2950 Ma event. Zircon has been formed in an igneous event around ~2650 Ma to ~2700 Ma although the complexity of this event has been obscured by a later metamorphic event at ~2630 Ma.

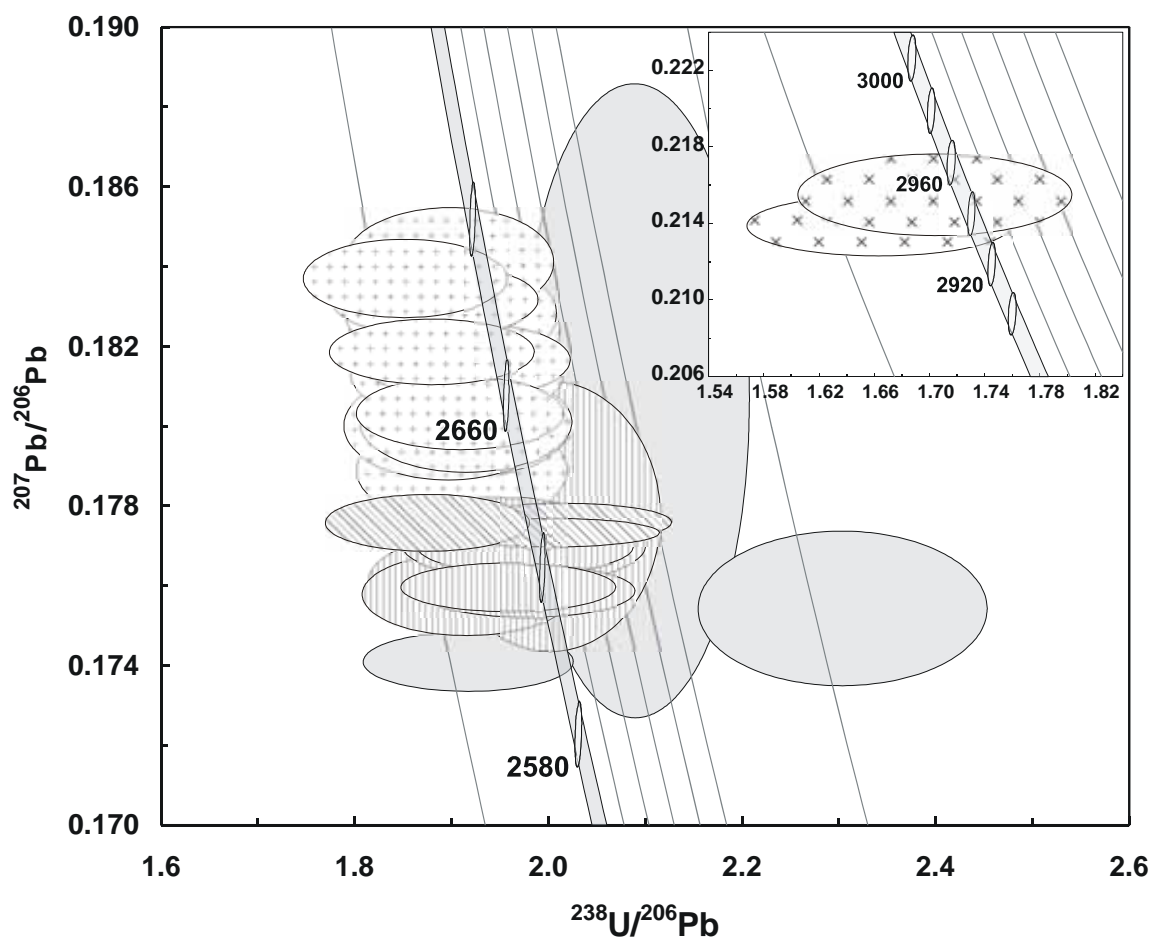


**Figure 30.** Tera-Wasserburg concordia plot for zircons from sample 2004967004: Gibraltar quartz monzonite. Plus-symbol hatching indicates older cluster and vertical hatching indicates younger cluster as discussed in text; diagonal hatching indicates group of analyses with >1000 ppm U; discordant and/or high common-Pb analyses are light grey; Inset: inherited analyses.

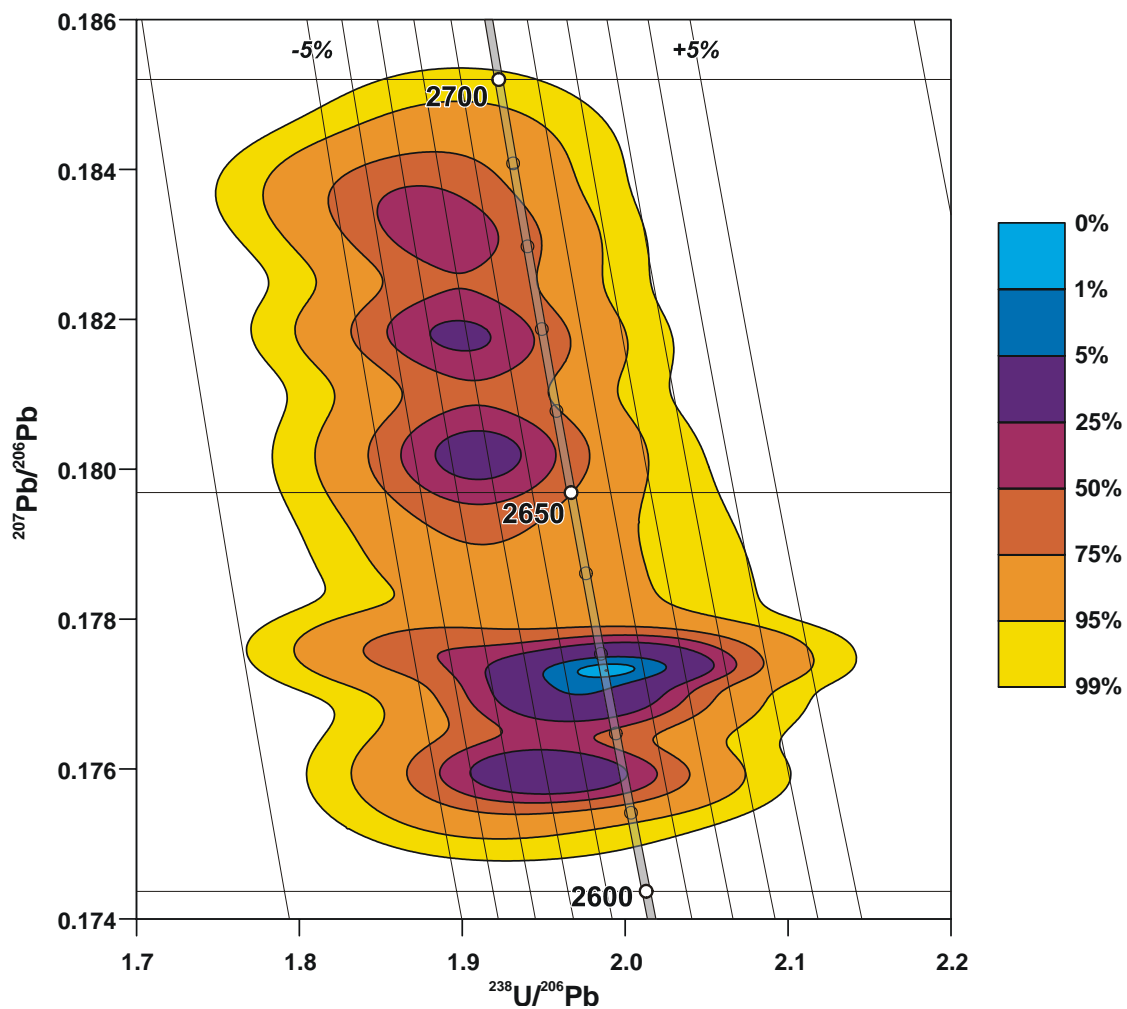


**Figure 31.** Concordia contour diagram of sample 2004967004: Gibraltar quartz monzonite illustrating concordant clusters: a dominant cluster 2630 – 2620 Ma and a broader cluster 2650 – 2690 Ma.

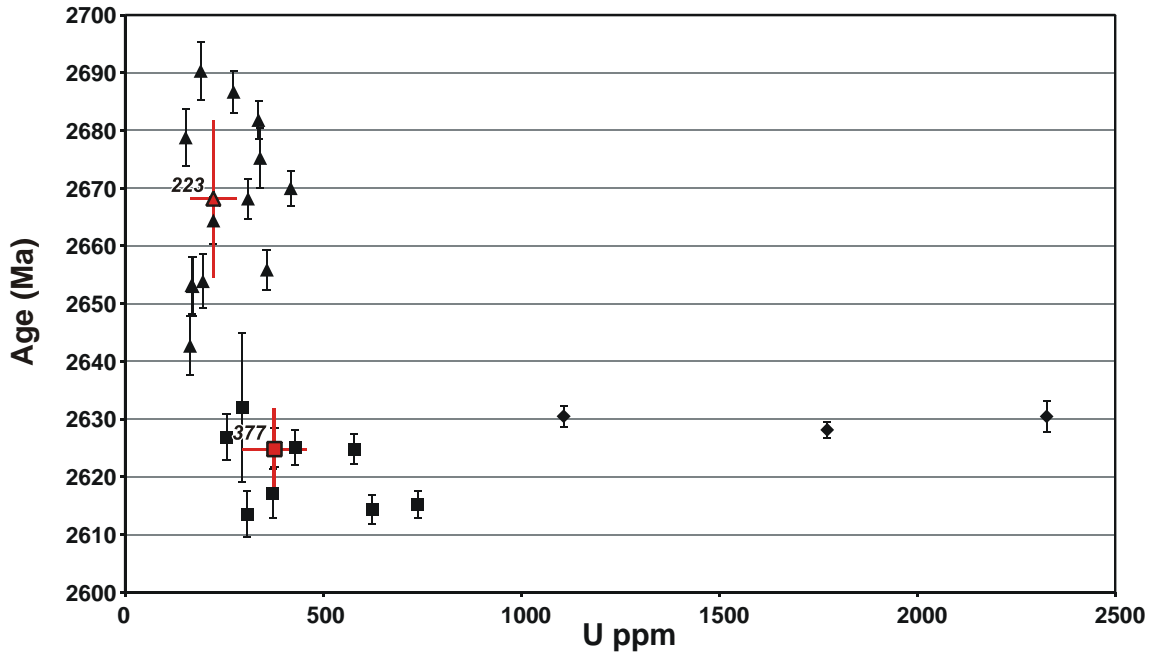


**Figure 32.** Plot of zircon age in relation to U content for zircons from sample 2004967004: Gibraltar quartz monzonite illustrating two potential clusters. As discussed in text: triangular markers indicate older cluster, square markers indicate younger cluster and diamond markers indicate concordant analyses with > 1000 ppm. The red markers and error bars indicate the median and median absolute deviation for each cluster.

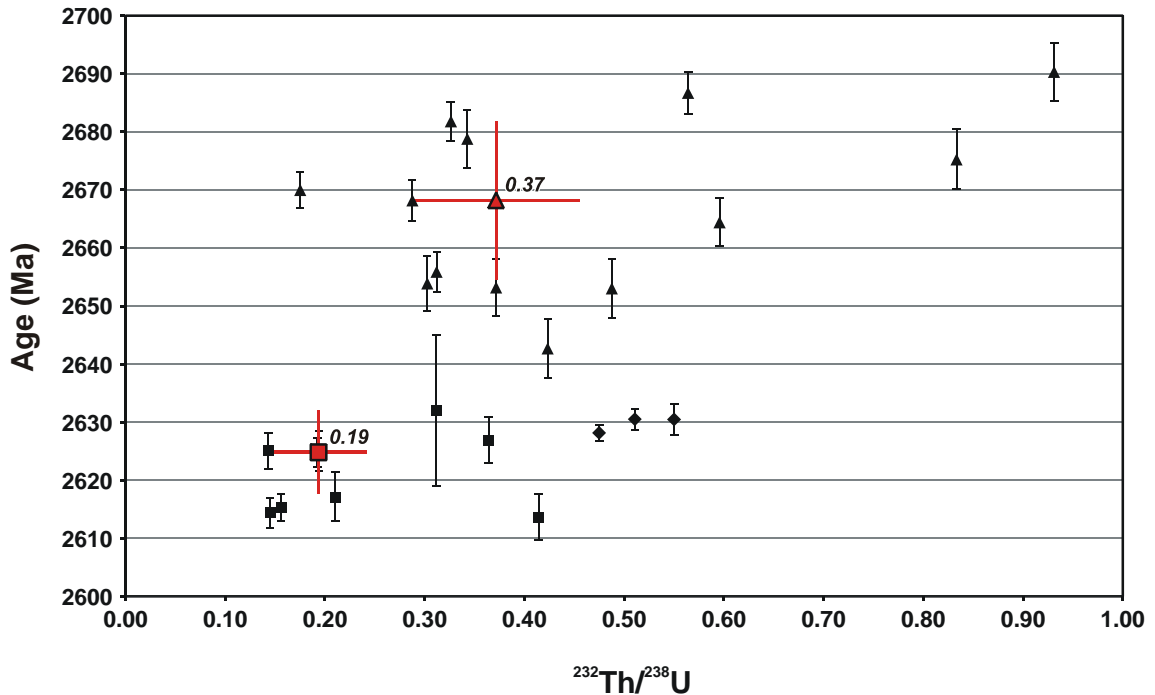


**Figure 33.** Plot of zircon age in relation to  $^{232}\text{Th}/^{238}\text{U}$  ratio for zircons from sample 2004967004: Gibraltar quartz monzonite illustrating two potential clusters. As discussed in text: triangular markers indicate older cluster, square markers indicate younger cluster and diamond markers indicate concordant analyses with > 1000 ppm. The red markers and error bars indicate the median and median absolute deviation for each cluster.

**Table 9.** SHRIMP analytical results for zircon from sample 2004967004: Gibraltar quartz monzonite.

Grain.Spot	U (ppm)	Th (ppm)	% comm 206	<sup>207</sup> Pb / <sup>206</sup> Pb	±	<sup>206</sup> Pb / <sup>238</sup> U	±	<sup>207</sup> Pb / <sup>235</sup> U	±	% Disc.	<sup>207</sup> Pb / <sup>206</sup> Pb Age (Ma)	±
<i>Metamorphic? cluster</i>												
31.1	308	123	0.052	0.1758	0.0004	0.5217	0.0121	12.6451	0.2940	-3.4	2613.6	4.0
7.1	623	88	0.006	0.1759	0.0003	0.5052	0.0116	12.2516	0.2826	-0.8	2614.4	2.6
30.1	738	112	0.084	0.1760	0.0002	0.5104	0.0118	12.3844	0.2868	-1.6	2615.3	2.3
12.1	373	76	0.029	0.1762	0.0004	0.5196	0.0121	12.6208	0.2945	-3.0	2617.1	4.2
28.1	578	108	0.014	0.1770	0.0003	0.5059	0.0116	12.3446	0.2847	-0.5	2624.8	2.5
3.1	429	59	0.012	0.1770	0.0003	0.5098	0.0118	12.4420	0.2888	-1.2	2625.1	3.1
1.1	377	71	0.024	0.1770	0.0004	0.5029	0.0117	12.2752	0.2873	-0.1	2625.1	3.5
27.1	256	90	0.022	0.1772	0.0004	0.5122	0.0119	12.5140	0.2912	-1.5	2626.9	3.9
5.1	1773	815	0.005	0.1773	0.0001	0.4992	0.0115	12.2069	0.2804	0.7	2628.1	1.4
15.1	2327	1239	0.000	0.1776	0.0003	0.5331	0.0123	13.0542	0.3015	-4.5	2630.5	2.7
18.1	1107	548	0.001	0.1776	0.0002	0.4963	0.0114	12.1523	0.2801	1.3	2630.5	1.8
11.1	295	89	0.425	0.1778	0.0014	0.4993	0.0116	12.2368	0.2989	0.8	2632.0	12.9
<i>Igneous? cluster</i>												
16.1	164	67	0.045	0.1789	0.0006	0.5233	0.0122	12.9080	0.3034	-2.6	2642.7	5.1
10.1	170	80	0.009	0.1800	0.0006	0.5270	0.0123	13.0817	0.3076	-2.8	2653.0	5.1
19.1	168	60	0.021	0.1800	0.0005	0.5225	0.0122	12.9697	0.3050	-2.1	2653.2	4.9
9.1	196	58	0.006	0.1801	0.0005	0.5219	0.0122	12.9617	0.3042	-2.0	2653.9	4.7
13.1	358	108	0.041	0.1803	0.0004	0.5236	0.0121	13.0197	0.3019	-2.2	2655.9	3.5
25.1	223	128	0.022	0.1813	0.0004	0.5247	0.0122	13.1132	0.3060	-2.0	2664.4	4.1
4.1	310	86	0.019	0.1817	0.0004	0.5222	0.0121	13.0795	0.3037	-1.5	2668.2	3.5
21.1	418	71	0.024	0.1819	0.0003	0.5318	0.0123	13.3351	0.3086	-2.9	2670.0	3.1
29.1	341	275	0.008	0.1824	0.0006	0.5253	0.0121	13.2136	0.3079	-1.7	2675.2	5.2
24.1	153	51	-0.011	0.1828	0.0005	0.5260	0.0123	13.2614	0.3118	-1.7	2678.8	4.9
26.1	337	106	0.023	0.1832	0.0004	0.5308	0.0123	13.4068	0.3111	-2.3	2681.8	3.3
20.1	273	149	0.024	0.1837	0.0004	0.5400	0.0125	13.6788	0.3179	-3.5	2686.7	3.6
17.1	191	172	0.015	0.1841	0.0006	0.5267	0.0123	13.3701	0.3138	-1.4	2690.3	5.0
<i>High-U</i>												
5.1	1773	815	0.005	0.1773	0.0001	0.4992	0.0115	12.2069	0.2804	0.7	2628.1	1.4
15.1	2327	1239	0.000	0.1776	0.0003	0.5331	0.0123	13.0542	0.3015	-4.5	2630.5	2.7
18.1	1107	548	0.001	0.1776	0.0002	0.4963	0.0114	12.1523	0.2801	1.3	2630.5	1.8
<i>Inherited</i>												
14.1	129	113	0.048	0.2139	0.0006	0.6012	0.0141	17.7304	0.4188	-3.3	2935.3	4.9
6.1	70	76	0.031	0.2155	0.0009	0.5868	0.0140	17.4368	0.4211	-1.0	2947.5	6.5
<i>Discordant</i>												
22.1	626	80	0.018	0.1741	0.0003	0.5215	0.0121	12.5186	0.2910	-4.0	2597.5	2.9
2.1	1447	314	0.006	0.1754	0.0008	0.4339	0.0115	10.4950	0.2823	12.4	2610.2	7.5
23.1	745	360	1.719	0.1806	0.0032	0.4783	0.0110	11.9141	0.3482	5.5	2658.8	29.8

Data are at 1 $\sigma$  precision. All Pb data are common-Pb corrected based on <sup>204</sup>Pb measurements. Mount: Z4437; Instrument: JdL Centre SHRIMP-A; Acquisition: 11 July 2004.



## 2004967007: biotite monzogranite dyke, Dinninup

### SAMPLE INFORMATION

**1:250,000 sheet:** Collie (SI5006)

**1:100,000 sheet:** Dinninup (2230)

**MGA:** 457550 mE 6257740 mN

**Location:** This sample taken from blasted rock on east side of road, approximately 1 km south of Dinninup.

**Description:** This rock is a grey, equigranular to sparsely feldspar-porphyrific, fine-grained, biotite monzogranite dyke. Alignment of biotite defines a very weak foliation. The dyke intrudes a fine- to coarse-grained, even-grained biotite granite, which forms the main rock type in the area. The area is intruded by several Proterozoic dolerite dykes.

The monzogranite has a granular texture. Principal minerals are quartz (35-40%), plagioclase (30%), K-feldspar (28-30%) and biotite (5-6%), with plagioclase  $\geq$  K-feldspar. Accessory phases include apatite, zircon and anhedral opaque minerals. Anhedral quartz is weakly recrystallised and displays minor undulose extinction, deformation lamellae and rare subgrains. Subhedral to anhedral plagioclase is weakly to locally moderately saussuritised to epidote, white mica and albite. K-feldspar, mainly microcline with minor perthite, is anhedral and unaltered, and forms a polygonal mosaic with quartz and plagioclase. Green-brown biotite flakes are moderately replaced by chlorite, epidote, opaque minerals and white mica.

### DESCRIPTION OF ZIRCONS

**Shape:** Sub-euhedral to euhedral prismatic grains ([Figure 34](#)).

**Size:** 50 to 300 microns.

**Colour/clarity:** Clear through pale yellow and hyacinth to turbid brown.

**Quality:** Poor to fair. Common cracks and inclusions.

**CL zoning:** Zoning generally bland although suggestions of concentric zoning, complex structures and cores ([Figure 34](#)).

### CONCURRENT STANDARD DATA

**Pb/U reprod.(2s):** 0.89%

**Err. of mean (2s):** 2.73%

**Standard:** QGNG

**Analyses:** 14 (one discarded with anomalously high U-Pb age)



## SAMPLE DATA

Thirty-two analyses were made on thirty-two grains (Table 10). Only one analysis (#9.1) is > 5% discordant and discarded from further interpretation (Figure 35). Analysis #5.1 yields an age significantly older than the remaining analyses that form a single cluster that yields a concordia age  $2610 \pm 6$  Ma (95% confidence; MSWD of concordance: 5.3; probability of concordance: 0.015). Although a reasonably good age, the relatively high MSWD and low probability of concordance would suggest some minor isotopic disturbance. A weak correlation of younger zircon ages tending to be associated with higher  $^{232}\text{Th}/^{238}\text{U}$  ratios hints that further complexity may exist in this sample (Figure 36).



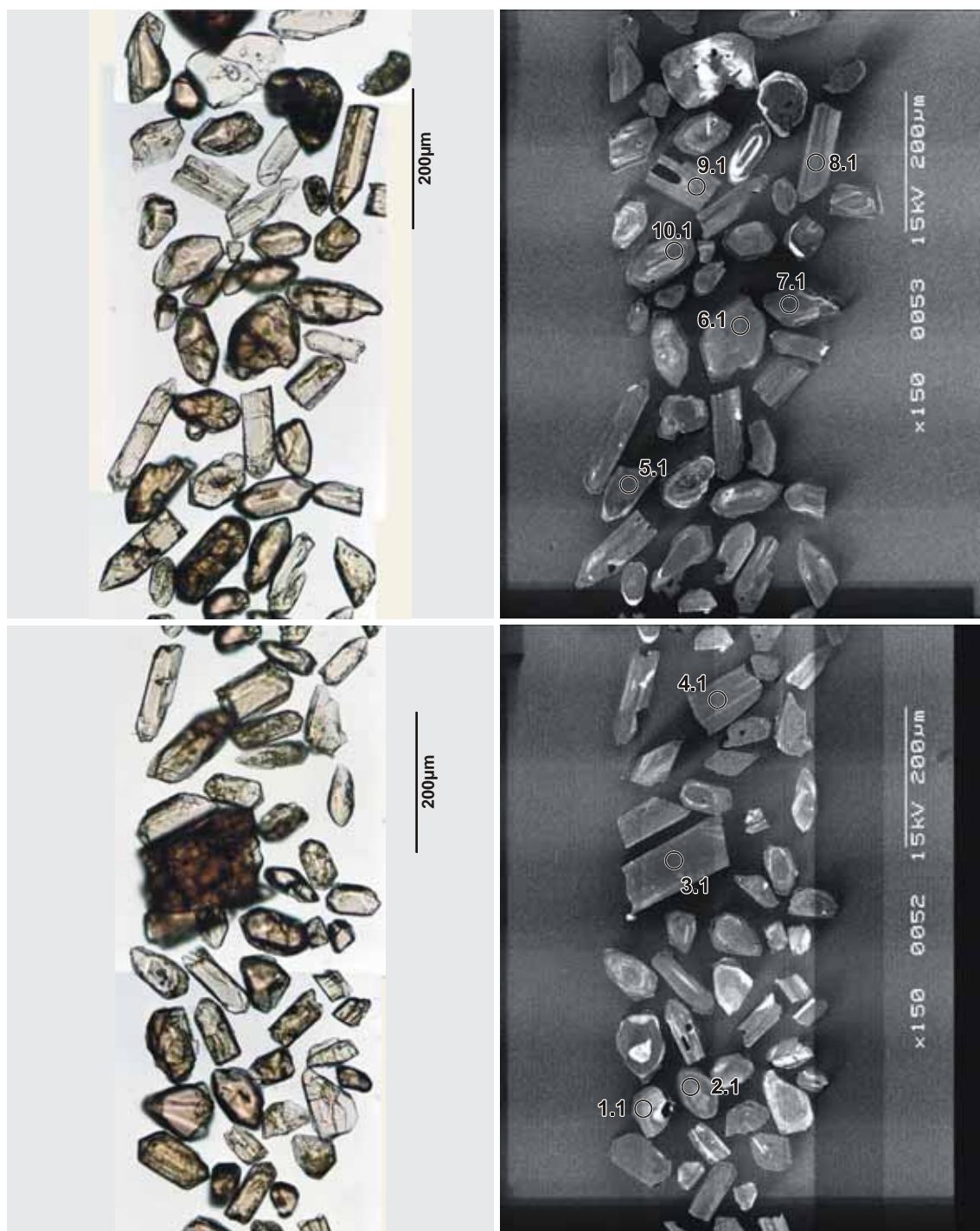


**Figure 34.** Representative images (transmitted light on left, cathodoluminescence on right) for sample 2004967007: biotite monzogranite dyke, Dinninup. SHRIMP analysis spots are labelled.

#### GEOCHRONOLOGICAL INTERPRETATION

The age of  $2610 \pm 6$  Ma is interpreted as the age of magmatic emplacement of the granitic dyke.

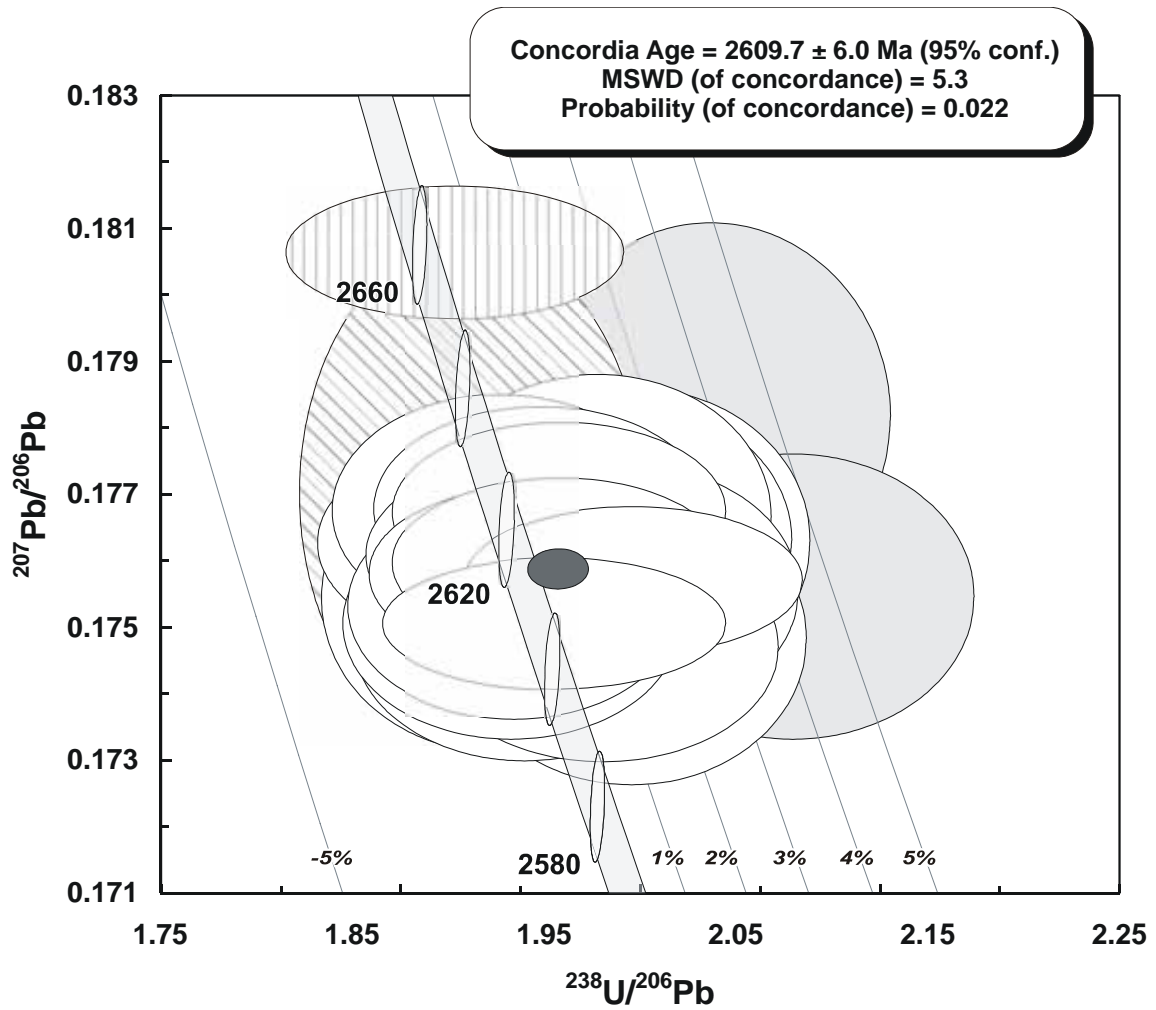


**Figure 35.** Tera-Wasserburg concordia plot for zircons from sample 2004967007: biotite monzogranite dyke, Dinninup. White-filled error ellipses indicate analyses used for calculating concordia age of  $2610 \pm 7$  Ma (indicated by dark grey error ellipse). Vertical hatch indicates analysis interpreted as inheritance; diagonal hatch indicates analysis considered as a blend; light-grey fill indicates analyses with high common-Pb.

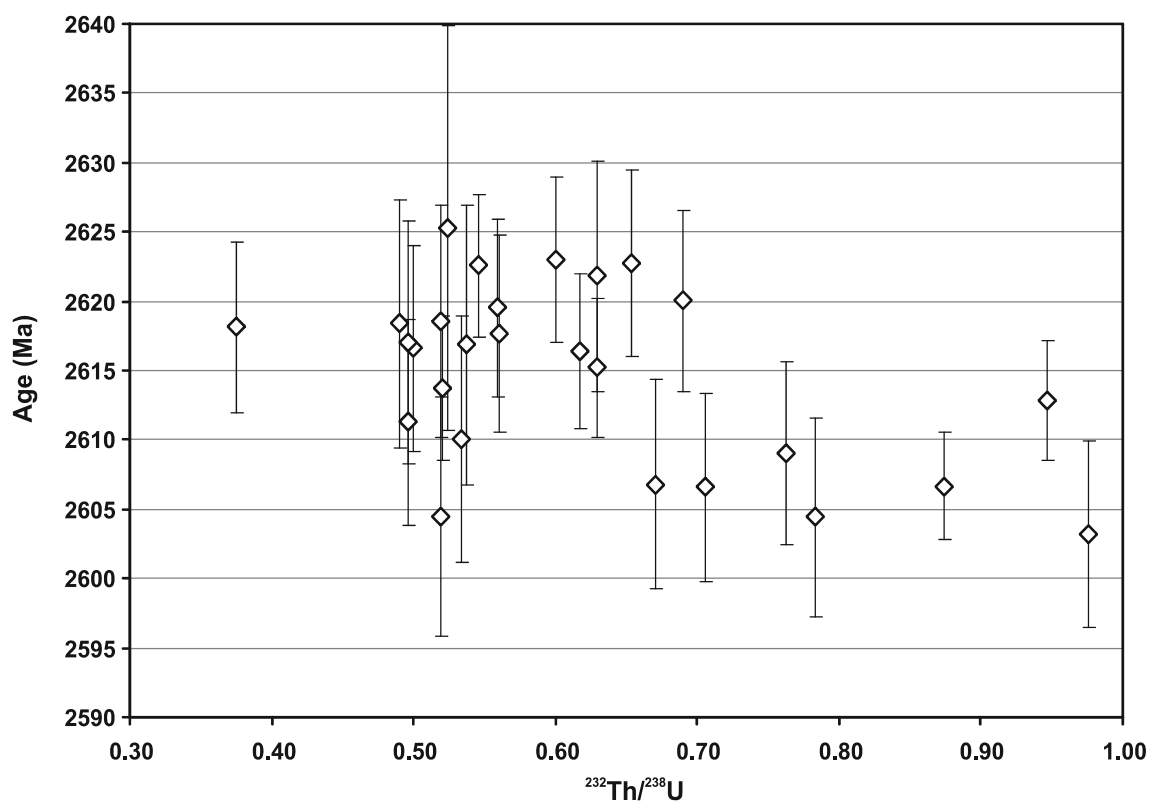


**Figure 36.** Plot of zircon age in relation to  $^{232}\text{Th}/^{238}\text{U}$  ratio for zircons from sample 2004967007: biotite monzogranite dyke, Dinninup illustrating a weak correlation toward higher ratio values for younger zircon analyses as discussed in text.

**Table 10.** SHRIMP analytical results for zircon from sample 2004967007: biotite monzogranite dyke, Dinninup.

Grain.Spot	U (ppm)	Th (ppm)	% comm 206	<sup>207</sup> Pb / <sup>206</sup> Pb	±	<sup>206</sup> Pb / <sup>238</sup> U	±	<sup>207</sup> Pb / <sup>235</sup> U	±	% Disc.	<sup>207</sup> Pb / <sup>206</sup> Pb Age (Ma)	±
<i>Magmatic</i>												
8.1	529	499	0.221	0.1747	0.0007	0.4916	0.0072	11.8411	0.1803	1.0	2603.1	6.7
15.1	608	461	0.161	0.1748	0.0008	0.4996	0.0073	12.0424	0.1829	-0.3	2604.4	7.2
32.1	321	161	0.140	0.1748	0.0009	0.4887	0.0071	11.7815	0.1821	1.5	2604.5	8.6
12.1	451	308	0.152	0.1751	0.0007	0.5010	0.0072	12.0932	0.1802	-0.4	2606.6	6.8
4.1	811	686	0.055	0.1751	0.0004	0.4966	0.0072	11.9867	0.1764	0.3	2606.6	3.9
27.1	476	309	0.046	0.1751	0.0008	0.4995	0.0071	12.0579	0.1807	-0.2	2606.8	7.5
7.1	571	421	0.273	0.1753	0.0007	0.5007	0.0071	12.1039	0.1784	-0.3	2609.1	6.6
1.1	249	129	0.121	0.1754	0.0009	0.5028	0.0074	12.1612	0.1910	-0.6	2610.0	8.9
24.1	592	285	0.282	0.1756	0.0008	0.4890	0.0069	11.8370	0.1758	1.7	2611.3	7.4
3.1	718	657	0.083	0.1757	0.0005	0.4885	0.0069	11.8353	0.1691	1.9	2612.8	4.3
22.1	773	389	0.029	0.1758	0.0006	0.4985	0.0070	12.0827	0.1741	0.2	2613.7	5.2
13.1	839	512	0.100	0.1760	0.0005	0.4961	0.0070	12.0362	0.1728	0.7	2615.2	5.0
25.1	649	387	0.072	0.1761	0.0006	0.4988	0.0071	12.1108	0.1760	0.3	2616.4	5.6
18.1	412	199	0.111	0.1761	0.0008	0.4981	0.0072	12.0961	0.1823	0.4	2616.6	7.4
30.1	295	153	0.444	0.1761	0.0011	0.4928	0.0072	11.9676	0.1896	1.3	2616.8	10.1
21.1	344	165	0.106	0.1762	0.0009	0.4926	0.0072	11.9642	0.1854	1.3	2617.0	8.8
17.1	624	339	0.106	0.1762	0.0008	0.4991	0.0071	12.1266	0.1793	0.3	2617.6	7.1
28.1	556	202	0.106	0.1763	0.0007	0.5022	0.0078	12.2066	0.1951	-0.2	2618.1	6.2
31.1	313	149	0.187	0.1763	0.0009	0.4885	0.0071	11.8745	0.1850	2.1	2618.4	8.9
26.1	402	202	0.053	0.1763	0.0009	0.4911	0.0075	11.9393	0.1931	1.6	2618.5	8.4
2.1	336	182	0.118	0.1764	0.0007	0.4964	0.0072	12.0752	0.1809	0.8	2619.5	6.4
10.1	628	419	0.049	0.1765	0.0007	0.4973	0.0071	12.1019	0.1780	0.7	2620.1	6.5
19.1	319	194	0.152	0.1767	0.0009	0.4922	0.0072	11.9903	0.1850	1.6	2621.8	8.3
16.1	690	364	0.046	0.1767	0.0006	0.4961	0.0070	12.0886	0.1747	1.0	2622.6	5.2
29.1	464	293	0.102	0.1768	0.0007	0.5022	0.0072	12.2404	0.1820	0.0	2622.7	6.7
20.1	645	374	0.082	0.1768	0.0006	0.4979	0.0070	12.1378	0.1771	0.7	2623.0	5.9
<i>Inheritance</i>												
5.1	837	606	0.048	0.1808	0.0004	0.5067	0.0071	12.6285	0.1791	0.6	2659.8	3.8
<i>Blended?</i>												
6.1	272	138	0.065	0.1770	0.0016	0.5053	0.0074	12.3336	0.2111	-0.4	2625.3	14.6
<i>Discordant/High common-Pb</i>												
9.1	449	189	1.321	0.1742	0.0018	0.3618	0.0052	8.6913	0.1554	23.4	2598.7	17.6
11.1	572	345	0.622	0.1755	0.0009	0.4732	0.0069	11.4470	0.1768	4.3	2610.4	8.4
14.1	302	153	0.676	0.1782	0.0012	0.4810	0.0070	11.8182	0.1903	4.0	2636.1	11.1

Data are at 1 $\sigma$  precision. All Pb data are common-Pb corrected based on <sup>204</sup>Pb measurements. Mount: Z4437; Instrument: JdL Centre SHRIMP-B; Acquisition: 31 July 2004.



## 2004967009: biotite granite, Wilyungulup Spring

### SAMPLE INFORMATION

**1:250,000 sheet:** Collie (SI5006)

**1:100,000 sheet:** Bridgetown (2130)

**MGA:** 440350 mE 6255070 mN

**Location:** This sample taken from blasted rock on north side of road, about 1.5 km north of Wilyungulup Spring and approximately 3 km west of Boyup Brook.

**Description:** This rock is a grey, foliated to weakly banded, seriate to sparsely feldspar-porphyritic, medium- to coarse-grained, biotite monzogranite. It is representative of the main rock type in the area. Incipient compositional layering mainly due to variations in grain size and biotite content, and biotite-rich seams and schlieren, result in the rock having a weakly banded appearance in places. Alignment of biotite defines a moderate foliation, parallel to banding. The monzogranite is cut by minor, thin quartz-feldspar veins.

The sample is characterised by a granular to granoblastic texture. Principal minerals are quartz (30%), plagioclase (35-40%), K-feldspar (25-30%) and biotite (5-7%), with plagioclase > K-feldspar. Accessory phases include minor titanite (~1%), apatite, zircon, and anhedral opaque minerals. Plagioclase forms subhedral to anhedral grains and minor phenocrysts to 1 cm in size and is incipiently altered to albite, white mica and epidote. K-feldspar, dominantly microcline, forms anhedral grains interstitial to plagioclase and quartz, and rare phenocrysts to 1 cm in length. Quartz is anhedral and displays weak subgrain development with sutured grain boundaries, deformation lamellae and undulose extinction. Plagioclase, K-feldspar and quartz are recrystallised along grain boundaries to a very fine-grained mosaic of quartz, feldspar, biotite, epidote, chlorite and opaque minerals. Aligned green-brown biotite flakes define a weak fabric. Biotite is weakly to locally moderately altered to epidote, chlorite, leucoxene and white mica, mainly along grain boundaries.

### DESCRIPTION OF ZIRCONS

**Shape:** Euhedral prismatic (Figure 37).

**Size:** 50 to 200 microns.

**Colour/clarity:** Brown and fairly clear.

**Quality:** Few cracks and inclusions.



**CL zoning:** Mixture of bright concentric zones and bland bands. Some complex core/rim associations (Figure 37).

#### CONCURRENT STANDARD DATA

**Pb/U reprod.(2s):** 1.84%

**Err. of mean (2s):** 6.33%

**Standard:** QGNG

**Analyses:** 15 (one discarded as anomalously young)

**Notes:** The reproducibility of this run was poor due to charging effects on the mount surface. While this will affect the calibration of the Pb/U values, Pb/Pb values are largely used here to calculate ages.

#### SAMPLE DATA

Thirty-five analyses were made on thirty-two grains (Table 11; Figure 38). Two analyses on grain #11 are > 5% discordant. Two analyses on a core/rim structure in grain #22 yielded two significantly different ages at  $2684 \pm 14$  Ma (#22.1 core) and  $2637 \pm 11$  Ma (#22.2 rim) indicating that there are two distinct zircon growth phases represented in this sample.

Further inspection of the data also confirms the presence of two zircon phases. A concordia contour plot of the data (Figure 39) shows two clusters at ~2690 Ma and ~2640 Ma with suggestion of smaller clusters or, more probably, analytical mixing between these ages. Plotting the zircon age against U content (Figure 40) and  $^{232}\text{Th}/^{238}\text{U}$  ratio (Figure 41) also demonstrates distinct differences between the clusters. The older cluster has a lower U content (median: 297 ppm) and higher  $^{232}\text{Th}/^{238}\text{U}$  ratio (median: 0.49); the CL pattern of zircons in this cluster also tends to be concentric. The younger cluster has a higher U content (median: 855 ppm) and lower  $^{232}\text{Th}/^{238}\text{U}$  ratio (median: 0.19) with a typically bland CL pattern.

Mixture modelling of the age results yields four model components at  $2635 \pm 5$ ,  $2651 \pm 7$  Ma,  $2672 \pm 8$  and  $2692 \pm 4$  Ma (Figure 42) with the first and last components being dominant.



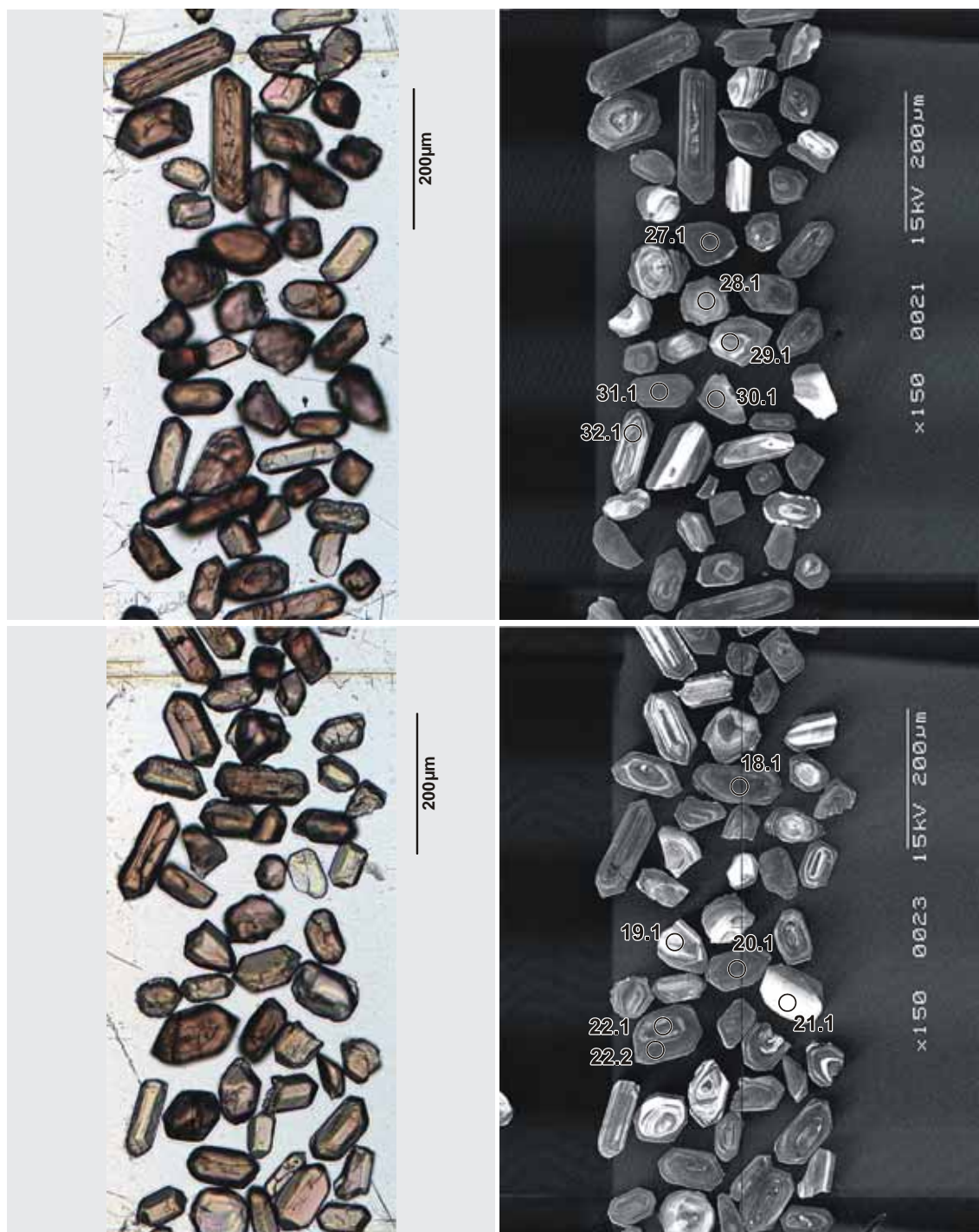


**Figure 37.** Representative images (transmitted light on left, cathodoluminescence on right) for sample 2004967009: biotite granite, Wilyungulup Spring. SHRIMP analysis spots are labelled.

### GEOCHRONOLOGICAL INTERPRETATION

The older mixture model age of  $2692 \pm 4$  Ma is interpreted as a magmatic protolith age with the younger mixture model age of  $2635 \pm 5$  Ma representing a metamorphic zircon growth event.

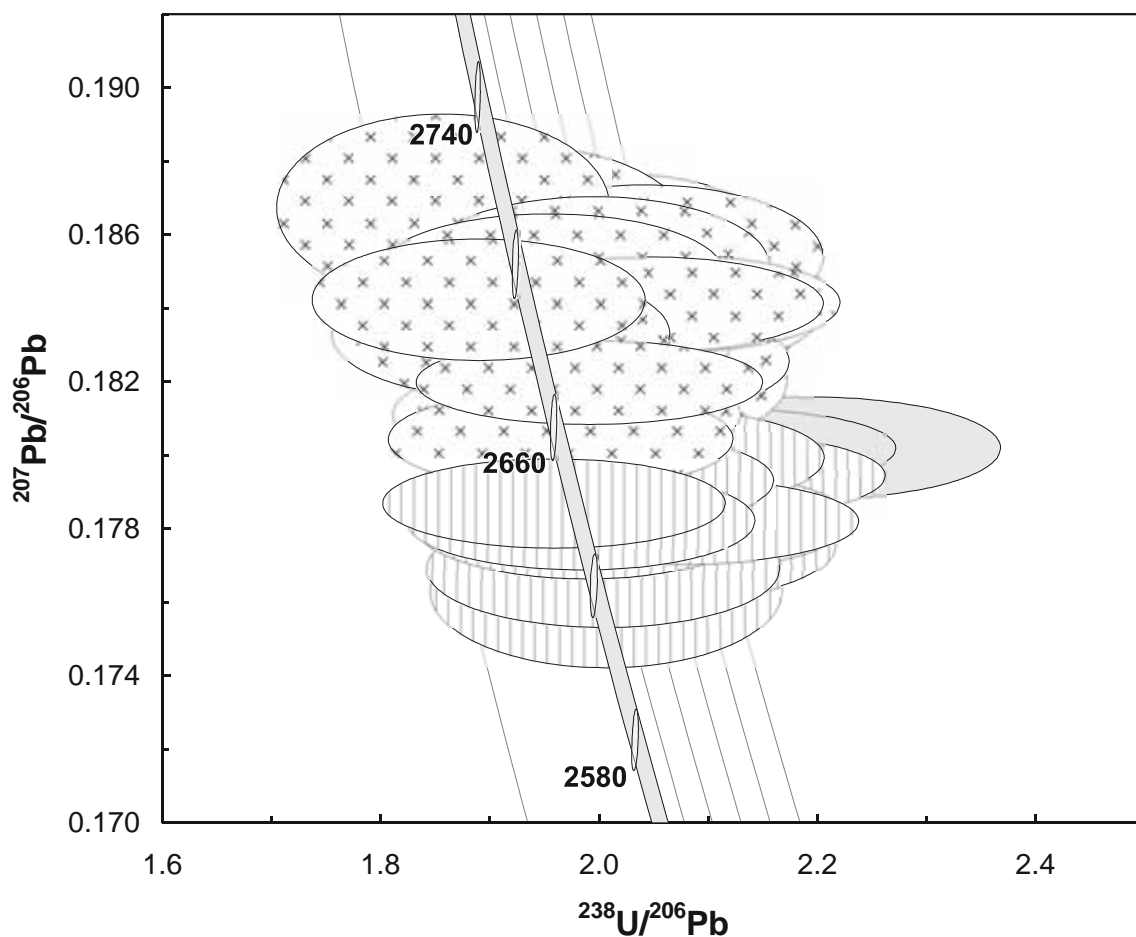


**Figure 38.** Tera-Wasserburg concordia plot for zircons from sample 2004967009: biotite granite, Wilyungulup Spring. The two concordant clusters discussed in text are indicated by vertical and cross hatching; discordant and/or high common-Pb analyses are light grey.

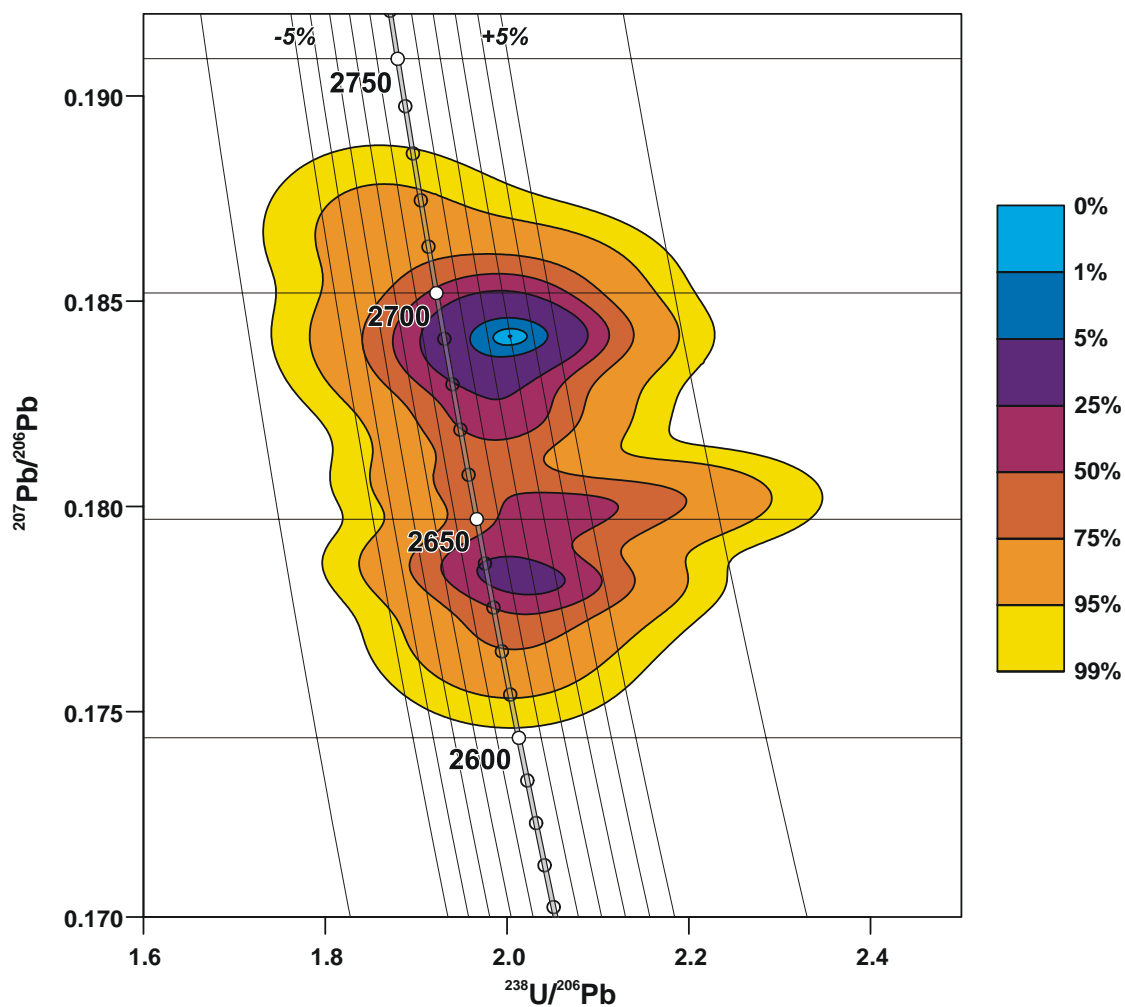


**Figure 39.** Concordia contour plot for zircons from sample 2004967009: biotite granite, Wilyungulup Spring (effectively the equivalent of [Figure 38](#)) illustrating the two clusters at ~2690 Ma and ~2640 Ma discussed in the text.

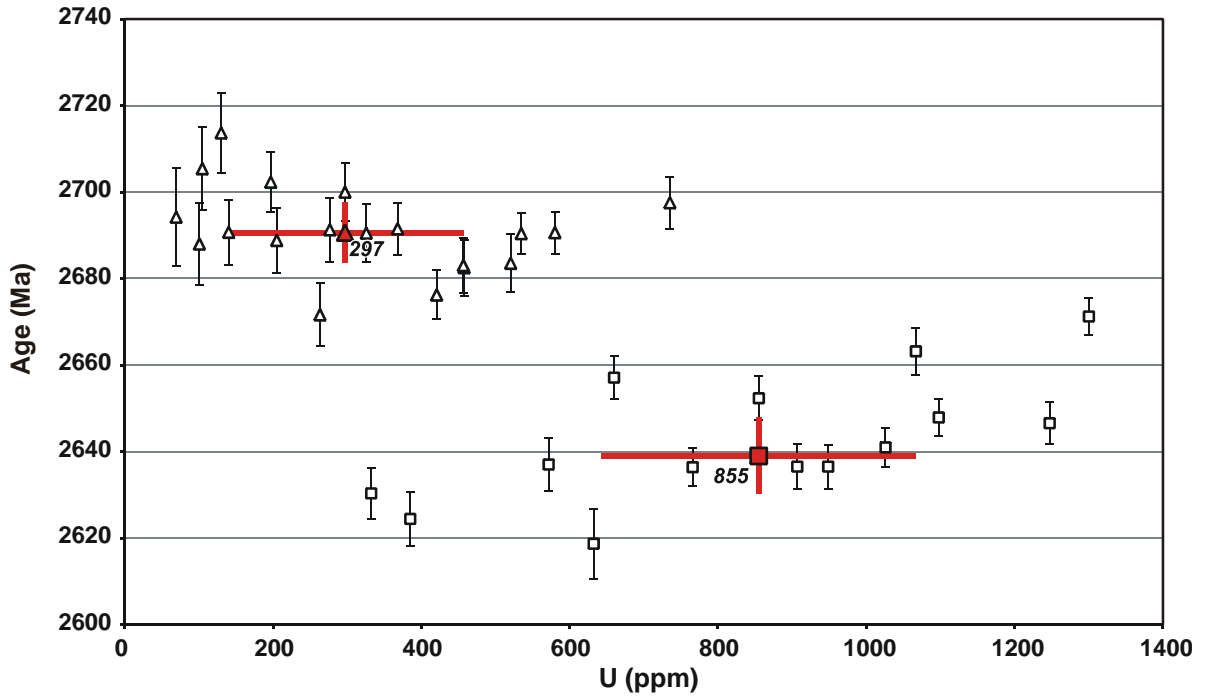


**Figure 40.** Plot of zircon age in relation to U content for zircons from sample 2004967009: biotite granite, Wilyungulup Spring illustrating two potential clusters. Triangular markers indicate the older cluster and square markers indicate the younger cluster. The red markers and error bars indicate the median and median absolute deviation for each cluster.

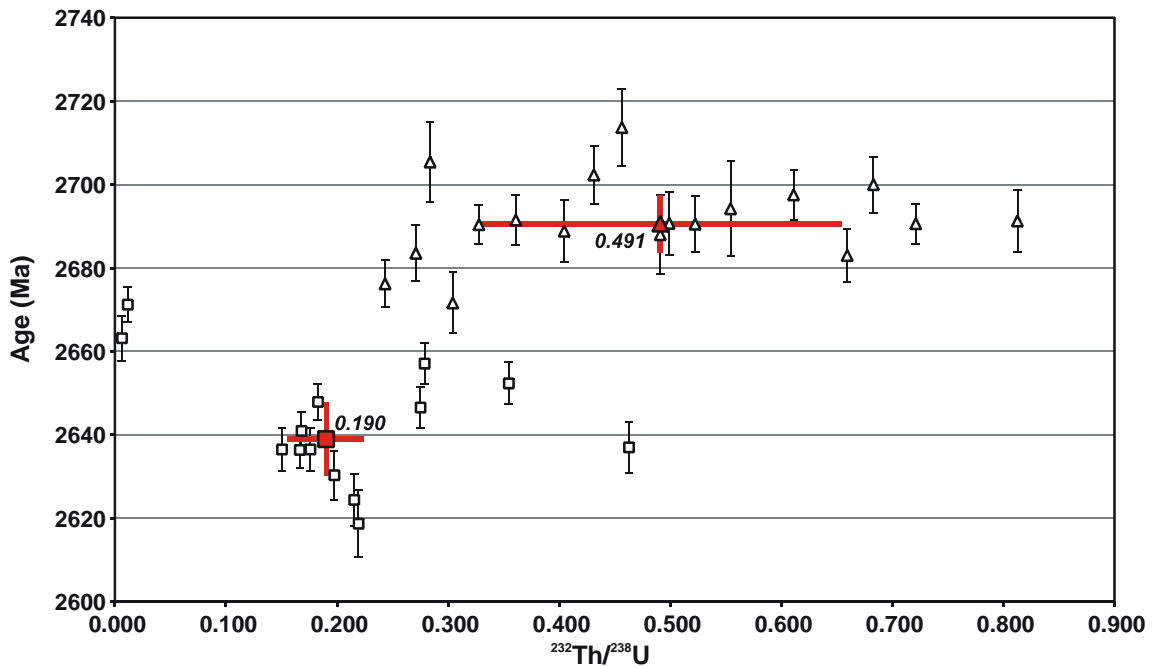


**Figure 41.** Plot of zircon age in relation to  $^{232}\text{Th}/^{238}\text{U}$  ratio for zircons from sample 2004967009: biotite granite, Wilyungulup Spring illustrating two potential clusters. Triangular markers indicate the older cluster and square markers indicate the younger cluster. The red markers and error bars indicate the median and median absolute deviation for each cluster.

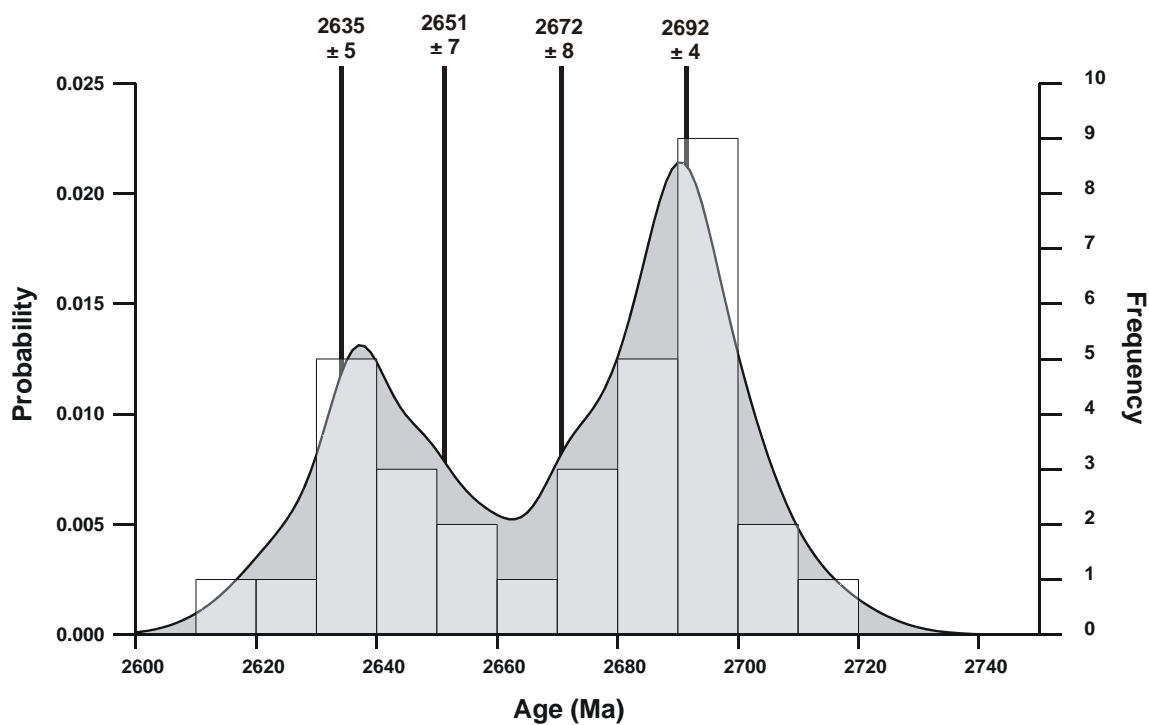


**Figure 42.** Probability density distribution and histogram plot of concordant  $^{207}\text{Pb}/^{206}\text{Pb}$  ages from sample 2004967009: biotite granite, Wilyungulup Spring with mixture modelled age components shown.

**Table 11.** SHRIMP analytical results for zircon from sample 2004967009: biotite granite, Wilyungulup Spring.

Grain.Spot	U (ppm)	Th (ppm)	% comm 206	<sup>207</sup> Pb / <sup>206</sup> Pb	±	<sup>206</sup> Pb / <sup>238</sup> U	±	<sup>207</sup> Pb / <sup>235</sup> U	±	% Disc.	<sup>207</sup> Pb / <sup>206</sup> Pb Age (Ma)	±
<i>Older cluster</i>												
16.1	660	178	-0.001	0.1805	0.0005	0.5096	0.0168	12.6801	0.4190	0.1	2657.1	5.0
10.1	1067	7	0.156	0.1811	0.0006	0.5083	0.0167	12.6945	0.4201	0.5	2663.2	5.4
18.1	1300	15	-0.003	0.1820	0.0005	0.5030	0.0165	12.6223	0.4147	1.7	2671.2	4.3
10.2	263	78	0.074	0.1821	0.0008	0.4989	0.0167	12.5226	0.4217	2.3	2671.7	7.3
1.1	421	99	0.029	0.1826	0.0006	0.4979	0.0165	12.5317	0.4184	2.7	2676.2	5.6
7.1	458	585	0.040	0.1833	0.0007	0.5055	0.0168	12.7726	0.4262	1.7	2682.5	6.5
32.1	457	291	0.053	0.1833	0.0007	0.5244	0.0174	13.2536	0.4437	-1.3	2683.0	6.4
22.1	521	137	0.473	0.1834	0.0008	0.5096	0.0169	12.8830	0.4295	1.1	2683.6	6.8
12.1	101	48	0.074	0.1839	0.0011	0.4963	0.0166	12.5808	0.4263	3.4	2688.0	9.5
28.1	205	80	0.059	0.1840	0.0008	0.5141	0.0171	13.0392	0.4382	0.5	2688.9	7.5
4.1	535	170	0.012	0.1841	0.0005	0.4903	0.0160	12.4463	0.4090	4.4	2690.4	4.7
29.1	326	165	0.059	0.1841	0.0007	0.4998	0.0166	12.6894	0.4245	2.9	2690.5	6.7
13.1	580	405	-0.007	0.1842	0.0005	0.4868	0.0159	12.3593	0.4055	5.0	2690.6	4.8
3.1	140	68	0.075	0.1842	0.0008	0.4964	0.0165	12.6040	0.4219	3.4	2690.7	7.5
19.1	276	217	0.019	0.1842	0.0008	0.4905	0.0164	12.4598	0.4191	4.4	2691.3	7.4
30.1	368	129	0.031	0.1843	0.0007	0.5300	0.0175	13.4639	0.4477	-1.9	2691.5	6.0
21.1	69	37	0.084	0.1846	0.0013	0.4940	0.0169	12.5708	0.4377	3.9	2694.2	11.4
2.1	735	435	0.035	0.1849	0.0007	0.5123	0.0172	13.0621	0.4419	1.2	2697.6	6.0
15.1	297	196	0.083	0.1852	0.0008	0.5020	0.0166	12.8198	0.4273	2.9	2700.0	6.7
9.1	197	82	0.044	0.1855	0.0008	0.4908	0.0162	12.5496	0.4179	4.7	2702.3	6.9
23.1	105	29	0.062	0.1858	0.0011	0.5190	0.0176	13.2952	0.4565	0.4	2705.4	9.5
24.1	130	57	0.088	0.1867	0.0010	0.5392	0.0181	13.8845	0.4733	-2.5	2713.7	9.2
<i>Younger cluster</i>												
14.1	632	134	0.828	0.1763	0.0009	0.4990	0.0164	12.1322	0.4026	0.4	2618.7	8.1
27.1	385	80	0.034	0.1769	0.0007	0.4998	0.0165	12.1935	0.4055	0.4	2624.5	6.2
8.1	332	64	0.032	0.1776	0.0006	0.4881	0.0160	11.9517	0.3948	2.6	2630.4	5.9
6.1	766	123	0.011	0.1782	0.0005	0.4831	0.0158	11.8717	0.3896	3.6	2636.4	4.4
22.2	949	138	0.130	0.1782	0.0005	0.5048	0.0166	12.4052	0.4106	0.1	2636.5	5.1
20.1	907	154	0.357	0.1782	0.0006	0.4852	0.0159	11.9229	0.3925	3.3	2636.5	5.2
26.1	571	256	0.090	0.1783	0.0007	0.5037	0.0168	12.3814	0.4144	0.3	2637.0	6.2
31.1	1026	167	0.023	0.1787	0.0005	0.5113	0.0168	12.5986	0.4154	-0.8	2641.0	4.6
25.1	1247	332	0.244	0.1793	0.0005	0.5008	0.0165	12.3825	0.4089	1.1	2646.6	4.9
5.1	1097	194	0.013	0.1795	0.0005	0.4780	0.0157	11.8279	0.3891	4.9	2647.9	4.4
17.1	855	293	0.030	0.1799	0.0006	0.4902	0.0161	12.1634	0.4018	3.0	2652.4	5.1
<i>Discordant</i>												
11.2	879	13	0.025	0.1802	0.0005	0.4756	0.0155	11.8184	0.3857	5.5	2654.8	4.2
11.1	451	7	0.039	0.1802	0.0006	0.4564	0.0149	11.3408	0.3716	8.7	2654.9	5.2

Data are at 1 $\sigma$  precision. All Pb data are common-Pb corrected based on <sup>204</sup>Pb measurements. Mount: Z4438; Instrument: JdL Centre SHRIMP-B; Acquisition: 24 October 2004.



## 2004967550: biotite syenogranite dyke, Nanicup Bridge

### SAMPLE INFORMATION

**1:250,000 sheet:** SI5007 Dumbleyung

**1:100,000 sheet:** 2530 Nyang

**MGA:** 620045 mE 6270742 mN

**Location:** The sample was taken from Dominion Mining Ltd diamond drill hole 04NBDH005, depth interval 102.00-102.47 m. The collar is located approximately 20 km southeast of Nyabing.

**Description:** This rock is from a grey-white, altered, seriate medium-coarse grained biotite syenogranite dyke. The dyke contains pegmatoid zones with prominent graphic intergrowth between quartz and K-feldspar. These dykes intrude garnet-bearing quartzofeldspathic gneisses and post date granulite facies regional metamorphism. Minor late brittle fractures and cataclastic zones, with quartz, prehnite and/or zeolite minerals in-fill, cut all lithologies.

The unit has a granular texture. Principal minerals are quartz (30%), K-feldspar (50%), plagioclase (~15%) and biotite (5-6%), with K-feldspar > plagioclase. K-feldspar, dominantly microcline with minor perthite, forms large, cloudy anhedral grains to 2 cm in length. Quartz is anhedral, interstitial to K-feldspar and plagioclase, and displays undulose extinction and patchy minor subgrain development. Plagioclase is anhedral to subhedral, cloudy and generally partly altered to albite, sericite, clinozoisite and chlorite. Biotite is mainly anhedral and interstitial and generally completely replaced by chlorite, clinozoisite/epidote and leucoxene. Accessory phases include trace zircon, titanite, monazite and anhedral opaque minerals.

### DESCRIPTION OF ZIRCONS

**Shape:** Largely euhedral and prismatic grains, with occasional rounded terminations (Figure 43). Two distinct morphological end-members occur with equant and elongated prismatic grains.

**Size:** 100 to 200 microns.

**Colour/clarity:** Mostly clear.

**Quality:** Very good. Cracks and inclusions uncommon.

**CL zoning:** Sector zoning prominent. Occasional complex embayment and truncation structures (Figure 43).

### CONCURRENT STANDARD DATA

**Pb/U reprod.(2s):** 0.65 %



**Err. of mean (2s):** 2.53 %

**Standard:** QGNG

**Analyses:** 21 (two discarded as anomalous)

#### **SAMPLE DATA**

Thirty-eight analyses were made on thirty-seven grains with only one analysis > 5% discordant ([Table 12](#)). These analyses form a remarkably homogeneous suite with no evidence of multiple zircon phases and no significant difference between the equant and elongated morphologies.

A concordia age of  $2638.4 \pm 6.5$  Ma is calculated with two analyses (#14.1 and #37.1) set aside as outliers ([Figure 44](#)).



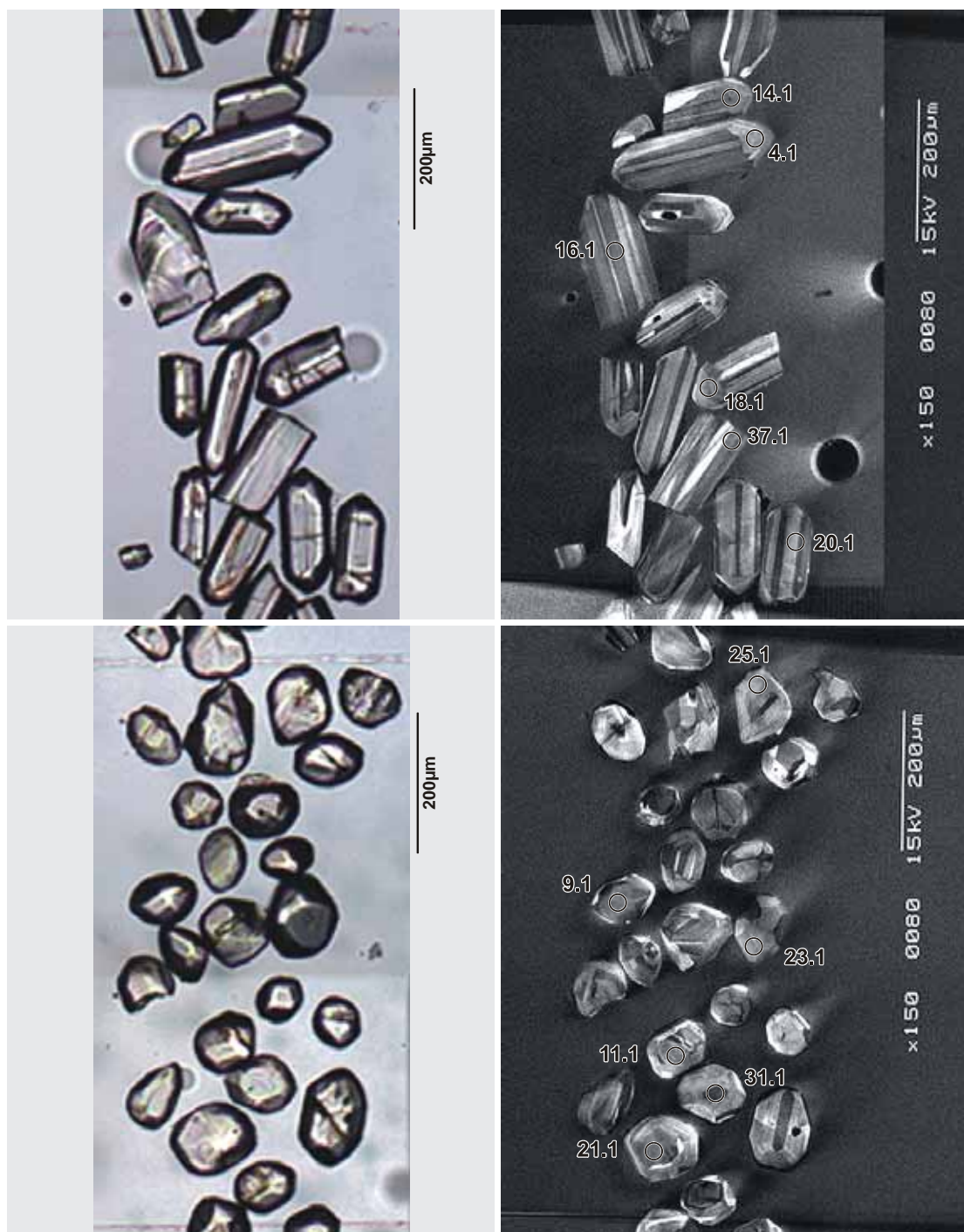


**Figure 43.** Representative images (transmitted light on left, cathodoluminescence on right) for sample 2004967550: biotite syenogranite dyke, Nanicup Bridge. SHRIMP analysis spots are labelled.

#### GEOCHRONOLOGICAL INTERPRETATION

The age of  $2638 \pm 7$  Ma is interpreted as the age of magmatic emplacement of the syenogranite.

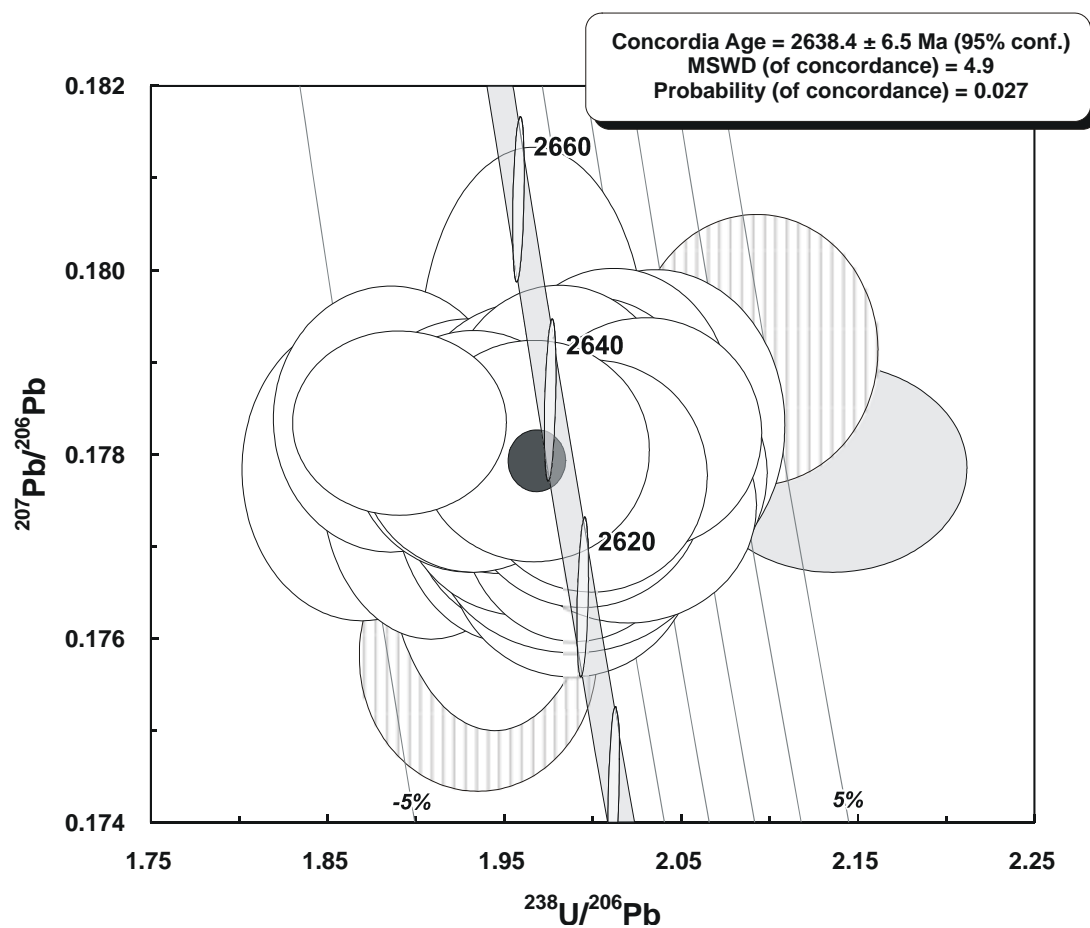


**Figure 44.** Tera-Wasserburg concordia plot for zircons from sample 2004967550: biotite syenogranite dyke, Nanicup Bridge. Two outliers are indicated by vertical hatching; discordant and/or high common-Pb analyses are light grey.

**Table 12.** SHRIMP analytical results for zircon from sample 2004967550: biotite syenogranite dyke, Nanicup Bridge.

Grain.Spot	U (ppm)	Th (ppm)	% comm 206	<sup>207</sup> Pb / <sup>206</sup> Pb	±	<sup>206</sup> Pb / <sup>238</sup> U	±	<sup>207</sup> Pb / <sup>235</sup> U	±	% Disc.	<sup>207</sup> Pb / <sup>206</sup> Pb Age (Ma)	±
<i>Main</i>												
28.1	156	175	0.000	0.1770	0.0006	0.5031	0.0073	12.2791	0.1824	-0.1	2625.1	5.4
15.1	180	196	-0.011	0.1771	0.0005	0.5029	0.0081	12.2802	0.2002	0.0	2626.0	4.7
7.1	136	146	-0.015	0.1774	0.0006	0.5025	0.0068	12.2917	0.1710	0.2	2628.9	5.5
31.1	174	230	0.021	0.1775	0.0005	0.4950	0.0073	12.1116	0.1821	1.4	2629.2	4.9
23.1	119	117	0.010	0.1775	0.0010	0.5144	0.0070	12.5888	0.1852	-1.7	2629.7	9.5
4.1	121	116	0.015	0.1776	0.0006	0.5060	0.0075	12.3896	0.1893	-0.3	2630.6	5.7
35.1	129	116	0.027	0.1776	0.0007	0.5122	0.0070	12.5432	0.1782	-1.3	2630.8	6.3
21.1	149	145	0.005	0.1776	0.0006	0.5098	0.0076	12.4849	0.1907	-0.9	2630.8	5.2
16.1	165	206	-0.008	0.1777	0.0005	0.5013	0.0071	12.2815	0.1784	0.5	2631.4	5.1
26.1	109	121	0.043	0.1777	0.0006	0.5106	0.0070	12.5097	0.1764	-1.0	2631.5	6.0
36.1	189	238	0.023	0.1777	0.0007	0.5240	0.0070	12.8409	0.1785	-3.2	2631.8	6.5
13.1	178	164	0.001	0.1778	0.0005	0.5002	0.0067	12.2605	0.1685	0.7	2632.3	4.8
30.1	147	159	0.018	0.1778	0.0006	0.4945	0.0077	12.1245	0.1916	1.6	2632.6	5.3
34.1	135	124	0.025	0.1778	0.0007	0.5350	0.0079	13.1200	0.2009	-4.9	2632.9	6.2
25.1	101	87	-0.031	0.1779	0.0007	0.5031	0.0069	12.3406	0.1755	0.2	2633.4	6.3
19.1	141	144	-0.015	0.1779	0.0006	0.5075	0.0078	12.4501	0.1946	-0.5	2633.6	5.4
1.1	128	123	0.016	0.1779	0.0006	0.4990	0.0087	12.2432	0.2178	0.9	2633.8	5.7
33.1	120	120	0.001	0.1780	0.0006	0.5077	0.0068	12.4588	0.1732	-0.5	2634.0	5.6
10.1	129	123	0.030	0.1780	0.0006	0.4979	0.0071	12.2227	0.1783	1.1	2634.8	5.7
17.1	183	155	-0.010	0.1780	0.0005	0.5175	0.0071	12.7048	0.1790	-2.0	2634.8	5.0
12.1	166	209	0.011	0.1781	0.0005	0.5133	0.0076	12.6019	0.1906	-1.4	2634.8	5.1
27.1	212	224	0.006	0.1781	0.0005	0.5085	0.0069	12.4839	0.1735	-0.6	2634.8	4.6
29.1	140	126	-0.011	0.1781	0.0006	0.5181	0.0074	12.7234	0.1866	-2.1	2635.4	5.2
22.1	160	203	0.002	0.1781	0.0005	0.5154	0.0083	12.6572	0.2066	-1.7	2635.5	4.9
3.1	118	96	0.014	0.1781	0.0006	0.5028	0.0071	12.3495	0.1797	0.4	2635.6	5.9
5.1	116	102	0.013	0.1782	0.0006	0.5063	0.0069	12.4400	0.1743	-0.2	2636.4	5.8
8.1	187	245	0.004	0.1782	0.0005	0.4927	0.0066	12.1081	0.1647	2.1	2636.6	4.8
2.1	149	180	0.002	0.1783	0.0006	0.5097	0.0071	12.5290	0.1792	-0.7	2636.8	5.3
11.1	141	113	0.015	0.1783	0.0006	0.5003	0.0067	12.2980	0.1703	0.8	2637.0	5.5
20.1	114	112	-0.002	0.1783	0.0007	0.4912	0.0072	12.0773	0.1832	2.3	2637.4	6.4
36.2	249	61	-0.006	0.1784	0.0004	0.5290	0.0069	13.0091	0.1731	-3.8	2637.6	3.8
32.1	166	154	-0.002	0.1784	0.0006	0.5305	0.0077	13.0480	0.1933	-4.0	2638.0	5.5
18.1	137	130	0.012	0.1784	0.0006	0.5047	0.0068	12.4176	0.1717	0.2	2638.5	5.3
24.1	135	143	-0.031	0.1786	0.0006	0.4970	0.0068	12.2359	0.1715	1.5	2639.5	5.6
9.1	145	120	0.021	0.1790	0.0009	0.5086	0.0068	12.5536	0.1814	-0.2	2643.9	8.8
<i>Outlier</i>												
37.1	122	132	0.056	0.1758	0.0006	0.5168	0.0073	12.5288	0.1832	-2.7	2614.0	5.7
14.1	181	166	0.006	0.1791	0.0006	0.4778	0.0064	11.8026	0.1638	4.8	2645.0	5.5
<i>Discordant</i>												
6.1	222	246	0.035	0.1779	0.0005	0.4681	0.0068	11.4806	0.1697	6.0	2633.1	4.3

Data are at 1 $\sigma$  precision. All Pb data are common-Pb corrected based on <sup>204</sup>Pb measurements. Mount: GA6009; Instrument: RSES SHRIMP-RG; Acquisition: 24 October 2006.



## 2004968001A: meta-psammite, Wheatley

### SAMPLE INFORMATION

**1:250,000 sheet:** SI5010 Pemberton

**1:100,000 sheet:** 2029 Donnelly

**MGA:** 407640 mE 6219876mN

**Location:** This sample was taken from Teck Cominco Australia Pty Ltd diamond drill hole WPD02, depth interval 235.22-237.05 m. The collar is located approximately 6 km south of Wheatley town site.

**Description:** This is a strongly deformed fine-grained meta-psammite. The meta-psammite forms part of a sequence of altered, deformed and metamorphosed mafic and felsic volcanic and sedimentary rocks. The unit has been recrystallised during amphibolite facies metamorphism and displays a strong fabric defined by mica, principally biotite. Limited secondary recrystallisation of quartz and alteration of other minerals is associated with late minor fractures that cross-cut the sequence.

Quartz is dominant (65-70%), with lesser K-feldspar (10-20%), plagioclase (5-10%), biotite (5-7%) and muscovite (3-5%). Accessory phases include tourmaline (trace to 1%) and carbonate and trace zircon, titanite, secondary clinozoisite and opaque minerals. Quartz, microcline and plagioclase form a weakly elongated, polygonal mosaic, with quartz grains displaying minor undulose extinction. Variations in modal abundance of the main phases may reflect original bedding. Pale yellow to red-brown biotite and elongate muscovite flakes are strongly aligned, form mica-rich layers to 1 mm thick, and define a strong foliation. Some muscovite flakes overprint the fabric, suggesting muscovite growth continued post the main phase of deformation and metamorphism. Small, blue-green, sub- to euhedral tourmaline grains are disseminated throughout the rock and also form thin tourmaline-rich layers in places. Anhedral carbonate is associated with biotite and muscovite.

### DESCRIPTION OF ZIRCONS

**Shape:** Variably euhedral and prismatic grains, with rounded edges and terminations (Figure 45).

**Size:** 50 to 200 microns.

**Colour/clarity:** Clear to light brown.

**Quality:** Fair to good. Cracks and inclusions uncommon.

**CL zoning:** Variable with concentric and sector zoning. Occasional complex embayment and truncation structures (Figure 45).



#### CONCURRENT STANDARD DATA

**Pb/U reprod.(2s):** 0.61%

**Err. of mean (2s):** 1.00%

**Standard:** QGNG

**Analyses:** 19

**Notes:** A remarkably good session yielded a high level of reproducibility. On the assumption that these zircons could be a detrital, the number of scans was reduced to four per analysis in order to increase number of analyses to meet statistical adequacy requirements.

#### SAMPLE DATA

Sixty-four analyses were made on sixty-four grains with seventeen analyses being outside 5% discordance (Table 13; Figure 46). The remaining forty-seven analyses yield a 5% chance of missing a component making up more than 0.105 of the total population (Vermeesch 2004). The concordant analyses form a band of ages from ~2700 to ~2600 Ma with a prominent mode around ~2640 Ma (Figure 47). Two analyses (#7.1 and #30.1) are significantly, although not distantly, older than the main cluster. There is a weak indication that younger ages are correlated with higher U (Figure 48). This can either indicate potential isotopic disturbance in high U grains or reflect an original provenance feature of the detrital grains. However, there does not appear to be any corresponding significant correlation with  $^{232}\text{Th}/^{238}\text{U}$  ratio (Figure 49) that might be expected if the U content and age correlation was a provenance feature. Mixture modelling on concordant analyses with U < 1000 ppm yields three modelled components at  $2646.0 \pm 4.9$ ,  $2670.4 \pm 6.9$  and  $2700.7 \pm 9.5$  (Figure 50).



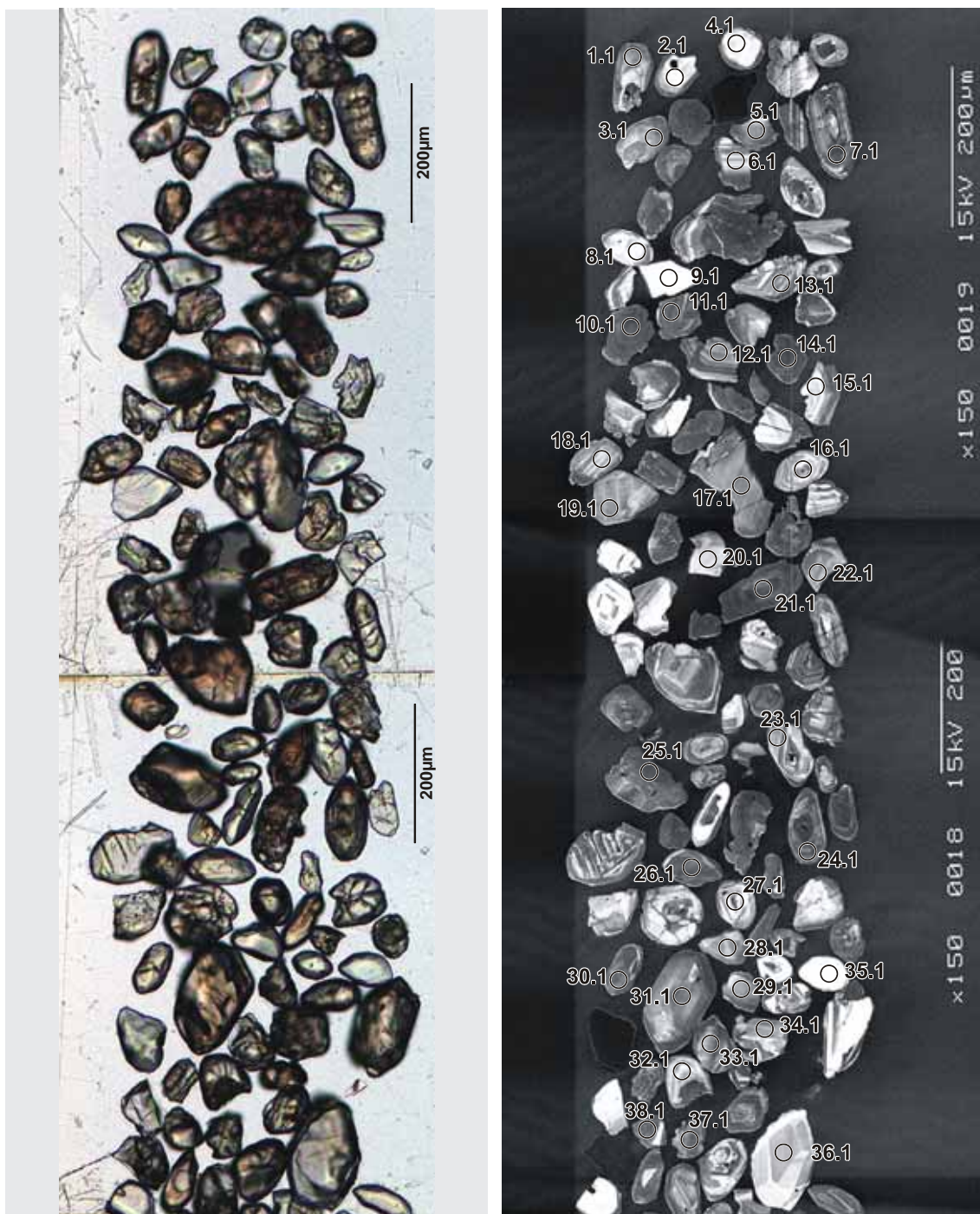


**Figure 45.** Representative images (transmitted light on left, cathodoluminescence on right) for sample 2004968001A: meta-psammite, Wheatley. SHRIMP analysis spots are labelled.

**GEOCHRONOLOGICAL INTERPRETATION**

The variety of CL patterns and lack of age correlation with compositional parameters suggests that the range is a remnant detrital pattern (albeit probably with minor Pb-loss and isotopic disruption in higher U grains). As such the mixture model ages potentially represent provenance components in the sedimentary protolith and indicate that the maximum age of deposition of that protolith was ~2646 Ma.

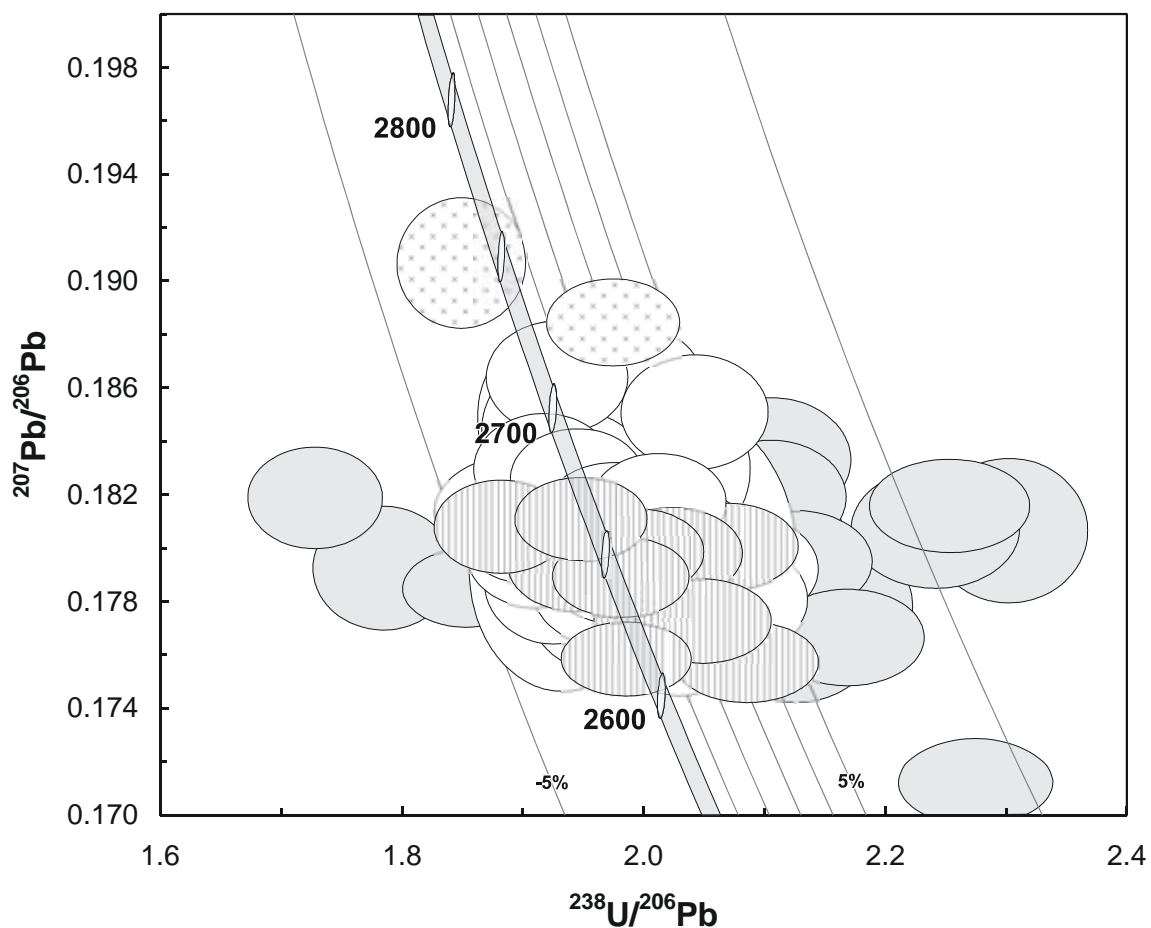


**Figure 46.** Tera-Wasserburg concordia plot for zircons from sample 2004968001A: meta-psammite, Wheatley. Cross-hatch pattern indicate distinctly older analyses; vertical hatch indicates analyses with  $U > 1000$  ppm; white filled ellipses indicate bulk of concordant analyses; discordant and/or high common-Pb analyses are light grey.

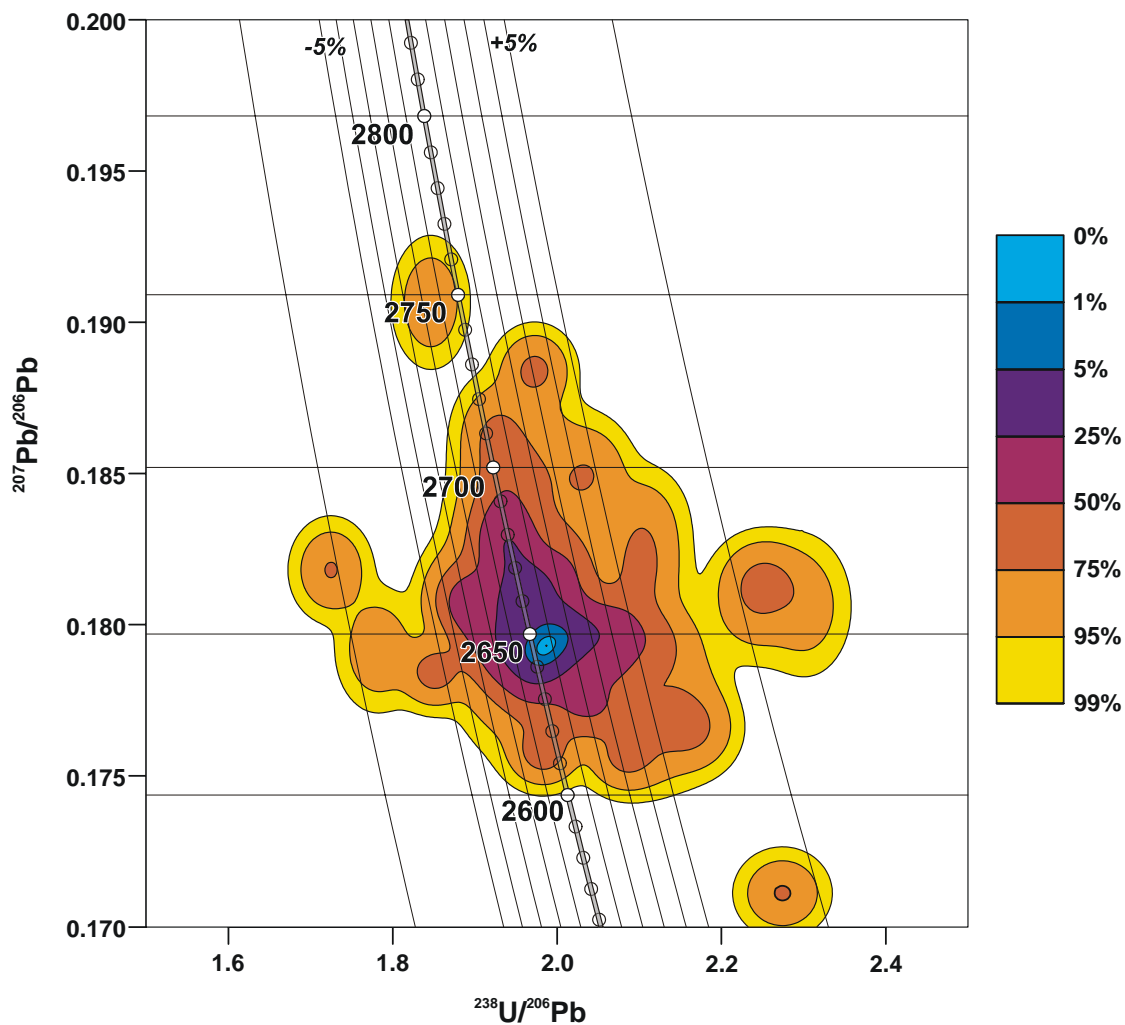


**Figure 47.** Concordia contour plot for zircons from sample 2004968001A: meta-psammite, Wheatley (effectively the equivalent of Figure 46) illustrating the broad range of analyses from 2700 to 2600 Ma with a dominant mode ~2640 Ma.

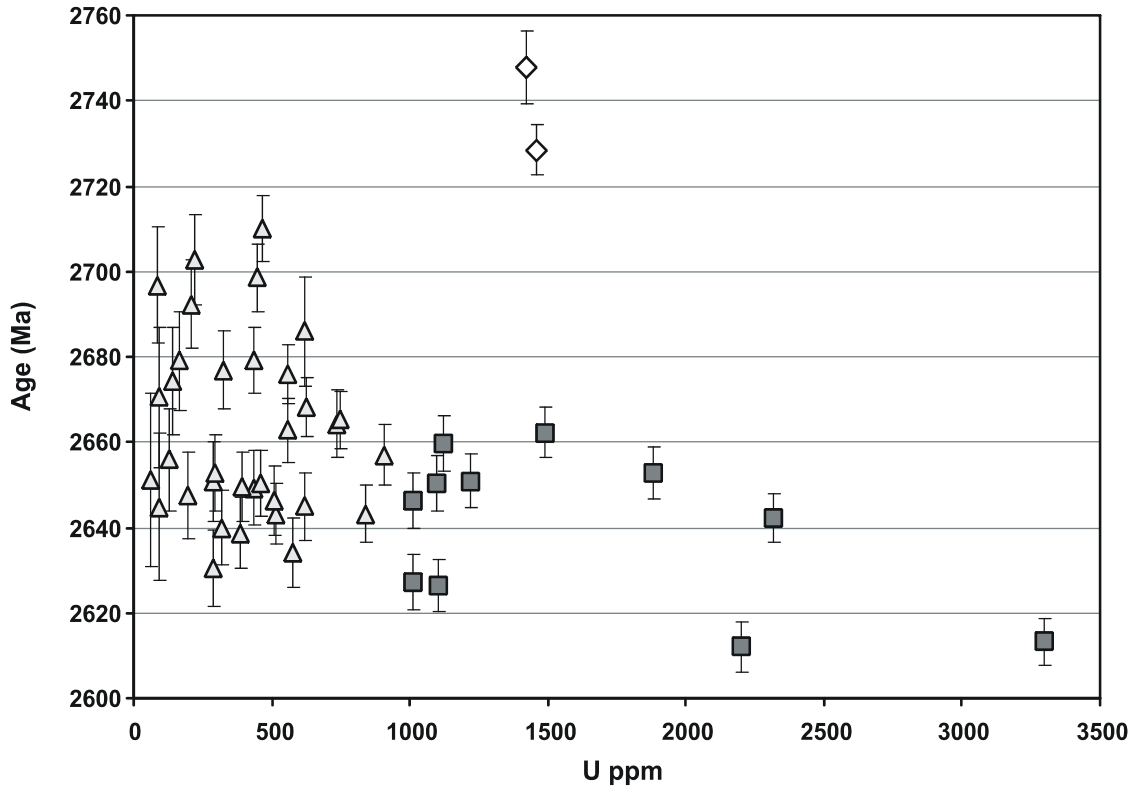


**Figure 48.** Plot of zircon age in relation to U content for concordant zircons from 2004968001A: meta-psammite, Wheatley illustrating a trend toward younger ages with higher U contents. Square markers indicate analyses U > 1000 ppm. Diamond markers indicate older analyses.

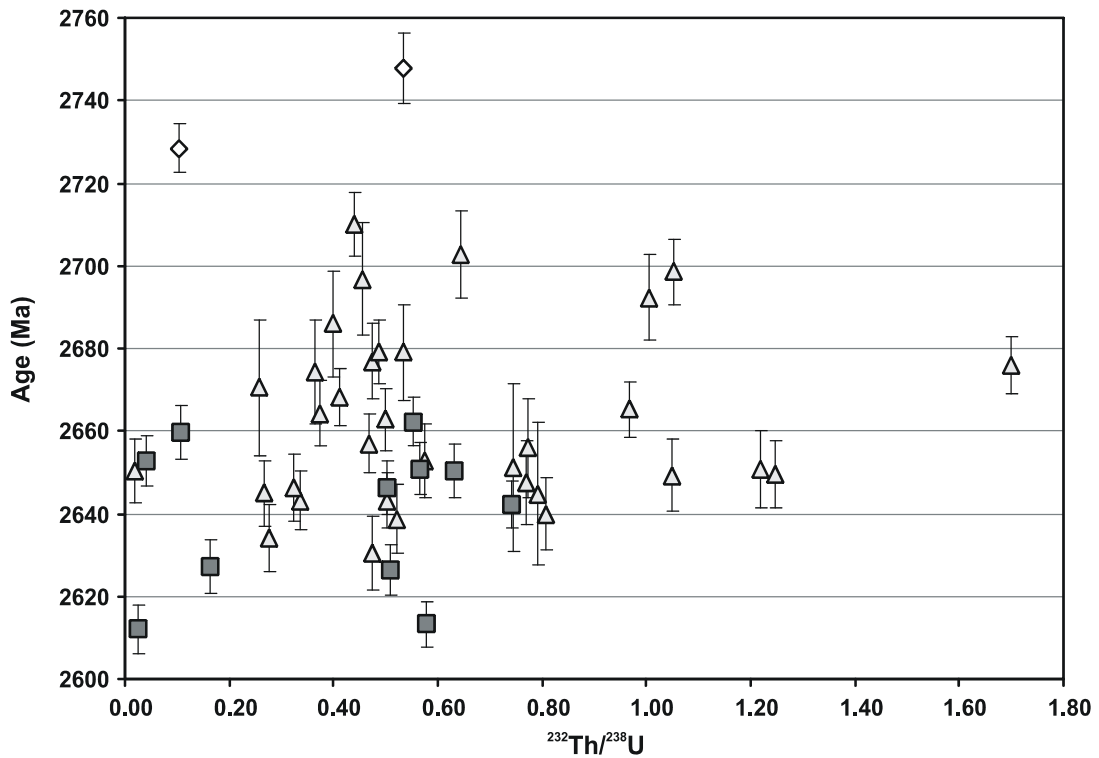


**Figure 49.** Plot of zircon age in relation to  $^{232}\text{Th}/^{238}\text{U}$  ratio for concordant zircons from 2004968001A: meta-psammite, Wheatley. Square markers indicate analyses U > 1000 ppm.

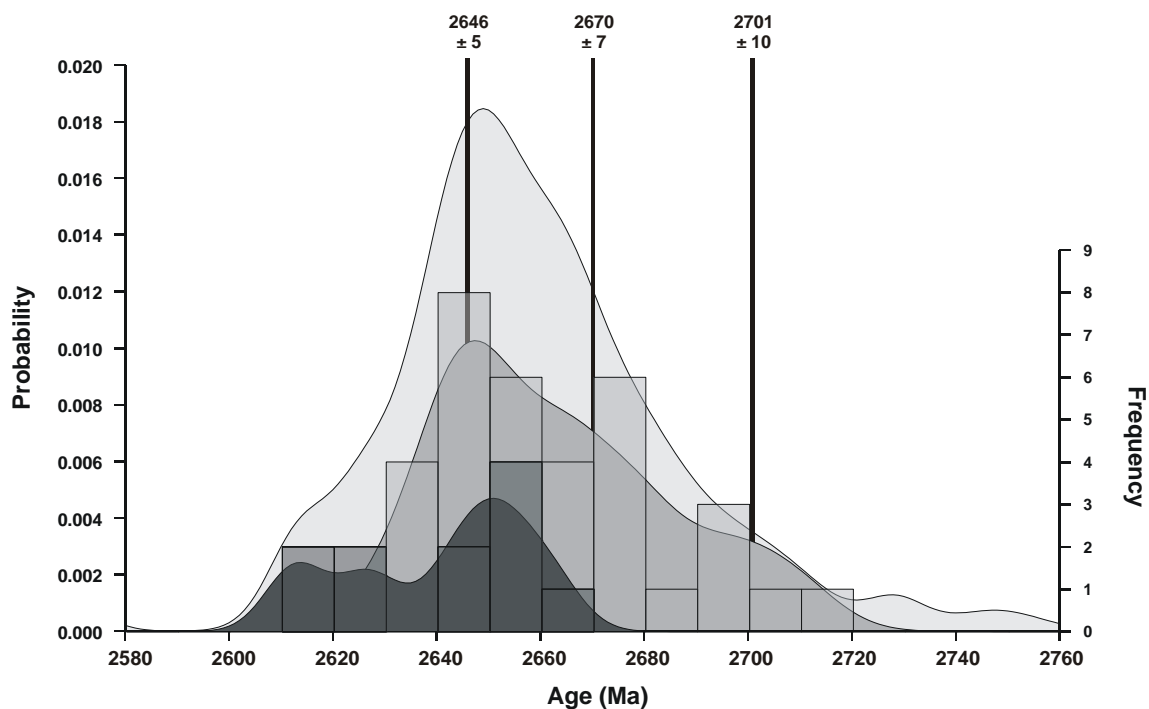


**Figure 50.** Probability density distribution and histogram plot of  $^{207}\text{Pb}/^{206}\text{Pb}$  ages from sample 2004968001A: meta-psammite, Wheatley with mixture modelled age components shown. Light grey distribution depicts all ages including discordant analyses – subsequent distributions have been scaled to this; medium grey distribution depicts concordant analyses with  $U < 1000$  ppm which is the basis for mixture modelled age components; dark grey distribution depicts concordant analyses with  $U > 1000$  ppm.

**Table 13.** SHRIMP analytical results for zircon from sample 2004968001A: meta-psammite, Wheatley.

Grain.Spot	U (ppm)	Th (ppm)	% comm 206	<sup>207</sup> Pb / <sup>206</sup> Pb	±	<sup>206</sup> Pb / <sup>238</sup> U	±	<sup>207</sup> Pb / <sup>235</sup> U	±	% Disc.	<sup>207</sup> Pb / <sup>206</sup> Pb Age (Ma)	±
<i>Detrital protolith</i>												
36.1	288	132	0.027	0.1776	0.0010	0.5089	0.0065	12.4614	0.1718	-0.8	2630.6	9.0
65.1	575	154	0.102	0.1780	0.0009	0.4824	0.0059	11.8397	0.1561	3.7	2634.2	8.0
12.1	389	196	0.013	0.1785	0.0009	0.5090	0.0063	12.5246	0.1675	-0.5	2638.7	8.3
18.1	318	249	0.043	0.1786	0.0009	0.5198	0.0064	12.8004	0.1721	-2.2	2640.0	8.7
17.1	514	167	0.018	0.1790	0.0008	0.5063	0.0059	12.4911	0.1547	0.1	2643.2	7.2
44.1	842	410	0.008	0.1790	0.0007	0.4991	0.0061	12.3138	0.1583	1.3	2643.2	6.8
50.1	92	71	0.114	0.1791	0.0019	0.5181	0.0085	12.7951	0.2479	-1.7	2644.8	17.3
53.1	622	161	0.014	0.1791	0.0008	0.4809	0.0060	11.8777	0.1587	4.3	2644.9	7.8
54.1	508	159	0.041	0.1793	0.0009	0.4874	0.0061	12.0481	0.1611	3.3	2646.3	8.1
20.1	194	145	0.053	0.1794	0.0011	0.5047	0.0066	12.4860	0.1797	0.5	2647.5	10.1
3.1	433	440	0.018	0.1796	0.0009	0.5037	0.0067	12.4740	0.1783	0.7	2649.3	8.7
23.1	392	473	0.001	0.1796	0.0009	0.4973	0.0059	12.3174	0.1577	1.8	2649.5	8.0
29.1	461	9	0.000	0.1797	0.0008	0.5243	0.0064	12.9933	0.1695	-2.5	2650.3	7.7
34.1	286	338	0.021	0.1798	0.0010	0.4934	0.0064	12.2309	0.1732	2.5	2650.8	9.4
56.1	62	45	0.250	0.1798	0.0022	0.4932	0.0096	12.2276	0.2819	2.5	2651.1	20.4
6.1	293	163	-0.038	0.1800	0.0010	0.5138	0.0065	12.7514	0.1766	-0.8	2652.8	9.0
62.1	127	95	-0.040	0.1803	0.0013	0.5030	0.0074	12.5063	0.2050	1.1	2655.9	11.9
25.1	908	410	-0.002	0.1804	0.0008	0.5253	0.0066	13.0696	0.1726	-2.4	2657.0	7.0
5.1	556	270	0.014	0.1811	0.0008	0.5083	0.0061	12.6923	0.1620	0.5	2662.8	7.5
47.1	736	265	0.026	0.1812	0.0009	0.5300	0.0072	13.2441	0.1902	-2.9	2664.2	7.9
33.1	747	699	0.023	0.1813	0.0007	0.5066	0.0060	12.6675	0.1591	0.9	2665.2	6.7
22.1	628	251	-0.017	0.1817	0.0008	0.4973	0.0057	12.4574	0.1513	2.5	2668.1	6.8
35.1	90	23	-0.043	0.1819	0.0018	0.5121	0.0088	12.8453	0.2550	0.2	2670.5	16.4
40.1	142	50	-0.026	0.1824	0.0014	0.5079	0.0075	12.7717	0.2117	1.0	2674.5	12.6
16.1	557	917	-0.020	0.1825	0.0008	0.5147	0.0060	12.9527	0.1617	0.0	2676.0	7.0
8.1	325	149	-0.024	0.1826	0.0010	0.5150	0.0067	12.9683	0.1818	0.0	2676.9	9.0
2.1	166	86	0.061	0.1829	0.0013	0.4959	0.0071	12.5049	0.1989	3.1	2679.1	11.5
27.1	437	207	-0.006	0.1829	0.0009	0.5221	0.0065	13.1653	0.1742	-1.1	2679.3	7.7
59.1	622	240	0.012	0.1836	0.0014	0.5141	0.0062	13.0169	0.1857	0.4	2686.0	12.7
4.1	205	200	-0.019	0.1843	0.0012	0.5187	0.0070	13.1833	0.1973	0.0	2692.3	10.4
9.1	84	37	-0.034	0.1848	0.0015	0.5170	0.0081	13.1759	0.2340	0.4	2696.7	13.6
31.1	446	455	0.049	0.1850	0.0009	0.4900	0.0060	12.5020	0.1645	4.7	2698.5	7.9
51.1	219	137	0.032	0.1855	0.0012	0.5036	0.0070	12.8803	0.1960	2.7	2702.7	10.6
61.1	466	198	0.007	0.1863	0.0009	0.5191	0.0065	13.3378	0.1778	0.5	2710.1	7.7
<i>High U</i>												
64.1	2198	53	0.015	0.1756	0.0006	0.4798	0.0056	11.6195	0.1417	3.3	2612.0	5.9
14.1	3298	1847	0.005	0.1758	0.0006	0.5042	0.0056	12.2179	0.1417	-0.7	2613.2	5.4
24.1	1102	542	0.002	0.1772	0.0006	0.4883	0.0055	11.9296	0.1409	2.4	2626.6	6.1
11.1	1011	160	0.003	0.1772	0.0007	0.4965	0.0057	12.1344	0.1479	1.1	2627.2	6.3
42.1	2319	1666	0.006	0.1788	0.0006	0.5051	0.0059	12.4557	0.1522	0.2	2642.2	5.8
58.1	1008	490	0.002	0.1793	0.0007	0.5149	0.0061	12.7294	0.1599	-1.2	2646.3	6.5
55.1	1100	671	0.007	0.1797	0.0007	0.4946	0.0058	12.2562	0.1512	2.3	2650.4	6.4
26.1	1221	667	0.026	0.1798	0.0007	0.5018	0.0057	12.4398	0.1492	1.1	2650.9	6.2
46.1	1884	77	0.002	0.1800	0.0007	0.4843	0.0059	12.0183	0.1529	4.0	2652.8	6.1
38.1	1121	115	0.021	0.1807	0.0007	0.5321	0.0064	13.2597	0.1680	-3.4	2659.6	6.6
10.1	1488	794	0.000	0.1810	0.0006	0.5138	0.0059	12.8246	0.1543	-0.4	2662.2	5.9
<i>Older inheritance</i>												



Compilation of SHRIMP U-Pb geochronological data, Yilgarn Craton, Western Australia, 2004-2006

7.1	1458	148	0.015	0.1884	0.0007	0.5069	0.0058	13.1684	0.1579	3.1	2728.4	5.8
30.1	1421	734	0.027	0.1907	0.0010	0.5416	0.0064	14.2383	0.1852	-1.5	2747.8	8.7
<i>Discordant</i>												
27.1	333	235	0.097	0.1639	0.0014	0.3232	0.0068	7.3038	0.1650	27.7	2496.2	14.4
39.1	1225	841	0.013	0.1711	0.0007	0.4397	0.0051	10.3742	0.1264	8.5	2568.6	6.5
32.1	296	115	0.038	0.1765	0.0010	0.4708	0.0061	11.4571	0.1611	5.1	2620.3	9.3
37.1	714	352	0.024	0.1766	0.0007	0.4613	0.0055	11.2292	0.1430	6.7	2620.7	7.0
15.1	235	122	0.051	0.1777	0.0012	0.4643	0.0060	11.3770	0.1647	6.6	2631.7	10.8
48.1	3023	994	0.040	0.1784	0.0006	0.5404	0.0063	13.2943	0.1607	-5.6	2638.3	5.6
19.1	601	350	0.004	0.1792	0.0010	0.5612	0.0075	13.8627	0.1999	-8.6	2645.2	8.8
1.1	739	297	0.023	0.1794	0.0008	0.4711	0.0059	11.6532	0.1549	6.0	2647.4	7.3
41.1	358	291	0.033	0.1802	0.0011	0.4773	0.0066	11.8567	0.1785	5.2	2654.3	10.2
21.1	1133	605	0.722	0.1806	0.0011	0.4343	0.0051	10.8148	0.1427	12.5	2658.2	10.2
43.1	430	171	0.044	0.1807	0.0009	0.4463	0.0057	11.1159	0.1525	10.5	2658.9	8.5
60.1	1707	722	0.099	0.1815	0.0007	0.4439	0.0054	11.1100	0.1424	11.2	2666.8	6.6
49.1	1349	67	0.013	0.1818	0.0008	0.5797	0.0076	14.5329	0.2015	-10.4	2669.4	7.1
63.1	1251	103	0.019	0.1818	0.0009	0.4753	0.0057	11.9153	0.1552	6.1	2669.6	8.0
52.1	1198	432	0.147	0.1823	0.0023	0.3860	0.0053	9.7049	0.1822	21.3	2674.3	21.1
45.1	395	586	0.055	0.1832	0.0010	0.4753	0.0061	12.0088	0.1675	6.6	2682.5	8.7
13.1	544	571	0.020	0.1834	0.0009	0.3920	0.0046	9.9158	0.1266	20.6	2684.3	7.8

Data are at  $1\sigma$  precision. All Pb data are common-Pb corrected based on  $^{204}\text{Pb}$  measurements. Mount: Z4438; Instrument: JdL Centre SHRIMP-B; Acquisition: 23 October 2004.

## 2004969008: biotite granodiorite, Newlgalup

### SAMPLE INFORMATION

**1:250,000 sheet:** Collie (SI5006)

**1:100,000 sheet:** Bridgetown (2130)

**MGA:** 449709 mE 6259066 mN

**Location:** This sample taken from blasted rock on the south side of road, about 1 km east of Newlgalup.

**Description:** This rock is a grey, banded, seriate to variably feldspar porphyritic, fine-grained biotite monzogranite. The banding is defined by compositional variation, principally changes in biotite content. The rock also contains felsic layers, possibly leucosome, which are generally associated with biotite-rich bands. Banding is highly variable in orientation, ranging from sub-horizontal to chaotic.

The sample is characterised by a granular to granoblastic texture. Principal minerals are quartz (32%), plagioclase (30%), K-feldspar (30%) and biotite (8-10%), with plagioclase≈K-feldspar. Accessory phases include apatite, titanite, zircon and anhedral opaque minerals. Plagioclase forms rarely oscillatory zoned, subhedral to anhedral grains and minor phenocrysts to 1 cm in size. K-feldspar, dominantly microcline with minor perthite, forms anhedral grains instital to plagioclase and quartz, and rare phenocrysts to 2 cm in length. Quartz is anhedral and displays subgrain development with sutured grain boundaries, deformation lamellae and strong undulose extinction. The rock has minor myrmekitic quartz-plagioclase intergrowth. Plagioclase, K-feldspar and quartz are variably recrystallised along grain boundaries to a very fine-grained mosaic of quartz, feldspar, biotite, epidote and opaque minerals. Aligned green-brown biotite flakes and zones of recrystallisation along partly aligned quartz and feldspar grains define a moderate fabric. Alteration is limited to very minor replacement of biotite by epidote, white mica and chlorite, and patchy minor saussuritisation of plagioclase to albite, white mica and epidote.

### DESCRIPTION OF ZIRCONS

**Shape:** Euhedral prismatic, some flattened tabular shapes ([Figure 51](#)).

**Size:** 50 to 200 microns.

**Colour/clarity:** Clear to brown.

**Quality:** Fair. Cracks and inclusions common.

**CL zoning:** Generally bland with complex concentric zoning when apparent ([Figure 51](#)).



#### CONCURRENT STANDARD DATA

**Pb/U reprod.(2s):** 0.89%

**Err. of mean (2s):** 2.80%

**Standard:** QGNG

**Analyses:** 15 (one discarded as anomalously young)

**Notes:** Calibration slope of 2.65 used.

#### SAMPLE DATA

Twenty-one analyses were made on twenty-one grains (Table 14; Figure 52). No discordant analyses were reported although 11 analyses showing high common-Pb on the first scan were aborted. There is one very old grain (#13.1) and analysis #17.1, which appears concordant although obviously younger than the bulk of the sample, is regarded as an analytical anomaly because of primary beam instability during this analysis.

The bulk of the analyses range in age between ~2680 and ~2600 Ma. The concordia contour plot (Figure 53) clearly indicates two clusters. However, there is no significant correlation between age and U content, Th/U ratio, and CL pattern, and the two clusters can only be subdivided on the basis of age.

The older cluster yields a vague concordia age of  $2651.4 \pm 11$  Ma (95% confidence; MSWD (of concordance) = 5.4; Probability of concordance = 0.020), while the younger cluster yields a better constrained concordia age of  $2610.0 \pm 7.8$  Ma (95% confidence; MSWD (of concordance) = 0.96; Probability of concordance = 0.33).





**Figure 51.** Representative images (transmitted light on left, cathodoluminescence on right) for sample 2004969008: biotite granodiorite, Newlgalup. SHRIMP analysis spots are labelled.

### GEOCHRONOLOGICAL INTERPRETATION

There have clearly been two phases of zircon growth in this sample although apart from age there appears to be little to distinguish them. The older age of  $2651 \pm 11$  Ma is tentatively interpreted as inheritance with the younger age of  $2610 \pm 8$  Ma is interpreted as an igneous phase.

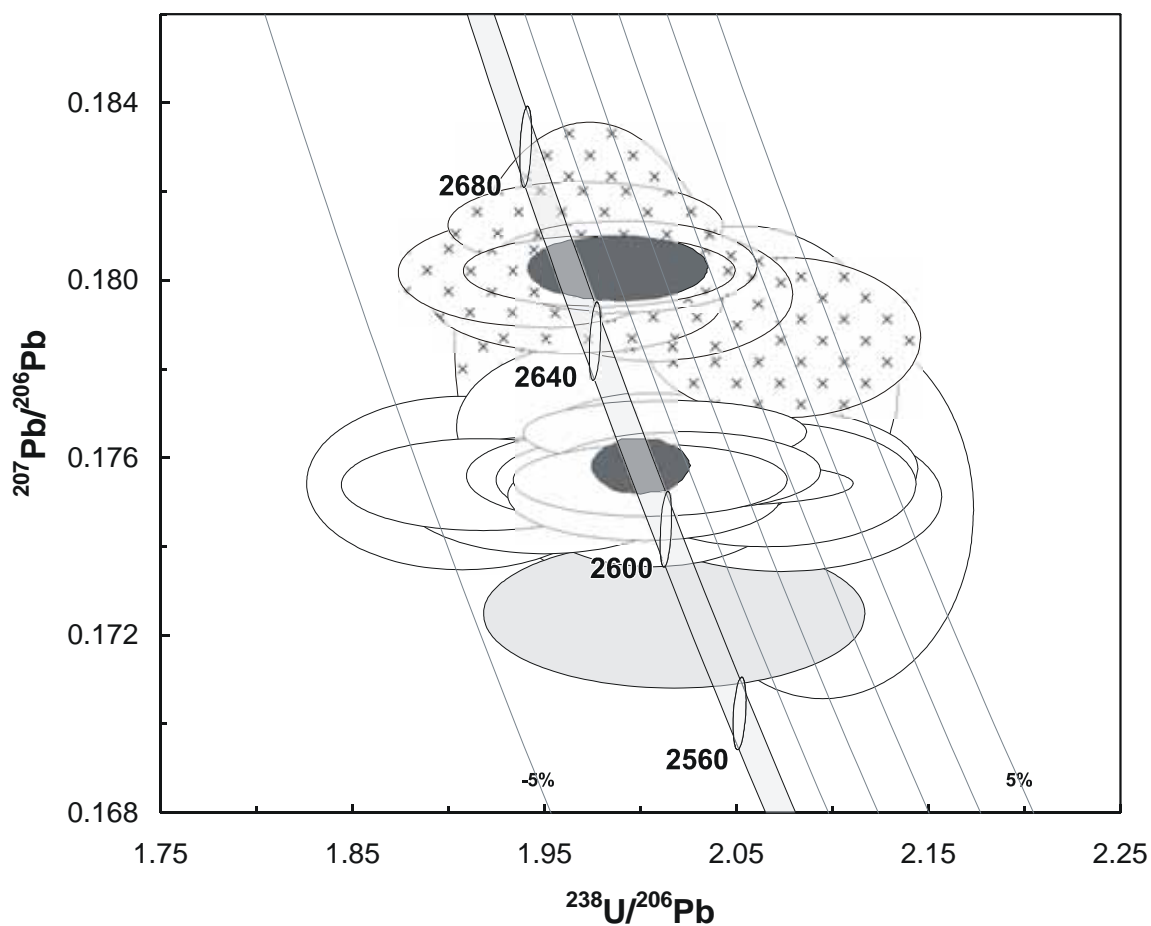


**Figure 52.** Tera-Wasserburg concordia plot for zircons from sample 2004969008: biotite granodiorite, Newlgalup. The two concordant clusters discussed in the text and interpreted from Figure 53 are indicated by white fill and cross hatching; an analytically suspicious result is indicated in light grey. The dark-grey ellipses indicate concordia ages calculated at  $2651 \pm 11$  Ma and  $2610 \pm 8$  Ma.

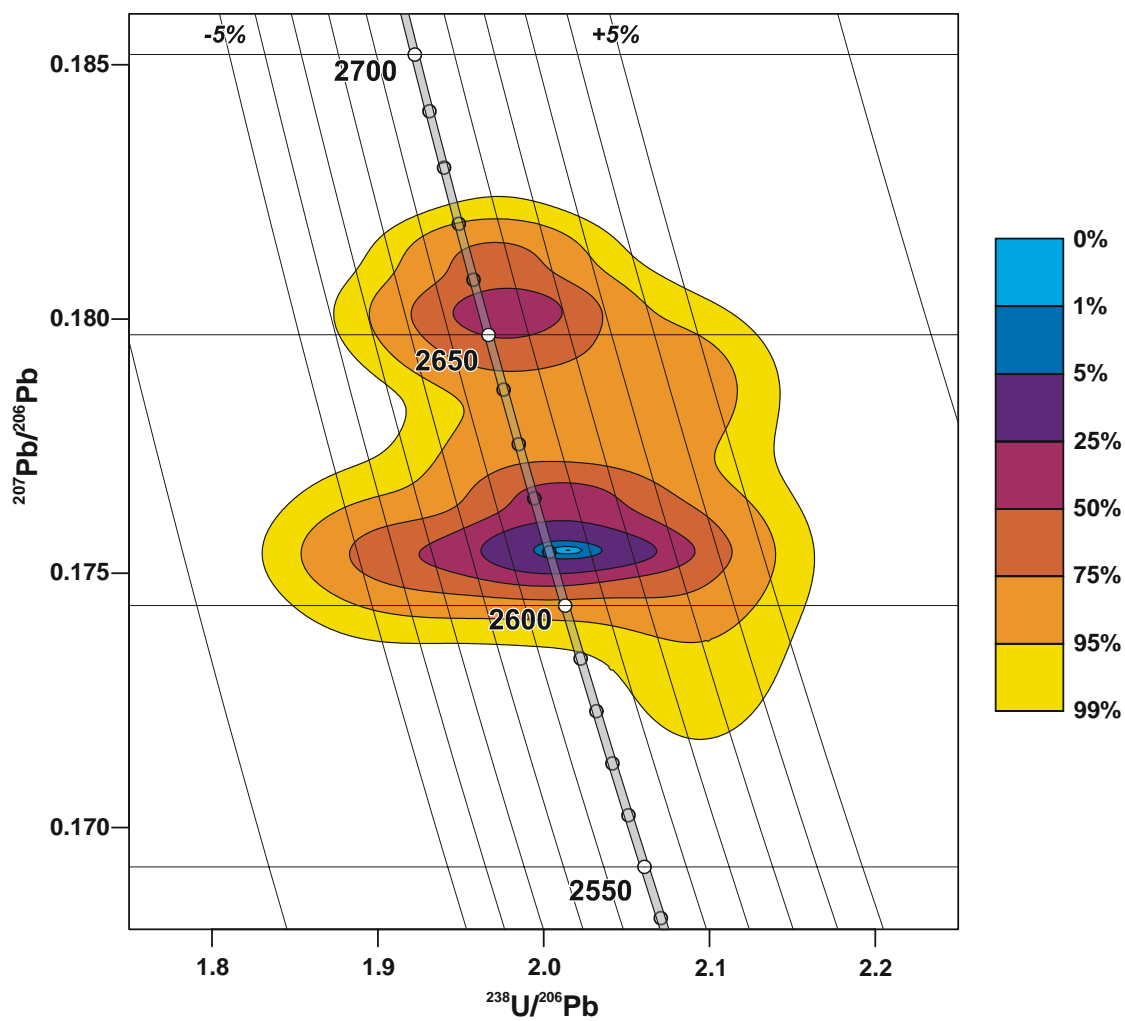


**Figure 53.** Concordia contour plot for zircons from sample 2004969008: biotite granodiorite, Newlgalup illustrating the two prominent clusters at ~2650 Ma and ~2610 Ma.

**Table 14.** SHRIMP analytical results for zircon from sample 2004969008: biotite granodiorite, Newlgalup.

Grain.Spot	U (ppm)	Th (ppm)	% comm 206	<sup>207</sup> Pb / <sup>206</sup> Pb	±	<sup>206</sup> Pb / <sup>238</sup> U	±	<sup>207</sup> Pb / <sup>235</sup> U	±	% Disc.	<sup>207</sup> Pb / <sup>206</sup> Pb Age (Ma)	±
<i>Igneous cluster</i>												
7.1	343	155	0.012	0.1748	0.0017	0.4775	0.0073	11.5074	0.2092	3.4	2604.0	16.5
31.1	457	259	0.037	0.1751	0.0007	0.4825	0.0080	11.6487	0.1977	2.6	2607.0	6.5
5.1	501	295	0.176	0.1751	0.0004	0.4995	0.0073	12.0626	0.1776	-0.2	2607.3	3.9
1.1	149	79	0.029	0.1751	0.0005	0.5130	0.0080	12.3873	0.1959	-2.4	2607.4	5.1
10.1	341	207	0.008	0.1753	0.0004	0.4992	0.0077	12.0685	0.1891	-0.1	2609.1	3.6
19.1	184	159	0.048	0.1754	0.0006	0.4844	0.0075	11.7145	0.1860	2.4	2609.7	5.4
25.1	288	123	0.018	0.1754	0.0004	0.5214	0.0082	12.6081	0.2014	-3.7	2609.7	4.0
18.1	1049	77	0.007	0.1754	0.0002	0.4910	0.0072	11.8738	0.1753	1.3	2609.9	1.9
4.1	68	46	-0.017	0.1754	0.0008	0.5244	0.0091	12.6840	0.2271	-4.1	2610.0	7.6
33.1	1867	99	0.001	0.1754	0.0002	0.4946	0.0074	11.9650	0.1792	0.8	2610.3	2.3
20.1	798	434	0.001	0.1755	0.0004	0.5009	0.0074	12.1189	0.1811	-0.3	2610.6	4.0
9.1	528	436	0.039	0.1755	0.0003	0.4988	0.0072	12.0696	0.1766	0.1	2610.7	3.1
26.1	161	102	0.077	0.1755	0.0008	0.4984	0.0078	12.0597	0.1954	0.1	2610.7	7.6
32.1	243	223	0.009	0.1756	0.0004	0.5046	0.0076	12.2146	0.1859	-0.8	2611.4	3.9
2.1	760	403	0.333	0.1757	0.0004	0.4945	0.0071	11.9790	0.1736	0.9	2612.6	3.4
6.1	236	144	-0.001	0.1757	0.0004	0.4973	0.0075	12.0491	0.1841	0.4	2613.0	4.1
28.1	144	102	0.006	0.1757	0.0006	0.4843	0.0076	11.7351	0.1872	2.6	2613.0	5.3
11.1	98	57	-0.053	0.1764	0.0007	0.4937	0.0082	12.0092	0.2063	1.2	2619.4	6.9
35.1	472	190	0.013	0.1766	0.0003	0.4969	0.0074	12.0967	0.1815	0.8	2620.8	2.8
41.1	106	64	0.019	0.1767	0.0008	0.5042	0.0082	12.2830	0.2081	-0.4	2622.1	7.5
16.1	168	144	0.131	0.1776	0.0015	0.4875	0.0079	11.9371	0.2179	2.7	2630.6	13.8
<i>Inherited cluster</i>												
8.1	669	67	0.070	0.1784	0.0021	0.5068	0.0074	12.4691	0.2320	-0.2	2638.5	19.3
38.1	1914	192	0.009	0.1787	0.0007	0.4823	0.0068	11.8827	0.1754	3.9	2640.7	6.8
3.1	335	269	0.107	0.1795	0.0005	0.5084	0.0079	12.5831	0.1991	-0.1	2648.2	4.3
39.1	402	223	0.011	0.1797	0.0006	0.4983	0.0073	12.3445	0.1862	1.6	2649.7	5.6
21.1	193	155	0.021	0.1802	0.0005	0.5137	0.0079	12.7605	0.1987	-0.7	2654.3	4.6
22.1	435	294	0.004	0.1802	0.0003	0.5055	0.0074	12.5585	0.1848	0.7	2654.6	3.0
14.1	893	66	0.010	0.1803	0.0004	0.5024	0.0072	12.4902	0.1818	1.2	2655.6	3.9
34.1	612	310	0.010	0.1812	0.0004	0.5074	0.0075	12.6795	0.1899	0.7	2664.1	3.7
<i>Inherited</i>												
13.1	176	156	0.100	0.2190	0.0040	0.5820	0.0095	17.5694	0.4285	0.5	2973.0	29.2
<i>Analytically low?</i>												
17.1	476	369	0.039	0.1725	0.0007	0.4958	0.0099	11.7894	0.2411	-0.5	2581.8	6.6

Data are at 1 $\sigma$  precision. All Pb data are common-Pb corrected based on <sup>204</sup>Pb measurements. Mount: Z4438; Instrument: JdL Centre SHRIMP-A; Acquisition: 8 November 2004.



## Part 2: Eastern Yilgarn

### 2002967002: biotite quartzofeldspathic gneiss, Moon Rock

#### SAMPLE INFORMATION

**1:250,000 sheet:** Edjudina (SH5106)

**1:100,000 sheet:** Mount Celia (3439)

**MGA:** 477040 mE 6743580 mN

**Location:** The sample was taken from a small pavement about 100 m northwest of Moon Rock, approximately 12 km north-northwest of the abandoned Elora homestead.

**Description:** The sample is from a grey, banded, medium-grained biotite quartzofeldspathic gneiss. The gneiss is the dominant phase of a granitic gneiss complex that contains foliation-parallel, thin aplite and pegmatite veins, possibly leucosome, and minor biotite-rich monzogranite disrupted dykes and xenoliths. The complex is cut by multiple generations of variably deformed biotite granite and pegmatite dykes.

The sample is characterised by a granular texture. Principal minerals are quartz (40%), plagioclase (45%), K-feldspar (<5%) and biotite (8-10%), with plagioclase>K-feldspar. Accessory phases include green amphibole (<1%) preserved in quartz grains, titanite (1%) and trace apatite, zircon, and anhedral opaque minerals. Plagioclase is subhedral, and is variably zoned. Very minor myrmekite is developed. K-feldspar is present as subhedral to anhedral grains and has moderate twinning and variable perthite. Anhedral quartz shows sutured grain boundaries with minor subgrain development. Biotite occurs as weakly aligned, light yellow to red-brown, elongate subhedral flakes. The rock is very weakly altered with minor replacement of biotite by chlorite and minor epidote, and minor saussuritisation of plagioclase by white mica, epidote/clinozoisite and carbonate.

#### DESCRIPTION OF ZIRCONS

**Shape:** Subhedral grains with moderate rounding of crystal faces; some elongate grains.

**Size:** 40 to 100 microns.

**Colour/clarity:** Colourless and clear.

**Quality:** Fair to good. Frequent fractures and inclusions.



**CL zoning:** Weak concentric zoning with complex embayments dominated by bright rims and wider mantles over dark cores with occasional very thin and dark outer rims (Figure 54).

#### CONCURRENT STANDARD DATA

**Pb/U reprod.(2s):** 3.7 %

**Err. of mean (2s):** 1.4 %

**Standard:** TEMORA

**Analyses:** 9 (one discarded because of high common-Pb)

**Notes:** The TEMORA standard was used on this sample as part of development trials early in this phase of the project. QGNG was also analysed concurrently to monitor  $^{207}\text{Pb}/^{206}\text{Pb}$  ratios. The Pb/U calibration slope is non-default at 2.15. The scatter most probably reflects poor instrument stability on SHRIMP-A and the resulting errors should be propagated through the unknowns. Although this large error will contribute to  $^{206}\text{Pb}/^{238}\text{U}$  age errors it will have no impact on  $^{207}\text{Pb}/^{206}\text{Pb}$  ages which are used here for interpretations.

#### SAMPLE DATA

Twenty-five analyses were made on twenty-four grains (Table 15). Thirteen of the analyses are >5% discordant, particularly the analyses associated with the bright CL zones which correspond to low U and Th content. After further discarding two outliers (#20.1 and #21.1) and one concordant analysis on a bright CL zone (#14.1), nine analyses yielded a concordia age of  $2752.1 \pm 4.1$  Ma (MSWD: 1.5; probability of concordance: 0.13). The one concordant age on a bright CL zone (#14.1) yields a younger age, but its position relative to the main cluster at ~2750 Ma and the dispersion of some of the discordant analyses suggest that this represents a later event that resulted in significant Pb-loss. This event could have been the migmatization of the precursor rock, but there is insufficient data to accurately define the age.





**Figure 54.** Representative images (transmitted light on left, cathodoluminescence on right) for sample 2002967002: biotite quartzofeldspathic gneiss, Moon Rock. SHRIMP analysis spots are labelled.

**GEOCHRONOLOGICAL INTERPRETATION**

The magmatic age of the precursor to the migmatite is interpreted as  $2752 \pm 5$  Ma. The age of the event that formed the migmatite is uncertain.

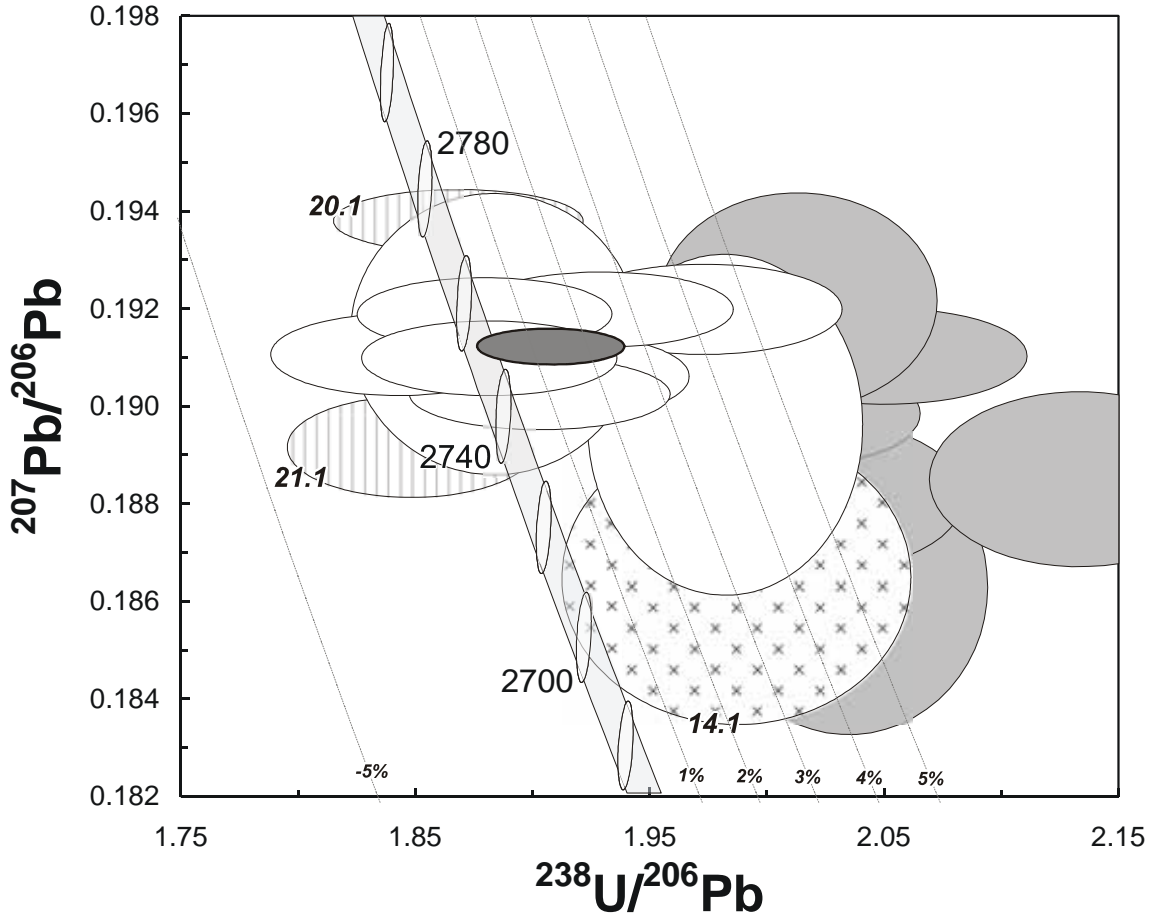


**Figure 55.** Tera-Wasserburg concordia plot for zircons from sample 2002967002: biotite quartzofeldspathic gneiss, Moon Rock. White-filled symbols are used to define the age of the sample; discordant and/or high common-Pb analyses are light grey; outliers have vertical hatching; the cross-pattern indicates one concordant analysis of bright CL zoning as described in the text.

**Table 15.** SHRIMP analytical results for zircon from sample 2002967002: biotite quartzofeldspathic gneiss, Moon Rock.

Grain. Spot	U (ppm)	Th (ppm)	% comm 206	<sup>207</sup> Pb / <sup>206</sup> Pb	±	<sup>206</sup> Pb / <sup>238</sup> U	±	<sup>207</sup> Pb / <sup>235</sup> U	±	% Disc.	<sup>207</sup> Pb / <sup>206</sup> Pb Age (Ma)	±
<i>Bright CL</i>												
14.1	32	0	0.201	0.1864	0.0020	0.5032	0.0124	12.93	0.35	3	2710.8	17.6
<i>Dark CL</i>												
1.1	283	125	1.619	0.1896	0.0023	0.5044	0.0098	13.18	0.30	4	2738.5	20.1
10.1	550	494	0.304	0.1902	0.0005	0.5253	0.0101	13.78	0.27	1	2743.9	4.2
11.1	632	508	0.458	0.1906	0.0006	0.5229	0.0099	13.74	0.26	1	2747.0	5.1
19.1	370	177	0.023	0.1909	0.0005	0.5314	0.0101	13.99	0.27	0	2750.2	4.4
7.1	393	155	0.045	0.1910	0.0006	0.5427	0.0105	14.29	0.28	-2	2750.8	4.8
22.1	398	222	0.282	0.1914	0.0019	0.5308	0.0114	14.01	0.33	0	2754.6	16.4
15.1	395	222	0.064	0.1919	0.0005	0.5320	0.0102	14.07	0.27	0	2758.1	4.2
8.1	395	333	0.119	0.1919	0.0005	0.5181	0.0099	13.71	0.26	2	2758.9	4.4
18.1	330	170	0.311	0.1920	0.0006	0.5067	0.0100	13.41	0.27	4	2759.0	5.2
<i>Outliers</i>												
21.1	546	221	0.065	0.1891	0.0007	0.5408	0.0102	14.10	0.27	-2	2734.4	6.0
20.1	684	439	0.179	0.1938	0.0004	0.5351	0.0101	14.30	0.27	0	2774.4	3.6
<i>Discordant bright</i>												
16.1	148	57	4.239	0.1739	0.0046	0.1239	0.0026	2.97	0.10	71	2595.4	44.0
4.1	45	1	4.409	0.1746	0.0051	0.3525	0.0086	8.49	0.32	25	2602.7	48.9
24.1	130	64	4.496	0.1767	0.0042	0.3139	0.0096	7.65	0.29	33	2622.6	39.1
23.1	43	2	1.372	0.1792	0.0031	0.3817	0.0088	9.43	0.27	21	2645.5	28.5
12.1	64	0	0.454	0.1818	0.0016	0.4330	0.0096	10.85	0.26	13	2669.0	14.6
<i>Discordant dark</i>												
17.1	655	218	0.352	0.1727	0.0007	0.4388	0.0083	10.45	0.20	9	2583.9	6.9
17.2	598	536	0.407	0.1789	0.0006	0.4707	0.0089	11.61	0.22	6	2643.0	5.8
6.1	395	190	1.328	0.1862	0.0020	0.4914	0.0094	12.62	0.28	5	2709.2	17.8
2.1	203	138	0.775	0.1881	0.0011	0.4960	0.0111	12.86	0.30	5	2725.7	9.3
5.1	367	205	1.479	0.1885	0.0012	0.4687	0.0093	12.18	0.25	9	2728.7	10.4
9.1	360	165	0.644	0.1898	0.0007	0.4982	0.0095	13.04	0.25	5	2740.3	6.2
3.1	497	243	0.455	0.1910	0.0007	0.4874	0.0093	12.83	0.25	7	2750.7	5.6
13.1	237	104	0.647	0.1921	0.0015	0.4966	0.0096	13.16	0.27	6	2760.5	12.6

Data are at 1 $\sigma$  precision. All Pb data are common-Pb corrected based on <sup>204</sup>Pb measurements. Mount: Z3580; Instrument: JdL Centre SHRIMP-B; Acquisition: 17 February 2004.



## 2002967003: biotite quartzofeldspathic gneiss, Kirgella Rockhole

### SAMPLE INFORMATION

**1:250,000 sheet:** Kurnalpi (SH5110)

**1:100,000 sheet:** Pinjin (3437)

**MGA:** 482940 mE 6677427 mN

**Location:** The sample was taken from an old blast site in the centre of a large pavement that contains the Kirgella Rockhole, west of a fence line and about 10 kms northeast of Pinjin.

**Description:** This blue-grey, seriate to sparsely feldspar-porphyrific, medium-grained, biotite-rich monzogranite is interlayered with light grey, equigranular to seriate, fine- to medium-grained, biotite-poor monzogranite. The bands of biotite-poor and biotite-rich monzogranite form folded, transposed and banded biotite quartzofeldspathic gneiss. Several generations of variably deformed biotite monzogranite and pegmatite dykes cross cut the banded gneiss.

Principal minerals in the granular to granoblastic rock are quartz (35%), K-feldspar (32%), plagioclase (28%) and biotite (8-10%), with K-feldspar > plagioclase. K-feldspar is anhedral to interstitial and locally poikilitic, with variably developed tartan twinning, and minor perthite. Plagioclase occurs as mostly anhedral to lesser subhedral grains with faint to no visible twinning, and no obvious zoning. Minor myrmekite is present. Quartz occurs as anhedral grains, with mild to locally moderately undulose extinction. Biotite is present as light yellow to medium red-brown, subhedral to irregular flakes. Accessory phases include trace secondary titanite, apatite, zircon, and anhedral opaque minerals. The rock is recrystallised, with a weak alignment of biotite and quartz displaying undulose extinction and minor subgrain development. Alteration is limited to weak saussuritisation of plagioclase by white mica, epidote, and minor replacement of biotite by chlorite and epidote/clinozoisite.

### DESCRIPTION OF ZIRCONS

**Shape:** Generally elongate subhedral grains with moderate rounding of crystal faces (Figure 56).

**Size:** ~100 - ~200 microns

**Colour/clarity:** Colourless and brown

**Quality:** Numerous cracks and inclusions



**CL zoning:** Weak concentric and sector zoning with complex embayments dominated by bright rims (Figure 56).

#### CONCURRENT STANDARD DATA

**Pb/U reprod.(2s):** 3.6%

**Err. of mean (2s):** 1.2%

**Standard:** QGNG

**Analyses:** 12

**Notes:** Reproducibility of Pb/U ratios is higher than the normal analytical dispersion. However, the ages of this sample have been determined by  $^{207}\text{Pb}/^{206}\text{Pb}$  ratio which is independent of reproducibility issues.

#### SAMPLE DATA

Twenty-seven analyses were made on twenty-six grains (Table 16). Eight analyses are >5% discordant. Ten analyses are scattered over a range of from ~3300 to ~3800 Ma, but do not have a distinctive morphology, composition or CL pattern (Figure 57). A well defined discordia chord is noted from a concordant group at ~2730 Ma.

Discarding discordant and the older analyses, the remaining nine analyses yield a weighted mean  $^{207}\text{Pb}/^{206}\text{Pb}$  age of  $2732 \pm 16$  Ma (95% conf., MSWD = 5.7). The MSWD is high suggesting that even concordant grains have been affected by Pb-loss. Discarding two analyses  $>3\sigma$  from the weighted mean (#2.1 and #24.1) yields a weighted mean  $^{207}\text{Pb}/^{206}\text{Pb}$  age of  $2722 \pm 15$  Ma (95% conf., MSWD = 3.2); further refinement is statistically unjustified. The smearing of ages in this group is clearly seen in the concordia contour diagram (Figure 58).



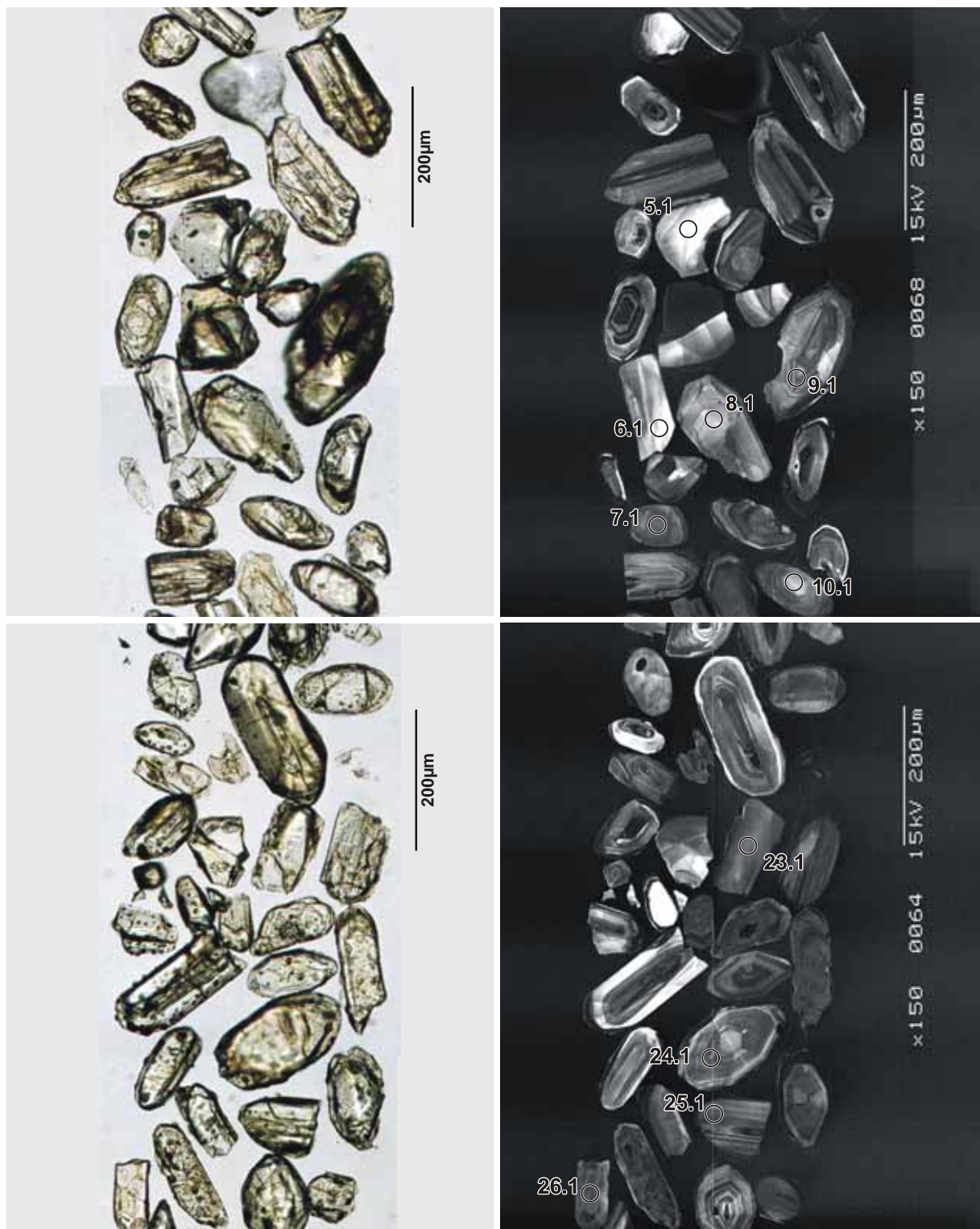


**Figure 56.** Representative images (transmitted light on left, cathodoluminescence on right) for sample 2002967003: biotite quartzofeldspathic gneiss, Kirgella Rockhole. SHRIMP analysis spots are labelled.



**GEOCHRONOLOGICAL INTERPRETATION**

The age of felsic igneous crystallisation is interpreted as  $2722 \pm 15$  Ma, although the age has been affected by a later Pb-loss event. Older ages represent an inherited mixed provenance in the protolith.

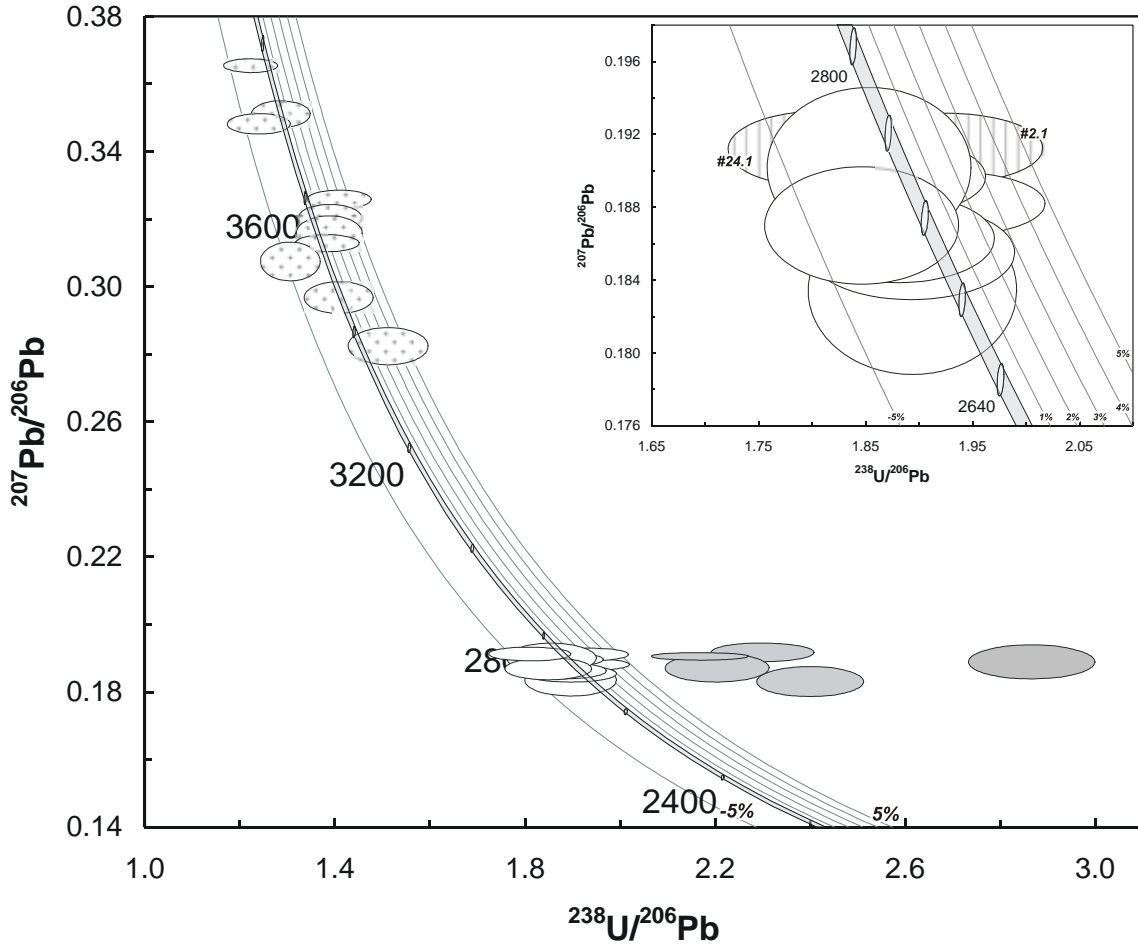


**Figure 57.** Tera-Wasserburg concordia plot for zircons from sample 2002967003: biotite quartzofeldspathic gneiss, Kirgella Rockhole. Insert diagram is a detailed view of the ~2730 Ma group. White-filled symbols are used to define the age of the sample; cross-hatch indicates analyses considered as inheritance; discordant and/or high common-Pb analyses are light grey; outliers have vertical hatching as described in the text.

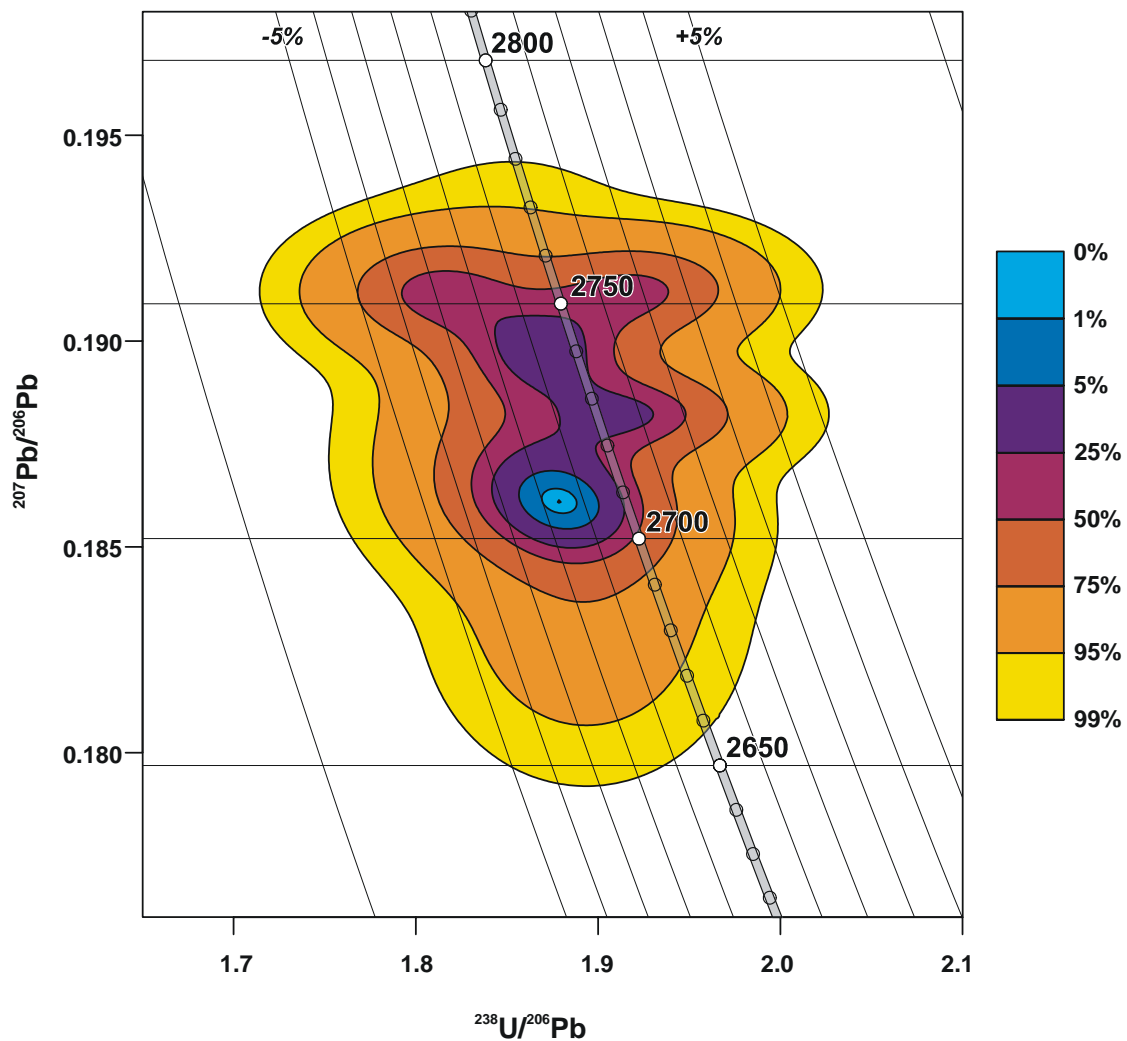


**Figure 58.** Concordia contour plot for zircons in the ~2730 Ma group from sample 2002967003: biotite quartzofeldspathic gneiss, Kirgella Rockhole.

**Table 16.** SHRIMP analytical results for zircon from sample 2002967003: biotite quartzofeldspathic gneiss, Kirgella Rockhole.

Grain. Spot	U (ppm)	Th (ppm)	% comm 206	<sup>207</sup> Pb / <sup>206</sup> Pb	±	<sup>206</sup> Pb / <sup>238</sup> U	±	<sup>207</sup> Pb / <sup>235</sup> U	±	% Disc.	<sup>207</sup> Pb / <sup>206</sup> Pb Age (Ma)	±
<i>Igneous crystallisation</i>												
3.1	229	105	0.023	0.1882	0.0007	0.5189	0.0099	13.4674	0.2619	1	2726.8	6.3
6.1	66	21	0.506	0.1835	0.0019	0.5281	0.0110	13.3609	0.3110	-2	2684.7	16.9
13.1	130	48	0.093	0.1856	0.0010	0.5283	0.0110	13.5170	0.2904	-1	2703.2	9.3
23.1	154	49	0.224	0.1863	0.0010	0.5317	0.0103	13.6583	0.2737	-1	2709.9	8.7
21.1	225	142	0.338	0.1897	0.0009	0.5334	0.0101	13.9515	0.2719	-1	2739.5	7.4
8.1	59	37	0.588	0.1902	0.0018	0.5396	0.0113	14.1492	0.3243	-1	2743.7	15.5
19.1	85	29	0.328	0.1870	0.0013	0.5416	0.0108	13.9675	0.2959	-3	2716.3	11.6
<i>Older outliers?</i>												
2.1	257	223	0.053	0.1913	0.0008	0.5195	0.0099	13.6985	0.2669	2	2753.0	6.7
24.1	160	89	0.062	0.1912	0.0008	0.5533	0.0106	14.5888	0.2880	-3	2752.6	7.3
<i>Inheritance</i>												
5.1	42	37	0.228	0.2823	0.0022	0.6624	0.0149	25.7872	0.6138	3	3375.9	12.3
7.1	182	73	0.495	0.3258	0.0012	0.7113	0.0138	31.9575	0.6320	4	3597.7	5.4
11.1	59	10	0.164	0.2969	0.0019	0.7114	0.0150	29.1180	0.6430	0	3454.0	9.9
22.1	120	103	1.049	0.3206	0.0016	0.7209	0.0140	31.8694	0.6398	2	3572.8	7.6
18.1	75	61	-0.002	0.3158	0.0021	0.7218	0.0146	31.4312	0.6705	1	3549.7	10.4
14.1	169	28	0.209	0.3129	0.0010	0.7236	0.0145	31.2221	0.6322	1	3535.4	5.1
15.1	224	49	0.059	0.3075	0.0023	0.7668	0.0152	32.5106	0.6894	-5	3508.4	11.7
10.1	129	79	0.070	0.3510	0.0016	0.7789	0.0153	37.6991	0.7596	0	3711.5	6.9
12.1	134	58	0.041	0.3482	0.0012	0.8084	0.0177	38.8110	0.8597	-3	3699.2	5.4
20.1	245	107	0.097	0.3655	0.0008	0.8202	0.0155	41.3295	0.7864	-2	3772.7	3.4
<i>Discordant</i>												
2.2	3159	211	18.615	0.1643	0.0150	0.1304	0.0032	2.9553	0.2799	68	790.3	18.3
4.1	135	26	1.289	0.1949	0.0031	0.1611	0.0032	4.3294	0.1115	65	963.0	18.0
9.1	375	107	0.570	0.1904	0.0011	0.1707	0.0036	4.4828	0.0975	63	1016.1	19.7
27.1	272	63	2.015	0.1890	0.0021	0.3493	0.0067	9.1036	0.2011	29	1931.1	31.9
25.1	221	128	1.653	0.1831	0.0018	0.4171	0.0080	10.5324	0.2273	16	2247.3	36.4
16.1	198	128	0.373	0.1917	0.0011	0.4351	0.0083	11.5007	0.2301	16	2328.5	37.4
17.1	85	53	0.370	0.1873	0.0017	0.4544	0.0092	11.7355	0.2602	11	2414.7	40.7
26.1	972	258	0.023	0.1906	0.0005	0.4620	0.0089	12.1390	0.2356	11	2448.5	39.2

Data are at 1 $\sigma$  precision. All Pb data are common-Pb corrected based on <sup>204</sup>Pb measurements. Mount: Z3580; Instrument: JdL Centre SHRIMP-A; Acquisition: 2 March 2004.



## 2002967004: biotite monzogranite, Lords Bore

### SAMPLE INFORMATION

**1:250,000 sheet:** Kurnalpi (SH5110)

**1:100,000 sheet:** Pinjin (3437)

**MGA:** 491600 mE 6673950 mN

**Location:** Sample taken from an old sample site located on large raised pavement about 100 m south of track, about 3.5 km east-southeast of Lords Bore.

**Description:** This rock is a fairly homogeneous, light grey-pink, seriate to sparsely K-feldspar-porphyrific, fine- to medium-grained biotite monzogranite. Minor biotite-rich schlieren as well as an alignment of biotite define a weak foliation in the monzogranite. The monzogranite intrudes banded, foliated and transposed biotite quartzofeldspathic gneiss. Minor thin pegmatite dykes and minor fractures cut the gneiss and monzogranite.

The unit has a granular texture. Principal minerals are quartz (40%), K-feldspar (35%), plagioclase (20%) and biotite (<5%), with K-feldspar > plagioclase. Accessory phases include trace apatite, allanite, zircon, fluorite and anhedral opaque minerals. K-feldspar is subhedral to anhedral, with moderate to well-developed tartan twinning and minor perthite. Plagioclase is subhedral to anhedral, and is generally faintly twinned. Biotite forms light yellow to reddish brown, subhedral to anhedral flakes. The rock has minor micrographic and myrmekitic intergrowth. The rock is weakly recrystallised with quartz mainly recrystallised to a fine-grained mosaic sporadically throughout and also displaying undulose extinction and moderate subgrain development with sutured grain boundaries. Alteration is limited to weak to moderate saussuritisation of plagioclase by white mica, carbonate, clinoziosite/epidote, moderate replacement of biotite by chlorite, epidote/clinoziosite, fluorite, opaque oxides and coarse white mica, and trace hematite staining.

### DESCRIPTION OF ZIRCONS

**Shape:** Sub-euhedral to euhedral prismatic grains. Grains generally stubby ([Figure 59](#)).

**Size:** 60 to 120 microns.

**Colour/clarity:** Clear to yellow. Generally clear, some staining.

**Quality:** Poor to fair. Common fractures and large inclusions.

**CL zoning:** Complex zoning; concentric zoned cores with unzoned, high-U rims common. Older zoning is truncated and often rounded, but there is little evidence of features associated with magmatic



resorption. Some cores, especially darker ones, display extensive alteration and complex zoning (Figure 59).

#### CONCURRENT STANDARD DATA

**Pb/U reprod.(2s):** 5.6%

**Err. of mean (2s):** 1.6%

**Standard:** QGNG

**Analyses:** 13 (two discarded due to U content > 1000 ppm)

**Notes:** Pb/U calibration slope is non-default at 2.2. The reproducibility error is very high. This sample was one of the first attempted on the new SHRIMP-B instrument and some procedures to improve primary beam stability were not developed. Although this large error will contribute to  $^{206}\text{Pb}/^{238}\text{U}$  age errors it will have no impact on  $^{207}\text{Pb}/^{206}\text{Pb}$  ages which are used here.

#### SAMPLE DATA

Twenty-eight analyses were made on twenty-six grains (Table 17). The poor quality of the zircon is reflected in the exclusion of 17 discordant and high common-Pb ages. The data fall into two clusters (Figure 60; Figure 61). The older cluster of five ages is associated with lower-U cores (median 117 ppm) with concentric CL zoning. The younger cluster of six ages is associated with higher-U rims and whole grains (median 395 ppm) with homogeneous CL zoning. One grain (#8) clearly demonstrates a significant age difference between core ( $2718.7 \pm 34.8$  Ma) and rim ( $2619.9 \pm 21.0$  Ma).

The weighted-mean  $^{207}\text{Pb}/^{206}\text{Pb}$  age of the older cluster is  $2700 \pm 13$  Ma (MSWD: 1.2) and the younger cluster is  $2636.8 \pm 8.7$  Ma (MSWD: 1.6). The higher U zircons have undergone significant Pb-loss since crystallisation, but it is unclear if this is simply zero-age Pb-loss or an earlier alteration event.



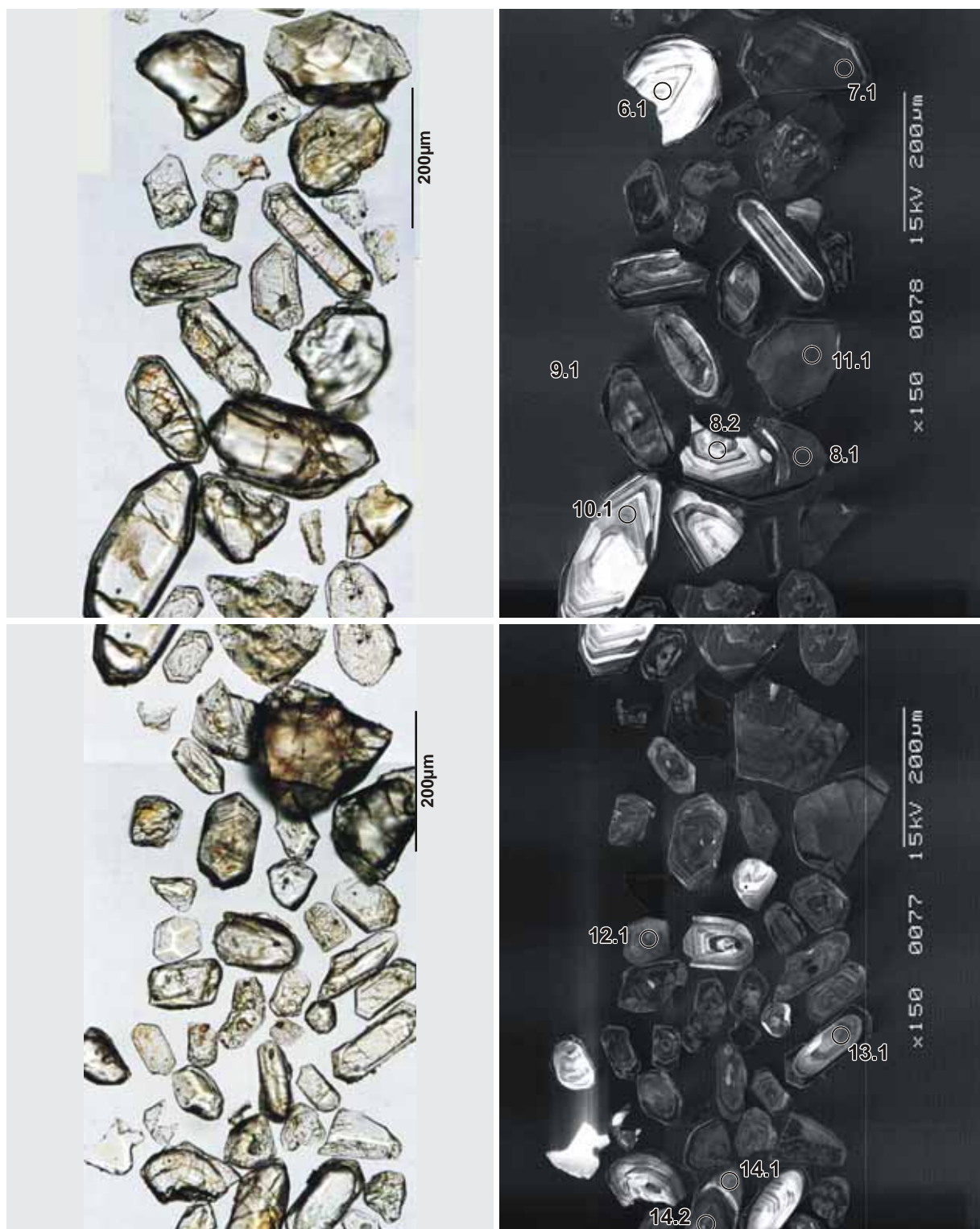


**Figure 59.** Representative images (transmitted light on left, cathodoluminescence on right) for sample 2002967004: biotite monzogranite, Lords Bore. SHRIMP analysis spots are labelled.

#### GEOCHRONOLOGICAL INTERPRETATION

The magmatic age of the monzogranite is interpreted as  $2638 \pm 9$  Ma, with a large proportion of zircon inherited from a precursor event at  $2700 \pm 13$  Ma.



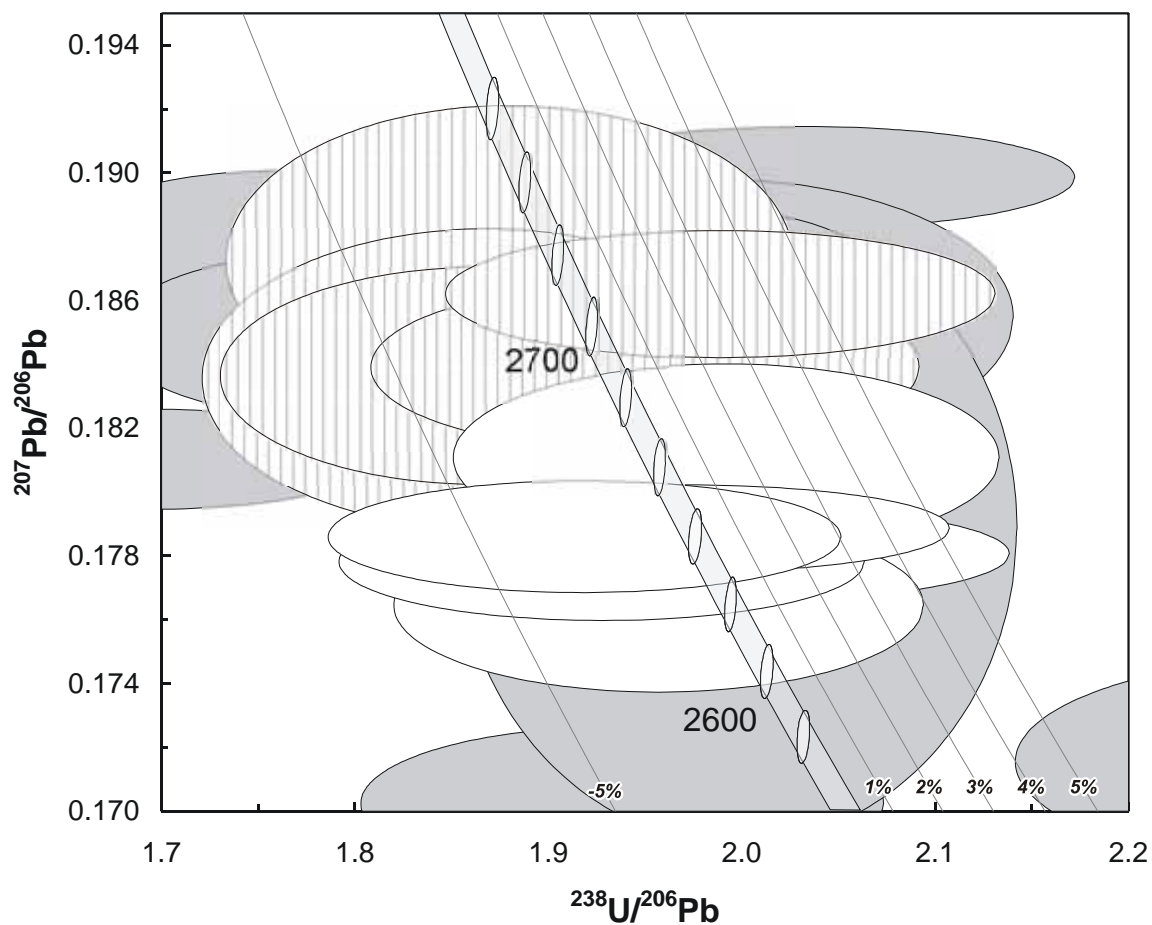


**Figure 60.** Tera-Wasserburg concordia plot for zircons from sample 2002967004: biotite monzogranite, Lords Bore. White-filled symbols are used to define the age of the sample; discordant and/or high common-Pb analyses are light grey; inherited analyses have vertical striping.

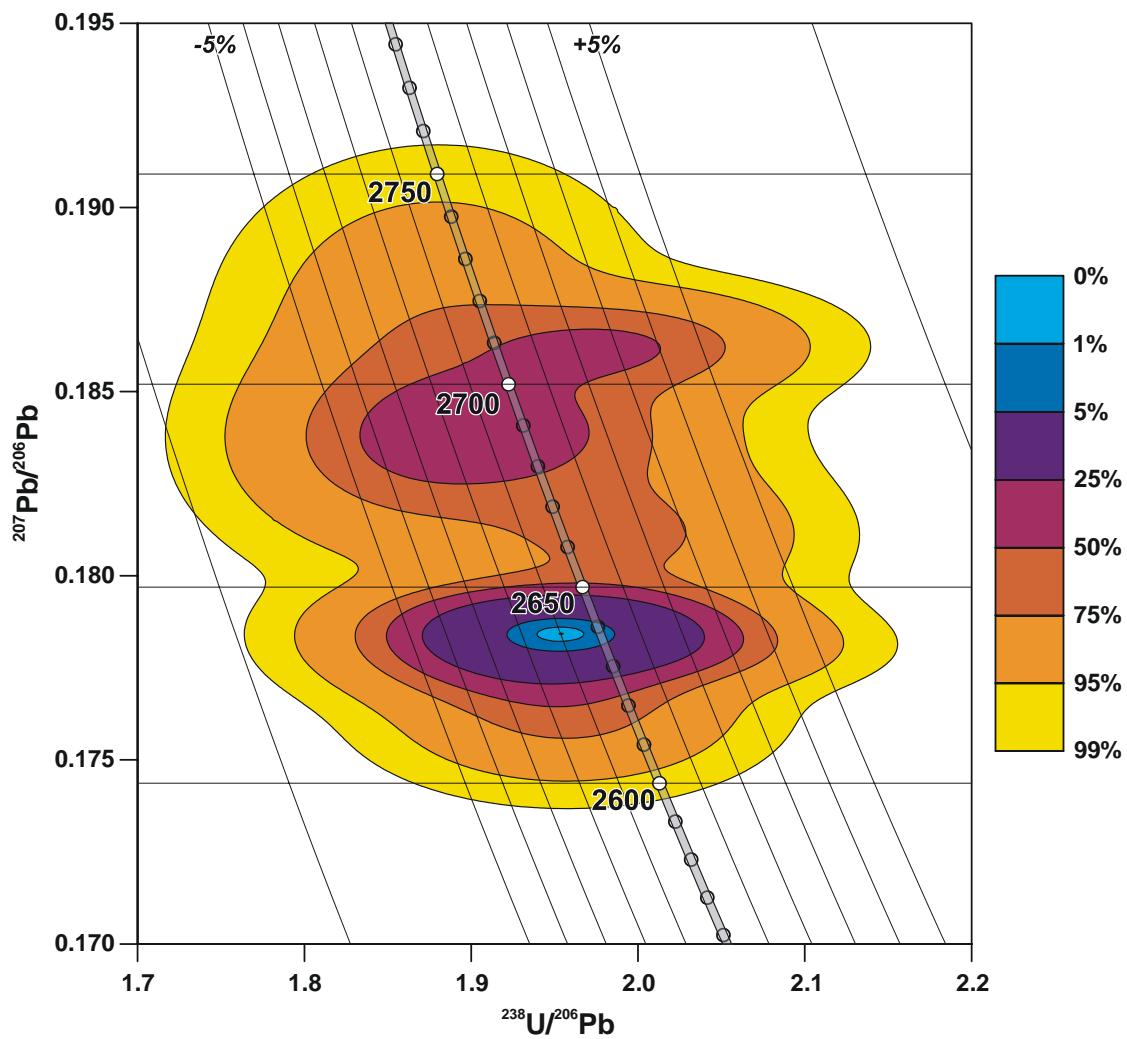


**Figure 61.** Tera-Wasserburg concordia contour plot of sample 2002967004: biotite monzogranite, Lords Bore illustrating the distinction between the two clusters at 2700 Ma and 2638 Ma. Only data within 5% discordance are included in the distribution.

**Table 17.** SHRIMP analytical results for zircon from sample 2002967004: biotite monzogranite, Lords Bore.

Grain. Spot	U (ppm)	Th (ppm)	% comm 206	<sup>207</sup> Pb / <sup>206</sup> Pb	±	<sup>206</sup> Pb / <sup>238</sup> U	±	<sup>207</sup> Pb / <sup>235</sup> U	±	% Disc.	<sup>207</sup> Pb / <sup>206</sup> Pb Age (Ma)	±
<i>Inheritance</i>												
9.1	66	24	0.50	0.1836	0.0019	0.5354	0.0171	13.55	0.46	-2.9	2685.4	17.3
13.1	117	36	0.23	0.1837	0.0014	0.5353	0.0160	13.55	0.42	-2.9	2686.2	12.6
5.1	136	68	0.02	0.1839	0.0011	0.5128	0.0152	13.00	0.39	0.7	2688.6	9.7
2.1	277	175	0.00	0.1862	0.0008	0.5028	0.0146	12.91	0.38	3.1	2709.2	7.2
8.2	58	25	0.26	0.1873	0.0020	0.5319	0.0169	13.74	0.46	-1.1	2718.7	17.4
<i>Magmatic/overgrowth</i>												
8.1	367	101	0.60	0.1765	0.0011	0.5110	0.0146	12.43	0.36	-1.6	2619.9	10.5
11.1	277	331	0.08	0.1778	0.0008	0.5188	0.0149	12.72	0.37	-2.3	2632.5	7.0
6.1	423	193	0.07	0.1781	0.0006	0.5009	0.0145	12.30	0.36	0.6	2634.8	5.7
20.1	545	602	0.19	0.1786	0.0007	0.5211	0.0147	12.83	0.37	-2.4	2639.9	6.7
7.1	546	433	0.07	0.1789	0.0006	0.5074	0.0144	12.51	0.36	-0.1	2642.3	5.2
14.2	281	91	0.64	0.1811	0.0012	0.5020	0.0145	12.54	0.37	1.5	2662.9	11.0
<i>Discordant/High common-Pb</i>												
3.1	7263	2875	3.83	0.1068	0.0059	0.1668	0.0048	2.46	0.15	43.0	1745.7	100.9
23.1	11383	6683	23.77	0.1081	0.0176	0.0820	0.0030	1.22	0.20	71.3	1768.3	296.7
21.2	1895	198	0.49	0.1172	0.0005	0.2741	0.0077	4.43	0.13	18.4	1913.5	7.2
18.1	1619	465	0.34	0.1391	0.0007	0.3494	0.0098	6.70	0.19	12.8	2216.0	8.4
4.2	2127	203	0.46	0.1445	0.0005	0.3533	0.0100	7.04	0.20	14.6	2282.4	5.6
21.1	913	61	0.11	0.1587	0.0010	0.3466	0.0098	7.58	0.22	21.4	2441.5	11.2
17.1	919	270	0.12	0.1656	0.0004	0.4166	0.0117	9.51	0.27	10.7	2513.6	3.9
15.1	806	977	0.11	0.1677	0.0004	0.4435	0.0125	10.25	0.29	6.6	2534.6	4.1
22.1	850	984	0.75	0.1702	0.0010	0.5159	0.0147	12.11	0.35	-4.8	2559.5	9.8
14.1	295	68	0.95	0.1715	0.0014	0.4341	0.0125	10.26	0.31	9.7	2572.5	13.2
12.1	677	948	1.91	0.1789	0.0041	0.5006	0.0148	12.35	0.46	1.0	2642.4	37.7
16.1	5441	3857	0.80	0.1810	0.0006	0.5898	0.0165	14.72	0.41	-12.2	2662.4	5.9
19.1	92	25	0.09	0.1849	0.0011	0.5543	0.0163	14.13	0.42	-5.4	2697.5	9.9
10.1	169	164	1.24	0.1855	0.0018	0.5038	0.0161	12.89	0.43	2.7	2702.9	15.8
24.1	113	48	0.00	0.1878	0.0009	0.5650	0.0165	14.63	0.43	-6.0	2723.1	8.3
1.1	432	104	0.18	0.1899	0.0007	0.4924	0.0140	12.89	0.37	5.8	2741.3	5.6
4.1	228	248	18.94	0.2066	0.0251	0.8558	0.0377	24.38	3.15	-38.4	2879.0	197.6

Data are at 1 $\sigma$  precision. All Pb data are common-Pb corrected based on <sup>204</sup>Pb measurements. Mount: Z3580; Instrument: JdL Centre SHRIMP-B; Acquisition: 13 February 2004.



## 2004967308: volcanic meta-sandstone, Kanowna Belle

### SAMPLE INFORMATION

**1:250,000 sheet:** SH5110 Kurnalpi

**1:100,000 sheet:** 3236 Kanowna

**MGA:** 362235 mE 6612685 mN

**Location:** This sample was taken from Placer Dome Asia Pacific diamond drill hole GVD97, depth interval 300.85-302.00 m. The collar is located approximately 1 km west of Kanowna Belle mine.

**Description:** It is a grey, altered, volcanic meta-sandstone. It contains cyclic graded beds of medium- to very coarse-grained sandstone, with pebbly horizons. The meta-sandstone contains a variety of altered, sub-mm to 3 mm size angular to sub-rounded crystal and lithic clasts and possible relict pumice or glassy shards consistent with a volcanoclastic origin. The unit is from the upper part of a sequence of sandstones and conglomerates that dips steeply to the east, is structurally dismembered and referred to as the Golden Valley conglomerate.

Principal minerals are discrete mono- and polycrystalline quartz (<10%), altered feldspar (~30%), microcrystalline quartz and/or feldspar (20%), chlorite (15%), sericite (~15%), carbonate (8-10%), opaque minerals (<2%), leucoxene (<2%), and trace zircon. The sample is an intensely altered, poorly-sorted, clast-rich rock with a very fine-grained chloritic and quartz-feldspar-rich matrix forming up to 20% of the rock. Crystal and lithic clasts, generally <3 mm, form about 80% of the rock and include monocrystalline quartz (7-8%) and feldspar (~30%), polycrystalline quartz (<1%), and a variety of altered rock fragments (40-45%). The quartz clasts are generally angular to rarely sub-rounded, feldspar clasts are angular and strongly altered to albite, sericite and carbonate, whereas alteration hampers identification of the other clast types. The lithic clasts have a variety of alteration assemblages, including quartz-feldspar, chlorite-feldspar-quartz-leucoxene, carbonate-chlorite-leucoxene, quartz-sericite carbonate, sericite-chlorite-carbonate-leucoxene assemblages, indicating a range of precursor lithologies. Aligned, elongate, angular to wispy chlorite-sericite-rich fragments (2-3%) may represent altered relict pumice and/or glassy shards. Opaque minerals occur as subhedral to anhedral and irregular grains disseminated throughout the matrix and concentrated in sericite-, chlorite- and carbonate-rich lithic clasts.



## DESCRIPTION OF ZIRCONS

- Shape:** Subhedral to euhedral prismatic grains (Figure 62).  
**Size:** 50 to 200 microns.  
**Colour/clarity:** Clear to brown, occasionally turbid.  
**Quality:** Generally good. Frequent fractures and inclusions.  
**CL zoning:** Prominent concentric zoning with occasional complex embayments. Occasional sector-zoning (Figure 62).

## CONCURRENT STANDARD DATA

- Pb/U reprod.(2s):** 0.50%  
**Err. of mean (2s):** 1.12%  
**Standard:** QGNG  
**Analyses:** 12 (one discarded as anomalous)  
**Notes:** This was a two-day session with occasional primary beam spiking problems which has caused the calculated uncertainty of some analyses to be exaggerated.

## SAMPLE DATA

Thirty-four analyses were made on thirty-four grains (Table 18). Only one analysis has been discarded because of high common-Pb (#5.1). There is also one clearly older analysis (#22.1) which is interpreted as inheritance (Figure 63). The remaining 32 analyses do not display any significant correlation between U/Th content, CL patterns and age. However, there does appear to be a possibly inherited component and an ancient Pb-loss component in the distribution (Figure 64). This dispersion is confirmed with an inability to derive a concordia age without arbitrary and statistically unjustified culling, and a weighted mean  $^{207}\text{Pb}/^{206}\text{Pb}$  age of  $2668.7 \pm 4.6$  (95% conf., MSWD = 3.5, 32 ages) with a notably large MSWD.

Applying mixture modelling to the age distribution yields three components at  $2657.2 \pm 17$ ,  $2667.8 \pm 6.5$  and  $2694.1 \pm 7.3$  Ma (Figure 65). The second component is dominant and also corresponds to the peak of the contoured distribution (Figure 64). The younger component could represent ancient Pb-loss and the older peak could reflect inheritance or analytical overlap with older zones.





*Figure 62. Representative images (transmitted light on left, cathodoluminescence on right) for sample 2004967308: volcanic meta-sandstone, Kanowna Belle. SHRIMP analysis spots are labelled.*

#### **GEOCHRONOLOGICAL INTERPRETATION**

The magmatic age of the dominant component of this meta-sandstone is interpreted as  $2668 \pm 7$  Ma with suggestion of an inherited component at  $\sim 2694$  Ma and an ancient Pb-loss event.



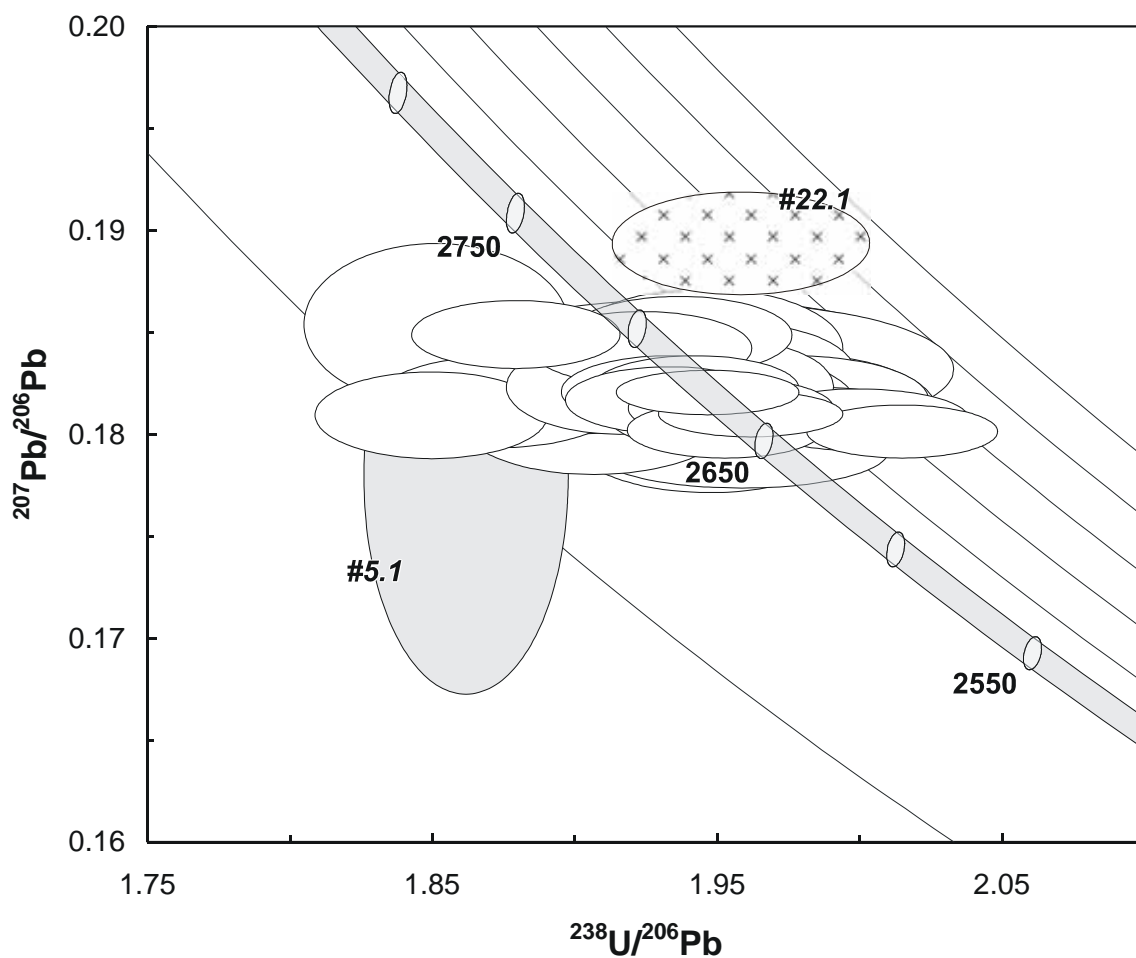


**Figure 63.** Tera-Wasserburg concordia plot for zircons from sample 2004967308: volcanic meta-sandstone, Kanowna Belle. White-filled symbols are used to define the age of the sample as discussed in text; discordant and/or high common-Pb analyses are light grey; cross hatch indicates analyses interpreted as inheritance.



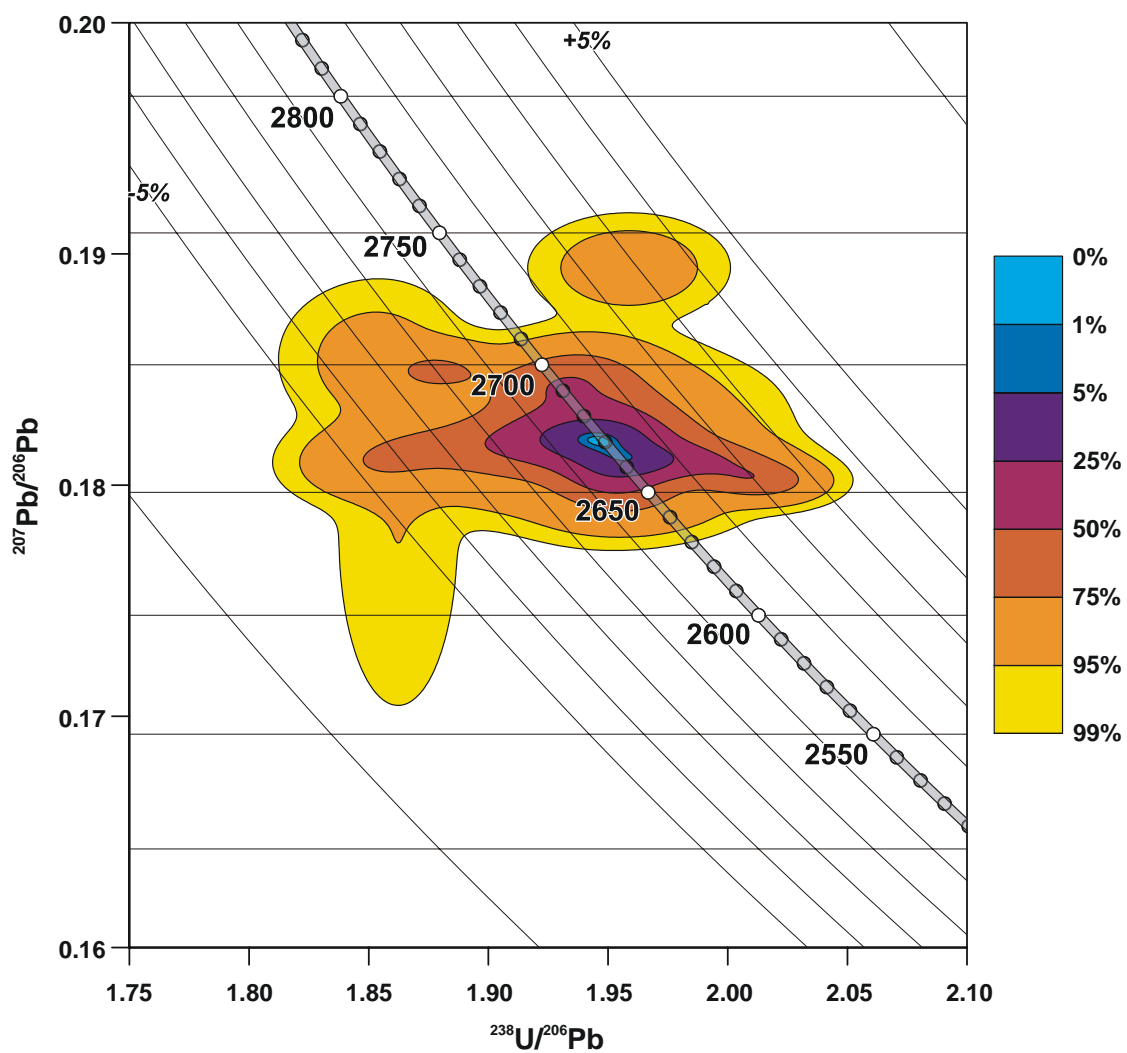


**Figure 64.** Tera-Wasserburg concordia contour plot for two sets of analyses from sample 2004967308: volcanic meta-sandstone, Kanowna Belle.

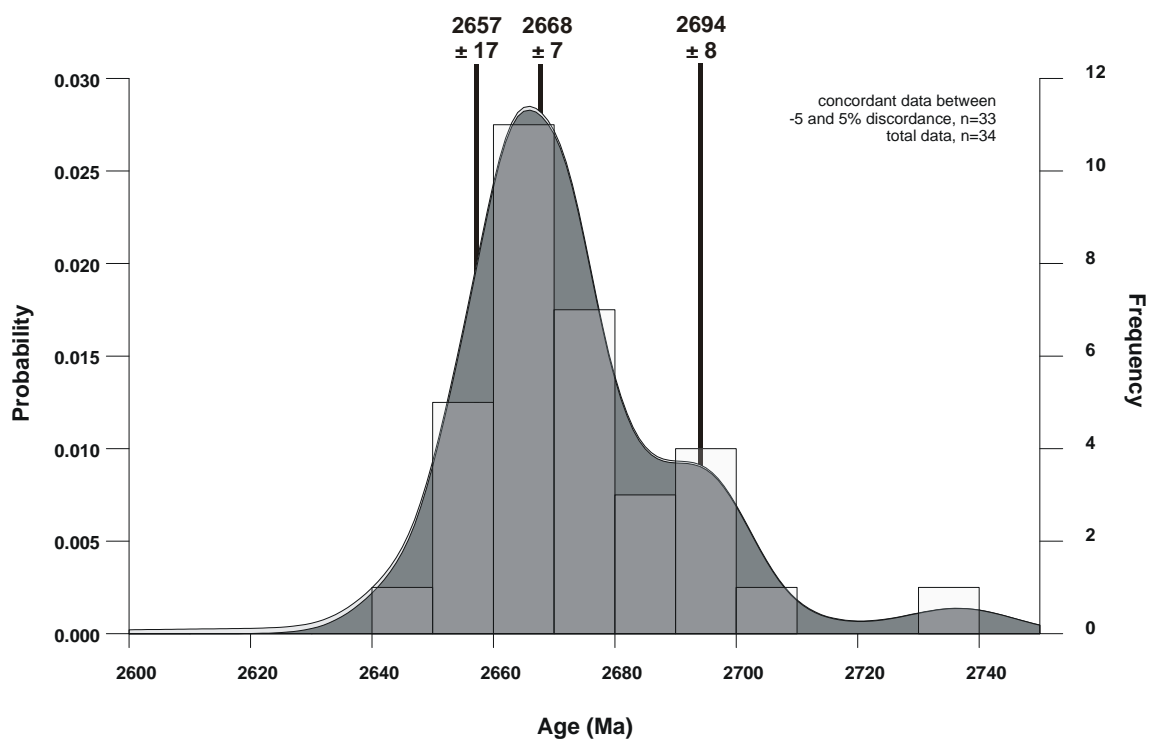


**Figure 65.** Probability density distribution and histogram plot of  $^{207}\text{Pb}/^{206}\text{Pb}$  ages from sample 2004967308: volcanic meta-sandstone, Kanowna Belle.

**Table 18.** SHRIMP analytical results for zircon from sample 2004967308: volcanic meta-sandstone, Kanowna Belle.

Grain. Spot	U (ppm)	Th (ppm)	% comm 206	<sup>207</sup> Pb / <sup>206</sup> Pb	±	<sup>206</sup> Pb / <sup>238</sup> U	±	<sup>207</sup> Pb / <sup>235</sup> U	±	% Disc.	<sup>207</sup> Pb / <sup>206</sup> Pb Age (Ma)	±
<i>Main</i>												
7.1	123	143	0.047	0.1792	0.0007	0.5104	0.0055	12.6103	0.1451	-0.5	2645.4	6.9
2.1	57	55	0.078	0.1800	0.0012	0.5135	0.0054	12.7459	0.1578	-0.7	2653.2	10.9
8.1	341	187	0.263	0.1802	0.0005	0.4962	0.0034	12.3270	0.0909	2.1	2654.4	4.9
34.1	241	122	0.117	0.1802	0.0006	0.5120	0.0037	12.7230	0.0992	-0.4	2655.0	5.2
27.1	62	51	0.029	0.1807	0.0011	0.5243	0.0053	13.0602	0.1527	-2.2	2658.9	9.8
21.1	189	164	0.016	0.1807	0.0006	0.4999	0.0039	12.4571	0.1068	1.7	2659.6	5.7
23.1	150	83	0.001	0.1809	0.0007	0.5128	0.0040	12.7900	0.1114	-0.3	2661.0	6.3
15.1	89	8	0.021	0.1809	0.0009	0.5405	0.0049	13.4840	0.1377	-4.7	2661.6	8.0
20.1	356	95	0.028	0.1810	0.0005	0.5096	0.0034	12.7212	0.0915	0.3	2662.4	4.2
33.1	303	133	0.017	0.1811	0.0005	0.5056	0.0050	12.6275	0.1285	1.0	2663.3	4.6
9.1	55	50	-0.015	0.1812	0.0011	0.5060	0.0053	12.6440	0.1548	0.9	2664.1	10.3
10.1	179	102	0.009	0.1813	0.0006	0.5114	0.0039	12.7821	0.1056	0.1	2664.5	5.6
32.1	78	34	0.062	0.1816	0.0010	0.5120	0.0048	12.8160	0.1399	0.1	2667.1	9.0
24.1	76	63	-0.002	0.1816	0.0009	0.5337	0.0050	13.3643	0.1433	-3.4	2667.6	8.4
14.1	170	88	0.128	0.1817	0.0007	0.5173	0.0039	12.9586	0.1099	-0.7	2668.4	6.2
4.1	92	32	0.004	0.1817	0.0009	0.5056	0.0049	12.6677	0.1376	1.1	2668.5	8.1
17.1	152	58	-0.007	0.1817	0.0007	0.5251	0.0054	13.1556	0.1428	-2.0	2668.6	6.1
28.1	85	24	-0.005	0.1820	0.0009	0.5132	0.0051	12.8797	0.1422	0.0	2671.5	8.2
31.1	369	177	0.002	0.1821	0.0004	0.5136	0.0035	12.8942	0.0924	0.0	2671.9	4.1
19.1	135	110	-0.005	0.1821	0.0007	0.5171	0.0042	12.9862	0.1166	-0.5	2672.5	6.5
25.1	164	92	0.042	0.1822	0.0007	0.5147	0.0040	12.9342	0.1102	-0.1	2673.4	6.1
1.1	65	68	-0.038	0.1823	0.0011	0.5243	0.0053	13.1763	0.1571	-1.7	2673.5	10.4
30.1	116	40	0.449	0.1824	0.0010	0.5218	0.0044	13.1204	0.1306	-1.2	2674.4	8.6
26.1	171	77	0.385	0.1824	0.0010	0.5121	0.0041	12.8770	0.1241	0.3	2674.5	8.7
18.1	70	55	0.019	0.1831	0.0010	0.5122	0.0050	12.9297	0.1447	0.6	2681.0	9.2
16.1	48	22	0.157	0.1832	0.0013	0.5124	0.0088	12.9430	0.2403	0.6	2682.1	11.9
29.1	73	22	0.037	0.1838	0.0012	0.5155	0.0091	13.0642	0.2447	0.3	2687.5	10.5
12.1	60	21	0.212	0.1842	0.0012	0.5139	0.0052	13.0528	0.1584	0.7	2691.2	10.8
6.1	133	39	-0.008	0.1843	0.0007	0.5198	0.0043	13.2056	0.1205	-0.2	2691.6	6.6
3.1	125	47	0.038	0.1849	0.0008	0.5161	0.0043	13.1589	0.1227	0.5	2697.3	7.0
11.1	179	92	0.051	0.1849	0.0007	0.5320	0.0042	13.5643	0.1190	-1.9	2697.6	6.2
13.1	75	44	0.017	0.1854	0.0016	0.5400	0.0055	13.8072	0.1862	-3.0	2702.1	14.5
<i>Inheritance</i>												
22.1	76	36	0.060	0.1894	0.0010	0.5105	0.0048	13.3320	0.1450	2.9	2737.0	9.0
<i>High common Pb</i>												
5.1	289	174	5.598	0.1778	0.0043	0.5370	0.0042	13.1661	0.3373	-5.2	2632.7	40.5

Data are at 1 $\sigma$  precision. All Pb data are common-Pb corrected based on <sup>204</sup>Pb measurements. Mount: Z4636; Instrument: JdL Centre SHRIMP-A; Acquisition: 11 October 2005.



## 2004967310: volcanic meta-sandstone, Kanowna Belle

### SAMPLE INFORMATION

**1:250,000 sheet:** SH5110 Kurnalpi

**1:100,000 sheet:** 3236 Kanowna

**MGA:** 365696 mE 6614032 mN

**Location:** This sample is from Placer Dome Asia Pacific diamond drill hole FED002, depth interval 320.00-321.00 m. The collar is located approximately 1 km east-northeast of Kanowna Belle mine.

**Description:** This rock is a white-grey, altered, volcanic meta-sandstone. The medium- to very coarse-grained sandstone contains a variety of altered, sub-mm to 2 cm size angular to sub-rounded, crystal and lithic clasts and possible relict pumice or glassy shards consistent with a volcanoclastic origin. The unit is from the lower part of a sequence of sandstone and conglomerate, which is locally referred to as the Ballarat Grit.

The sample is an intensely altered, poorly-sorted, clast-rich rock with a very fine-grained sericitic and quartz-feldspar-rich matrix forming up to 30% of the rock. Crystal and lithic clasts, generally <1 cm, form about 70% of the rock and include monocrystalline quartz (20%) and feldspar (10-15%), polycrystalline quartz (~5%), and a variety of altered rock fragments (30-35%). The quartz clasts are generally angular to rarely sub-rounded, and locally resorbed. Feldspar clasts are angular and intensely altered to albite, sericite and carbonate. The lithic clasts include intensely altered dacitic, andesitic, rhyolitic and rare fuchsite-bearing mafic lithologies. Alteration has resulted in a variety of assemblages, including quartz-albite, chlorite-albite-quartz-leucoxene, carbonate-chlorite-leucoxene, quartz-sericite carbonate, and sericite-chlorite-carbonate-leucoxene. Elongate, angular to wispy sericite-carbonate-opaque mineral-rich fragments (3-4%) possibly represent altered relict pumice and/or glassy shards. Opaque minerals occur as subhedral to anhedral and irregular grains disseminated throughout the matrix and concentrated in sericite-, carbonate- and chlorite-rich lithic clasts. Carbonate also forms irregular to anhedral grains disseminated throughout the various rock fragments and matrix. Accessory phases include trace zircon.

### DESCRIPTION OF ZIRCONS

**Shape:** Subhedral prismatic grains with minor rounding of crystal faces (Figure 66).

**Size:** 50 to 200 microns.



- Colour/clarity:** Generally clear.
- Quality:** Good to fair. Frequent fractures and inclusions.
- CL zoning:** Complex concentric zoning with frequent embayment patterns (Figure 66).
- Notes:** Zircon yield from this sample was very limited.

#### CONCURRENT STANDARD DATA

- Pb/U reprod.(2s):** 1.15%
- Err. of mean (2s):** 3.35%
- Standard:** QGNG
- Analyses:** 12 (two discarded as anomalous)
- Notes:** This one day session was marked by frequent primary beam failures resulting in a marked diminution of reproducibility.

#### SAMPLE DATA

Because of limited sample yield only six analyses were made on six grains (Table 19). These analyses have a range of common-Pb and discordance which would normally be largely discarded. For the sake of limited reconnaissance these faults have been ignored and yield a reasonable discordia chord with intercepts at  $2693 \pm 18$  and  $732 \pm 110$  Ma (MSWD = 0.95) (Figure 67). The upper intercept is very tentatively interpreted as a determined age, but the result should be treated with extreme caution.



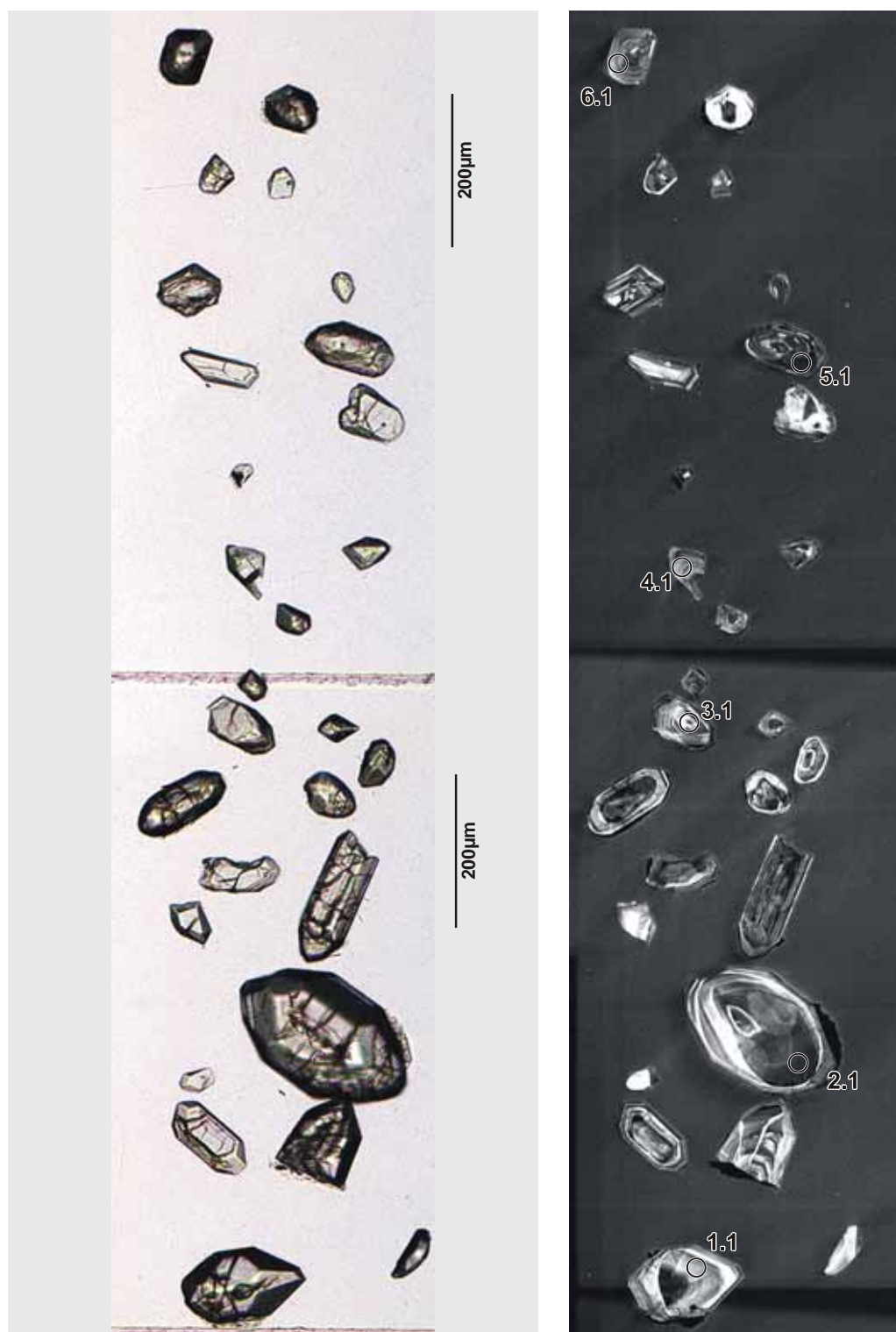


**Figure 66.** Complete image (transmitted light on left, cathodoluminescence on right) for sample 2004967310: volcanic meta-sandstone, Kanowna Belle. SHRIMP analysis spots are labelled.

#### **GEOCHRONOLOGICAL INTERPRETATION**

The magmatic age of the volcanoclastic rock is very tentatively interpreted as  $2693 \pm 18$  Ma. The zircons have been strongly influenced by a Neoproterozoic Pb-loss event.



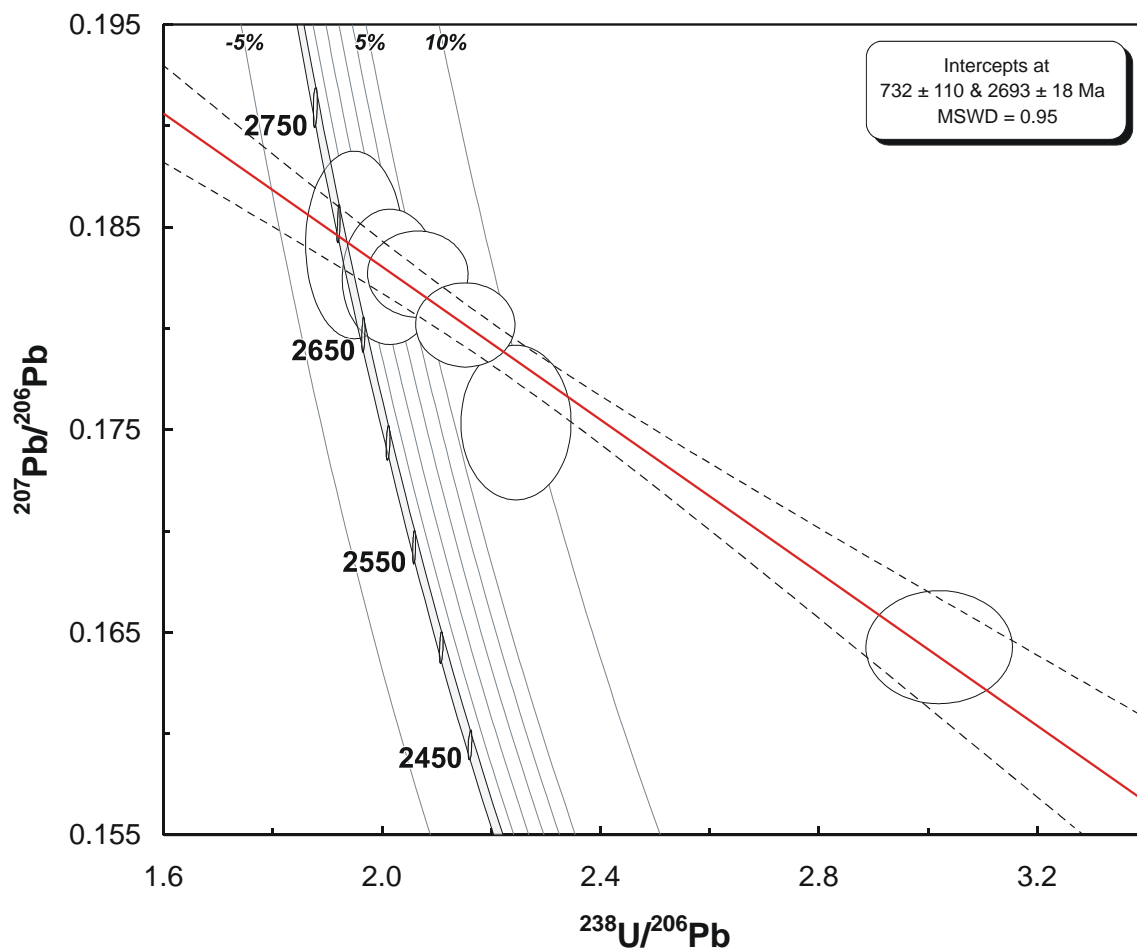


**Figure 67.** Tera-Wasserburg concordia plot for zircons from sample 2004967310: volcanic meta-sandstone, Kanowna Belle. White-filled symbols are used to define the age of the sample as discussed in text.

**Table 19.** SHRIMP analytical results for zircon from sample 2004967310: volcanic meta-sandstone, Kanowna Belle.

Grain. Spot	U (ppm)	Th (ppm)	% comm 206	<sup>207</sup> Pb / <sup>206</sup> Pb	±	<sup>206</sup> Pb / <sup>238</sup> U	±	<sup>207</sup> Pb / <sup>235</sup> U	±	% Disc.	<sup>207</sup> Pb / <sup>206</sup> Pb Age (Ma)	±
<i>Main</i>												
3.1	524	212	0.818	0.1643	0.0011	0.3309	0.0060	7.4943	0.1454	26.3	2500.2	11.7
5.1	377	175	0.681	0.1754	0.0016	0.4451	0.0082	10.7616	0.2207	9.1	2609.5	14.8
6.1	304	159	1.219	0.1802	0.0008	0.4641	0.0080	11.5300	0.2063	7.4	2654.5	7.8
1.1	94	34	0.495	0.1826	0.0014	0.4960	0.0089	12.4861	0.2429	3.0	2676.3	12.3
2.1	335	154	0.449	0.1827	0.0009	0.4837	0.0088	12.1839	0.2284	5.0	2677.5	7.9
4.1	154	49	1.808	0.1841	0.0019	0.5126	0.0096	13.0139	0.2772	0.8	2690.4	17.0

Data are at 1σ precision. All Pb data are common-Pb corrected based on <sup>204</sup>Pb measurements. Mount: Z4636; Instrument: RSES SHRIMP-RG; Acquisition: 4 July 2005.

## 2004967316: volcanic meta-sandstone, Kanowna Belle

### SAMPLE INFORMATION

**1:250,000 sheet:** SH5110 Kurnalpi

**1:100,000 sheet:** 3236 Kanowna

**MGA:** 364794 mE 6613193 mN

**Location:** This sample was taken from Placer Dome Asia Pacific diamond drill hole GVD51, depth interval 325.15-326.30 m. The collar is located approximately 1 km east-northeast of Kanowna Belle mine.

**Description:** It is a grey, altered, volcanic meta-sandstone. The medium- to very coarse-grained sandstone contains a variety of altered, sub-mm to 3 cm size, angular to sub-rounded, crystal and lithic clasts and relict pumice or glassy shards consistent with a volcanoclastic origin. The unit is from the lower part of a sequence of sandstone and conglomerate, which is locally referred to as the Ballarat Grit. The rock is cut by rare carbonate-filled fractures.

This is a moderately altered, poorly-sorted, clast-rich rock with a very fine-grained chloritic and quartz-feldspar-rich matrix forming up to 25% of the rock. Crystal and lithic clasts, generally <1 cm, form about 75% of the rock and include monocrystalline quartz (10-15%) and feldspar (40-45%), polycrystalline quartz (5-8%), and altered rock fragments (8-10%). Elongate, angular to wispy chlorite-carbonate-sericite-opaque mineral-rich fragments (4-5%) possibly represent altered relict pumice and/or glassy shards. The quartz clasts are generally angular to rarely sub-rounded, and rarely resorbed. Feldspar clasts are angular and moderately altered to albite, sericite and carbonate. The lithic clasts include altered porphyritic dacitic and andesitic lithologies. Alteration has resulted in a variety of assemblages with variable amounts of chlorite, carbonate, sericite, albite, opaque minerals, tourmaline and relict biotite. Sericite is locally aligned and wraps some crystal and lithic clasts. Carbonate also forms irregular to anhedral grains disseminated throughout the various rock fragments and matrix. Opaque minerals occur as subhedral to anhedral and irregular grains disseminated throughout the matrix and concentrated in sericite-, carbonate- and chlorite-rich lithic clasts. Accessory phases include minor blue-green subhedral tourmaline and trace zircon.



#### DESCRIPTION OF ZIRCONS

<b>Shape:</b>	Euhedral to subhedral prismatic grains with frequently rounded crystal tips (Figure 68).
<b>Size:</b>	100 to 200 microns.
<b>Colour/clarity:</b>	Clear to brown, frequently turbid.
<b>Quality:</b>	Fair to poor. Frequent fractures and inclusions.
<b>CL zoning:</b>	Prominent concentric zoning with common complex embayment structures (Figure 68).

#### CONCURRENT STANDARD DATA

<b>Pb/U reprod.(2s):</b>	1.11%
<b>Err. of mean (2s):</b>	3.23%
<b>Standard:</b>	QGNG
<b>Analyses:</b>	12 (two discarded as anomalous)
<b>Notes:</b>	This one day session was marked by frequent primary beam failures resulting in a marked diminution of reproducibility.

#### SAMPLE DATA

Twenty-nine analyses were made on twenty-five grains (Table 20). The poor quality of the zircon is indicated by seventeen of the analyses having >1% common-Pb which is also associated with high U and Th content. The remaining analyses with <1% common-Pb are also reasonably concordant although do not produce a singular cluster (Figure 69).

Further visualisation of the data suggests three components (Figure 70) and this is also indicated by mixture modelling of  $^{207}\text{Pb}/^{206}\text{Pb}$  ages yields components at  $2651.9 \pm 12$ ,  $2681.1 \pm 11$  and  $2694.9 \pm 5.7$  Ma (Figure 71). The distribution suggests a systematic miscalibration causing the older components to appear slightly reversely discordant. The whole distribution is also suggestive of an ancient Pb-loss discordia. The ~2681 Ma component is either a result of ancient Pb-loss, analytical mixing or may represent a subsidiary magmatic component in the volcanoclastic rock. Any interpretation of this age is thus considered very tentative.

It is interesting to note that the tentative age of zircon in the other Ballarat Grit (sample 2004967310) is ~2693 Ma.





**Figure 68.** Representative images (transmitted light on left, cathodoluminescence on right) for sample 2004967316: volcanic meta-sandstone, Kanowna Belle. SHRIMP analysis spots are labelled.

#### GEOCHRONOLOGICAL INTERPRETATION

The magmatic age of the dominant component of the meta-sandstone is interpreted as  $2695 \pm 6$  Ma and the zircons have been influenced by an ancient Pb-loss event.



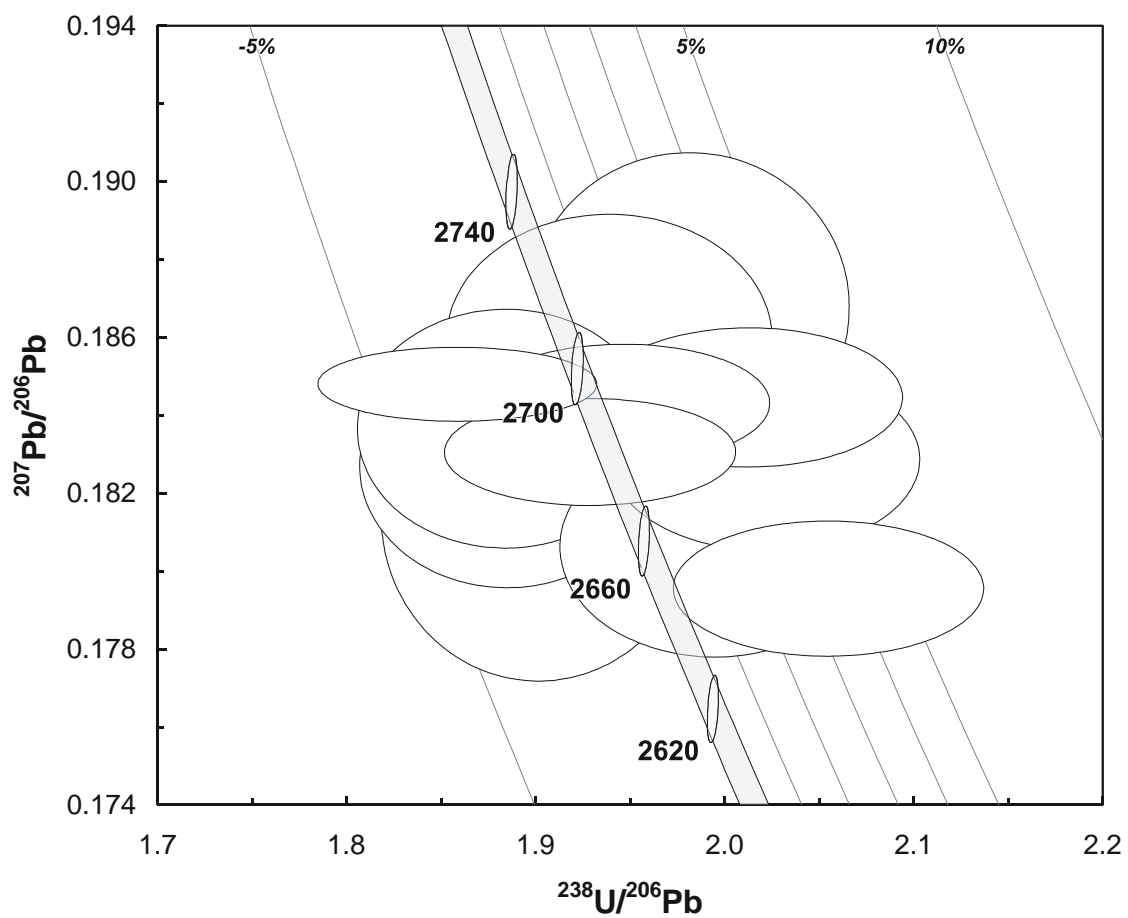


**Figure 69.** Tera-Wasserburg concordia plot for zircons from sample 2004967316: volcanic meta-sandstone, Kanowna Belle. Only analyses with <1% common-Pb have been plotted as white-filled symbols.

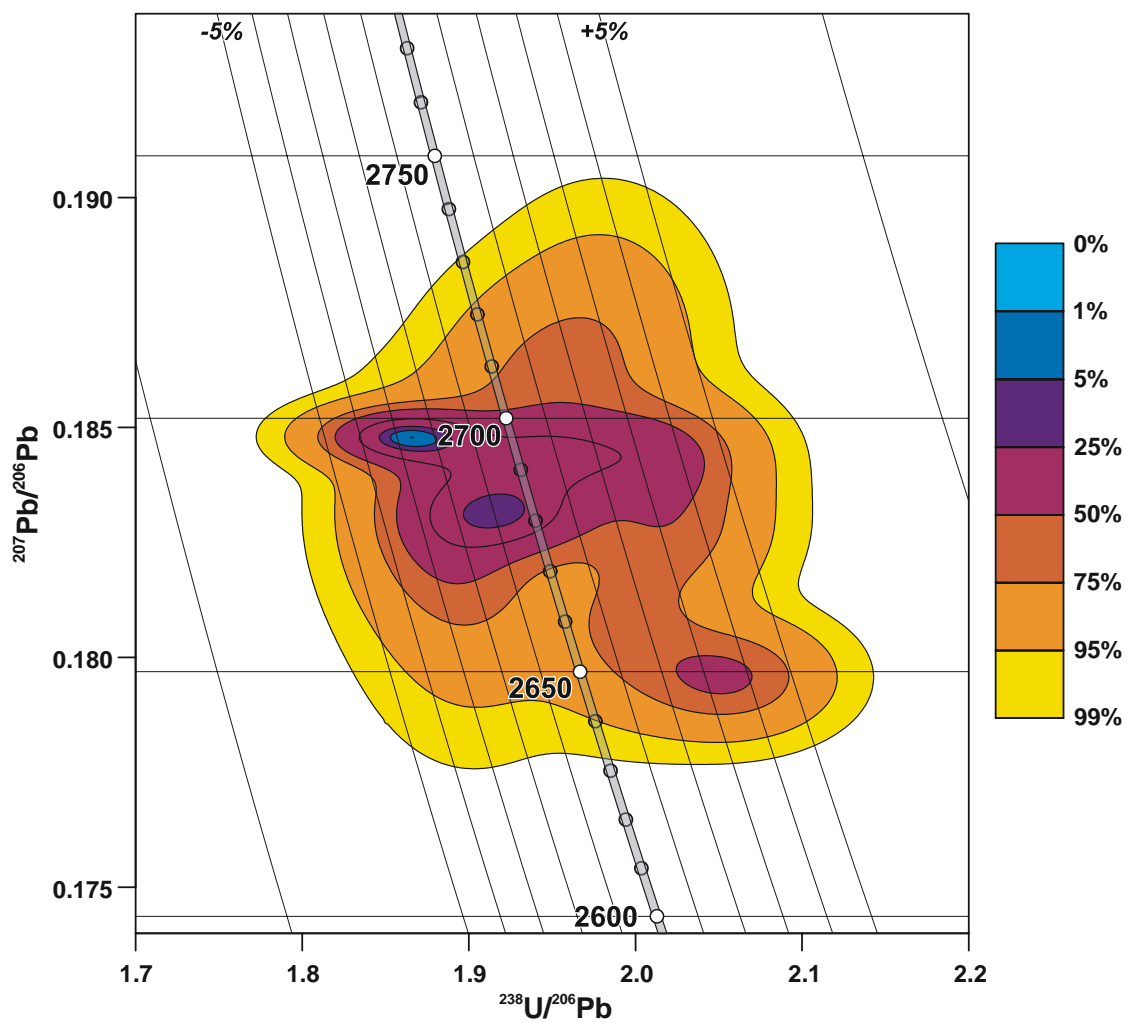


**Figure 70.** Tera-Wasserburg concordia plot for concordant zircons from sample 2004967316: volcanic meta-sandstone, Kanowna Belle. Only analyses with <1% common-Pb have been used to calculate the distribution.

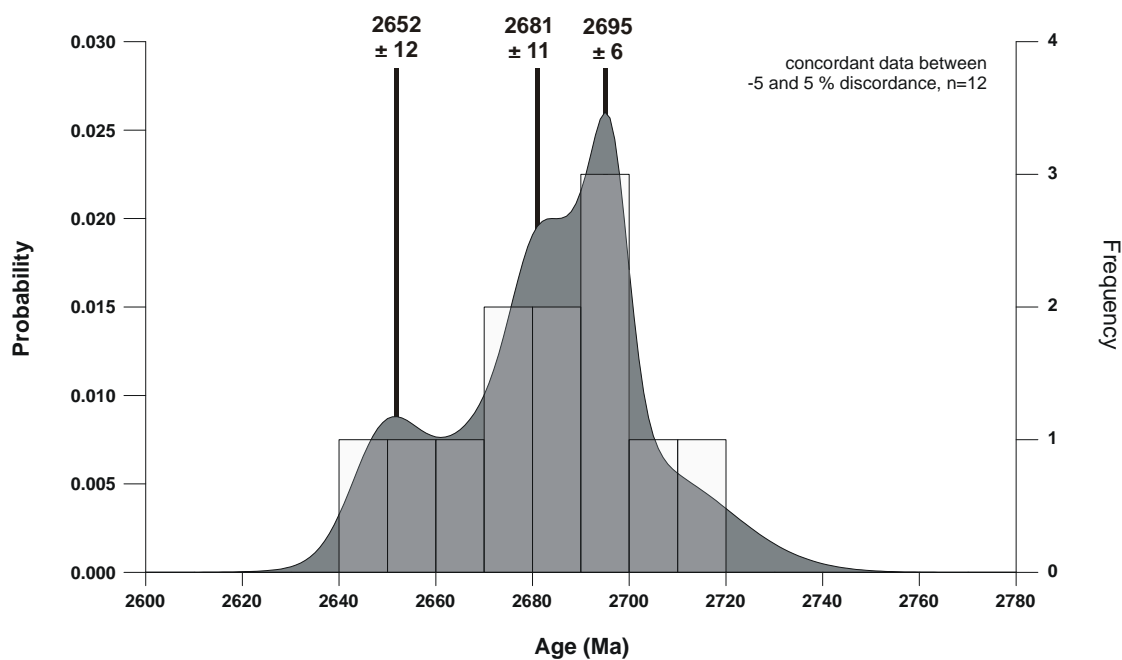


**Figure 71.** Probability density distribution and histogram plot of  $^{207}\text{Pb}/^{206}\text{Pb}$  ages from sample 2004967316: volcanic meta-sandstone, Kanowna Belle with mixture modelled age components shown. Only analyses with <1% common-Pb have been used to calculate the distribution and age components. Because of the low quantity of data the modelled age components should be considered as tentative.

**Table 20.** SHRIMP analytical results for zircon from sample 2004967316: volcanic meta-sandstone, Kanowna Belle.

Grain Spot	U (ppm)	Th (ppm)	% comm 206	$^{207}\text{Pb}/^{206}\text{Pb}$	$\pm$	$^{206}\text{Pb}/^{238}\text{U}$	$\pm$	$^{207}\text{Pb}/^{235}\text{U}$	$\pm$	% Disc.	$^{207}\text{Pb}/^{206}\text{Pb}$ Age (Ma)	$\pm$
<i>Main</i>												
10.1	323	46	0.546	0.1796	0.0007	0.4865	0.0080	12.0439	0.2029	3.5	2648.8	6.5
14.1	109	38	0.379	0.1806	0.0012	0.5012	0.0084	12.4816	0.2243	1.5	2658.7	10.6
16.1	38	13	0.002	0.1814	0.0017	0.5257	0.0094	13.1518	0.2667	-2.2	2666.1	15.9
18.1	87	42	0.526	0.1827	0.0013	0.5304	0.0090	13.3639	0.2446	-2.4	2677.8	11.6
25.1	182	102	0.667	0.1829	0.0010	0.4945	0.0082	12.4697	0.2163	3.3	2679.3	8.7
12.1	384	121	0.035	0.1831	0.0006	0.5183	0.0085	13.0833	0.2173	-0.4	2680.8	5.0
2.1	72	24	-0.113	0.1837	0.0012	0.5307	0.0090	13.4383	0.2459	-2.2	2686.2	11.2
26.3	426	37	0.623	0.1843	0.0006	0.5137	0.0084	13.0556	0.2176	0.7	2692.1	5.6
26.1	240	14	0.130	0.1845	0.0007	0.4966	0.0082	12.6316	0.2142	3.5	2693.4	6.5
7.1	1105	81	0.078	0.1848	0.0004	0.5380	0.0087	13.7076	0.2247	-2.9	2696.5	3.5
15.1	63	45	-0.029	0.1859	0.0013	0.5156	0.0094	13.2178	0.2581	1.0	2706.4	11.7
13.1	47	17	-0.134	0.1868	0.0016	0.5046	0.0088	12.9946	0.2538	3.0	2713.9	14.3
<i>High common-Pb</i>												
4.1	1823	595	14.388	0.1328	0.0047	0.5021	0.0085	9.1925	0.3607	-22.9	2135.0	62.0
21.1	716	617	4.318	0.1650	0.0038	0.5126	0.0088	11.6591	0.3375	-6.4	2507.1	39.1
9.1	1075	371	3.459	0.1662	0.0016	0.3044	0.0056	6.9739	0.1451	32.0	2519.4	16.6
6.1	516	262	8.854	0.1726	0.0027	0.5220	0.0086	12.4192	0.2798	-4.8	2582.7	25.8
23.1	99	58	3.636	0.1743	0.0025	0.4038	0.0069	9.7049	0.2172	15.9	2599.4	24.0
1.1	991	479	2.209	0.1747	0.0006	0.5006	0.0081	12.0564	0.2007	-0.5	2603.1	6.0
17.1	622	291	15.489	0.1759	0.0203	0.6114	0.0186	14.8261	1.7705	-17.6	2614.3	192.2
19.1	318	134	1.066	0.1782	0.0010	0.5383	0.0090	13.2240	0.2324	-5.3	2635.9	9.5
5.1	313	112	1.383	0.1787	0.0021	0.4422	0.0076	10.8933	0.2266	10.6	2640.6	19.6
22.1	113	34	4.107	0.1794	0.0021	0.5253	0.0091	12.9941	0.2689	-2.8	2647.3	19.0
25.2	179	60	11.349	0.1796	0.0025	0.5787	0.0106	14.3306	0.3317	-11.1	2649.1	23.5
24.1	105	44	1.284	0.1801	0.0014	0.5171	0.0087	12.8408	0.2378	-1.3	2653.7	12.9
3.2	189	49	4.293	0.1811	0.0015	0.5277	0.0090	13.1726	0.2508	-2.6	2662.6	13.9
11.1	231	117	2.397	0.1823	0.0013	0.5097	0.0084	12.8131	0.2314	0.7	2674.2	12.2
20.1	196	96	3.950	0.1825	0.0043	0.3977	0.0069	10.0082	0.2936	19.3	2676.0	39.0
26.2	85	75	2.721	0.1901	0.0022	0.5395	0.0101	14.1421	0.3106	-1.4	2743.2	18.9
3.1	288	109	22.606	0.2008	0.0302	0.5658	0.0239	15.6627	2.4457	-2.1	2832.4	245.2

Data are at  $1\sigma$  precision. All Pb data are common-Pb corrected based on  $^{204}\text{Pb}$  measurements. Mount: Z4636; Instrument: RSES SHRIMP-RG; Acquisition: 29 August 2005.



## 2004967325: meta-dacite, Kanowna Belle

### SAMPLE INFORMATION

**1:250,000 sheet:** Kurnalpi (SH5110)

**1:100,000 sheet:** Kanowna (3236)

**MGA:** 362795 mE 6614292 mN

**Location:** The sample is from Placer Dome Asia Pacific diamond drillhole GVD65, interval 386.75–387.90 m. The collar for the north-plunging drillhole is located 2 km north of Kanowna Belle mine.

**Description:** This is from a grey, altered, meta-dacite unit. The fine-grained dacite contains a variety of altered quartz and feldspar phenocrysts, minor xenoliths, and a number of textures consistent with the rock being a coherent volcanic flow. The unit is part of a felsic volcanic package this is intimately associated with ultramafic rocks. The rock is cut by minor, thin quartz-carbonate veinlets.

This is a moderately altered, quartz-feldspar-porphyrific dacite with a very fine-grained chlorite-sericite-bearing quartz-feldspar-rich groundmass. Phenocrysts constitute about 55-60% of the rock and include partly resorbed, subrounded quartz (~10%), altered, sub- to euhedral plagioclase (40-45%) and minor irregular-shaped aggregates of chlorite-carbonate±secondary biotite±sericite± opaque minerals (~5%) that may represent intensely altered FeMg-bearing phenocrysts. Minor subhedral to subrounded aggregates of polycrystalline quartz (<2%) have shapes that are outlined by opaque minerals. Plagioclase phenocrysts are generally moderately altered to albite-carbonate±sericite. The groundmass is mainly microcrystalline quartz and elongate feldspar that exhibits a preferred alignment, as well as aligned sericite, chlorite and minor secondary biotite, which locally wraps relict phenocrysts. Alteration has resulted in a variety of assemblages with variable amounts of chlorite, carbonate, sericite, albite, opaque minerals and secondary biotite. Opaque minerals occur as subhedral to anhedral irregular grains disseminated throughout the groundmass and concentrated in chlorite-, sericite- and carbonate-rich aggregates. Accessory phases include trace zircon and fine dusting of secondary hematite.

### DESCRIPTION OF ZIRCONS

**Shape:** Sub-euhedral to euhedral prismatic grains ([Figure 72](#)).

**Size:** 100 to 300 microns.

**Colour/clarity:** Clear.

**Quality:** Fair to good.



**CL zoning:** Complex zoning; sector zoning and dark rims common. Evidence of embayments and resorption in some zones (Figure 72).

#### CONCURRENT STANDARD DATA

**Pb/U reprod.(2s):** 2.9%

**Err. of mean (2s):** 0.6%

**Standard:** QGNG

**Analyses:** 31 (multi-day session, one discarded as anomalously young)

**Notes:** Reproducibility of Pb/U ratios is reasonable.

#### SAMPLE DATA

Forty-one analyses were made on thirty-nine grains with only one analysis (#11.1) being > 5% discordant (Table 21; Figure 73). A concordia contour diagram indicates a dominant cluster ~2700 Ma along with a tail extending down to ~2665 Ma (Figure 74). There appears to be a weak correlation between  $^{232}\text{Th}/^{238}\text{U}$  ratio and age (Figure 75) and the oldest age mode tends to associated with bright CL broad-zoned cores and the youngest mode tends to, but not exclusively, occur in darker CL rims with concentric zoning. One grain (#2) clearly demonstrates a significant difference between core and rim, although both ages are younger than the ~2700 Ma mode.

Mixture modelling of  $^{207}\text{Pb}/^{206}\text{Pb}$  ages indicates four age model components:  $2663 \pm 7$ ,  $2681 \pm 9$ ,  $2704 \pm 5$  and  $2727 \pm 18$  Ma, dominated by the  $2704 \pm 5$  Ma mode (Figure 76).





**Figure 72.** Representative images (transmitted light on left, cathodoluminescence on right) for sample 2004967325: meta-dacite, Kanowna Belle. SHRIMP analysis spots are labelled.

### GEOCHRONOLOGICAL INTERPRETATION

A range of ages and complex CL patterns are present suggesting a complicated history. Unlike other samples which show a distinct compositional change between age clusters, this samples appears to be more transitory suggesting a long-lived period of multiple events leading to zircon formation.

The dominant age mode of  $2704 \pm 5$  Ma is interpreted as the age of original zircon crystallisation, which was followed by a series of magmatic events that caused some



resorption and new zircon growth, possibly culminating in an event around  $2663 \pm 7$  Ma.

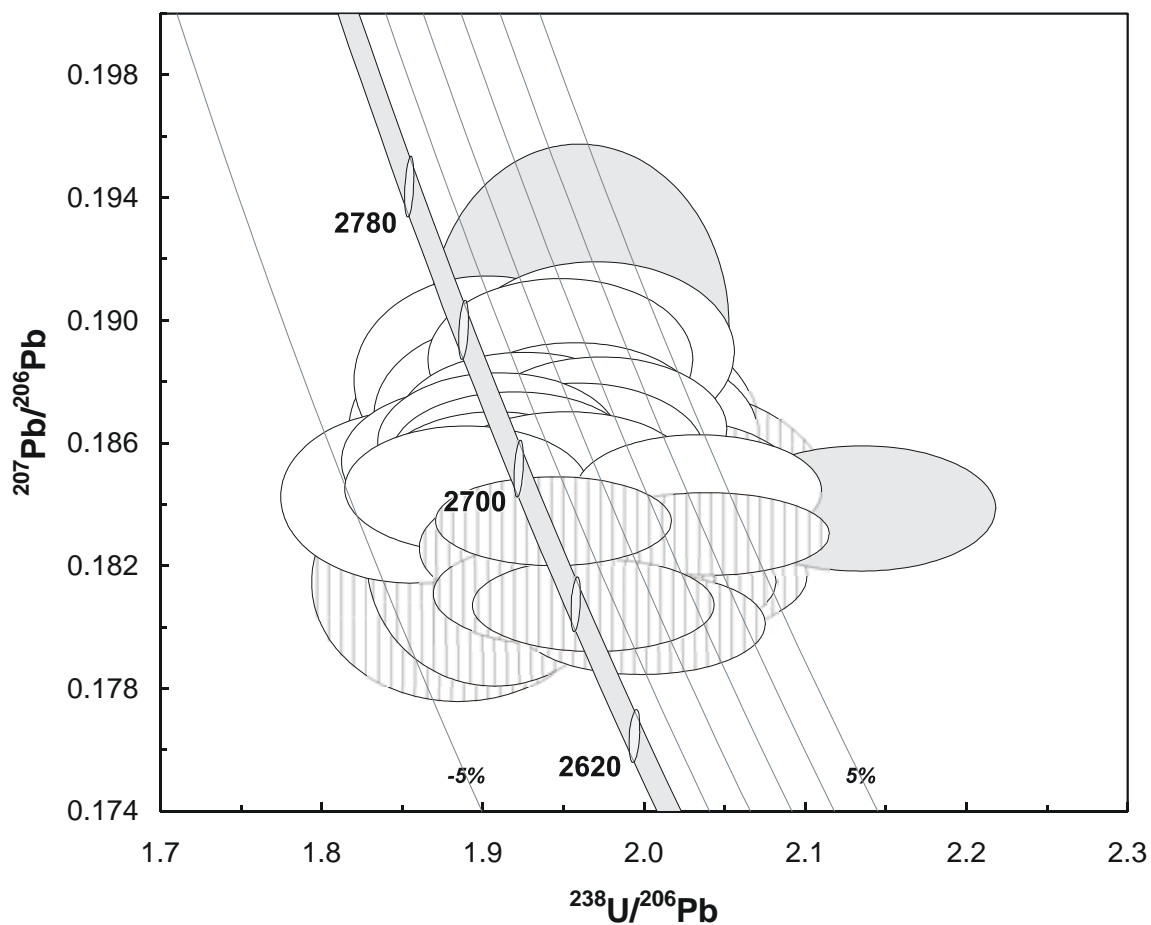


**Figure 73.** Tera-Wasserburg concordia plot for zircons from sample 2004967325: meta-dacite, Kanowna Belle. The two concordant clusters discussed in text are indicated by white fill and vertical hatching; discordant and/or high common-Pb analyses are light grey.

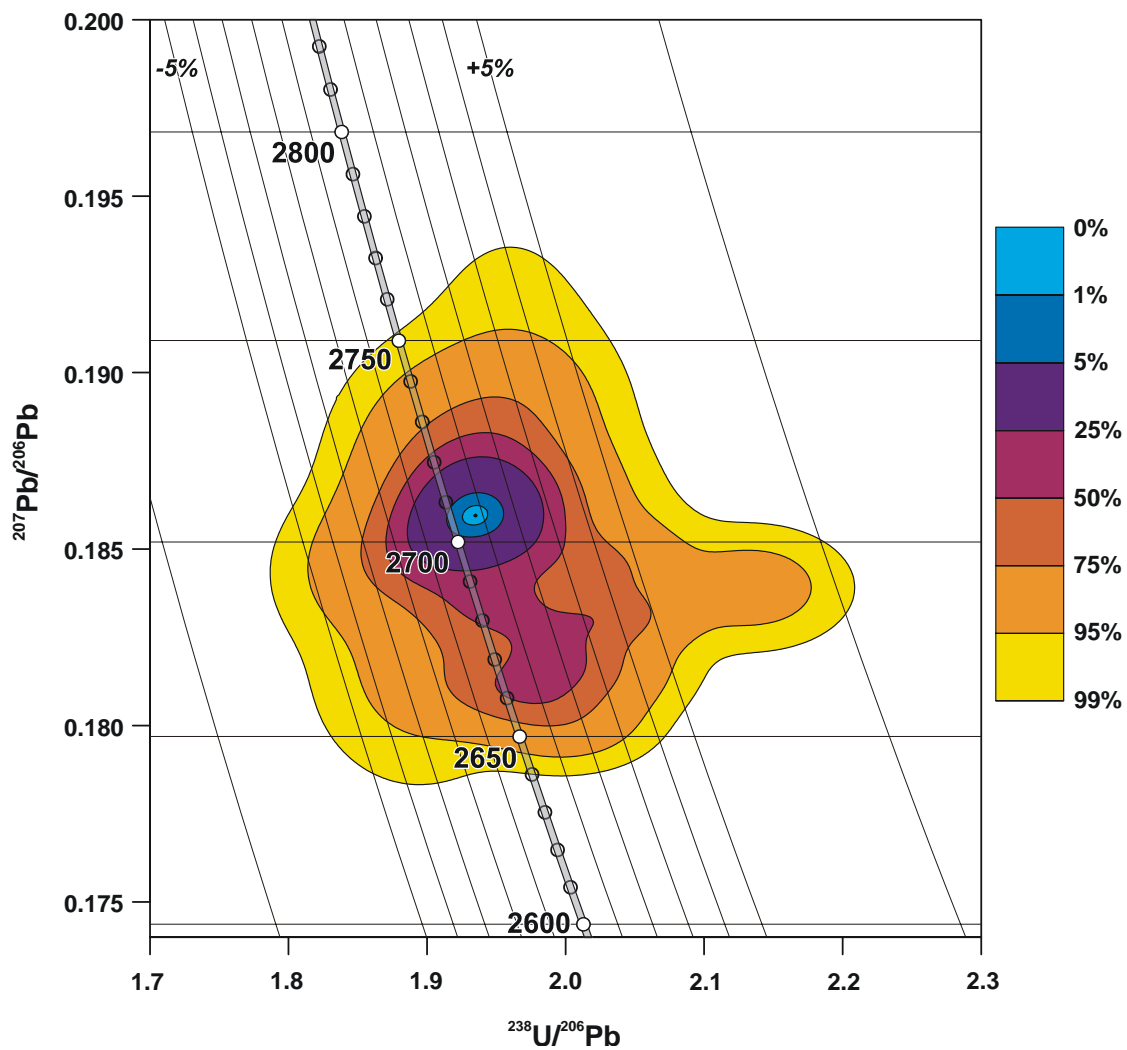


**Figure 74.** Concordia contour plot for zircons from sample 2004967325: meta-dacite, Kanowna Belle illustrating the dominant cluster at ~2700 Ma and a minor cluster at ~2665 Ma.

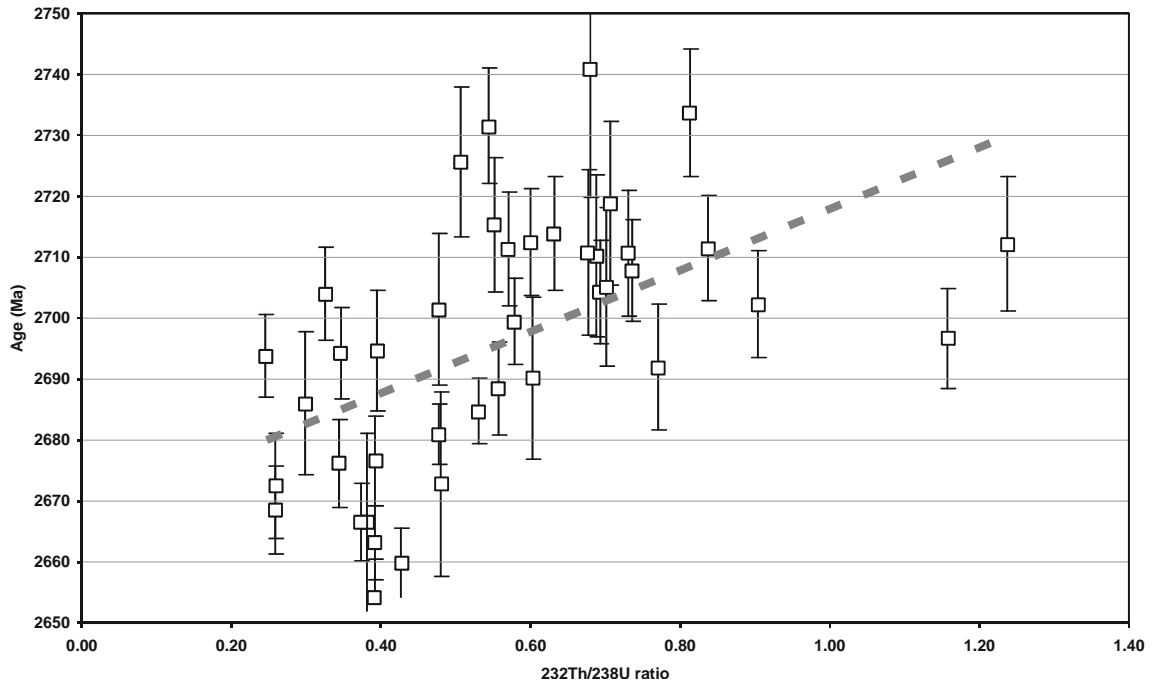


**Figure 75.** Plot of zircon age in relation to  $^{232}\text{Th}/^{238}\text{U}$  ratio for zircons from sample 2004967325: meta-dacite, Kanowna Belle illustrating possible weak correlation ( $\rho^2: 0.28$ ).

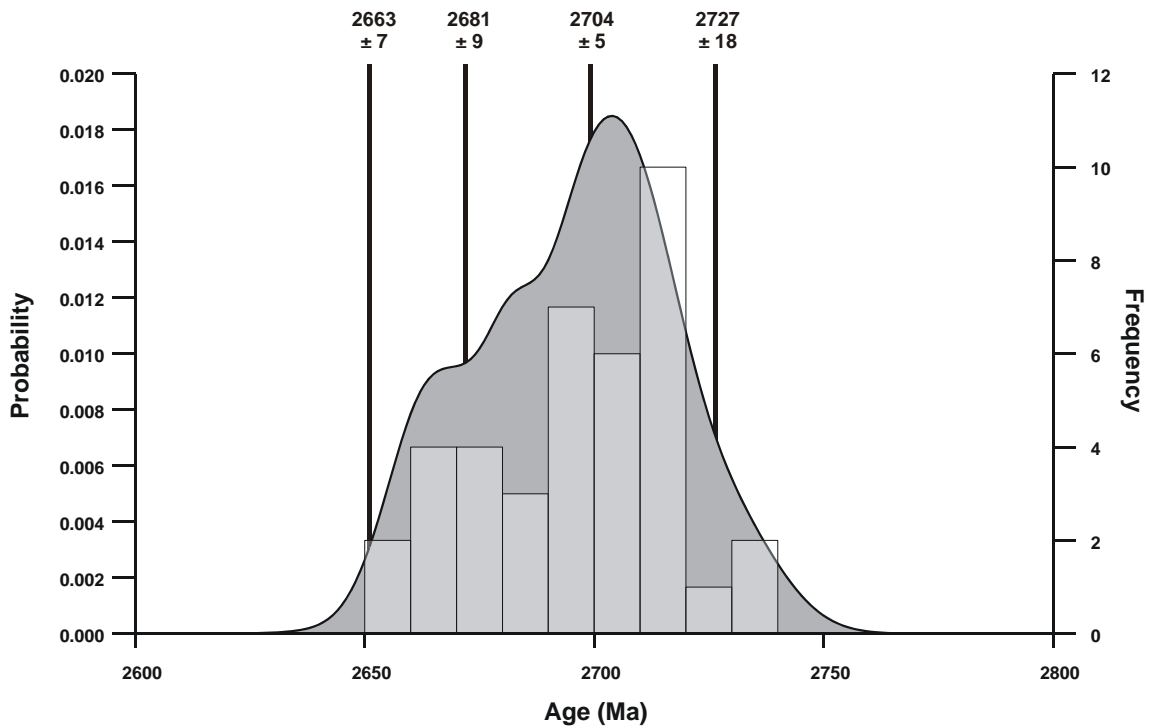


**Figure 76.** Probability density distribution and histogram plot of concordant  $^{207}\text{Pb}/^{206}\text{Pb}$  ages from sample 2004967325: meta-dacite, Kanowna Belle with mixture modelled age components shown.

**Table 21.** SHRIMP analytical results for zircon from sample 2004967325: meta-dacite, Kanowna Belle.

Grain.Spot	U (ppm)	Th (ppm)	% comm 206	<sup>207</sup> Pb / <sup>206</sup> Pb	±	<sup>206</sup> Pb / <sup>238</sup> U	±	<sup>207</sup> Pb / <sup>235</sup> U	±	% Disc.	<sup>207</sup> Pb / <sup>206</sup> Pb Age (Ma)	±
<i>Main cluster</i>												
7.1	65	48	0.063	0.1843	0.0011	0.5391	0.0095	13.6989	0.2563	-3.3	2691.8	10.3
16.1	297	71	0.750	0.1845	0.0007	0.4916	0.0075	12.5056	0.1980	4.3	2693.8	6.7
5.1	111	37	0.078	0.1846	0.0008	0.5290	0.0086	13.4622	0.2279	-1.6	2694.3	7.5
28.1	79	30	0.101	0.1846	0.0011	0.5076	0.0088	12.9203	0.2374	1.8	2694.6	9.9
9.1	159	178	0.704	0.1848	0.0009	0.5243	0.0083	13.3606	0.2212	-0.8	2696.7	8.2
10.1	119	66	0.029	0.1851	0.0008	0.5123	0.0082	13.0772	0.2176	1.2	2699.4	7.1
30.1	52	24	0.037	0.1854	0.0014	0.5158	0.0098	13.1819	0.2694	0.7	2701.4	12.5
6.1	73	64	0.028	0.1854	0.0010	0.5290	0.0089	13.5264	0.2396	-1.3	2702.2	8.8
19.1	115	36	0.116	0.1856	0.0009	0.5210	0.0085	13.3347	0.2252	0.0	2703.9	7.6
35.1	92	62	0.053	0.1857	0.0009	0.5105	0.0084	13.0692	0.2249	1.7	2704.3	8.4
23.1	45	30	0.069	0.1858	0.0015	0.5144	0.0099	13.1748	0.2749	1.1	2705.1	13.1
12.1	131	93	0.040	0.1861	0.0009	0.5236	0.0084	13.4328	0.2261	-0.2	2707.8	8.2
3.1	36	24	0.190	0.1863	0.0015	0.5249	0.0100	13.4856	0.2782	-0.4	2710.2	13.2
22.1	86	61	0.038	0.1864	0.0012	0.5058	0.0098	12.9990	0.2641	2.7	2710.7	10.3
24.1	38	25	0.000	0.1864	0.0015	0.5059	0.0099	13.0031	0.2761	2.6	2710.7	13.5
1.1	67	37	0.030	0.1865	0.0010	0.5157	0.0089	13.2594	0.2403	1.1	2711.3	9.3
17.1	101	82	0.237	0.1865	0.0010	0.5068	0.0082	13.0314	0.2220	2.5	2711.4	8.6
27.1	66	78	0.100	0.1866	0.0012	0.5143	0.0092	13.2282	0.2517	1.4	2712.1	11.0
4.1	78	45	0.079	0.1866	0.0010	0.5192	0.0087	13.3589	0.2346	0.6	2712.4	8.7
20.1	75	46	0.016	0.1868	0.0010	0.5109	0.0087	13.1555	0.2354	2.0	2713.8	9.3
31.1	77	41	0.069	0.1869	0.0012	0.5216	0.0094	13.4447	0.2582	0.3	2715.3	11.0
34.1	54	37	-0.064	0.1873	0.0015	0.5209	0.0101	13.4534	0.2838	0.6	2718.8	13.4
15.1	54	27	0.051	0.1881	0.0014	0.5255	0.0093	13.6293	0.2622	0.1	2725.6	12.2
26.1	75	40	-0.042	0.1888	0.0011	0.5133	0.0088	13.3583	0.2420	2.2	2731.4	9.5
25.1	62	49	0.032	0.1890	0.0012	0.5074	0.0090	13.2229	0.2489	3.2	2733.7	10.5
<i>Young cluster</i>												
8.1	74	35	0.058	0.1822	0.0017	0.5242	0.0089	13.1668	0.2549	-1.6	2672.8	15.1
39.1	111	37	0.058	0.1826	0.0008	0.5050	0.0081	12.7102	0.2126	1.5	2676.2	7.2
2.2	165	63	0.337	0.1826	0.0008	0.5168	0.0081	13.0110	0.2128	-0.3	2676.6	7.4
21.1	262	121	0.085	0.1831	0.0005	0.4904	0.0075	12.3797	0.1931	4.0	2680.9	5.0
36.1	242	124	0.082	0.1835	0.0006	0.5143	0.0079	13.0124	0.2050	0.4	2684.6	5.3
33.1	78	23	0.140	0.1836	0.0013	0.4951	0.0089	12.5344	0.2412	3.5	2685.9	11.7
32.1	54	32	0.224	0.1841	0.0015	0.4945	0.0093	12.5526	0.2570	3.7	2690.2	13.3
2.1	176	67	0.178	0.1801	0.0007	0.5002	0.0078	12.4228	0.1997	1.5	2654.1	6.2
14.1	207	86	0.000	0.1808	0.0006	0.5079	0.0079	12.6590	0.2021	0.5	2659.8	5.7
37.1	188	71	0.039	0.1811	0.0007	0.5143	0.0081	12.8450	0.2073	-0.4	2663.2	6.1
37.2	193	70	0.018	0.1815	0.0007	0.4989	0.0079	12.4836	0.2033	2.2	2666.5	6.4
13.1	37	14	0.131	0.1815	0.0016	0.5305	0.0105	13.2746	0.2865	-2.9	2666.5	14.5
29.1	214	54	0.059	0.1817	0.0008	0.4958	0.0085	12.4212	0.2198	2.7	2668.5	7.2
18.1	85	21	0.091	0.1821	0.0010	0.5035	0.0084	12.6455	0.2204	1.6	2672.5	8.6
<i>Discordant/High common-Pb</i>												
11.1	151	81	0.303	0.1839	0.0008	0.4683	0.0074	11.8743	0.1962	7.9	2688.5	7.5
38.1	35	23	1.038	0.1898	0.0024	0.5102	0.0099	13.3544	0.3102	3.0	2740.9	21.1

Data are at 1 $\sigma$  precision. All Pb data are common-Pb corrected based on <sup>204</sup>Pb measurements. Mount: Z4562; Instrument: RSES SHRIMP-RG; Acquisition: 22 January 2005.



## 2004967366: meta-sandstone, Long Wong prospect

### SAMPLE INFORMATION

**1:250,000 sheet:** Kalgoorlie (SH5109)

**1:100,000 sheet:** Davyhurst (3037)

**MGA:** 304172 mE 6632853 mN

**Location:** This sample was taken from Placer Dome Asia Pacific diamond drill hole LWD001, depth interval 91.45-92.16 m. The collar is located approximately 2.5 km north of Brown Dam.

**Description:** This rock is from a grey, altered, meta-sandstone. The fine- to medium-grained sandstone forms a metre-thick lens in the upper part of the Kurrawang Conglomerate. The sandstone contains a variety of altered, sub-mm to 1 mm size angular to sub-rounded, quartz, feldspar and lithic clasts. The lithic clasts include intergrown quartz-feldspar and chert as well as minor altered mafic lithologies. The rock contains a strong anastomosing fabric defined by chlorite, biotite and sericite. Clasts in the conglomerate on either side of the sandstone lens exhibit evidence of minor flattening. The unit is cut by rare carbonate fractures.

Principal minerals are micro-crystalline quartz and/or feldspar (50-55%), discrete quartz (~35%) and feldspar (5-10%), very-fine-grained biotite (~5%), with lesser sericite, chlorite, carbonate, epidote/clinozoisite, leucoxene, opaque minerals and trace zircon. The sample exhibits a strongly recrystallised, granulated quartz, feldspar and biotite mosaic, with a typical grain size of 0.1 to 0.2 mm, forming up to 30% of the rock, through which larger, recrystallised clasts are disseminated. Crystal and lithic clasts, generally <1 mm, form about 70% of the rock and include monocrystalline quartz (~25%) and feldspar (5-10%), polycrystalline quartz and quartz-feldspar (~40%), and minor altered mafic clasts (1-2%). The quartz clasts are generally angular to rounded, whereas feldspar clasts are angular and strongly altered to albite, sericite, epidote and carbonate. Polycrystalline quartz and quartz-feldspar-rich clasts include rare chert that are identified by fine-grained disseminated opaque minerals, and variably recrystallised relict granitoid clasts with altered quartz and feldspar grains in a finer-grained quartz-feldspathic matrix. The rock is strongly foliated, as defined by aligned, elongate clusters of yellow to red-brown biotite flakes and the fine-grained quartzofeldspathic mosaic. Carbonate also occurs as irregular to anhedral grains. Retrograde alteration minerals include minor chlorite and white mica.



## DESCRIPTION OF ZIRCONS

- Shape:** Euhedral to sub-euhedral squat prismatic grains (Figure 77).  
**Size:** 100 to 150 microns.  
**Colour/clarity:** Clear to pale brown.  
**Quality:** Fair, numerous crack and inclusions.  
**CL zoning:** Generally concentric (Figure 77).

## CONCURRENT STANDARD DATA

- Pb/U reprod.(2s):** 0.67%  
**Err. of mean (2s):** 4.68%  
**Standard:** QGNG  
**Analyses:** 56 (two analyses rejected as anomalously young)  
**Notes:** A multi-day session.

## SAMPLE DATA

This sample was analysed as if it were a detrital sample with the number of scans reduced to five in order to increase the total number of analyses for statistical adequacy.

Eighty analyses were made on eighty grains with twenty-one analyses > 5% discordant or with high common-Pb (Table 22; Figure 78). The remaining fifty-nine analyses yield a 5% chance of missing a component making up more than 0.088 of total population (Vermeesch 2004). Four analyses are clearly inherited with ages > 3200 Ma. The bulk of the analyses from a dispersed cluster between 2750 and 2650 Ma with a dominant mode ~2720 Ma and possible Pb-loss toward younger ages (Figure 79). There are no significant correlations between  $^{207}\text{Pb}/^{206}\text{Pb}$  ages, U content or  $^{232}\text{Th}/^{238}\text{U}$  ratio and the CL patterns are generally homogeneous concentric zoning.

Mixture modelling yields model components at  $2657.4 \pm 6.5$ ,  $2679.6 \pm 5.0$ ,  $2690.9 \pm 8.1$ ,  $2712.9 \pm 3.7$ ,  $2720.1 \pm 4.9$  and  $2741.7 \pm 16$  Ma where the 2712.9 and 2720.1 Ma components are dominant (Figure 80).





**Figure 77.** Representative images (transmitted light on left, cathodoluminescence on right) for sample 2004967366: meta-sandstone, Long Wong prospect. SHRIMP analysis spots are labelled.

### GEOCHRONOLOGICAL INTERPRETATION

The mixture model components ( $2657 \pm 7$ ,  $2680 \pm 5$ ,  $2691 \pm 8$ ,  $2713 \pm 4$ ,  $2720 \pm 5$  and  $2742 \pm 16$  Ma) most probably represent the original detrital provenance to the meta-sandstone, possibly overprinted by later events causing variable Pb-loss. The  $2713 \pm 4$  and  $2720 \pm 5$  Ma modes dominate, with  $2657 \pm 7$  Ma tentatively representing a maximum age of deposition as defined by these data.



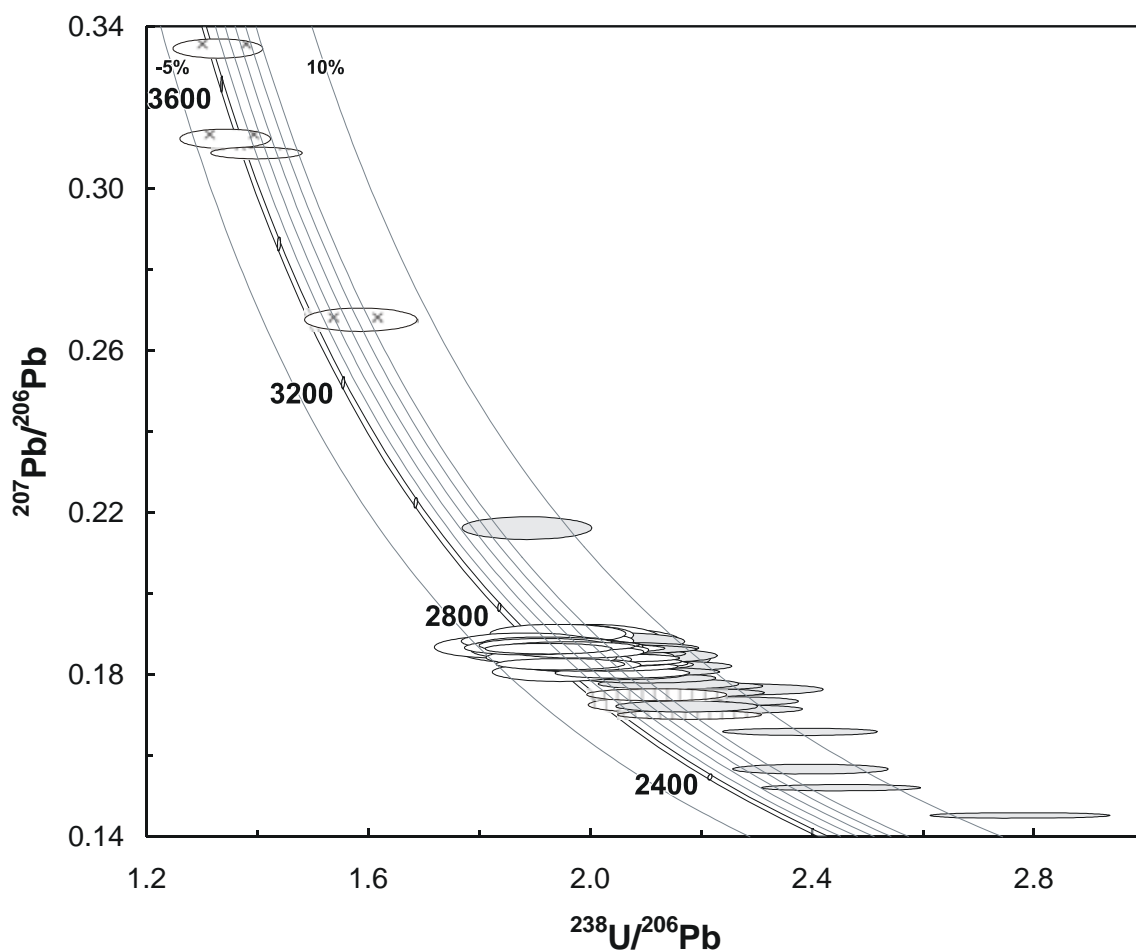


**Figure 78.** Tera-Wasserburg concordia plot for zircons from sample 2004967366: meta-sandstone, Long Wong prospect. Analyses in the main concordant cluster are indicated by white fill; analyses possibly affected by Pb-loss have vertical hatching; inherited analyses have a cross-hatch fill and discordant and/or high common-Pb analyses are light grey.

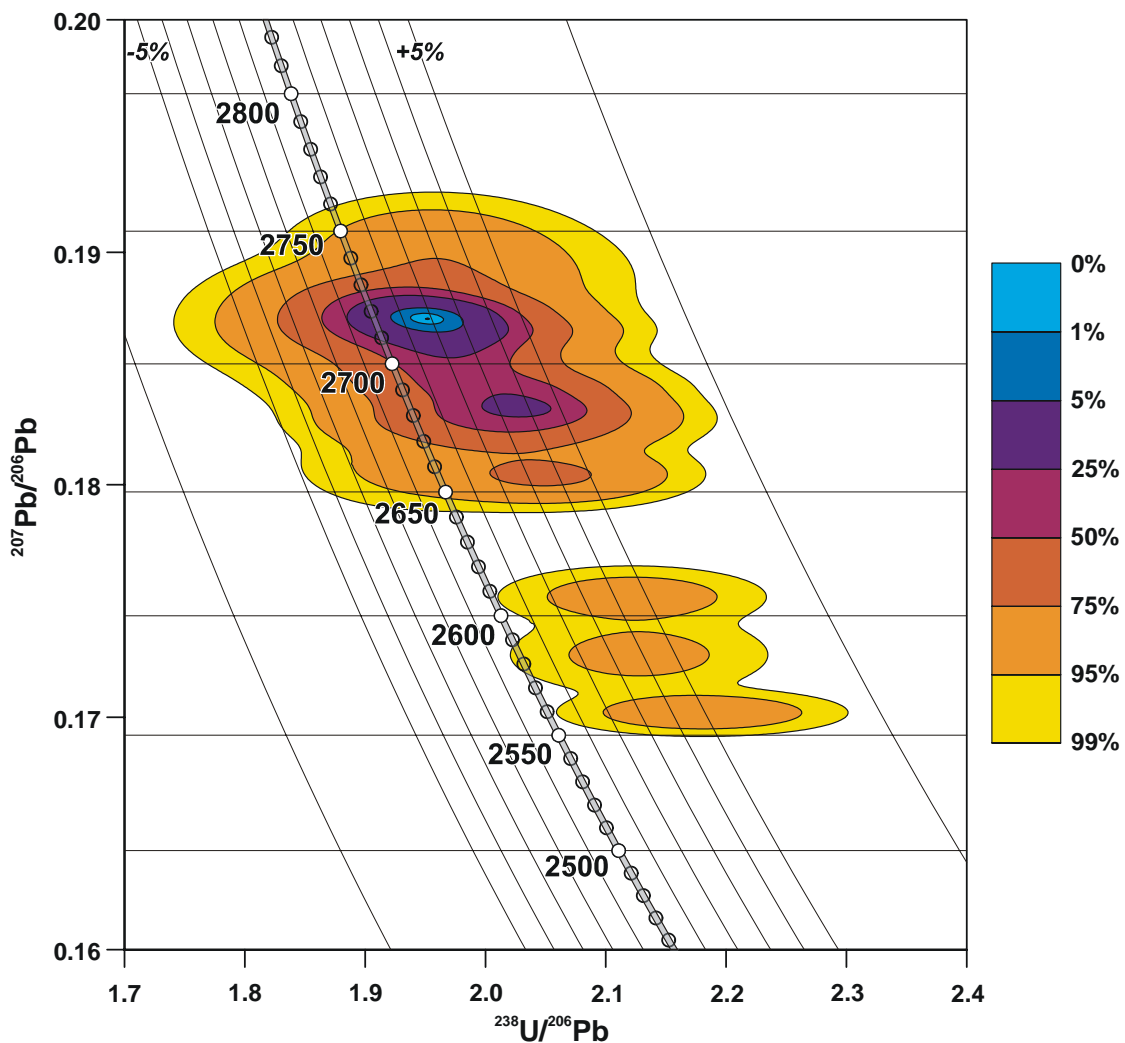


**Figure 79.** Concordia contour plot for zircons from sample 2004967366: meta-sandstone, Long Wong prospect illustrating the dominant cluster at ~2720 Ma and probable dispersion toward lower left.

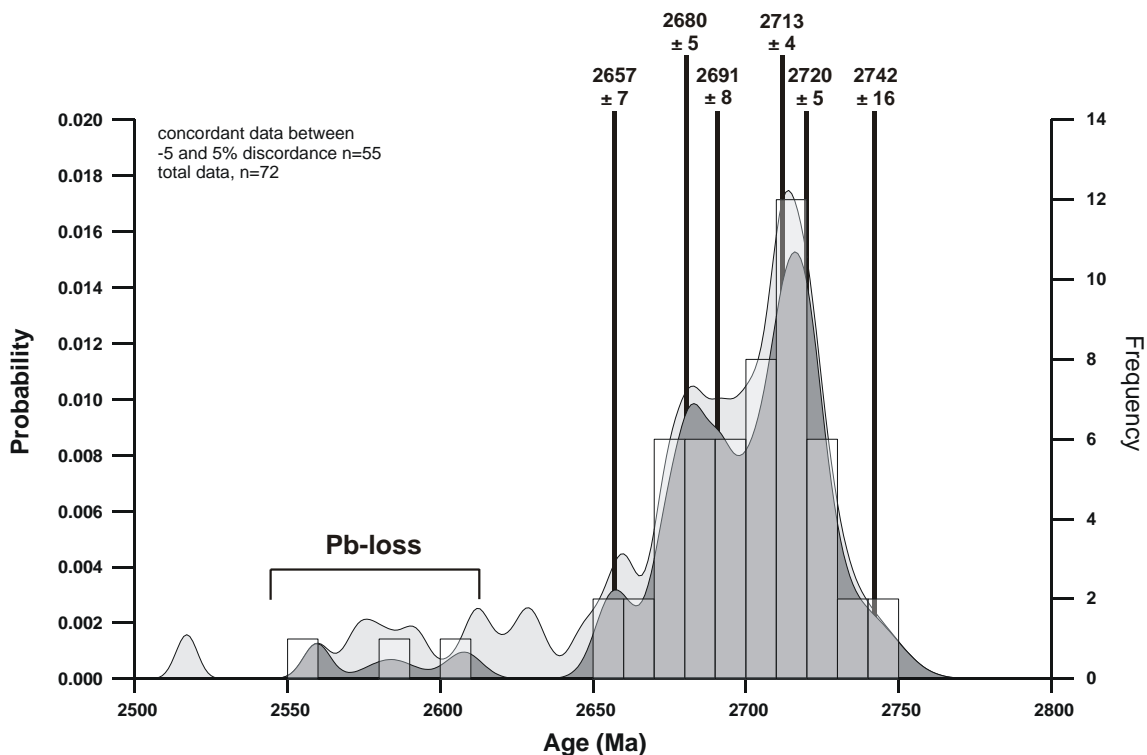


**Figure 80.** Probability density distribution and histogram plot of concordant  $^{207}\text{Pb}/^{206}\text{Pb}$  ages from sample 2004967366: meta-sandstone, Long Wong prospect with mixture modelled age components shown.

**Table 22.** SHRIMP analytical results for zircon from sample 2004967366: meta-sandstone, Long Wong prospect.

Grain.Spot	U (ppm)	Th (ppm)	% comm 206	<sup>207</sup> Pb / <sup>206</sup> Pb	±	<sup>206</sup> Pb / <sup>238</sup> U	±	<sup>207</sup> Pb / <sup>235</sup> U	±	% Disc.	<sup>207</sup> Pb / <sup>206</sup> Pb Age (Ma)	±
<i>Main detrital cluster</i>												
52.1	384	197	0.055	0.1801	0.0005	0.4877	0.0120	12.1142	0.2996	3.5	2654.1	5.0
31.1	463	350	0.495	0.1806	0.0006	0.4857	0.0118	12.0931	0.2949	4.0	2658.1	5.1
36.1	126	88	0.097	0.1808	0.0009	0.5137	0.0132	12.8101	0.3346	-0.5	2660.6	8.6
68.1	169	132	0.094	0.1810	0.0008	0.4912	0.0136	12.2612	0.3434	3.2	2662.3	7.8
69.1	335	211	0.045	0.1821	0.0006	0.4984	0.0123	12.5156	0.3122	2.5	2672.4	5.5
34.1	572	308	0.121	0.1822	0.0005	0.4906	0.0118	12.3211	0.2987	3.7	2672.6	4.2
84.1	503	325	0.220	0.1826	0.0005	0.4842	0.0117	12.1937	0.2963	4.9	2677.0	4.6
26.1	341	243	0.098	0.1827	0.0006	0.5066	0.0125	12.7602	0.3175	1.3	2677.2	5.5
25.1	372	210	0.049	0.1827	0.0006	0.5134	0.0125	12.9323	0.3174	0.2	2677.5	5.1
77.1	578	144	0.055	0.1829	0.0005	0.4864	0.0118	12.2671	0.2982	4.6	2679.3	4.4
13.1	712	357	0.039	0.1831	0.0004	0.4919	0.0118	12.4201	0.3003	3.8	2681.5	3.8
27.1	574	444	0.143	0.1834	0.0005	0.4890	0.0118	12.3641	0.2998	4.4	2683.7	4.2
18.1	648	440	0.026	0.1836	0.0004	0.4903	0.0118	12.4089	0.3001	4.2	2685.4	3.8
61.1	428	148	0.399	0.1839	0.0006	0.4923	0.0120	12.4786	0.3065	4.0	2687.9	5.8
19.1	203	127	0.085	0.1839	0.0008	0.5110	0.0127	12.9538	0.3274	1.0	2688.0	6.8
65.1	234	144	0.111	0.1839	0.0007	0.4985	0.0124	12.6411	0.3179	3.0	2688.6	6.6
56.1	761	377	0.028	0.1842	0.0004	0.4898	0.0118	12.4404	0.3018	4.5	2691.1	3.6
78.1	174	132	0.103	0.1843	0.0010	0.5076	0.0128	12.8986	0.3329	1.7	2691.8	8.6
11.1	222	121	0.280	0.1844	0.0008	0.5178	0.0129	13.1615	0.3324	0.1	2692.4	7.2
57.1	397	202	0.131	0.1847	0.0006	0.4925	0.0120	12.5427	0.3078	4.2	2695.5	5.4
16.1	143	106	0.077	0.1849	0.0009	0.5091	0.0130	12.9779	0.3382	1.7	2697.3	8.2
66.1	233	157	0.085	0.1850	0.0007	0.5030	0.0135	12.8308	0.3486	2.6	2698.2	6.6
72.1	131	56	0.030	0.1857	0.0010	0.5141	0.0132	13.1628	0.3451	1.1	2704.5	8.5
21.1	459	290	0.196	0.1857	0.0006	0.5047	0.0122	12.9237	0.3159	2.6	2704.7	5.6
51.1	107	68	0.058	0.1858	0.0011	0.5026	0.0131	12.8738	0.3425	3.0	2705.1	9.4
76.1	178	75	0.063	0.1859	0.0008	0.5086	0.0128	13.0354	0.3331	2.0	2706.0	7.4
9.1	86	97	0.152	0.1860	0.0013	0.5261	0.0154	13.4911	0.4065	-0.7	2706.9	11.4
24.1	137	77	0.122	0.1861	0.0009	0.5247	0.0134	13.4622	0.3498	-0.4	2707.9	8.3
81.1	358	103	0.379	0.1861	0.0007	0.5031	0.0123	12.9124	0.3194	3.0	2708.4	6.0
3.1	227	121	0.277	0.1862	0.0009	0.4997	0.0124	12.8325	0.3251	3.6	2709.3	7.7
40.1	372	131	0.049	0.1866	0.0006	0.5192	0.0126	13.3558	0.3274	0.6	2712.0	4.9
79.1	379	343	0.054	0.1866	0.0006	0.5054	0.0125	13.0032	0.3231	2.8	2712.5	5.1
74.1	170	88	0.101	0.1866	0.0009	0.5069	0.0128	13.0440	0.3351	2.5	2712.6	7.7
62.1	688	331	0.081	0.1866	0.0005	0.4961	0.0119	12.7665	0.3089	4.3	2712.8	4.0
81.1	257	146	0.095	0.1868	0.0007	0.5294	0.0131	13.6372	0.3423	-0.9	2714.3	6.6
17.1	91	98	0.106	0.1870	0.0011	0.5439	0.0144	14.0222	0.3802	-3.1	2715.9	9.8
54.1	73	75	0.333	0.1871	0.0014	0.5102	0.0138	13.1588	0.3704	2.2	2716.5	12.5
30.1	671	558	0.040	0.1872	0.0004	0.5086	0.0122	13.1236	0.3172	2.5	2717.4	3.7
64.1	322	120	0.032	0.1872	0.0006	0.5058	0.0124	13.0553	0.3227	2.9	2717.7	5.4
20.1	226	248	0.046	0.1873	0.0007	0.5240	0.0130	13.5282	0.3404	0.1	2718.2	6.5
60.1	300	108	0.012	0.1873	0.0007	0.5219	0.0128	13.4779	0.3351	0.4	2718.6	6.1
8.1	336	131	0.027	0.1874	0.0006	0.5173	0.0133	13.3657	0.3463	1.2	2719.5	5.3
23.1	783	574	0.009	0.1876	0.0004	0.5067	0.0122	13.1061	0.3157	2.9	2721.3	3.4
73.1	187	74	0.057	0.1876	0.0008	0.5172	0.0130	13.3793	0.3414	1.2	2721.3	7.2
32.1	273	113	0.022	0.1877	0.0006	0.5148	0.0133	13.3199	0.3469	1.7	2721.9	5.6
15.1	478	226	0.047	0.1882	0.0005	0.5196	0.0127	13.4807	0.3319	1.1	2726.3	4.5
14.1	166	201	0.097	0.1883	0.0008	0.5305	0.0134	13.7759	0.3542	-0.6	2727.6	7.4
80.1	157	160	0.142	0.1885	0.0010	0.5109	0.0130	13.2752	0.3443	2.5	2728.7	8.5



Compilation of SHRIMP U-Pb geochronological data, Yilgarn Craton, Western Australia, 2004-2006

2.1	79	76	0.128	0.1887	0.0013	0.4984	0.0158	12.9646	0.4212	4.5	2730.6	11.5
53.1	80	93	0.373	0.1893	0.0014	0.5011	0.0134	13.0763	0.3626	4.3	2735.8	11.9
29.1	100	154	0.116	0.1900	0.0011	0.5118	0.0134	13.4076	0.3600	2.8	2742.0	9.6
58.1	121	52	0.058	0.1903	0.0010	0.5148	0.0133	13.5052	0.3560	2.5	2744.5	8.7
<i>Inheritance</i>												
47.1	132	136	0.042	0.2680	0.0012	0.6299	0.0163	23.2754	0.6124	4.4	3294.4	7.0
35.1	485	226	0.007	0.3093	0.0006	0.7142	0.0173	30.4568	0.7390	1.2	3517.3	3.0
83.1	190	115	0.047	0.3129	0.0010	0.7442	0.0186	32.1024	0.8067	-1.4	3535.2	4.8
22.1	194	62	0.058	0.3352	0.0010	0.7520	0.0187	34.7584	0.8711	0.7	3641.2	4.4
<i>Pb-loss??</i>												
70.1	572	407	0.059	0.1702	0.0004	0.4586	0.0111	10.7617	0.2615	4.9	2559.6	4.4
49.1	475	283	0.085	0.1727	0.0008	0.4700	0.0118	11.1903	0.2863	3.9	2583.8	8.0
12.1	645	302	0.110	0.1752	0.0006	0.4713	0.0114	11.3837	0.2790	4.5	2607.8	5.8
<i>Discordant/High common-Pb</i>												
33.1	1656	846	0.162	0.1453	0.0003	0.3602	0.0086	7.2153	0.1727	13.4	2290.9	3.3
5.1	1536	1745	0.135	0.1521	0.0003	0.4076	0.0097	8.5502	0.2048	7.0	2370.1	3.4
55.1	1265	490	0.117	0.1568	0.0005	0.4169	0.0100	9.0130	0.2172	7.2	2421.2	5.4
75.1	1121	193	0.105	0.1659	0.0003	0.4203	0.0101	9.6153	0.2311	10.1	2517.0	3.5
7.1	604	448	0.139	0.1715	0.0004	0.4442	0.0107	10.5064	0.2551	7.9	2572.8	4.4
37.1	696	392	0.361	0.1723	0.0006	0.4597	0.0110	10.9223	0.2647	5.5	2580.2	5.5
38.1	586	439	0.175	0.1735	0.0004	0.4457	0.0107	10.6634	0.2583	8.3	2592.0	4.3
28.1	815	786	0.068	0.1757	0.0004	0.4573	0.0110	11.0743	0.2670	7.1	2612.3	3.7
71.1	646	469	0.151	0.1765	0.0005	0.4394	0.0115	10.6922	0.2820	10.4	2620.2	5.0
67.1	716	360	0.055	0.1773	0.0004	0.4581	0.0110	11.1997	0.2708	7.5	2628.0	3.9
46.1	434	228	0.059	0.1778	0.0005	0.4668	0.0113	11.4419	0.2787	6.2	2632.3	4.6
39.1	533	313	0.058	0.1793	0.0005	0.4756	0.0115	11.7550	0.2853	5.2	2646.1	4.3
50.1	753	625	0.060	0.1809	0.0004	0.4737	0.0114	11.8118	0.2850	6.1	2660.8	3.8
4.1	567	438	0.304	0.1823	0.0005	0.4696	0.0113	11.8011	0.2870	7.2	2673.7	4.7
6.1	61	42	-0.022	0.1842	0.0013	0.4827	0.0140	12.2572	0.3662	5.6	2690.6	12.0
45.1	347	211	0.952	0.1849	0.0007	0.4750	0.0115	12.1094	0.2977	7.1	2697.2	6.4
59.1	476	202	0.171	0.1853	0.0005	0.4879	0.0119	12.4647	0.3065	5.2	2700.9	4.8
1.1	765	464	0.021	0.1864	0.0004	0.4829	0.0116	12.4128	0.2991	6.3	2710.9	3.5
63.1	642	280	0.130	0.1867	0.0005	0.4820	0.0116	12.4077	0.3008	6.5	2713.4	4.6
48.1	158	193	0.059	0.1884	0.0009	0.4895	0.0126	12.7178	0.3315	5.9	2728.4	7.5
10.1	165	140	0.244	0.2164	0.0011	0.5298	0.0133	15.8060	0.4069	7.2	2954.0	8.5

Data are at  $1\sigma$  precision. All Pb data are common-Pb corrected based on  $^{204}\text{Pb}$  measurements. Mount: Z4799; Instrument: JdL Centre SHRIMP-B; Acquisition: 2 October 2005.



## 2004967367: volcanic meta-sandstone, Three-in-Hand prospect

### SAMPLE INFORMATION

**1:250,000 sheet:** Kalgoorlie (SH5109)

**1:100,000 sheet:** Kalgoorlie (3136)

**MGA:** 331206 mE 6615758 mN

**Location:** This composite sample is from Placer Dome Asia Pacific diamond drill hole THD001, depth interval 123.10-136.95 m. The collar is located approximately 1 km south of Four-in-Hand Dam.

**Description:** This rock is a grey, altered, volcanic meta-sandstone. The medium- to coarse-grained, graded sandstone is from a sequence of interbedded, immature sandstones, siltstones and mudstones, which form the basal part of a thick felsic volcanoclastic and siliciclastic sequence that conformably overlies mafic volcanic rocks. The unit contains a variety of altered, sub-mm to 2 mm size, mainly angular to rare sub-rounded quartz, feldspar and lithic clasts.

The sample is an intensely altered, poorly-sorted, clast-rich rock with a very fine-grained chlorite-, carbonate- and quartz-feldspar-rich matrix forming up to 15 % of the rock. Crystal and lithic clasts form about 85% of the rock and include monocrystalline quartz (~10%) and feldspar (~65%), and altered relict mafic fragments (~10%). The quartz clasts are generally very angular to rarely sub-rounded. Feldspar clasts are angular and strongly altered to albite, sericite, carbonate and leucoxene. Alteration hampers identification of the mafic clasts, with opaque minerals outlining their precursor shapes. These clasts comprise aggregates of fine-grained chlorite, carbonate, leucoxene and opaque minerals, with rare relict biotite. Opaque minerals occur as subhedral to anhedral and irregular grains disseminated throughout the matrix and concentrated in sericite-, chlorite- and carbonate-rich lithic clasts. Accessory minerals include trace zircon.

### DESCRIPTION OF ZIRCONS

**Shape:** Euhedral squat prismatic grains ([Figure 81](#)).

**Size:** 50 to 150 microns.

**Colour/clarity:** Clear to pale brown.

**Quality:** Fair, frequent cracking parallel to internal zoning, rare inclusions. Concentric zoning apparent in optical transmission imaging.



**CL zoning:** Concentric zoning prominent, frequently with unconformable core and rim banding (Figure 81).

#### CONCURRENT STANDARD DATA

**Pb/U reprod.(2s):** 0.67%

**Err. of mean (2s):** 4.68%

**Standard:** QGNG

**Analyses:** 56 (two analyses rejected as anomalously young)

**Notes:** A multi-day session.

#### SAMPLE DATA

Fifty-six analyses were made on fifty-two grains with fourteen analyses >5% discordant (Table 23, Figure 82). Analysis of three grains (#1, #34 and #35) revealed a significant age difference between rims and cores (Figure 83). However, the younger rim ages are more dispersed than the core ages suggesting possible effects of Pb-loss (Figure 84, Figure 85). There is no significant correlation with  $^{207}\text{Pb}/^{206}\text{Pb}$  age and U content or  $^{232}\text{Th}/^{238}\text{U}$  ratio. CL patterns generally show homogeneous concentric zoning, although there is frequently an discontinuous relationship between core and rim zoning.

Mixture modelling of the concordant distribution yields three model components at  $2638.1 \pm 4.6$ ,  $2669.5 \pm 3.9$  and  $2696.4 \pm 1.9$  Ma, with the latter mode dominant. The middle mode may represent an accidental analytical mixing of the two end-member ages (Figure 85).





**Figure 81.** Representative images (transmitted light on left, cathodoluminescence on right) for sample 2004967367: volcanic meta-sandstone, Three-in-Hand prospect. SHRIMP analysis spots are labelled.

### GEOCHRONOLOGICAL INTERPRETATION

The sample is unusual in possibly having two significant zircon phases at  $2696 \pm 2$  and  $2638 \pm 5$  Ma which is an unusually long interval, but there is no other apparent significant difference between the two phases. The younger mode is dispersed,



suggesting that it has been affected by ancient Pb-loss and there is the possibility that the apparent clustering of the younger ages is an artefact of that event.

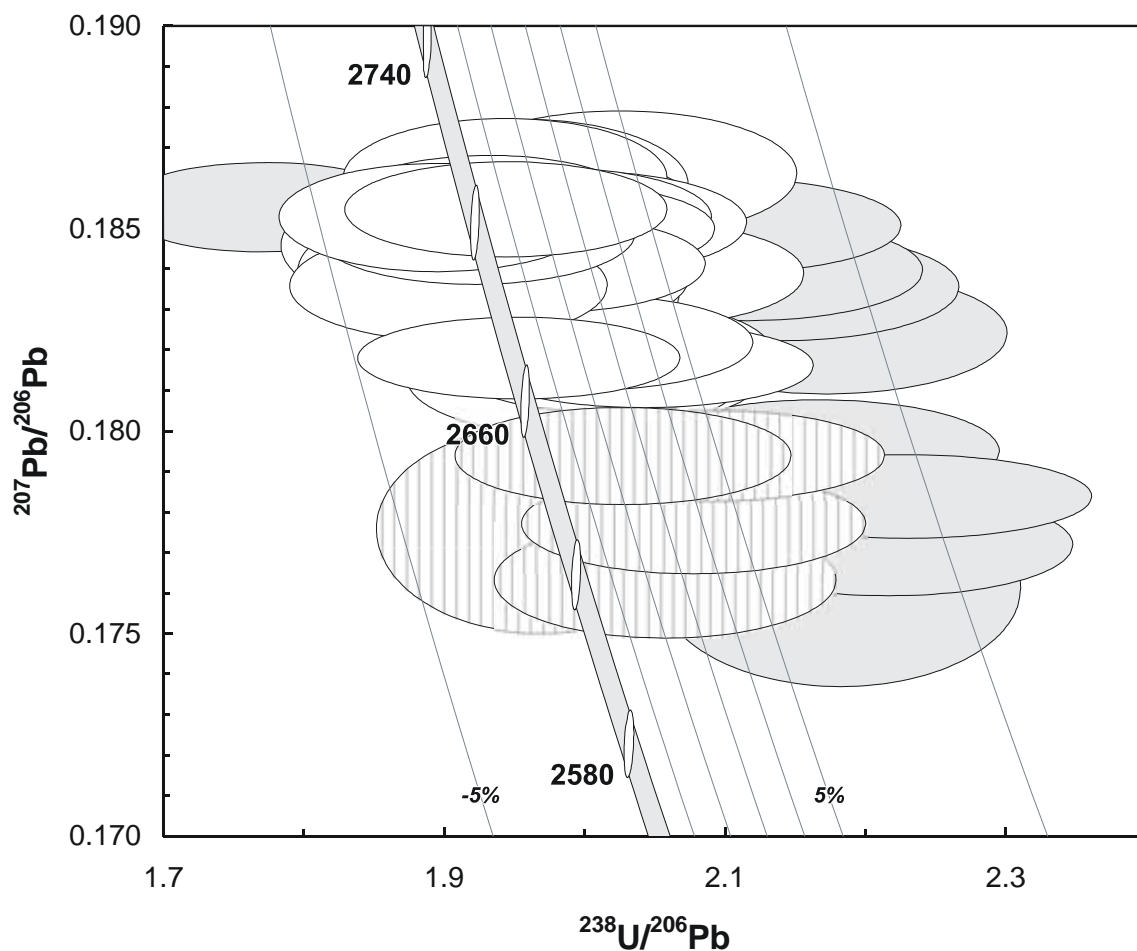


**Figure 82.** Tera-Wasserburg concordia plot for zircons from sample 2004967367: volcanic meta-sandstone, Three-in-Hand prospect. Analyses in the main concordant cluster are indicated by white fill; rims have vertical hatching; discordant and/or high common-Pb analyses are light grey.

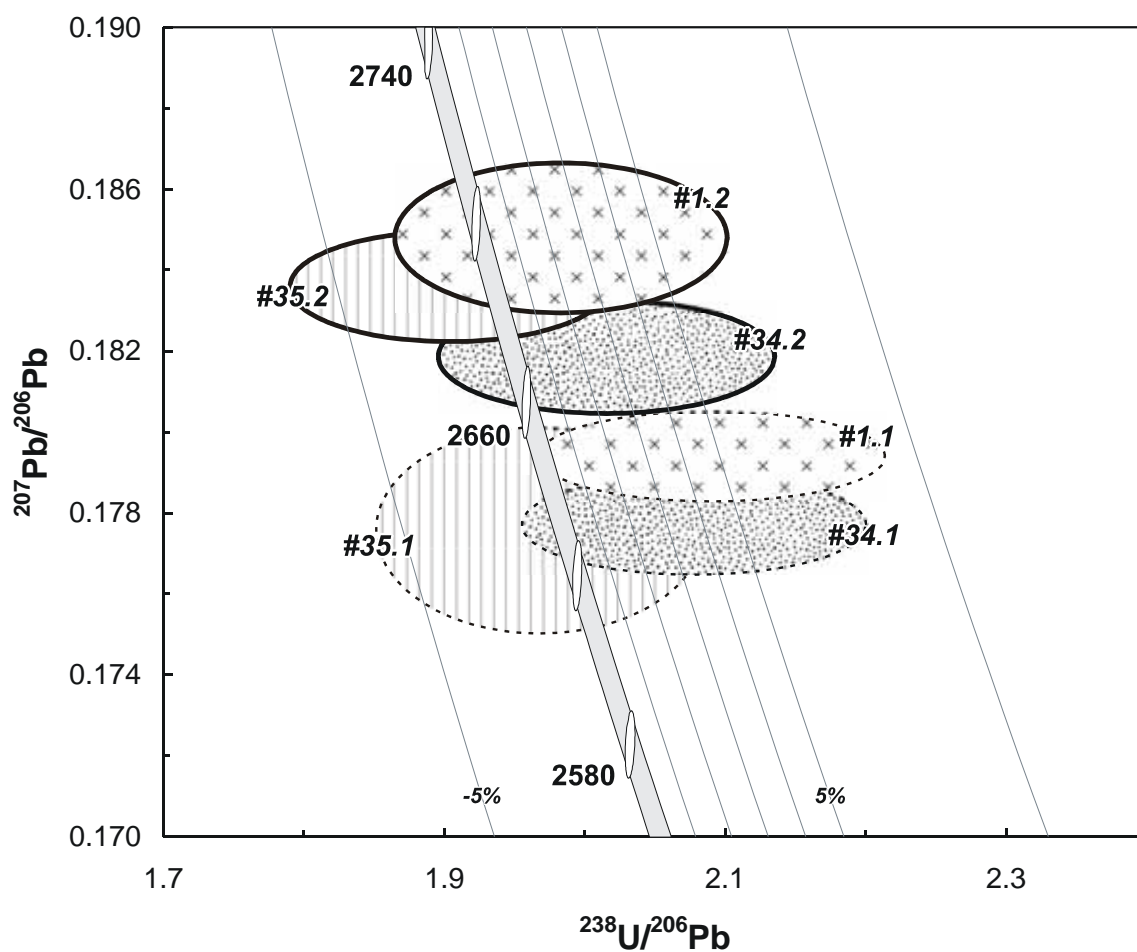


**Figure 83.** Tera-Wasserburg concordia plot for core and rim analyses from sample 2004967367: volcanic meta-sandstone, Three-in-Hand prospect. Analyses from zircon cores are indicated by thick line on the error ellipses; dashed error ellipses indicate corresponding analyses from rims.

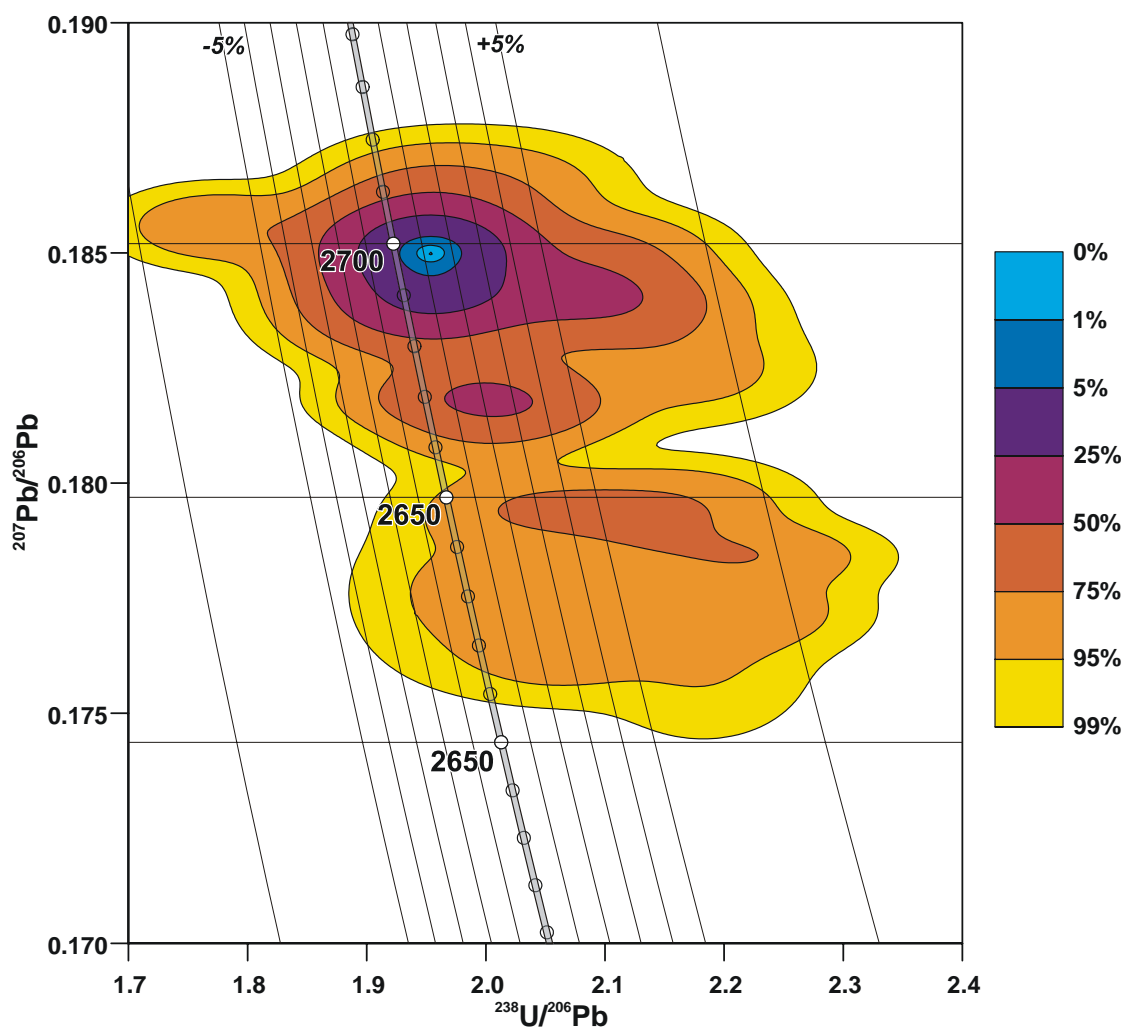


**Figure 84.** Concordia contour plot for zircons from sample 2004967367: volcanic meta-sandstone, Three-in-Hand prospect illustrating the dominant cluster at ~2700 Ma and probable dispersion toward lower left.

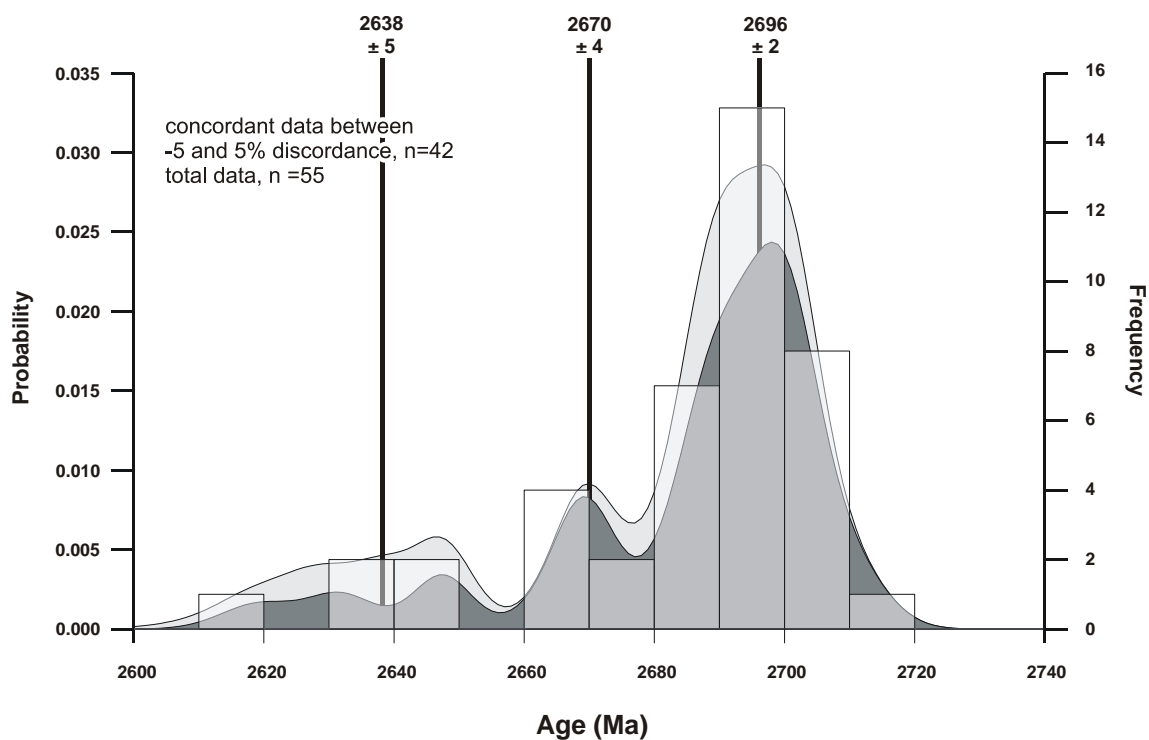


**Figure 85.** Probability density distribution and histogram plot of concordant  $^{207}\text{Pb}/^{206}\text{Pb}$  ages from sample 2004967367: volcanic meta-sandstone, Three-in-Hand prospect with mixture modelled age components shown.

**Table 23.** SHRIMP analytical results for zircon from sample 2004967367: volcanic meta-sandstone, Three-in-Hand prospect.

Grain.Spot	U (ppm)	Th (ppm)	% comm 206	<sup>207</sup> Pb / <sup>206</sup> Pb	±	<sup>206</sup> Pb / <sup>238</sup> U	±	<sup>207</sup> Pb / <sup>235</sup> U	±	% Disc.	<sup>207</sup> Pb / <sup>206</sup> Pb Age (Ma)	±
<i>Rim</i>												
25.1R	461	377	0.213	0.1763	0.0006	0.4859	0.0118	11.8149	0.2886	2.5	2618.8	5.5
35.1R	490	398	0.309	0.1776	0.0010	0.5081	0.0122	12.4431	0.3087	-0.7	2630.6	9.8
34.1R	569	438	0.140	0.1777	0.0005	0.4813	0.0116	11.7938	0.2857	3.8	2631.8	4.7
15.1	479	312	0.131	0.1794	0.0005	0.4932	0.0119	12.1999	0.2967	2.4	2647.5	4.5
1.1R	562	401	0.112	0.1794	0.0005	0.4784	0.0115	11.8348	0.2868	4.8	2647.6	4.2
<i>Main</i>												
17.1	314	173	0.071	0.1814	0.0006	0.5018	0.0123	12.5482	0.3095	1.7	2665.5	5.4
16.1	381	276	0.519	0.1816	0.0006	0.4981	0.0126	12.4692	0.3171	2.3	2667.2	5.5
38.1	584	571	0.121	0.1816	0.0004	0.4894	0.0118	12.2576	0.2961	3.7	2668.0	3.9
23.1	633	539	0.012	0.1818	0.0004	0.5120	0.0123	12.8364	0.3097	0.2	2669.7	3.7
34.2C	379	234	0.158	0.1819	0.0006	0.4961	0.0120	12.4431	0.3045	2.7	2670.3	5.2
27.1	467	265	0.019	0.1822	0.0005	0.4996	0.0121	12.5527	0.3052	2.3	2673.3	4.4
22.1	344	236	0.035	0.1833	0.0006	0.5125	0.0125	12.9560	0.3178	0.6	2683.4	5.2
30.1	247	118	0.041	0.1836	0.0007	0.5099	0.0126	12.9097	0.3215	1.1	2685.9	5.9
35.2C	381	231	0.090	0.1836	0.0006	0.5255	0.0127	13.3043	0.3252	-1.4	2686.0	5.0
37.1	537	416	0.494	0.1839	0.0006	0.5104	0.0123	12.9404	0.3144	1.1	2688.1	5.3
10.1	349	239	0.103	0.1839	0.0006	0.5018	0.0122	12.7236	0.3129	2.5	2688.3	5.2
36.1	396	303	0.204	0.1839	0.0005	0.4912	0.0119	12.4563	0.3037	4.2	2688.7	4.8
7.1	319	157	0.319	0.1840	0.0007	0.5235	0.0128	13.2805	0.3278	-0.9	2689.1	5.9
11.1	397	272	0.144	0.1841	0.0006	0.5121	0.0124	13.0011	0.3183	0.9	2690.3	4.9
42.1	421	262	0.066	0.1842	0.0005	0.5076	0.0123	12.8906	0.3135	1.6	2690.8	4.4
41.1	272	155	0.036	0.1843	0.0006	0.5040	0.0123	12.8045	0.3167	2.3	2691.7	5.6
32.1	352	213	0.196	0.1843	0.0006	0.5121	0.0125	13.0137	0.3196	1.0	2692.1	5.4
39.1	375	186	0.005	0.1844	0.0006	0.5182	0.0126	13.1727	0.3225	0.0	2692.5	5.3
14.1	273	143	0.095	0.1846	0.0007	0.5269	0.0129	13.4138	0.3327	-1.2	2694.9	6.0
1.2C	315	197	0.732	0.1849	0.0008	0.5042	0.0123	12.8504	0.3176	2.4	2696.9	6.8
18.1	296	148	0.071	0.1849	0.0007	0.5239	0.0128	13.3541	0.3309	-0.7	2697.1	6.0
24.1	351	222	0.330	0.1849	0.0007	0.5097	0.0124	12.9959	0.3197	1.6	2697.6	6.2
20.1	414	256	0.160	0.1850	0.0005	0.5202	0.0126	13.2661	0.3241	-0.1	2697.9	4.7
29.1	249	165	0.331	0.1850	0.0007	0.5217	0.0129	13.3092	0.3328	-0.3	2698.4	6.5
40.1	345	192	0.037	0.1850	0.0005	0.5071	0.0123	12.9362	0.3168	2.0	2698.4	4.8
8.1	417	236	0.019	0.1850	0.0005	0.5120	0.0124	13.0607	0.3191	1.2	2698.4	4.6
28.1	509	416	0.037	0.1850	0.0005	0.5061	0.0122	12.9126	0.3133	2.2	2698.6	4.1
43.1	398	263	0.191	0.1852	0.0005	0.5006	0.0121	12.7836	0.3115	3.1	2699.9	4.6
45.1	301	161	0.037	0.1852	0.0006	0.5063	0.0124	12.9299	0.3198	2.2	2700.2	5.7
19.1	364	213	0.022	0.1853	0.0005	0.5276	0.0128	13.4818	0.3301	-1.1	2701.2	4.9
12.1	464	297	0.025	0.1853	0.0005	0.5066	0.0123	12.9476	0.3152	2.2	2701.3	4.4
31.1	306	148	0.047	0.1854	0.0006	0.5178	0.0127	13.2369	0.3262	0.5	2701.9	5.3
33.1	303	190	0.039	0.1855	0.0006	0.5093	0.0124	13.0264	0.3208	1.8	2702.6	5.3
26.1	486	378	0.057	0.1855	0.0005	0.5144	0.0124	13.1572	0.3196	1.0	2702.9	4.3
9.1	316	181	0.225	0.1862	0.0006	0.5111	0.0125	13.1191	0.3242	1.7	2708.6	5.8
21.1	332	260	0.129	0.1863	0.0006	0.5146	0.0125	13.2180	0.3252	1.2	2709.9	5.3
13.1	296	229	0.129	0.1864	0.0006	0.4937	0.0126	12.6885	0.3261	4.6	2710.8	5.6
<i>Discordant/High common-Pb</i>												
25.2C	590	600	2.006	0.1762	0.0010	0.4581	0.0110	11.1274	0.2750	7.1	2617.0	9.4
53.1	413	325	0.081	0.1772	0.0005	0.4511	0.0109	11.0216	0.2682	8.6	2627.0	4.8
56.1	592	465	0.153	0.1784	0.0004	0.4483	0.0108	11.0291	0.2662	9.5	2638.2	4.0
49.1	331	198	0.093	0.1788	0.0006	0.4670	0.0115	11.5135	0.2855	6.5	2641.7	5.4



Compilation of SHRIMP U-Pb geochronological data, Yilgarn Craton, Western Australia, 2004-2006

55.1	450	328	0.160	0.1795	0.0005	0.4613	0.0111	11.4201	0.2778	7.7	2648.7	4.8
46.1	418	320	0.715	0.1825	0.0006	0.4602	0.0111	11.5777	0.2827	8.8	2675.4	5.6
50.1	389	264	0.202	0.1836	0.0005	0.4672	0.0113	11.8282	0.2884	8.0	2685.7	4.9
52.1	262	155	0.470	0.1836	0.0008	0.4802	0.0118	12.1566	0.3020	5.9	2685.8	6.8
51.1	420	249	0.048	0.1840	0.0005	0.4726	0.0114	11.9900	0.2918	7.2	2689.4	4.6
47.1	293	166	0.179	0.1842	0.0006	0.4793	0.0117	12.1696	0.3001	6.2	2690.7	5.6
54.1	371	226	0.290	0.1842	0.0006	0.4813	0.0117	12.2276	0.2994	5.9	2691.5	5.2
57.1	399	234	0.105	0.1843	0.0005	0.4766	0.0115	12.1111	0.2956	6.7	2692.1	4.8
48.1	491	433	0.093	0.1851	0.0005	0.4757	0.0115	12.1429	0.2945	7.1	2699.3	4.3
44.1	492	364	0.056	0.1856	0.0005	0.5640	0.0137	14.4326	0.3520	-6.7	2703.4	4.0

Data are at  $1\sigma$  precision. All Pb data are common-Pb corrected based on  $^{204}\text{Pb}$  measurements.  
Mount: Z4799; Instrument: JdL Centre SHRIMP-B; Acquisition: 1 October 2005.



## 2004967369: porphyritic micro-diorite sill, Three-in-Hand prospect

### SAMPLE INFORMATION

**1:250,000 sheet:** Kalgoorlie (SH5109)

**1:100,000 sheet:** Kalgoorlie (3136)

**MGA:** 331207 mE 6615769 mN

**Location:** This composite sample was taken from Placer Dome Asia Pacific diamond drill hole THD001, depth interval 157.62-168.61 m. The collar is located approximately 1 km south of Four-in-Hand Dam.

**Description:** This rock is a grey, weakly altered, feldspar-amphibole-porphyritic micro-diorite sill. The sill intrudes the basal part of a thick felsic volcanoclastic and siliciclastic sequence that conformably overlies mafic volcanic rocks. The rock is cut by minor chlorite- and/or carbonate-bearing fractures.

Principal minerals in the rock include plagioclase (~65%), altered amphibole (~30%), minor quartz (<5%), apatite (<1%) and opaque minerals (<1%), and trace zircon. Phenocrysts constitute about 45% of the rock and include mostly 1 mm to ~1 cm, sub- to euhedral plagioclase (~20%), and generally <1 mm to 3 mm sub- and euhedral amphibole (~20-25%). Plagioclase phenocrysts are locally weakly altered to oligoclase, carbonate, clinzoisite/epidote, sericite and quartz. Rare hornblende inclusions are preserved in some plagioclase phenocrysts. Amphibole phenocrysts are generally hornblende that is partly to completely replaced by chlorite, actinolite, epidote, carbonate, leucoxene, and minor opaque minerals and secondary biotite. The phenocrysts are disseminated throughout a fine-grained groundmass (~55%) comprising interlocking to irregular grains of feldspar (~45%) and minor amphibole, quartz, epidote, carbonate, leucoxene and opaque minerals. Quartz is likely both primary and secondary in origin.

### DESCRIPTION OF ZIRCONS

**Shape:** Sub-euhedral to euhedral prismatic grains ([Figure 86](#)).

**Size:** 50 to 300 microns.

**Colour/clarity:** Clear to brown.

**Quality:** Fair with common cracks.

**CL zoning:** Complex mixture of bland zoned cores, dark concentric mantles and bright very narrow rims ([Figure 86](#)).



#### CONCURRENT STANDARD DATA

**Pb/U reprod.(2s):** 2.9%

**Err. of mean (2s):** 0.6%

**Standard:** QGNG

**Analyses:** 31 (one discarded as anomalously young)

**Notes:** Reproducibility of Pb/U ratios is reasonable.

#### SAMPLE DATA

Forty-nine analyses were made on forty-four grains with 11 analyses > 5% discordant (Table 24; Figure 87). The cumulated analyses are dominated by a mode ~2680 Ma with some possible Pb-loss dispersion (Figure 88).

This is a complex sample. Subdivision of results is based on observed CL patterns and Pb-loss may obscure statistically significant age differences. Discarding discordant and high Pb grains, the analyses can be subdivided into four groups on the basis of CL patterns: zoned cores, concentric mantles, concentric grains and bright rims. A number of grains (e.g. #6 and #24) clearly demonstrate a significant difference between zoned cores and concentric mantle, although overall the two sets overlap considerably and there is no statistical justification in subdividing the calculated ages. The concentric grains appear to have ages similar to the zoned cores and defining a meaningful age for the bright rims is difficult. The difficulty in subdividing the ages of the groups is a result of high-U content (particularly in the concentric mantle) causing Pb-loss.

Discarding discordant and high Pb grains and the youngest three of the concentric mantle ages (#24.1, #23.1, #6.1), the weighted mean  $^{207}\text{Pb}/^{206}\text{Pb}$  age is:  $2689.3 \pm 1.8$  (95% conf), MSWD = 1.16.





**Figure 86.** Representative images (transmitted light on left, cathodoluminescence on right) for sample 2004967369: porphyritic micro-diorite sill, Three-in-Hand prospect. SHRIMP analysis spots are labelled.

### GEOCHRONOLOGICAL INTERPRETATION

The most robust interpretation is that zoned cores and concentric zones are very close in age, but the higher U content of the mantles has caused discordance and difficulty in accurately defining the age. The age of  $2689 \pm 2$  Ma is a best approximation of two very close magmatic events.



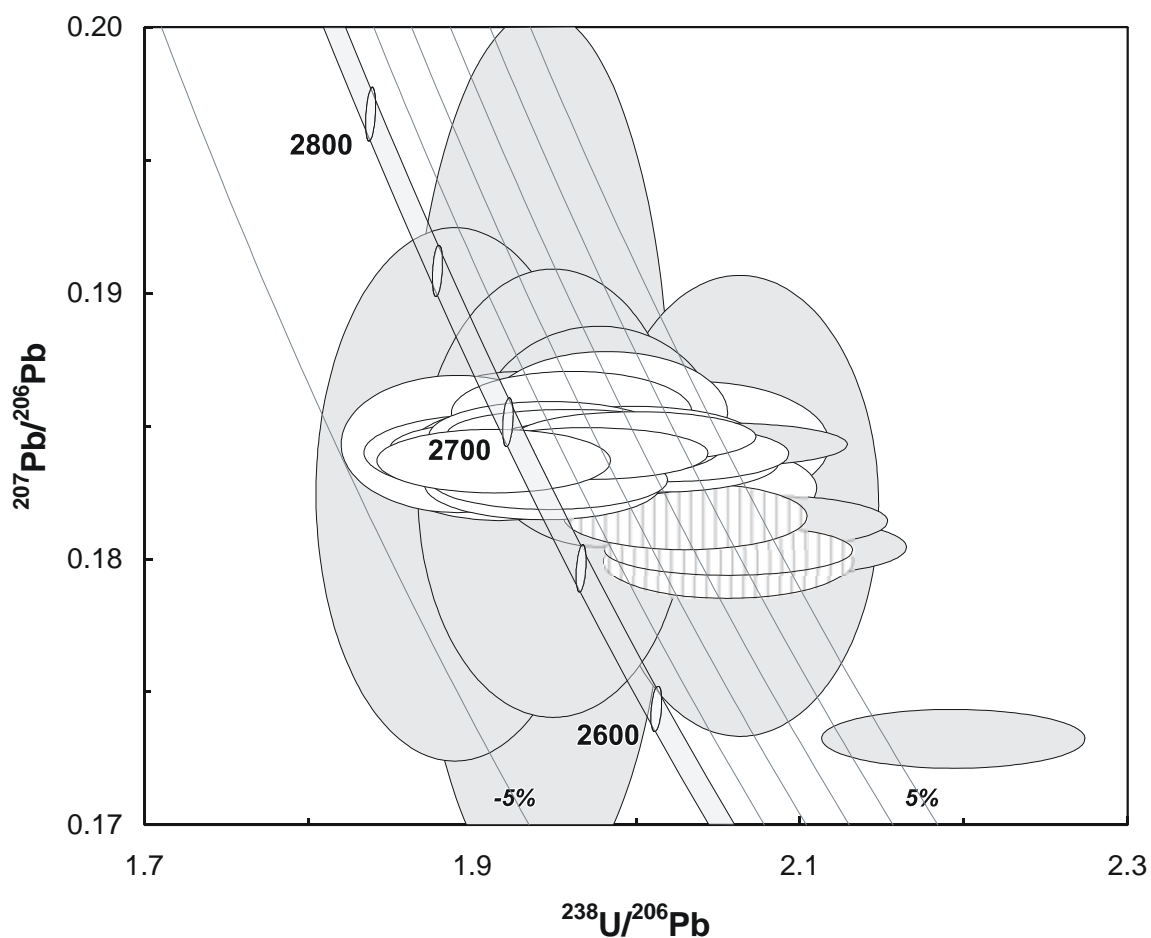


**Figure 87.** Tera-Wasserburg concordia plot for zircons from sample 2004967369: porphyritic micro-diorite sill, Three-in-Hand prospect. The main concordant clusters discussed in the text text are represented by white-filled symbols and the young outliers from this group are indicated by vertical hatching; discordant and/or high common-Pb analyses are light grey.

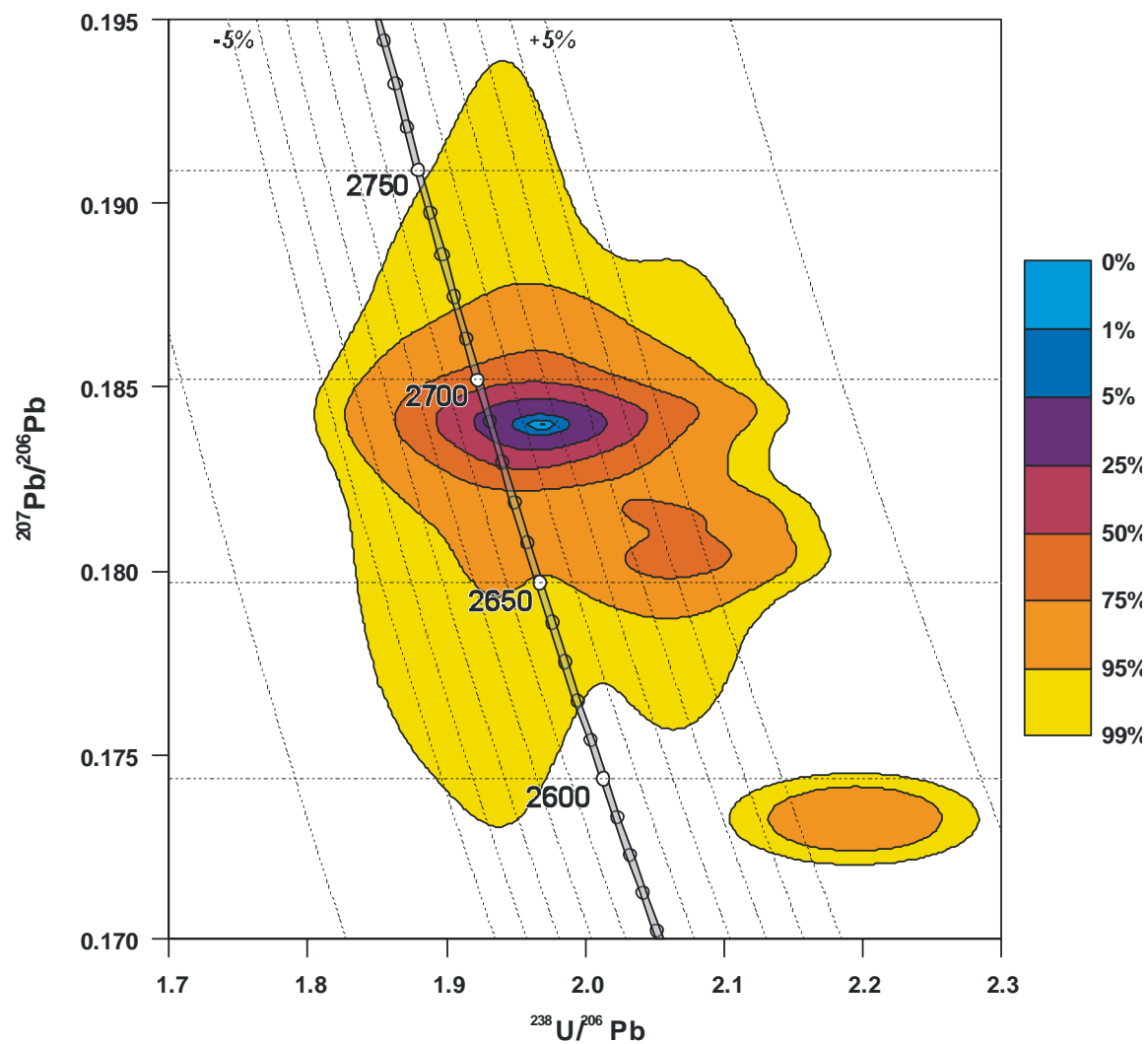


**Figure 88.** Concordia contour plot for zircons from sample 2004967369: porphyritic micro-diorite sill, Three-in-Hand prospect, illustrating the dominant cluster at ~2680 Ma with minor dispersion toward lower right.

**Table 24.** SHRIMP analytical results for zircon from sample 2004967369: porphyritic micro-diorite sill, Three-in-Hand prospect.

Grain.Spot	U (ppm)	Th (ppm)	% comm 206	$^{207}\text{Pb}/^{206}\text{Pb}$	$\pm$	$^{206}\text{Pb}/^{238}\text{U}$	$\pm$	$^{207}\text{Pb}/^{235}\text{U}$	$\pm$	% Disc.	$^{207}\text{Pb}/^{206}\text{Pb}$ Age (Ma)	$\pm$
<i>Zoned cores</i>												
16.1	369	155	0.341	0.1828	0.0006	0.5146	0.0078	12.97	0.20	0.1	2678.6	5.2
35.1	248	151	0.024	0.1829	0.0005	0.5079	0.0078	12.81	0.20	1.2	2679.6	4.9
22.1	190	66	0.025	0.1835	0.0006	0.5046	0.0084	12.77	0.22	1.9	2684.8	5.5
26.1	293	106	0.014	0.1837	0.0005	0.5074	0.0078	12.85	0.20	1.5	2686.5	4.4
06.2	271	120	0.022	0.1837	0.0005	0.5226	0.0080	13.24	0.21	-0.9	2687.0	4.4
32.1	143	53	0.022	0.1838	0.0007	0.5093	0.0095	12.91	0.25	1.3	2687.8	6.5
37.1	242	95	0.026	0.1838	0.0005	0.5126	0.0079	12.99	0.20	0.7	2687.8	4.9
40.1	222	109	0.030	0.1839	0.0006	0.5136	0.0080	13.02	0.21	0.6	2687.9	5.2
24.2	266	85	-0.018	0.1839	0.0005	0.5183	0.0091	13.14	0.23	-0.1	2688.7	4.7
36.1	250	103	0.649	0.1840	0.0009	0.5136	0.0079	13.03	0.21	0.6	2689.2	7.9
24.3	252	73	0.024	0.1840	0.0006	0.5227	0.0088	13.26	0.23	-0.8	2689.7	5.3
39.1	167	59	0.012	0.1840	0.0006	0.5000	0.0078	12.69	0.20	2.8	2689.7	5.7
22.2	189	65	0.015	0.1841	0.0006	0.5085	0.0079	12.91	0.20	1.5	2690.2	5.5
12.2	143	55	0.003	0.1841	0.0007	0.5163	0.0082	13.11	0.21	0.3	2690.5	6.2
10.1	206	88	0.036	0.1842	0.0006	0.5002	0.0077	12.70	0.20	2.8	2691.1	5.2
19.2	395	119	0.015	0.1842	0.0004	0.5193	0.0083	13.19	0.21	-0.2	2691.4	3.8
13.2	232	96	0.012	0.1844	0.0011	0.5287	0.0081	13.44	0.22	-1.6	2692.6	9.5
04.1	226	80	0.018	0.1844	0.0006	0.5247	0.0093	13.34	0.24	-1.0	2692.9	4.9
<i>Concentric mantle</i>												
24.1	604	109	0.238	0.1799	0.0006	0.4863	0.0073	12.07	0.19	3.7	2652.4	5.5
23.1	516	173	0.061	0.1804	0.0004	0.4862	0.0073	12.09	0.18	3.8	2656.2	3.5
06.1	540	234	0.028	0.1816	0.0005	0.4925	0.0074	12.33	0.19	3.2	2667.9	4.6
41.1	372	64	0.430	0.1827	0.0007	0.4914	0.0074	12.38	0.19	3.8	2677.4	6.7
17.1	355	179	0.011	0.1830	0.0004	0.5136	0.0078	12.96	0.20	0.3	2680.4	4.0
13.1	427	96	0.172	0.1834	0.0004	0.5059	0.0078	12.79	0.20	1.7	2684.0	4.1
37.2	522	240	0.277	0.1837	0.0005	0.4967	0.0075	12.58	0.19	3.2	2686.4	4.5
34.1	294	87	0.030	0.1837	0.0005	0.5029	0.0077	12.74	0.20	2.3	2687.0	4.6
01.1	374	181	0.048	0.1839	0.0004	0.4963	0.0075	12.58	0.19	3.4	2688.3	3.7
33.1	525	161	0.203	0.1840	0.0004	0.4952	0.0075	12.56	0.19	3.6	2689.2	4.0
11.1	444	152	0.054	0.1840	0.0004	0.5072	0.0076	12.87	0.20	1.7	2689.5	3.6
02.1	312	110	0.016	0.1842	0.0004	0.5054	0.0077	12.84	0.20	2.0	2691.2	3.9
<i>Concentric grains</i>												
25.1	353	135	0.176	0.1846	0.0005	0.5001	0.0076	12.73	0.20	3.0	2694.4	4.6
38.1	554	158	0.022	0.1847	0.0004	0.5000	0.0075	12.73	0.19	3.0	2695.1	3.5
30.1	241	89	0.012	0.1847	0.0005	0.5136	0.0079	13.08	0.20	0.9	2695.2	4.8
31.1	572	225	0.007	0.1848	0.0004	0.5103	0.0079	13.00	0.20	1.4	2696.4	3.2
08.2	291	77	0.679	0.1855	0.0011	0.5044	0.0077	12.90	0.21	2.6	2702.5	9.5
44.1	289	79	0.381	0.1856	0.0007	0.5099	0.0078	13.05	0.21	1.7	2703.2	6.1
<i>Bright rims</i>												
21.1	79	22	0.040	0.1839	0.0010	0.5219	0.0087	13.23	0.23	-0.7	2688.5	8.9
15.1	110	39	0.059	0.1844	0.0010	0.4910	0.0080	12.48	0.21	4.4	2692.5	8.7
<i>Discordant/High Pb</i>												
14.1	594	164	0.080	0.1682	0.0004	0.4243	0.0064	9.84	0.15	10.2	2539.9	3.7
19.1	655	204	0.185	0.1733	0.0005	0.4557	0.0068	10.89	0.17	6.5	2589.4	4.5
12.1	356	128	0.048	0.1805	0.0004	0.4790	0.0073	11.92	0.18	5.1	2657.3	4.0
27.1	578	133	0.206	0.1814	0.0004	0.4812	0.0072	12.04	0.18	5.0	2666.1	3.9
07.1	596	172	0.000	0.1844	0.0003	0.4868	0.0073	12.37	0.19	5.0	2692.5	3.0
05.1	77	34	6.840	0.1816	0.0059	0.4836	0.0085	12.11	0.45	4.7	2667.7	53.7



Compilation of SHRIMP U-Pb geochronological data, Yilgarn Craton, Western Australia, 2004-2006

28.1	73	34	1.648	0.1825	0.0036	0.5128	0.0089	12.91	0.34	0.3	2675.8	32.9
03.1	43	19	4.239	0.1825	0.0051	0.5293	0.0099	13.32	0.45	-2.3	2676.0	46.0
43.1	202	87	3.068	0.1839	0.0072	0.5149	0.0087	13.05	0.56	0.4	2688.2	64.5
03.2	209	78	1.005	0.1845	0.0013	0.5180	0.0080	13.18	0.22	0.1	2694.0	11.3
42.1	319	116	3.901	0.1845	0.0032	0.5055	0.0079	12.86	0.30	2.1	2694.1	28.3

---

*Data are at 1 $\sigma$  precision. All Pb data are common-Pb corrected based on  $^{204}\text{Pb}$  measurements. Mount: Z4562; Instrument: RSES SHRIMP-RG; Acquisition: 21 January 2005.*

## 2004967372: meta-conglomerate, Bee-Eater prospect

### SAMPLE INFORMATION

**1:250,000 sheet:** Kalgoorlie (SH5109)

**1:100,000 sheet:** Bardoc (3137)

**MGA:** 335400 mE 6608534 mN

**Location:** This sample is from Placer Dome Asia Pacific diamond drill hole WTD2, depth interval 115.10-117.20 m. The collar is located approximately 7 km east-southeast of White Flag Dam.

**Description:** This rock is from a grey-white altered, volcanic meta-conglomerate. The meta-conglomerate contains a variety of altered, <1 to >5 cm size sub-rounded sandstone, quartzofeldspathic, and lithic clasts. The lithic clasts include dacitic and andesitic lithologies. The unit is part of a thick felsic volcanic, volcanoclastic and siliciclastic sequence, which is locally referred to as the White Flag Formation. The rock is cut by minor quartz-filled fractures.

The sample is an intensely altered, poorly-sorted, clast-rich rock with a fine-grained chloritic and quartz-feldspar-rich matrix forming up to 30% of the rock. Individual clasts form about 70% of the rock and include re-sedimented sandstone and dacite porphyry. A sandstone clast contains angular to rare rounded monocrystalline quartz (20%) and feldspar (20%) and polycrystalline quartz-feldspar (40%) in a very-fine-grained chloritic and quartz-feldspar-rich matrix (20%). A dacite porphyry clast comprises quartz (10%) and altered feldspar (25%) phenocrysts in a recrystallised, fine-grained quartzofeldspathic groundmass. Aggregates of fine-grained chlorite, sericite and carbonate are possibly relict Fe-Mg silicates in the dacite. The matrix to these large clasts contains micro-clasts of angular to rounded monocrystalline quartz (25%) and feldspar (30%) and polycrystalline quartz-feldspar (20%) in a very fine-grained chloritic and quartz-feldspar-rich matrix. The rock is moderately to strongly altered, with abundant secondary albite, sericite, chlorite, carbonate and minor clinozoisite/epidote, leucoxene and opaque minerals. Opaque minerals occur as subhedral to anhedral and irregular grains disseminated throughout the matrix and are concentrated in sericite-, carbonate- and chlorite-rich aggregates in the clasts. Carbonate forms irregular to anhedral grains disseminated throughout the various rock fragments and matrix. Accessory phases include trace zircon.



#### DESCRIPTION OF ZIRCONS

- Shape:** Euhedral, squat prismatic ([Figure 89](#)).
- Size:** 50 to 150 microns.
- Colour/clarity:** Clear to brown.
- Quality:** Fair to poor, cracks concentric to zoning.
- CL zoning:** Generally concentric zoning ([Figure 89](#)).
- Notes:** Zircon yield from this sample was very limited (18 grains only) and to ensure a reasonable sized selection for analysis there was no quality discrimination.

#### CONCURRENT STANDARD DATA

- Pb/U reprod.(2s):** 0.67%
- Err. of mean (2s):** 4.68%
- Standard:** QGNG
- Analyses:** 56 (two analyses rejected as anomalously young)
- Notes:** A multi-day session.

#### SAMPLE DATA

The low zircon yield of this sample greatly restricted analytical opportunities. Ten analyses were made on ten grains ([Table 25](#), [Figure 90](#)). Five analyses are >5% discordant or have high common-Pb.

The remaining five analyses yield a concordia age of  $2689.7 \pm 8.6$  Ma with a relatively high MSWD of 5.4 suggesting isotopic perturbation in this sample ([Figure 90](#)). The low volume of data does not allow further statistical discrimination.



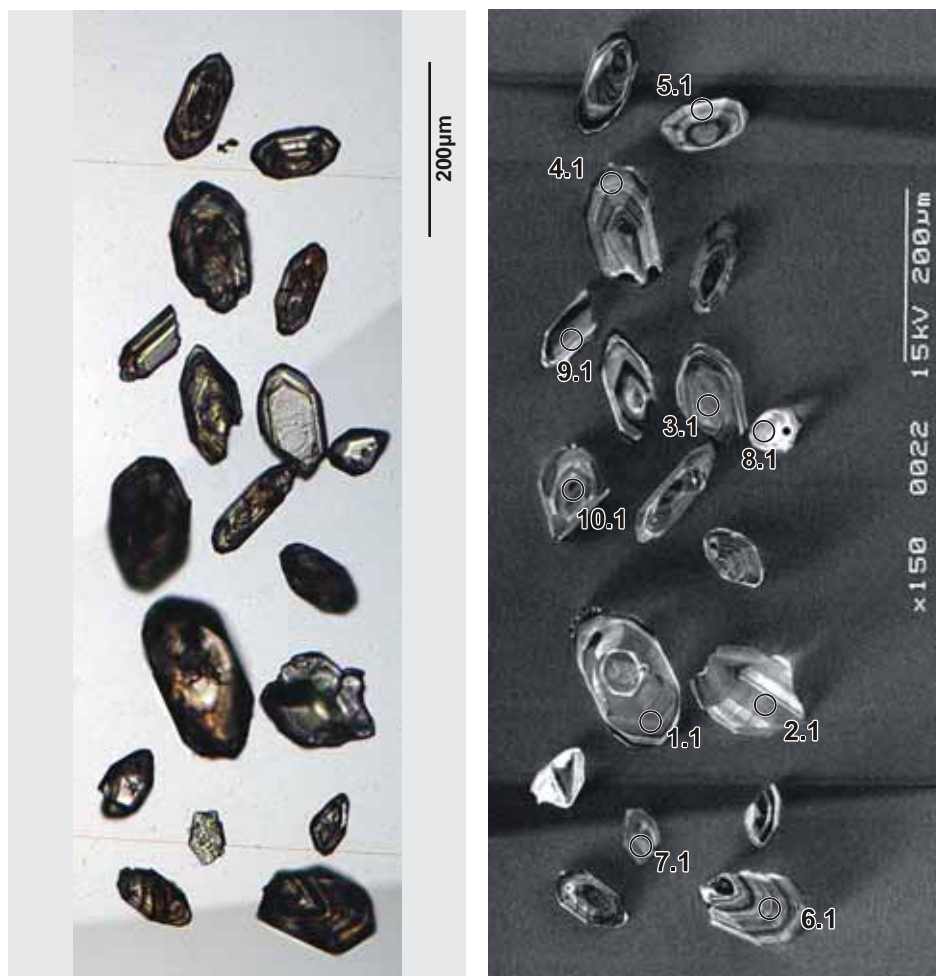


**Figure 89.** Complete image (transmitted light on left, cathodoluminescence on right) of sample 2004967372: meta-conglomerate, Bee-Eater prospect. SHRIMP analysis spots are labelled.

#### **GEOCHRONOLOGICAL INTERPRETATION**

The age of  $2690 \pm 9$  Ma is tentatively interpreted as the age of zircon crystallisation for an igneous contribution to this volcanoclastic rock.

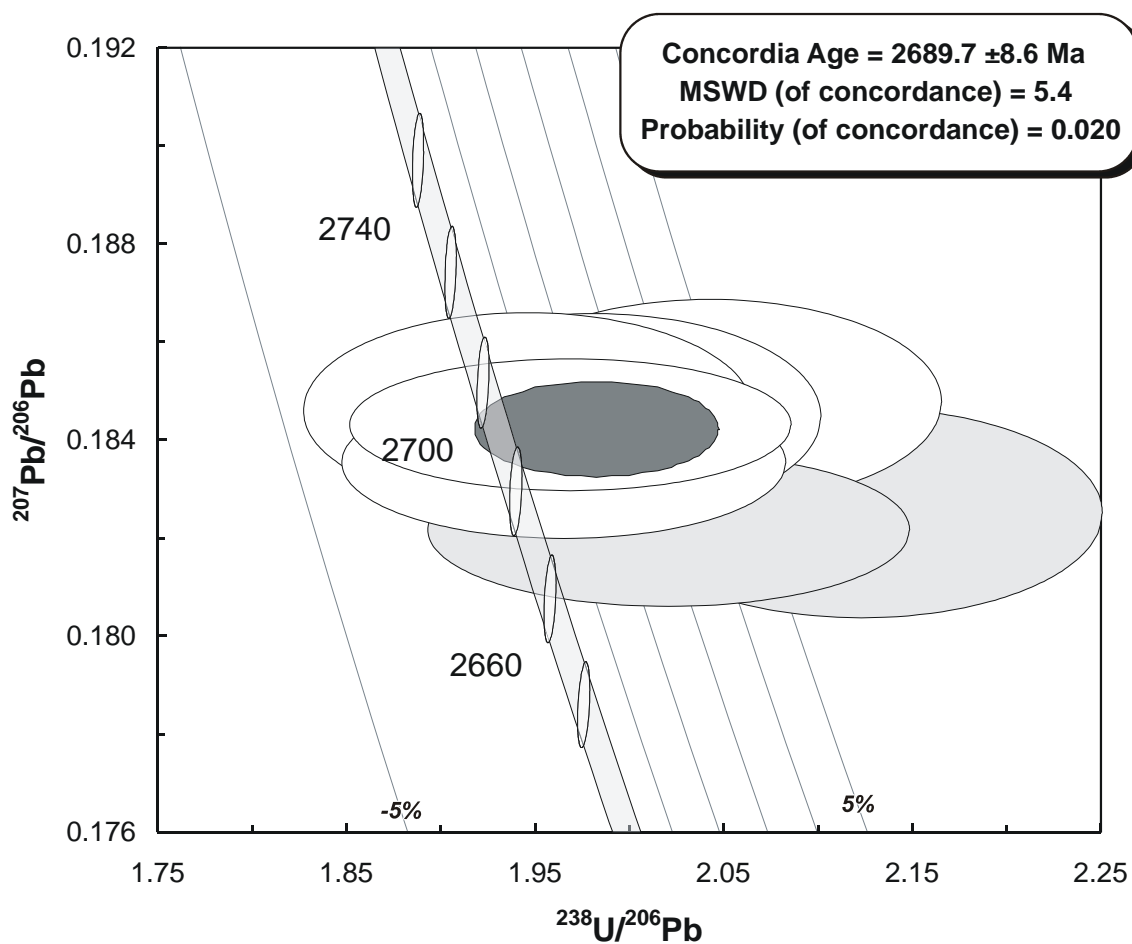


**Figure 90.** Tera-Wasserburg concordia plot for zircons from sample 2004967372: meta-conglomerate, Bee-Eater prospect. The main concordant cluster discussed in text is represented by white-filled symbols with the concordant age ellipse represented by the dark grey fill; discordant and/or high common-Pb analyses are light grey.

**Table 25.** SHRIMP analytical results for zircon from sample 2004967372: meta-conglomerate, Bee-Eater prospect.

Grain.Spot	U (ppm)	Th (ppm)	% comm 206	$^{207}\text{Pb}/^{206}\text{Pb}$	$\pm$	$^{206}\text{Pb}/^{238}\text{U}$	$\pm$	$^{207}\text{Pb}/^{235}\text{U}$	$\pm$	% Disc.	$^{207}\text{Pb}/^{206}\text{Pb}$ Age (Ma)	$\pm$
<i>Main</i>												
2.1	211	193	0.153	0.1836	0.0006	0.5088	0.0124	12.8768	0.3180	1.3	2685.3	5.7
1.1	276	169	0.117	0.1843	0.0005	0.5080	0.0123	12.9111	0.3154	1.6	2692.3	4.9
3.1	175	85	0.152	0.1845	0.0009	0.5045	0.0124	12.8347	0.3217	2.3	2693.9	7.7
8.1	119	58	0.160	0.1846	0.0008	0.5138	0.0128	13.0802	0.3317	0.8	2694.9	7.3
9.1	175	93	0.361	0.1848	0.0009	0.4896	0.0120	12.4755	0.3119	4.7	2696.5	7.6
<i>Discordant/High common-Pb</i>												
5.1	226	111	0.476	0.1822	0.0009	0.3320	0.0081	8.3395	0.2085	30.9	2672.7	8.0
7.1	260	154	0.664	0.1822	0.0006	0.4948	0.0128	12.4306	0.3238	3.0	2672.9	5.8
4.1	178	101	0.271	0.1825	0.0009	0.4711	0.0116	11.8559	0.2974	7.0	2676.0	7.9
6.1	430	145	1.778	0.1837	0.0012	0.1961	0.0047	4.9686	0.1244	57.0	2686.9	10.9
10.1	529	293	1.703	0.1867	0.0008	0.1999	0.0048	5.1459	0.1255	56.7	2713.6	7.4

Data are at  $1\sigma$  precision. All Pb data are common-Pb corrected based on  $^{204}\text{Pb}$  measurements. Mount: Z4799; Instrument: JdL Centre SHRIMP-B; Acquisition: 4 October 2005.



## 2004967377: Owen monzogranite

### SAMPLE INFORMATION

**1:250,000 sheet:** Kalgoorlie (SH5109)

**1:100,000 sheet:** Bardoc (3137)

**MGA:** 331321 mE 6630085 mN

**Location:** This sample was taken from outcrop 2 km west-southwest of Mount Ellis.

**Description:** This rock is a light grey, foliated, seriate to rarely feldspar-porphyrific, medium-coarse-grained, biotite monzogranite. The monzogranite forms the part of the southern end of a composite granitoid batholith. The rock is weakly sheared with the resulting anastomosing fabric defined by strained and recrystallised quartz and elongate partly-altered biotite that locally wrap feldspar phenocrysts.

Principal minerals in the granular textured rock are quartz (30-35%), plagioclase (30-35%), K-feldspar (28-30%) and biotite (-5-6%), with plagioclase>K-feldspar. Plagioclase occurs as subhedral grains that locally display broad oscillatory to complex zoning. The plagioclase is locally weakly saussuritised to fine-grained white mica and minor epidote. Quartz displays textures consistent with shearing including recrystallisation along grain boundaries, variable subgrain development with sutured boundaries and undulose extinction. K-feldspar is anhedral to interstitial, dominantly microcline and locally perthitic. Biotite occurs as brown to green ragged flakes, and commonly displays minor chlorite alteration, with minor epidote, white mica and leucoxene. Accessory phases include zircon and opaque minerals, and trace apatite and hematite staining.

### DESCRIPTION OF ZIRCONS

**Shape:** Euhedral prismatic grains, frequent fractures ([Figure 91](#)).

**Size:** 50 to 100 microns

**Colour/clarity:** Generally dark and turbid, few clear grains.

**Quality:** Fair to poor, frequent cracks and inclusions.

**CL zoning:** Generally concentric zoning, but frequently dark, bland patterns with complex embayment structures ([Figure 91](#)).

**Notes:** Zircon yield from this sample was very limited (~60 grains) and to ensure a reasonable sized selection for analysis there was no quality discrimination.



#### CONCURRENT STANDARD DATA

**Pb/U reprod.(2s):** 2.9%

**Err. of mean (2s):** 0.6%

**Standard:** QGNG

**Analyses:** 31 (one discarded as anomalous)

**Notes:** Reproducibility of Pb/U ratios is reasonable.

#### SAMPLE DATA

The low zircon yield of this sample greatly restricted analytical opportunities. Nine analyses were made on nine grains ([Table 26](#); [Figure 92](#)) with five other analyses aborted due to high common-Pb noted in the first scan. Four analyses are > 5% discordant or have high common-Pb.

The remaining five analyses form a concordant cluster that yields a concordant age of  $2655 \pm 15$  Ma. Because of the small number of analyses this result has to be treated with considerable caution.



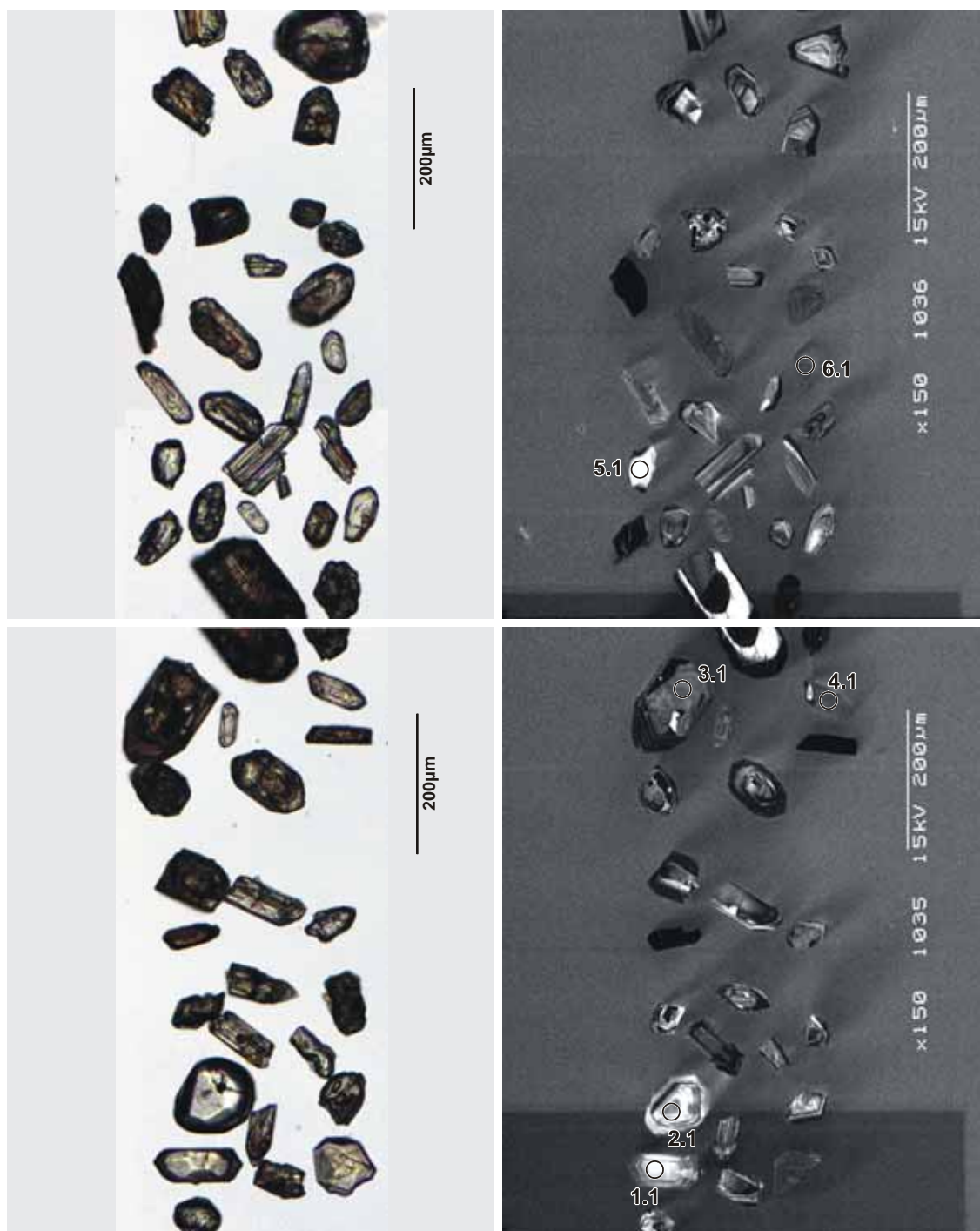


**Figure 91.** Representative images (transmitted light on left, cathodoluminescence on right) for sample 2004967377: Owen monzogranite. SHRIMP analysis spots are labelled.

#### GEOCHRONOLOGICAL INTERPRETATION

The age of  $2655 \pm 15$  Ma is interpreted, very tentatively, as the magmatic age of this monzogranite.



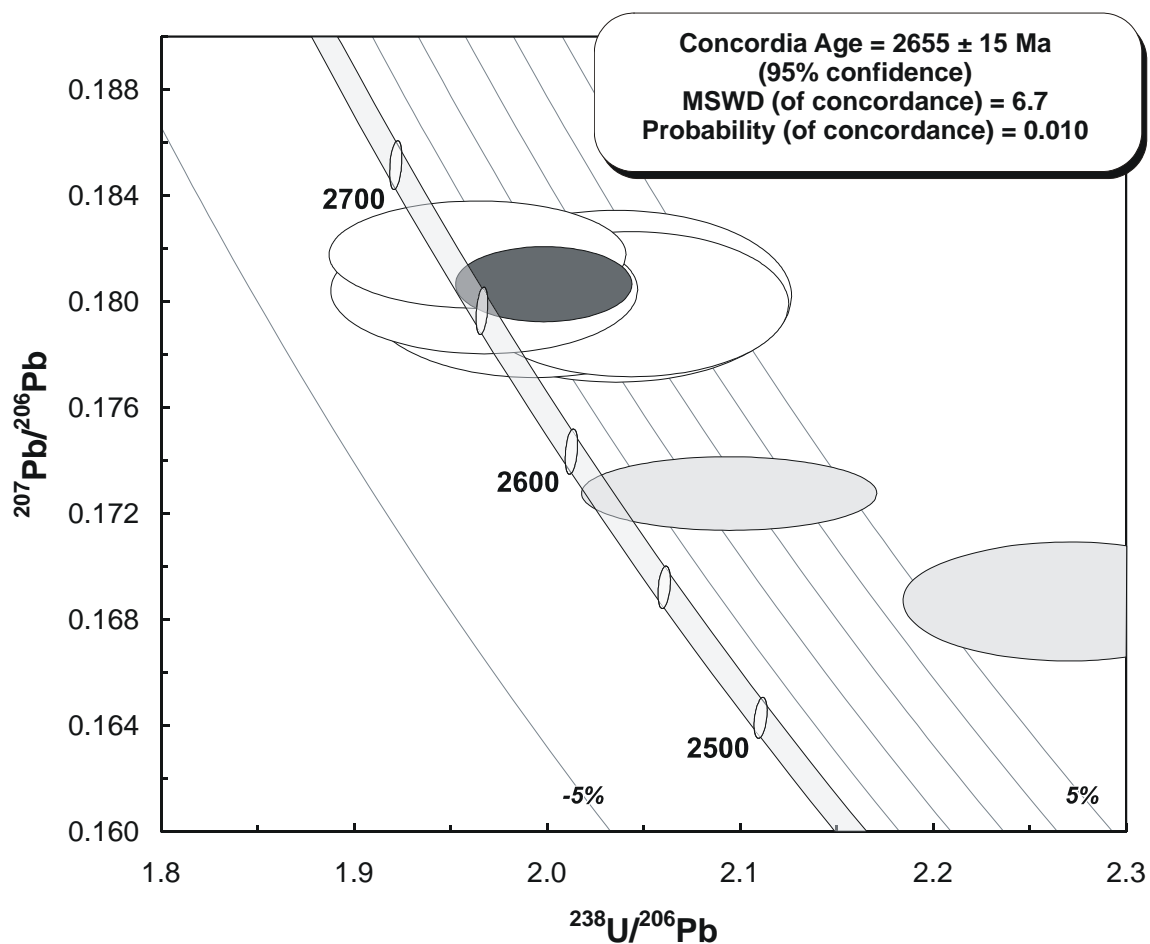


**Figure 92.** Tera-Wasserburg concordia plot for zircons from sample 2004967377: Owen monzogranite. The main concordant cluster used to calculate a concordia age of  $2655 \pm 15$  Ma is represented by white-filled symbols; discordant and/or high common-Pb analyses are light grey.

**Table 26.** SHRIMP analytical results for zircon from sample 2004967377: Owen monzogranite.

Grain.Spot	U (ppm)	Th (ppm)	% comm 206	<sup>207</sup> Pb / <sup>206</sup> Pb	±	<sup>206</sup> Pb / <sup>238</sup> U	±	<sup>207</sup> Pb / <sup>235</sup> U	±	% Disc.	<sup>207</sup> Pb / <sup>206</sup> Pb Age (Ma)	±
<i>Magmatic?</i>												
3.1	101	40	0.756	0.1799	0.0011	0.4892	0.0079	12.1380	0.2110	3.2	2652.3	10.4
1.1	56	34	0.095	0.1800	0.0012	0.5015	0.0087	12.4449	0.2310	1.2	2652.8	10.6
5.1	45	36	0.115	0.1802	0.0013	0.4912	0.0089	12.2068	0.2399	3.0	2655.1	12.3
2.1	90	77	0.078	0.1805	0.0010	0.5081	0.0084	12.6439	0.2193	0.3	2657.3	9.0
7.1	128	148	0.055	0.1818	0.0008	0.5090	0.0081	12.7606	0.2119	0.6	2669.5	7.6
<i>Discordant/High common-Pb</i>												
4.1	638	508	0.080	0.1687	0.0009	0.4407	0.0067	10.2502	0.1663	7.5	2544.6	9.1
6.1	853	820	0.550	0.1728	0.0006	0.4775	0.0071	11.3749	0.1733	2.7	2584.8	5.5
9.1	221	164	2.305	0.1828	0.0015	0.2681	0.0047	6.7550	0.1310	42.8	2678.1	13.7
8.1	277	621	7.778	0.1869	0.0315	0.2724	0.0081	7.0213	1.2028	42.8	2715.5	278.2

Data are at 1 $\sigma$  precision. All Pb data are common-Pb corrected based on <sup>204</sup>Pb measurements. Mount: Z4562; Instrument: RSES SHRIMP-RG; Acquisition: 22 January 2005.



## 2004967500: meta-sandstone, Toppin Hill

### SAMPLE INFORMATION

**1:250,000 sheet:** Rason (SH5103)

**1:100,000 sheet:** Toppin (3640)

**MGA:** 593670 mE 6829800 mN

**Location:** This sample taken from Anglogold Ashanti Australia Ltd diamond drill hole YMD002, depth interval 113.90-115.50 m. The collar is located approximately 5.5 km north of Toppin Hill.

**Description:** This rock is from a grey, altered, graded meta-sandstone unit, which is part of an altered felsic volcanoclastic and siliciclastic sequence. The fine- to medium-grained sandstone contains a variety of altered, sub-mm sub-rounded, quartz, quartzofeldspathic, and feldspar clasts. A strong anastomosing fabric defined by fine-grained biotite wraps the recrystallised quartz and quartzofeldspathic clasts. Overgrowing the foliation are oikocrysts of biotite of likely metamorphic origin.

Principal minerals are micro-crystalline quartz and/or feldspar (75%), discrete monocrystalline quartz (~5%) and feldspar (10%), very-fine grained biotite (8-10%), and trace opaque minerals and zircon. Metamorphic and/or alteration minerals include secondary biotite, fine-grained white mica, carbonate, leucoxene and opaque minerals. The sample is a strongly recrystallised, and intensely altered, clast-rich rock with a very fine-grained biotite and quartz-feldspar-rich matrix forming up to 35% of the rock. Recrystallised and altered clasts, generally < 2 mm, form about 65% of the rock and include mono- (~5%) and rare poly-crystalline quartz, monocrystalline feldspar (~10%) and abundant very fine-grained quartz-feldspar-rich (~40%) lithic clasts. Recrystallisation and alteration hamper identification of the clast types. The (sub-)rounded quartz clasts exhibit undulose extinction and are rimmed by very fine-grained polycrystalline quartz mosaics. There are also rare polycrystalline quartz clasts, which may represent either recrystallised chert clasts or recrystallised monocrystalline quartz grains. The feldspar clasts are intensely altered to albite, white mica and carbonate. Aggregates of red-brown biotite flakes both aligned parallel to, and overprinting, the dominant foliation, form 8-10% of the rock.

### DESCRIPTION OF ZIRCONS

**Shape:** Subhedral prismatic grains with minor rounding of crystal faces (Figure 93).

**Size:** 50 to 150 microns.

**Colour/clarity:** Clear to dark brown, frequently turbid.



**Quality:** Fair to poor. Frequent fractures and inclusions.  
**CL zoning:** Prominent concentric zoning with occasional complex embayments. Occasional sector-zoned core (Figure 93).

#### CONCURRENT STANDARD DATA

**Pb/U reprod.(2s):** 0.39%

**Err. of mean (2s):** 2.06%

**Standard:** QGNG

**Analyses:** 34 (two discarded as anomalous)

**Notes:** This was a two-day session with occasional primary beam spiking problems which has caused the calculated uncertainty of some analyses to be exaggerated.

#### SAMPLE DATA

Thirty-six analyses were made on thirty grains (Table 27). Unfortunately five analyses experienced primary beam instability during analysis resulting in apparently large uncertainties and these have been discarded from further interpretation. Fourteen analyses are >5% discordant although these analyses produce a good discordia chord and concordia intercepts at  $2710 \pm 22$  Ma and  $1041 \pm 140$  Ma (Figure 94). The lower intercept value clearly indicates a non-zero age Pb-loss event.

Although six grains were analysed for possible core-rim associations only two, #1 and #4, yielded age differences (Figure 95). However, while these core ages appear to be older than the associated rims there is no statistically significant difference between the ages. This suggests that although there is a prominent difference in CL pattern between sector-zoned cores and concentric-zoned rims that there is insufficient resolution in these data to clearly resolve an age difference.

On the basis of CL patterns three 'inherited core' analyses (#1.1, #4.1 and #33.1) plus one analysis indicative of Pb-loss (#25.1) are discarded from the concordant analyses yielding a weighted mean  $^{207}\text{Pb}/^{206}\text{Pb}$  age of  $2682.3 \pm 4.6$  (95% conf., MSWD = 1.8, 13 ages). A concordia age cannot be calculated from these data suggesting that these analyses may be affected by a minor ancient Pb-loss event and/or represent mixture of two unresolvable age components. The determined age should be treated with caution.





**Figure 93.** Representative images (transmitted light on left, cathodoluminescence on right) for sample 2004967500: meta-sandstone, Toppin Hill. SHRIMP analysis spots are labelled. The white streaking is due to the over-bright luminescence of accidentally included apatite grains.

#### GEOCHRONOLOGICAL INTERPRETATION

The magmatic age of the dominant component of this meta-sandstone is interpreted as  $2682 \pm 5$  Ma with suggestion of an unresolvable inherited component at  $\sim 2700$  Ma. The zircons have been strongly influenced by a Neoproterozoic Pb-loss event.



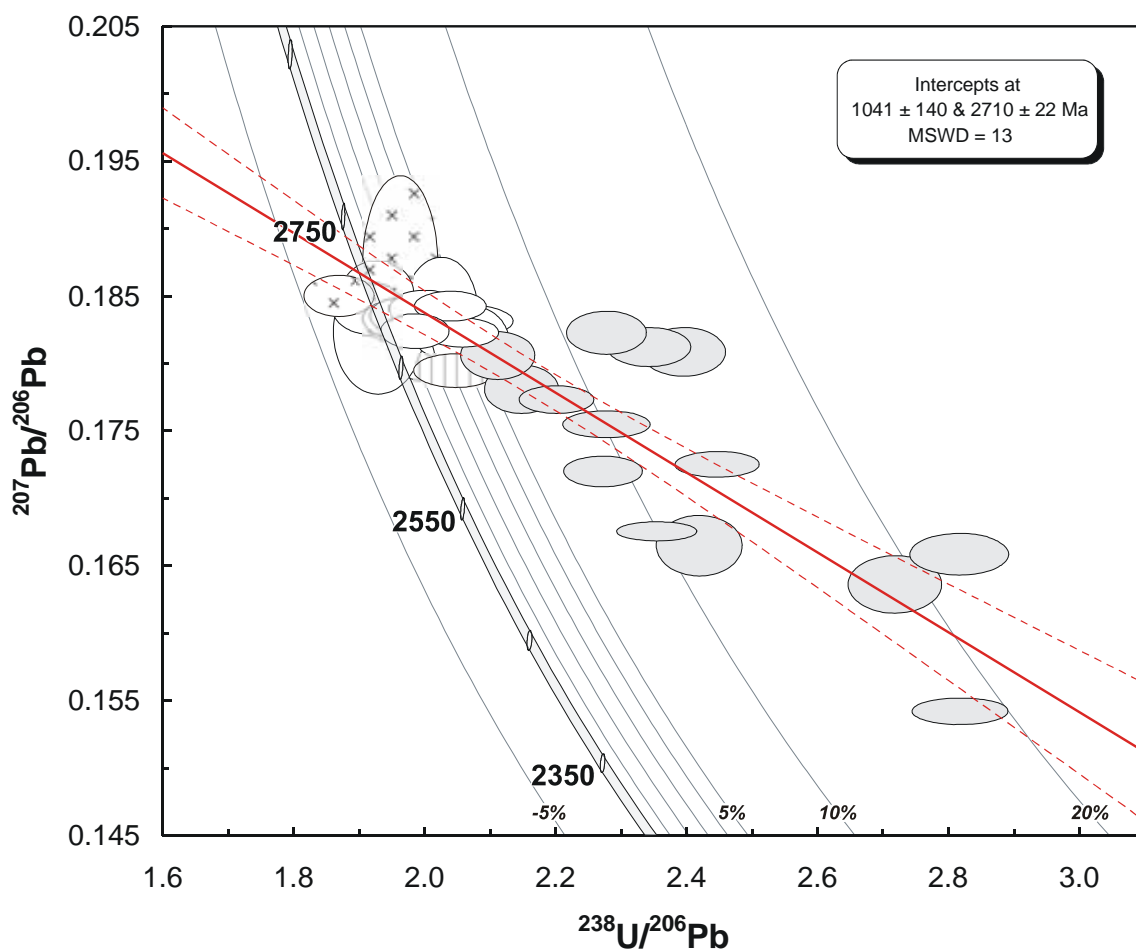


**Figure 94.** Tera-Wasserburg concordia plot for zircons from sample 2004967500: meta-sandstone, Toppin Hill. White-filled symbols are used to define the age of the sample; discordant and/or high common-Pb analyses are light grey; vertical hatch indicates analyses with possible Pb-loss; cross hatch indicates analyses on cores identified by CL imaging. Data with instrument induced exaggerated uncertainties have not been plotted.

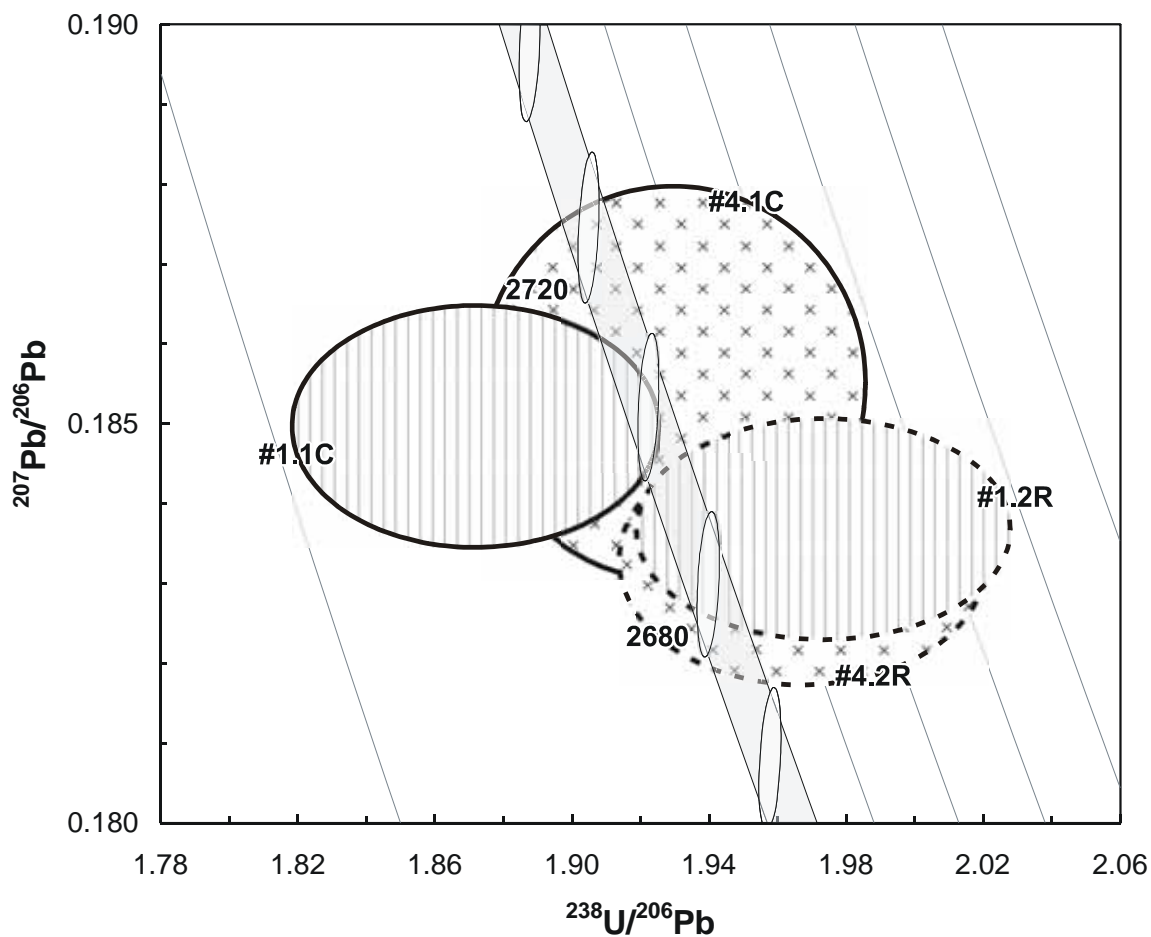


**Figure 95.** Tera-Wasserburg concordia plot for two sets of analyses from sample 2004967500: meta-sandstone, Toppin Hill with potential core-rim relationship. Core analyses are indicated by thick border on error ellipses; corresponding rim analyses have dashed borders. Although the ages suggest that core analyses are older than rim analyses, there is no significant statistical difference between the two.

**Table 27.** SHRIMP analytical results for zircon from sample 2004967500: meta-sandstone, Toppin Hill.

Grain. Spot	U (ppm)	Th (ppm)	% comm 206	<sup>207</sup> Pb / <sup>206</sup> Pb	±	<sup>206</sup> Pb / <sup>238</sup> U	±	<sup>207</sup> Pb / <sup>235</sup> U	±	% Disc.	<sup>207</sup> Pb / <sup>206</sup> Pb Age (Ma)	±
<i>Main</i>												
24.1	183	64	0.009	0.1815	0.0012	0.4947	0.0105	12.3771	0.2753	2.8	2666.3	10.6
9.2	130	71	0.044	0.1816	0.0011	0.4823	0.0056	12.0782	0.1576	4.9	2667.7	9.9
27.1	221	95	0.017	0.1823	0.0004	0.4854	0.0052	12.2004	0.1351	4.6	2673.8	3.9
29.1	265	106	0.004	0.1824	0.0005	0.5029	0.0054	12.6465	0.1403	1.8	2674.8	4.8
16.2	150	59	0.035	0.1824	0.0019	0.5174	0.0075	13.0143	0.2321	-0.5	2675.1	17.4
4.2	142	62	0.020	0.1831	0.0006	0.5082	0.0056	12.8293	0.1496	1.2	2681.2	5.8
21.1	183	87	0.040	0.1831	0.0005	0.4867	0.0081	12.2901	0.2069	4.7	2681.5	4.6
26.1	128	58	0.018	0.1834	0.0006	0.5092	0.0057	12.8727	0.1497	1.1	2683.5	5.1
1.2	128	63	0.008	0.1836	0.0006	0.5067	0.0057	12.8266	0.1494	1.6	2685.6	5.1
8.1	102	39	0.018	0.1841	0.0008	0.5212	0.0062	13.2280	0.1663	-0.5	2689.9	7.1
5.1	144	85	0.035	0.1841	0.0005	0.4995	0.0055	12.6780	0.1451	2.9	2690.1	4.8
15.1	264	94	0.019	0.1841	0.0015	0.4931	0.0054	12.5189	0.1731	4.0	2690.5	13.8
22.1	200	140	0.002	0.1843	0.0005	0.4896	0.0053	12.4383	0.1389	4.6	2691.6	4.1
<i>Possible inherited cores?</i>												
1.1	108	53	-0.007	0.1850	0.0006	0.5342	0.0062	13.6266	0.1650	-2.2	2698.4	5.5
4.1	138	67	0.040	0.1851	0.0010	0.5180	0.0061	13.2231	0.1728	0.3	2699.5	9.1
33.1	78	39	0.099	0.1871	0.0028	0.5086	0.0061	13.1240	0.2510	2.4	2717.1	24.5
<i>Pb-loss</i>												
25.1	336	197	0.011	0.1795	0.0005	0.4879	0.0062	12.0735	0.1573	3.3	2648.0	4.8
<i>Discordant</i>												
2.1	493	371	0.087	0.1542	0.0004	0.3550	0.0037	7.5476	0.0821	18.1	2392.8	4.5
13.2	271	155	0.061	0.1636	0.0009	0.3680	0.0039	8.3023	0.0993	19.0	2493.5	8.9
28.1	336	148	0.038	0.1659	0.0006	0.3551	0.0039	8.1214	0.0938	22.1	2516.2	6.4
3.1	439	234	0.022	0.1665	0.0009	0.4131	0.0045	9.4838	0.1165	11.6	2522.8	9.2
6.1	506	262	0.027	0.1676	0.0003	0.4245	0.0045	9.8076	0.1049	10.0	2533.5	2.9
18.1	226	120	0.053	0.1720	0.0005	0.4396	0.0048	10.4251	0.1164	8.9	2577.1	4.5
11.1	455	275	0.030	0.1725	0.0004	0.4085	0.0043	9.7186	0.1054	14.5	2582.3	3.8
14.1	274	167	0.024	0.1755	0.0004	0.4387	0.0053	10.6151	0.1296	10.2	2610.6	3.9
7.1	319	190	0.024	0.1773	0.0004	0.4538	0.0049	11.0957	0.1216	8.2	2628.0	3.9
16.1	282	133	0.011	0.1781	0.0007	0.4651	0.0050	11.4219	0.1322	6.6	2635.4	6.9
10.1	204	109	0.079	0.1806	0.0007	0.4730	0.0051	11.7777	0.1367	6.1	2658.4	6.7
9.1	210	89	0.034	0.1809	0.0007	0.4172	0.0045	10.4029	0.1206	15.5	2660.7	6.7
23.1	131	71	0.062	0.1812	0.0006	0.4265	0.0047	10.6593	0.1234	14.0	2664.3	5.4
19.1	170	95	0.041	0.1823	0.0007	0.4388	0.0048	11.0267	0.1270	12.3	2673.6	6.0
<i>Instrument induced uncertainties</i>												
17.1	341	194	0.070	0.1320	0.0147	0.3528	0.0203	6.4192	0.8044	8.3	2124.2	195.0
24.2	269	161	0.586	0.1485	0.0064	0.3682	0.0142	7.5417	0.4349	13.2	2329.1	73.5
20.1	275	118	0.029	0.1713	0.0051	0.4459	0.0072	10.5315	0.3538	7.5	2570.3	49.3
13.1	123	66	0.031	0.1738	0.0050	0.4549	0.0052	10.8991	0.3363	6.8	2594.5	47.8
12.1	178	114	0.144	0.1821	0.0075	0.3949	0.0194	9.9139	0.6360	19.7	2672.0	68.3

Data are at 1σ precision. All Pb data are common-Pb corrected based on <sup>204</sup>Pb measurements. Mount: GA6009; Instrument: RSES SHRIMP-RG; Acquisition: 16 August 2006.



## 2004967506: meta-rhyolite, Toppin Hill

### SAMPLE INFORMATION

**1:250,000 sheet:** Rason (SH5103)

**1:100,000 sheet:** Toppin (3640)

**MGA:** 594130 mE 6830200 mN

**Location:** This sample taken from Anglogold Ashanti Australia Ltd diamond drill hole YMD003, depth interval 107.00-108.85 m. The collar is located approximately 6 km north-northeast of Toppin Hill.

**Description:** This rock is from a grey-white, altered, meta-rhyolite, which is part of an altered felsic volcanoclastic and sedimentary sequence. The quartz-feldspar-phyric rhyolite has variably recrystallised quartz and feldspar phenocrysts in a strongly recrystallised very fine-grained quartzofeldspathic groundmass. The rock is cut by thin (<1 mm) quartz-rich veinlets and fractures and late carbonate-rich fractures. The quartz-rich veins exhibit strong recrystallisation to very fine-grained granoblastic polygonal quartz aggregates indicating the veins are themselves strongly deformed and metamorphosed.

This is an intensely altered, quartz-feldspar-porphyrific rhyolite with a very fine-grained sericitic and quartz-feldspar-rich groundmass. Phenocrysts constitute about 20% of the rock and include recrystallised, subrounded quartz (~5%), altered, subhedral plagioclase (15%) and minor irregular-shaped aggregates of biotite-quartz-opaque minerals (~5%) that may represent altered FeMg-bearing phenocrysts. Quartz phenocrysts are mainly strongly recrystallised to a fine-grained mosaic, with rare single crystals preserved with moderate undulose extinction and minor subgrain development. Plagioclase phenocrysts are generally moderately altered to albite-sericite±carbonate. Biotite-quartz-rich clusters are moderately altered to chlorite, leucoxene, sericite and carbonate. The groundmass forms over 75% of the rock and is mainly micro-crystalline quartz and feldspar that exhibits a preferred alignment, as well as aligned sericite, secondary biotite, chlorite and opaque minerals, which locally wrap relict phenocrysts. Sericite, chlorite and carbonate define a late fabric that cuts earlier recrystallised quartz-rich veinlets. Accessory phases include trace zircon and fine dusting of secondary hematite.

### DESCRIPTION OF ZIRCONS

**Shape:** Euhedral to subhedral prismatic grains (Figure 96).

**Size:** 50 to 100 microns.

**Colour/clarity:** Clear to brown, frequently turbid.



**Quality:** Fair to poor. Frequent fractures and inclusions.  
**CL zoning:** Prominent concentric zoning with occasional complex embayments (Figure 96).

#### CONCURRENT STANDARD DATA

**Pb/U reprod.(2s):** 0.39%

**Err. of mean (2s):** 2.06%

**Standard:** QGNG

**Analyses:** 34 (two discarded as anomalous)

**Notes:** This was a two-day session with occasional primary beam spiking problems which has caused the calculated uncertainty of some analyses to be exaggerated.

#### SAMPLE DATA

Thirty-eight analyses were made on thirty-four grains (Table 28). The poor quality of the zircon is indicated by thirty-one of the analyses being >5% discordant. Unfortunately these analyses also produce a poor discordia chord and concordia intercepts at  $2684 \pm 56$  Ma and  $541 \pm 180$  Ma (Figure 97).

Two further concordant analyses are discarded as representing inheritance (#3.1) and possible Pb-loss (#23.1). The remaining five analyses yield a weighted mean  $^{207}\text{Pb}/^{206}\text{Pb}$  age of  $2698.7 \pm 4.8$  Ma (95% conf. MSWD: 0.28).



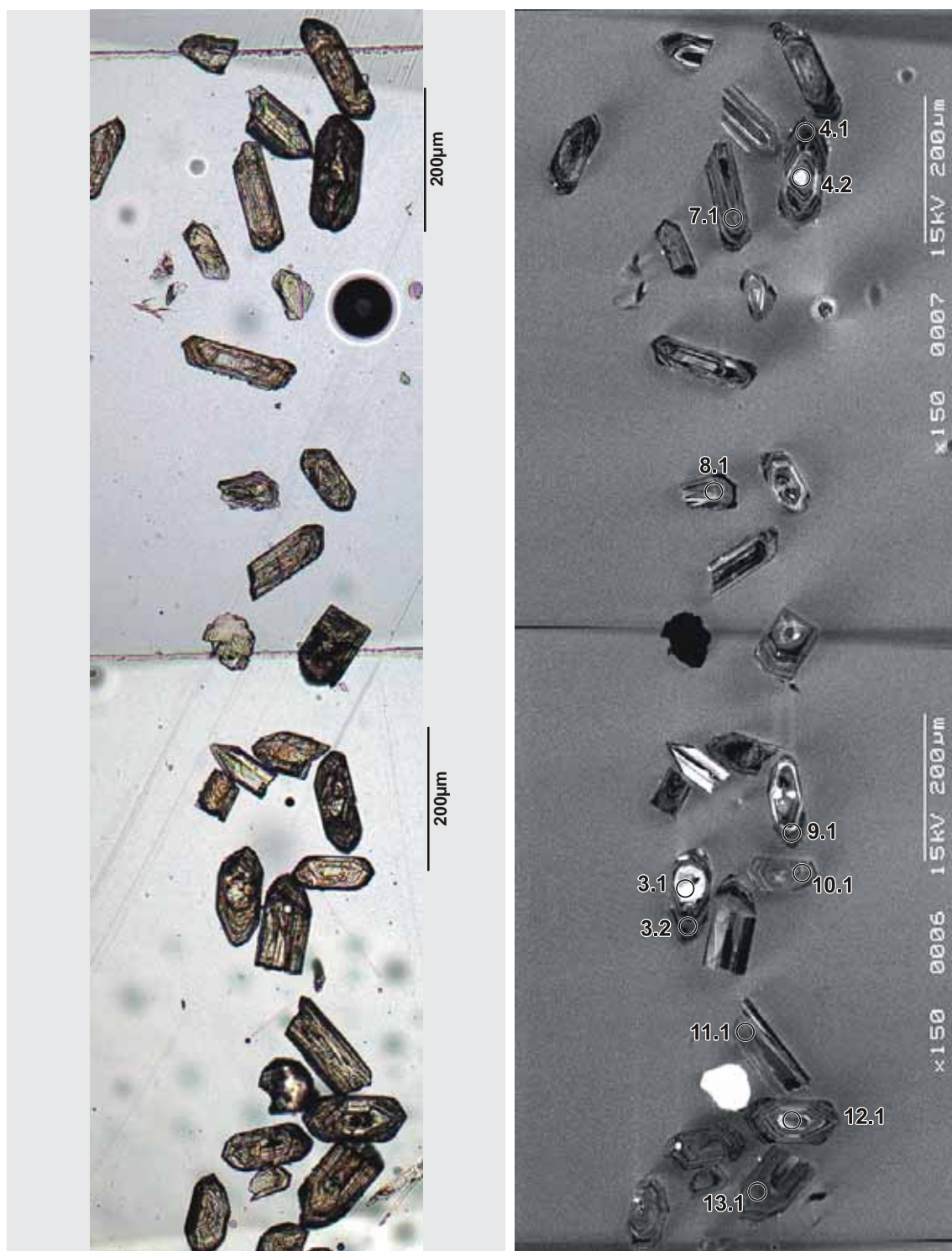


**Figure 96.** Representative images (transmitted light on left, cathodoluminescence on right) for sample 2004967506: meta-rhyolite, Toppin Hill. SHRIMP analysis spots are labelled.

#### GEOCHRONOLOGICAL INTERPRETATION

The magmatic age of the meta-rhyolite is interpreted as  $2699 \pm 5$  Ma and the zircons have been strongly influenced by a Neoproterozoic Pb-loss event.



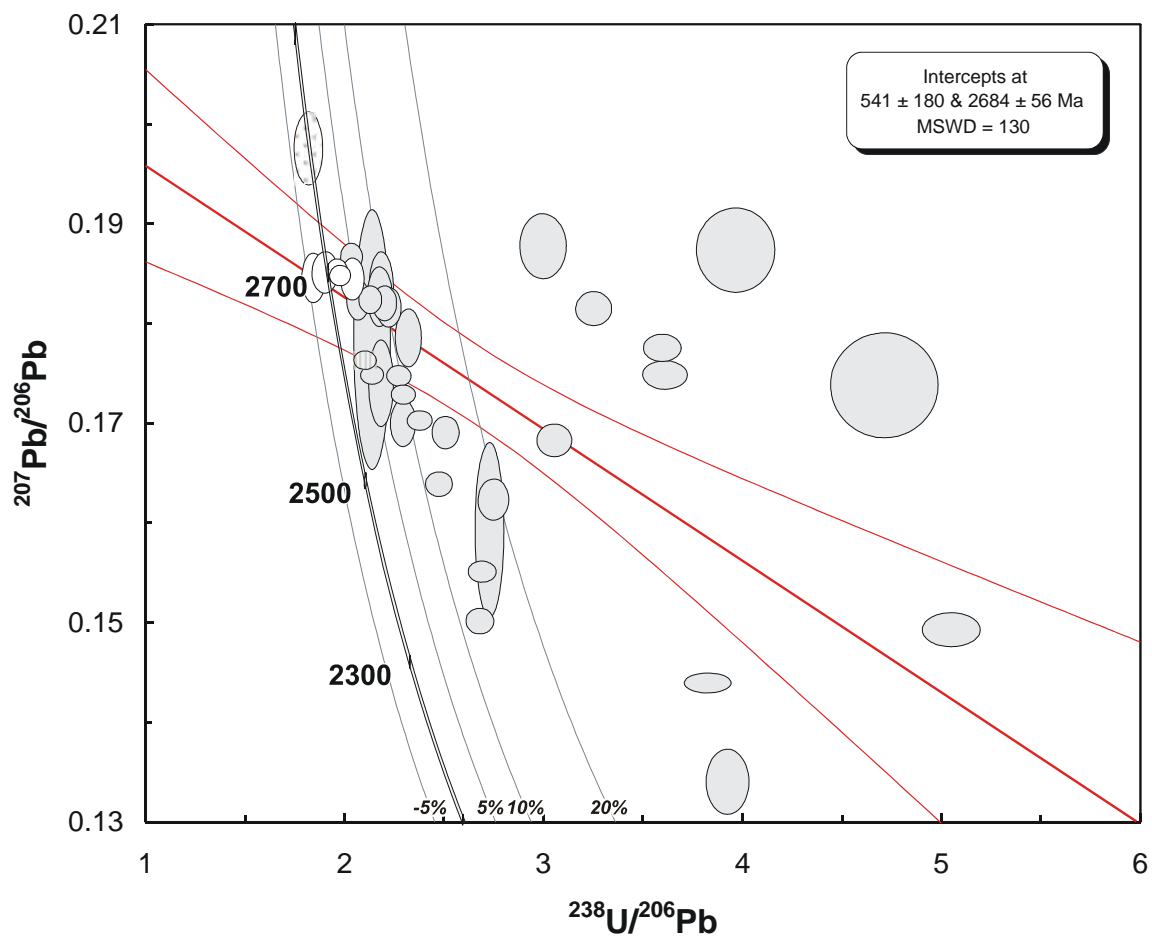


**Figure 97.** Tera-Wasserburg concordia plot for zircons from sample 2004967506: meta-rhyolite, Toppin Hill. White-filled symbols are used to define the age of the sample; discordant and/or high common-Pb analyses are light grey; cross-hatch fill indicates possible inheritance; vertical hatch fill indicates possible Pb-loss.

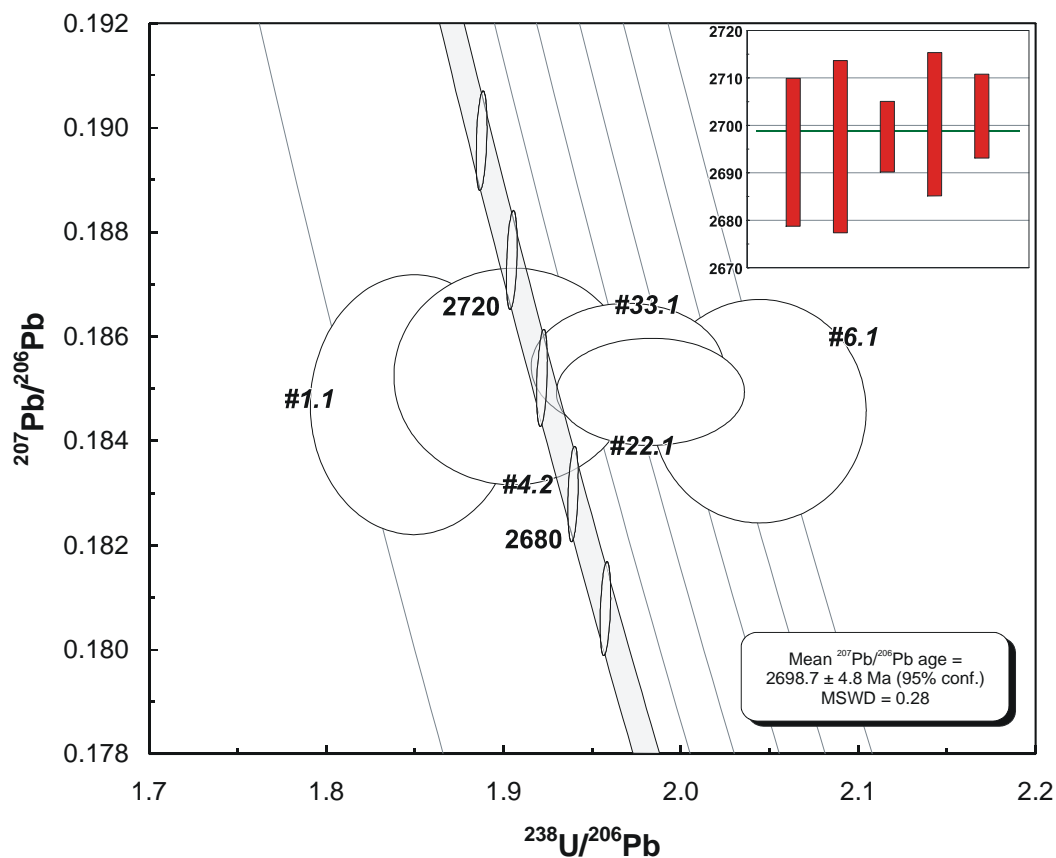


**Figure 98.** Tera-Wasserburg concordia plot for concordant zircons from sample 2004967506: meta-rhyolite, Toppin Hill.  $^{207}\text{Pb}/^{206}\text{Pb}$  ages ( $\pm 2\sigma$ ) uncertainties used for calculating weighted mean shown in inset.

**Table 28.** SHRIMP analytical results for zircon from sample 2004967506: meta-rhyolite, Toppin Hill.

Grain Spot	U (ppm)	Th (ppm)	% comm 206	$^{207}\text{Pb}/^{206}\text{Pb}$	$\pm$	$^{206}\text{Pb}/^{238}\text{U}$	$\pm$	$^{207}\text{Pb}/^{235}\text{U}$	$\pm$	% Disc.	$^{207}\text{Pb}/^{206}\text{Pb}$ Age (Ma)	$\pm$
<i>Main</i>												
6.1	186	75	0.038	0.1846	0.0009	0.4891	0.0059	12.4471	0.1606	4.7	2694.3	7.8
1.1	60	32	0.039	0.1847	0.0010	0.5404	0.0069	13.7626	0.1922	-3.3	2695.5	9.1
22.1	305	257	0.017	0.1849	0.0004	0.5043	0.0055	12.8589	0.1430	2.4	2697.6	3.7
4.2	77	50	0.020	0.1852	0.0008	0.5246	0.0075	13.3973	0.2018	-0.7	2700.2	7.6
33.1	334	261	0.016	0.1854	0.0005	0.5075	0.0057	12.9748	0.1492	2.1	2701.9	4.4
<i>Inherited</i>												
3.1	39	19	0.250	0.1977	0.0015	0.5479	0.0091	14.9337	0.2728	-0.3	2807.1	12.4
<i>Pb-loss?</i>												
23.1	375	138	0.218	0.1764	0.0004	0.4740	0.0051	11.5296	0.1256	4.5	2619.3	3.6
<i>Discordant/High comm. Pb</i>												
27.1	710	609	0.319	0.1339	0.0013	0.2546	0.0028	4.7016	0.0702	32.0	2150.0	17.5
4.1	550	1351	0.106	0.1439	0.0004	0.2613	0.0033	5.1848	0.0670	34.2	2275.1	4.9
3.2	741	3350	0.662	0.1492	0.0007	0.1981	0.0023	4.0771	0.0519	50.1	2337.2	8.0
7.1	571	247	0.086	0.1501	0.0005	0.3721	0.0039	7.7016	0.0860	13.1	2347.1	6.0
19.1	811	286	0.192	0.1551	0.0004	0.3710	0.0039	7.9344	0.0860	15.4	2403.0	4.6
18.1	416	319	0.015	0.1593	0.0036	0.3662	0.0040	8.0440	0.2020	17.8	2448.3	38.3
25.1	385	241	0.025	0.1623	0.0008	0.3633	0.0041	8.1325	0.1004	19.4	2480.1	8.8
28.1	706	330	0.013	0.1639	0.0005	0.4034	0.0043	9.1186	0.1016	12.5	2496.7	5.2
34.1	267	1262	0.238	0.1683	0.0007	0.3272	0.0038	7.5939	0.0924	28.2	2541.1	6.6
16.1	377	232	0.153	0.1691	0.0007	0.3978	0.0043	9.2751	0.1063	15.3	2548.7	6.5
14.1	445	244	0.022	0.1701	0.0010	0.4352	0.0048	10.2034	0.1268	9.0	2558.2	9.5
10.1	361	147	0.106	0.1703	0.0004	0.4193	0.0045	9.8464	0.1081	11.9	2560.8	4.0
8.1	308	84	0.023	0.1729	0.0004	0.4345	0.0047	10.3563	0.1136	10.1	2585.8	3.8
35.1	298	606	0.073	0.1739	0.0022	0.2122	0.0049	5.0873	0.1342	52.2	2595.3	20.7
19.2	295	157	0.076	0.1741	0.0018	0.4570	0.0054	10.9697	0.1710	6.6	2597.3	17.1
13.1	310	96	0.022	0.1748	0.0004	0.4387	0.0049	10.5735	0.1209	10.0	2604.1	4.0
21.1	364	220	0.011	0.1749	0.0004	0.4665	0.0050	11.2514	0.1234	5.3	2605.3	3.7
2.1	310	250	0.083	0.1749	0.0006	0.2768	0.0036	6.6756	0.0887	39.5	2605.3	5.6
9.1	327	525	0.042	0.1776	0.0006	0.2778	0.0030	6.8037	0.0769	39.9	2630.9	5.2
32.1	197	97	0.033	0.1785	0.0053	0.4667	0.0083	11.4849	0.3997	6.4	2638.8	49.6
20.1	225	110	0.021	0.1786	0.0012	0.4297	0.0048	10.5821	0.1384	12.7	2640.1	11.0
1.2	186	417	0.080	0.1816	0.0007	0.3073	0.0035	7.6923	0.0913	35.2	2667.2	6.4
29.1	78	59	0.241	0.1817	0.0008	0.4486	0.0052	11.2371	0.1405	10.5	2668.3	7.4
24.1	173	48	0.050	0.1821	0.0007	0.4534	0.0050	11.3833	0.1331	9.8	2672.0	6.5
26.1	170	79	0.034	0.1824	0.0006	0.4689	0.0051	11.7949	0.1345	7.3	2675.2	5.1
11.1	434	367	0.029	0.1825	0.0008	0.4824	0.0053	12.1373	0.1447	5.2	2675.6	7.6
31.1	143	198	0.134	0.1828	0.0012	0.4579	0.0053	11.5381	0.1539	9.3	2678.2	11.1
30.1	177	67	0.043	0.1837	0.0015	0.4562	0.0050	11.5526	0.1564	9.8	2686.4	13.2
12.1	207	112	0.011	0.1868	0.0006	0.4900	0.0054	12.6219	0.1442	5.3	2714.3	5.0
17.1	236	1554	0.150	0.1875	0.0017	0.2521	0.0051	6.5162	0.1449	46.7	2720.1	15.1
5.1	148	59	0.034	0.1879	0.0013	0.3329	0.0053	8.6230	0.1505	32.0	2723.5	11.7

Data are at  $1\sigma$  precision. All Pb data are common-Pb corrected based on  $^{204}\text{Pb}$  measurements. Mount: GA6009; Instrument: RSES SHRIMP-RG; Acquisition: 15 August 2006.



## Acknowledgements

Drillcore samples were kindly provided by:

- PlacerDome Asia Pacific (Gerald Tripp, Jamie Rogers)
- Dominion Mining Ltd (Tony Poustie)
- AngloGold Ashanti Australia Limited (Mark Doyle)
- Teck-Cominco Australia Pty Ltd (Michael Taylor)

Sample preparation, mount preparation and imaging were by Tas Armstrong, Chris Foudoulis, Lauren Jackson, Bozana Krsteska, Gerald Kuehlich and Stephen Ridgway (Mineral Separation Laboratory, Geoscience Australia).

The Curtin University of Technology–Geoscience Australia Agreement for Access to SHRIMP Analytical Facilities provided access to facilities at John de Laeter Centre of Mass Spectrometry. Special thanks go to Peter Cawood (John de Laeter Centre), Chris Pigram and Peter Southgate (Geoscience Australia) for establishing and maintaining the agreement.

The SHRIMP-II instruments at the John de Laeter Centre of Mass Spectrometry are operated by a consortium consisting of Curtin University of Technology, the Geological Survey of Western Australia and the University of Western Australia with the support of the Australian Research Council.

Agreements managed by Trevor Ireland (RSES), Richard Stern and Peter Southgate (Geoscience Australia) provided access to the SHRIMP instruments at the Research School of Earth Sciences. Peter Holden (RSES) kindly provided technical assistance as required and Chris Foudoulis (Geoscience Australia) provided critical session start-up assistance and call-out support.

SHRIMP analytical sessions were assisted by Matt Baggott, Andrea Biondo, Julie Brown, Karl Bunney, Matthew Cobb, Huntly Cutten, Raul Fonseca, Matt Godfrey, Joe Heiss, Antii Kallio, Stephen Kulic, Nick McNaughton, Robbie Morris, Stefan Mueller, Rowena Pallister, April Pickard and Carl Young.

Adam Frew and Eric Thern are especially thanked for their efforts assisting Geoscience Australia operations at the Curtin facility.

Natalie Kositcin and Kurt Worden are thanked for their thorough reviews.



## References

- Black, L. P., Kamo, S. L., Allen, C. M., Aleinikoff, J. N., Davis, D. W., Korsch, R. J. and Foudoulis, C., 2003. TEMORA 1: A new zircon standard for Phanerozoic U-Pb geochronology. *Chemical Geology*, **200**, 155-170.
- Black, L. P., Kamo, S. L., Williams, I. S., Mundil, R., Davis, D. W., Korsch, R. J. and Foudoulis, C., 2003. The application of SHRIMP to Phanerozoic geochronology; a critical appraisal of four zircon standards. *Chemical Geology*, **200**, 171-188.
- Black, L. P., Kamo, S. L., Allen, C. M., Davis, D. W., Aleinikoff, J. N., Valley, J. W., Mundil, R., Campbell, I. H., Korsch, R. J., Williams, I. S. and Foudoulis, C., 2004. Improved Pb/U microprobe geochronology by the monitoring of a trace-element-related matrix effect; SHRIMP, ID-TIMS, ELA-ICP-MS and oxygen isotope documentation for a series of zircon standards. *Chemical Geology*, **205**, 115-140.
- Bollhöfer, A. and Rosman, K. J. R., 2000. Isotopic source signatures for atmospheric lead: The Southern Hemisphere. *Geochimica et Cosmochimica Acta*, **64**, 3251-3262.
- Claoue-Long, J. C., Compston, W., Roberts, J. and Fanning, C.M., 1995. Two Carboniferous ages; a comparison of SHRIMP zircon dating with conventional zircon ages and  $^{40}\text{Ar}/^{39}\text{Ar}$  analysis. *Geochronology, time scales and global stratigraphic correlation*. A. Berggren William, V. Kent Dennis, P. Aubry Marie and J. Hardenbol. Tulsa, OK, United States, SEPM (Society for Sedimentary Geology). **54**, 3-21.
- Compston, W., Williams, I. S. and Meyer, C., 1984. U-Pb geochronology of zircons from lunar breccia 73217 using a sensitive high mass-resolution ion microprobe. *Journal of Geophysical Research*, **89**, B525-B534.
- Daly, S. J., Fanning, C. M. and Fairclough, M. C., 1998. Tectonic evolution and exploration potential of the Gawler Craton, South Australia. *AGSO Journal of Australian Geology and Geophysics*, **17**, 145-168.
- Dunphy, J. M., Fletcher, I. R., Cassidy, K.F. and Champion, D.C., 2003. Compilation of SHRIMP U-Pb geochronological data, Yilgarn Craton, Western Australia, 2001-2002. *Geoscience Australia Record* **2003/15**.
- Fletcher, I. R., Dunphy, J. M., Cassidy, K.F. and Champion, D.C., 2001. Compilation of SHRIMP U-Pb geochronological data, Yilgarn Craton, Western Australia, 2000-2001. *Geoscience Australia Record* **2001/47**.
- Ludwig, K. R., 1998. On the treatment of concordant uranium-lead ages. *Geochimica et Cosmochimica Acta*, **62**, 665-676.
- Ludwig, K. R., 2000. Decay constant errors in U-Pb concordia-intercept ages. *Chemical Geology*, **166**, 315-318.
- Ludwig, K. R., 2002. SQUID 1.02: a user's manual. Berkeley Geochronology Center Special Publication **2**.
- Sambridge, M. S. and Compston, W., 1994. Mixture modelling of multi-component data sets with application to ion-probe zircon ages. *Earth and Planetary Science Letters*, **128**, 373-390.
- Sircombe K. N., 2006. Mountains in the shadows of time: Three-dimensional density distribution mapping of U-Pb isotopic data as a visualization aid for geochronological information in concordia diagrams, *Geochemistry Geophysics Geosystems*, **7**, Q07013, doi:10.1029/2005GC001052.
- Stacey, J. S. and Kramers, J. D., 1975. Approximation of terrestrial lead isotope evolution by two-stage model. *Earth and Planetary Science Letters*, **26**, 207-221.
- Tera, F. and Wasserburg, G. J., 1972. U-Th-Pb systematics in three Apollo 14 basalts and the problem of initial Pb in lunar rock. *Earth and Planetary Science Letters*, **14**, 281-304.
- Vermeesch, P., 2004. How many grains are needed for a provenance study? *Earth and Planetary Science Letters*, **224**, 441-451.
- Wetherill, G. W., 1956. Discordant uranium-lead ages. *Transactions, American Geophysical Union*, **37**, 320-326.

